UNIVERSITY OF CATANIA

DEPARTMENT OF CIVIL ENGINEERING AND ARCHITECTURE
(DICAR)

Ph.D. COURSE IN "EVALUATION AND MITIGATION OF TERRITORIAL AND URBAN RISKS" – XXXII CICLO

INNOVATIVE SOLUTIONS AND PERFORMANCE ASSESSMENT OF GREEN ROOFS

Ph.D. Thesis

Ph.D. Candidate

Stefano Cascone

Tutor

Prof. Gaetano Sciuto

University of Catania

Thesis group

Prof. Antonio Gagliano

University of Catania

Prof.ssa Tiziana Poli

Politecnico di Milano

Mail: stefano.cascone@unict.it

Riassunto

La ricerca di dottorato affronta lo studio di differenti configurazioni di tetto verde, al variare dei materiali impiegati, al fine di proporre una soluzione tecnologica innovativa sviluppata per aree con clima mediterraneo. Inoltre, la ricerca mira ad incrementare la conoscenza scientifica sul tema del raffrescamento passivo degli edifici che rappresenta uno dei principali benefici dei tetti verdi.

Preliminarmente, è stata condotta un'approfondita ricerca bibliografica inerente sia gli aspetti tecnologici sia il raffrescamento evapotraspirativo conseguito mediante i tetti verdi.

La sperimentazione numerica ha riguardato l'analisi delle prestazioni di diverse soluzioni commerciali, al fine di identificare quelle che determinano le prestazioni energetiche più elevate in clima mediterraneo, anche nel caso di impiego dei tetti verdi per la riqualificazione di edifici esistenti.

Sulla base della letteratura scientifica di riferimento e dei risultati delle analisi numeriche, sono stati progettati e installati due set-up sperimentali. Il primo, costruito presso l'Università di Catania, ha mirato a determinare le prestazioni energetiche di una soluzione innovativa che ha previsto l'impiego del granulo di polietilene come materiale di drenaggio, proveniente dalla rigenerazione dei film dismessi utilizzati in agricoltura. Per valutare gli impatti ambientali del processo di produzione del granulo, è stata eseguita un'analisi LCA, individuando le possibili azioni migliorative. Inoltre, è stato formulato un substrato con una percentuale maggiore di materia organica rispetto a quelli tradizionali, con l'obiettivo di incrementare la ritenzione idrica e, quindi, diminuire la quantità di acqua fornita dal sistema di irrigazione. Il secondo, realizzato presso l'Università di Lleida (Spagna), ha avuto l'obiettivo di valutare il raffrescamento passivo dovuto a fenomeni evapotraspirativi del tetto verde al variare del regime di irrigazione e di correlarlo alle prestazioni energetiche e alle condizioni microclimatiche.

Abstract

The Ph.D. research deals with the study of different green roof configurations by varying the materials used, in order to propose an innovative technological solution developed for areas with Mediterranean climate. In addition, this research aims to increase the scientific knowledge on building passive cooling, which is one of the main benefits of green roofs.

Firstly, a thorough bibliographical survey was carried out, concerning both the technological aspects and the evapotranspirative cooling due to green roofs.

The numerical analysis involved the performance of different commercial solutions, in order to identify those with the highest energy performance in Mediterranean climate, even in the case of building retrofitting. Based on scientific literature and numerical analysis results, two experimental set-ups have been designed and installed. The first, built at the University of Catania, aimed to determine the thermal performance of an innovative technology that involved the polyethylene granule, coming from the regeneration of films released in agriculture, as drainage material. Furthermore, an LCA analysis was performed to assess the environmental impacts of the granule production process, identifying possible improvements. In addition, a substrate, with a higher percentage of organic matter than traditional ones, was created with the aim of increasing water retention and decreasing the amount of water provided by the irrigation system. The second, built at the University of Lleida (Spain), had the objective of assessing the passive cooling due to evapotranspirative phenomena of green roof, varying the irrigation regime, and correlating it both to the energy performance and the microclimatic conditions.

Keywords: Recycled material; thermal performance; evaporative cooling; building retrofitting; LCA

Experimental set-up for thermal performance comparison at the University of Catania, Italy

Experimental set-up for passive cooling assessment at the University of Lleida, Spain

Summary

Objectives of the thesis

The objectives of the Ph.D. thesis were achieved through both numerical analysis and experimental research.

The objectives of numerical analyses are summarized in the following list:

1. To identify substrate-vegetation combinations that determine the highest thermal performance in the Mediterranean climate. The best green roof configuration was identified by a ranking based on the values of three indices representing the mitigation of the urban heat island, the reduction in energy consumption for air conditioning and the decrease in temperature fluctuations on the waterproofing membrane, respectively. In addition, the surface temperatures and energy savings of the different green roofs were analyzed by varying the substrate, vegetation and drainage layer and compared to those of the traditional roof. Substrate-vegetation combinations were characterized by physical parameters from previous experimental studies and, therefore, such materials are currently available for extensive green roofs.
2. To determine the performance of green roofs used for the retrofitting of existing buildings. Several extensive green roofs were considered as the drainage layer, substrate and vegetation changed. In addition, numerous combinations of such materials were hypothesized for the retrofitting of a residential multi-storey building in Catania (Mediterranean climate). The saturated weight of each green roof was compared to the load limits prescribed by European standard for the redevelopment of existing roofs. In addition, energy performance, in terms of reduction in surface temperature and energy savings due to green roof, was determined and compared to the performance of the existing roof. Finally, the economic costs and environmental benefits of the green roof, such as the reduction in harmful gases and the water management, were assessed.

The literature review, which covered both the technology and performance (passive cooling) of green roofs, and results from numerical analyses led to the design and installation of two experimental set-up. The objectives of the experimental research are summarized in the following list:

1. To propose an innovative green roof using low-density polyethylene (LDPE) granules as drainage layer. The polyethylene granules come from the regeneration of films used in agriculture for greenhouse cover and mulch. In the first phase, a life cycle assessment (LCA) of the granule production process was carried out, using the data provided by the manufacturer, in order to assess

its environmental impacts and to identify possible improvements. In the second phase, the thermal performance of a green roof installed at the University of Catania, specially developed for the Mediterranean climate, was assessed. This green roof uses recycled polyethylene granule as drainage layer and a substrate with a higher percentage of organic matter than commercial ones, in order to increase water retention and reduce irrigation. The thermal performance of the proposed system is compared to two commercial green roofs and existing roof without green roof.

2. To validate an innovative set-up for the evaluation of evaporative cooling due to extensive green roofs at the University of Lleida and to correlate the evaporation process with the thermal performance of the green roof. This set-up allowed to correlate the weight of the green roof, measured with high-precision scales, with the surface temperatures in the different layers, the water content in the substrate with the climatic conditions. Given that evapotranspiration mainly depends on the water content in the substrate, evaporative cooling was determined by varying the amount of water provided by the irrigation system, i.e. green roof saturation and drainage layer saturation.

The Ph.D. thesis is divided into 8 chapters. Chapter 1 presented the problem within the general scope of the doctoral course in “Evaluation and mitigation of urban and territorial risks”, Chapter 2 analyzed the literature in order to identify the technology and materials used in green roofs and chapter 7 synthesized and organized scientific knowledge on the evaporative cooling of green roofs. The other chapters represent the proposal phase of the research, where numerical analyses (chapters 3, 4 and 5) and experimental evaluations (chapters 6 and 8) are described. Chapters 3 and 4 determined the performance of different green roof configurations, also for the retrofitting existing buildings, Chapter 6 proposed an innovative technology using recycled polyethylene granules as drainage layer and the environmental impacts of which were assessed through an LCA analysis (Chapter 5). Finally, in Chapter 8, an innovative set-up was designed, built and validated to determine the evapotraspirative cooling of green roofs. These chapters were organized following the approach of scientific papers published in international journals and, therefore, each chapter includes a literature analysis on the specific topic, the description of the methodology adopted, the discussion of the results and the main conclusions that can be drawn. In addition, in order to facilitate the reading of the thesis, the bibliography was reported at the end of each chapter rather than at the conclusion of the thesis. This structure and organization of the Ph.D. thesis is widely used in other European countries, such as Spain.

1. Introducing the problem

1.1. Introduction

Currently, climate change and the scarcity of natural energy resources are topics of interest in many countries [1]. Furthermore, cities continue to grow and expand their peripheries to accommodate increases in rural migration to urban areas. According to a recent report of the United Nations, urbanization is forecasted to attain 83% by 2030 in developed countries [2]. This results in several environmental issues on a global scale, such as increased greenhouse gas emissions.

Due to this worldwide urbanization, the demand for new buildings, land, water, and energy have drastically increased over the last four decades. According to United Nations Environmental Program, the construction and maintenance of buildings account for about 40% of the global primary energy requirement and buildings account for 33% of the global greenhouse gas emissions [3]. Therefore, the building sector is of particular interest in the reduction of energy use, in order to limit global warming and mitigate the impacts of climate change [4,5].

The effect of building envelope technologies on the design and construction of sustainable buildings and urban spaces is undeniable [6,7]. Implementing various sustainable approaches and designing more environmentally friendly components for buildings leads to the realization of low-energy buildings [8]. In addition, roofs are important components of buildings, accounting for nearly 20–25% of the overall urban surface area [9]. Therefore, efficiently designed and integrated green roofs have great potential to affect the building and urban environments, replacing the lost green spaces and habitats in modern cities. Specifically, green roofs are engineered roofing systems, planted with different kind of plants on the top of a growth medium [10].

In recent years, the number of studies carried out on green roofs has considerably increased and several review papers have been published, in an attempt to summarize and organize the scientific knowledge on this topic. One of the first reviews was carried out in 2010 by Berndtsson [11], which addressed the role of green roofs in urban drainage, considering the management of both water quantity and quality. Factors which affect the influence of a vegetative roof on runoff water quality were discussed in general terms, followed by a review of data regarding the concentrations of phosphorus, nitrogen, and heavy metals in the runoff, pH, and the first-flush effect. Likewise, Akther et al. [12] statistically synthesized the effects of the influential factors, including design and hydrologic variables, on green roof performance, to explore their effects in different climatic zones. Castleton et al. [13] reviewed the current literature and highlighted the situations in which the greatest building energy savings can be made. Similarly, Saadatian et al. [14] focused on energy-related topics. Berardi et al. [15] presented a state-of-the-art of green roofs emphasizing current implementations, technologies, and benefits. The authors reviewed the benefits related to the reduction of building energy consumption, mitigation of the urban heat island effect, improvement of air pollution, water management, an increase of sound insulation, and ecological preservation. In 2015, Hashemi et al. [16] provided an overview of the effects of the application of the green roof strategy on the quality of runoff water and the reduction of energy consumption. Shafique et al. [17] included in their review the history, components, and multiple benefits (environmental, social, and economic) associated with green roof technology. In addition, the authors also emphasized its performance in reducing stormwater and energy costs, improving air quality, and ecological benefits. Recently, Cascone et al. [18] carried out a comprehensive review of the cooling effect, due to the evapotranspiration process, as most of the benefits of green roofs are related to this phenomenon. These previous studies were mainly focused on reviewing the performance and benefits, without providing a description of their technology and materials.

Vijayaraghavan [19] analyzed desirable characteristics for the growth substrate and vegetation and suggested a methodology for constructing green roofs. Dvorak and Volder [20] conducted a review in order to investigate what is known about the application of plants on vegetative roofs across North America and their ecological implications. However, these review papers addressed mainly the roles and the performance of vegetation and substrate, providing little information with both of the materials and of the other primary layers, such as the waterproof and anti-root membranes, and the protection, filter, and drainage layers. In addition, the most used international guidelines are the German FLL 2018 [21], concerning the planning, construction and maintenance of green roofs. However, these guidelines are mainly developed for Northern Europe, characterized by cold and rainy days during most of the year. Mediterranean area, characterized by hot and sunny days, has requirements that are not fulfilled by the green roof designed, according to the German FLL standard. This is mainly due to the absence of water for extended periods. Actually, several regional guidelines exist. For example, in Italy, the guideline is the standard UNI 11235:2015 [22]. However, this standard is written in Italian and, therefore, it is not suitable as an international guideline for the Southern Europe countries.

Differently from both the review carried out by Vijayaraghavan [19] and the international FLL guidelines [21], the novelty of this thesis chapter consists in comparing it to a conventional roof technology, in terms of both materials and thermal and economic performance, in assessing the Mediterranean climate conditions and their influence on green roof design, also comparing it with Tropical area and focusing on irrigation systems, in providing examples about the commercial materials and products available in the market and in analyzing innovative materials coming from recycled sources, as possible components. All these aspects related to green roof materials and technology are not fully described neither by previous articles nor by international guidelines. In addition, for each layer, the roles, requirements, performance, and materials are assessed. The information provided in this thesis chapter will be useful for both researchers and designers to develop Mediterranean guidelines for selecting suitable components and materials during the design and installation phases.

First, the history and modern applications are discussed, in order to present a state of the art of this technology and their benefits and classification into extensive and intensive are described.

1.2. History and modern applications

Existing literature shows that covering the building rooftop with soil, wetting the soil, and shading the surface of the wet soil have been used for centuries as passive cooling practices in different countries with confirmed benefits in different climatic conditions and building characteristics [23].

One of the most famous ancient green roofs dates to the fifth century when the Hanging Gardens of Babylon was constructed that is admitted as the earliest examples of greenery systems [24]. Living roofs were also utilized in the ziggurats of ancient Mesopotamia. Like Babylon, the Roman and Greek architecture also employed these systems at their own eras. For example, the Mysteries Villa represents such integration and offers an example of space that enhances human activities while improving the aesthetic value and roof life. In the Mediterranean region, different plants notably vines were utilized to prevent the building envelope from excessive sunlight in the summertime and to provide cooler and comfortable indoor conditions to occupants. Green roofs have also been presented in vernacular architecture in different countries. For example, the usage of the plants climbing the building greatly expanded in the UK and Central and Northern Europe (especially in Norway) during 17th and 18th centuries to increase the thermal insulation [25]. After many centuries of rare utilization in European cities, during the modern age green roofs have been rediscovered in the twentieth century by the Swiss architect Le Corbusier who included them in the five points of modern architecture [26]. Around the same time, American organic architects proposed vegetative roofs as a method to integrate buildings and nature.

Modern green roofs, therefore, may acquire their concept from ancient technique; however technological advances have made this technology far more efficient, practical and beneficial than their ancient counterparts. An intensive implementation started from Germany in the early 1960s when there were energy crises arose [27]. Several investigations have been carried out with emphasis on biodiversity, substrate, roof construction and design guidelines. Green roofs gained popularity also in Austria, Switzerland and United Kingdom (UK) in the same years, however, Germany is regarded as the world leader in the employment of this strategy, because green roofs on the large scale were being developed, designed and implemented [28]. In this respect, the first comprehensive program was put into practice from the early 20th century by retrofitting the houses with greenery surfaces. Nowadays, as Table 1 shows, research and application at the building in Germany are very popular and green roof coverage increases by approximately eight million square meters per year, which is remarkable. The total value of this technology in Germany was estimated to be worth Eur 254 million in the year 2015.

Table 1. Estimated market figures [29].

Target Country	**Green Roof Total m^2 (2014)**	**Green Roofs New/year m^2**	**Ratio extensive**	**Ratio intensive**	**Yearly sales figures €**
Austria	4,500,000	500,000	73%	27%	27,350,000
Germany	86,000,000	8,000,000	85%	15%	254,000,000
Hungary	1,250,000	100,000	35%	65%	5,662,500
Scandinavia	-	600,000	85%	15%	16,050,000
Switzerland	-	1,800,000	95%	5%	51,300,000
United Kingdom	3,700,000	250,000	80%	20%	28,000,000

1.3. Green roof benefits

Green roofs are a solution to increase the sustainability and energy conservation of buildings, but they produce several other benefits to urban areas in terms of social, economic, and environmental advantages. Some of these benefits can be illustrated as reducing greenhouse gas emissions and the urban heat island effect [30], preventing acid rain by escalating pH values [31], improving air quality [32] by producing more oxygen and sequestering carbon dioxide and decreasing traffic noise pollution within urban areas [33]. Other benefits of green roofs are the enhancement of aesthetic value in urban environments and the improvement of life quality of dwellers by creating recreational activities [34].

Several studies stressed the advantages for urban hydrology and storm water management, focusing on the ability of green roofs to minimize the risks of flooding by reducing water runoff while improving its quality [35]. As a result of this improvement, due to the absorption of rainfall in the soil, the burden on water treatment facilities is reduced.

Green roofs can reduce the sound exposure near or inside a building by mitigating diffracting sound waves over (parts of) roofs and by reducing sound transmission through the roof system [36]. Commonly used porous growing substrates were shown to have good sound absorbing properties when dry [37].

Based on the current literature, the energy-related performance of green roofs is still the most common benefit for which they are promoted and adopted [38]. Therefore, energy designers are very interested in their application, due to the reduction in roof surface temperature and solar heat to the covered building components [39], highlighting their contributions to both overall building thermal performance and microclimatic conditions in urban environments [40,41]. Green roofs improve the thermal performance of a building through different mechanisms:

- Shading: Vegetation provides an additional layer that shades the substrate and the roof, blocking part of the incoming solar radiation;
- Evapotranspiration: Plant transpiration and soil evaporation cool the surface of the plants, decreasing the heat flux toward the interior of the building and the urban heat island effect;
- Thermal inertia: The substrate increases the roof thermal mass, delaying and reducing incoming heat fluxes;
- Thermal insulation: The substrate and drainage layers increase the heat resistance of the roof by providing an additional thermal layer.

Therefore, this strategy is a sustainable roof design that saves energy for cooling and heating purposes [42]. Despite its high initial cost, in the long term, green roofs are an economical option considering their energy savings. However, the focus of developers has been limited to achieving basic aesthetic benefits. This is generally due to a lack of research on different aspects of vegetative roofs and the premature introduction of products into the market [43].

1.4. Technology classification

Green roofs are broadly classified into intensive and extensive roofs, though some authors include a semi-intensive classification, based on the depth of the substrate layer, maintenance, cost, vegetation type, construction material, and irrigation [44].

Intensive green roofs are generally roof gardens designed with a considerable substrate depth—more than 15–20 cm—a wide variety of plants (similar to ground-level landscapes), high water retention capacity (over 50%), high capital costs ($25 per square foot), and heavy weight (180–500 kg/m^2). Typically, this type is installed when the slope is less than 10°. Due to the increased soil depth, the plant selection can be more diverse, including small trees, shrubs, and bushes [24,45]. Therefore, it requires a high level of maintenance, in the form of fertilizing, weeding, and watering. One of the main advantages of an intensive roofing system is the creation of a natural environment with improved biodiversity, providing a recreation space, as they are normally designed for the use of humans for entertainment [46]. Intensive roofs encompass a comparatively better potential than extensive green roofs in terms of stormwater management, decreasing runoff by 85% when compared to traditional roofs [47]. Likewise, intensive green roof runoff has three times less lead contamination, 1.5 times less zinc contamination, 2.5 times less cadmium contamination, and three times less copper contamination [47]. On the other hand, their greater weight may require additional structural reinforcement, and drainage and irrigation must generally be utilized, increasing the technical complexity and associated costs [27].

Extensive green roofs are characterized by a shallower depth of substrate layer (less than 15 cm) and have a lower weight in comparison to intensive ones. Owing to the thin substrate layer, extensive roofs can utilize only limited types of plants, including grasses, mosses, and a few succulents. The main advantages of extensive roofing systems are the low capital cost and maintenance and water requirements, compared to intensive roofs [11]. These roofs are usually very lightweight and useful, especially where no additional structural support is desired. Furthermore, an extensive roof can be installed on a larger slope, their construction process is technically simple, and it is appropriate for large-sized rooftops. However, both the energy performance and storm water management potentials of extensive green roofs are relatively low [48].

Of the two types, extensive roofs are most common around the world, due to their low weight, not requiring irrigation, and having less capital and maintenance costs [49]. Table 2 compares intensive and extensive green roofs.

Table 2. Main features of intensive and extensive green roofs.

Main characteristics	Intensive	Extensive
Maintenance	High	Low
Irrigation	Periodically	Regularly
Plant diversity	Sedum-Herb-Moss-Grass	Lawn-Perennial-Shrub-Tree
Cost	Low	High
Weight	Lightweight (60–150 kg/m^2)	Heavy (180–500 kg/m^2)
Thickness	60–200 mm	140–400 mm
Use	Accessible	Inaccessible

2. Green roof design: State of the art on technology and materials

2.1. Materials and components

A green roof generally consists of several components, including, from bottom to top [19]: A waterproofing membrane, an anti-root barrier, a protection layer, a water storage and drainage layer, a filter layer, substrate (growing medium or soil), and vegetation (plants). These components are shown in Figure 1.

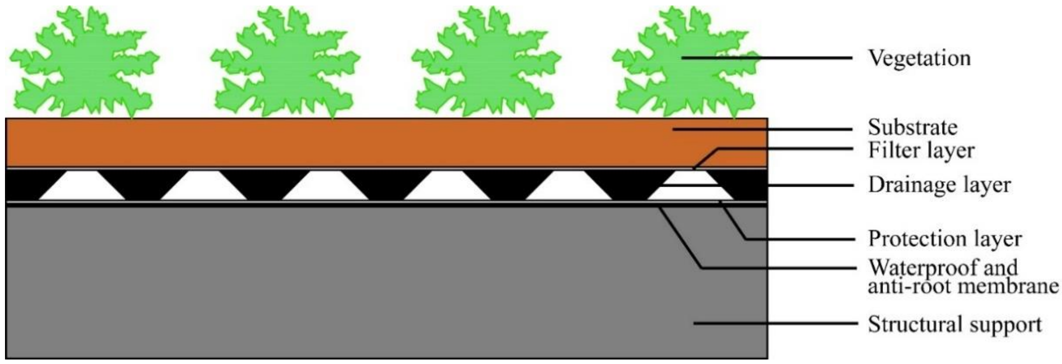

Figure 1. Green roof layers.

2.1.1. Waterproof membrane

The waterproof membrane is one of the most important components of the green roof technology. It protects the building against any infiltration resulting from the large water content of the upper layers and, in turn, it is protected by the vegetative roof against temperature fluctuations and solar radiation, which may cause performance decay of the membrane in a short time. The primary requirement for this layer is water-tightness. In addition, it should be considered that the maintenance of this layer is very complex because, in the case of a leak in an operating green roof, all the layers need to be removed. Therefore, it is necessary to foresee solutions to prevent horizontal water flow below the membrane, to reduce degradation, and to allow the location of any infiltration points. These results can be achieved either through the perfect adhesion of the waterproof membrane to the bearing structure, or through compartmented sectors in the membrane.

The design of the waterproofing membrane is similar to traditional roofing. However, compared to a traditional roof, the waterproofing membrane of a green roof is protected against UV rays, thermal fluctuations, and hail shocks. On the other hand, the membrane can be exposed to the biological and chemical agents contained in the substrate and vegetation.

Bituminous flexible membranes are the most common and they can be classified, further, as:

- Elastomeric membranes: Characterized by an elastomeric polymer mixed with bitumen, which gives flexibility at low temperatures and excellent elasticity;
- Plastomeric membranes: Characterized by a plastomeric polymer mixed with bitumen, which gives stability at high temperatures and offers high resistance to UV exposure;
- Elasto-Plastomeric membranes: Combines the characteristics of the two membranes above-described.

The bituminous membranes can be laid in a monolayer or as a double layer. Thicknesses of 3 or 4 mm are generally used. These membranes have different characteristics and behaviors, but a common stratigraphy is realized by the compound, the glass or polyester reinforcement, and the protective surface finish.

The main characteristics of the waterproofing membrane to be controlled, in addition to water tightness, are the dimensional stability (since as long as the green roof is not installed the membrane is exposed to solar radiation and to high daily thermal fluctuations), cold flexibility, resistance to static loads (in order to verify that the membrane resists permanent and accidental loads), and artificial ageing (through long-term exposure to high temperatures). The waterproofing membrane does not necessarily meet the requirement of protection from the roots. If the membrane is exposed to the roots and there is no anti-root layer, it would be necessary to verify this resistance, too.

The type of green roof, along with cost, availability, and life expectation, determines the type of waterproofing. Once the suitable typology of waterproofing membrane has been identified, it must be laid on a sloping screen (allowing an adequate flow of water) and turned over at the edges by at least 15 cm.

2.1.2. Anti-root membrane

In the design of a green roof, the aggressive capacity of the root system should not be underestimated. The objective of a root-barrier is to defend the waterproof membrane and the roof structure from vegetative roots penetrating from the upper layers, which could mechanically disrupt and chemically alter the waterproofing membrane. The consequence of these two combined actions is the drilling of the waterproofing membrane and penetration into the underlying layers, causing water infiltrations in the building. Therefore, the anti-root layer must always be laid out in a green roof and, in almost all cases, it is integrated into the waterproofing membrane. When installing a living roof on an existing building with an efficient waterproofing membrane, the additional anti-root protection layer will be overlaid onto the waterproofing membrane.

The main characteristics and materials of this layer are similar to those reported for the waterproofing membrane. However, the anti-root membrane must be characterized by high resistance to micro-organisms contained in the soil, adding some repellent ingredients to the chemical composition of the anti-root membrane. Anti-root membranes are characterized by thicknesses around 4 mm and are placed with hot-air welding or a chemical solvent.

The use of concrete as an anti-root barrier is not possible, as it can be attacked by roots over time and makes it very difficult to maintain the waterproofing membrane. In addition, felts, polyethylene films, or the like, do not meet the performance requirements in terms of resistance to root penetration. An alternative material for the anti-root layer is a metal sheet.

2.1.3. Protection layer

To protect the waterproofing and anti-root membrane, a good practice is to provide a separation and protection layer among the green roof layers. The requirement for this layer is the ability to withstand loads and stresses during both the construction and operational phases. Therefore, it is necessary to place it after the anti-root membrane. Normally, the loads it needs to withstand are, due to the weight of the layers above the anti-root membrane.

The materials used are either geogrids and geotextiles or polystyrene, with a minimum thickness of 3 mm and compression resistance >150 kPa. These materials may not replace the anti-root membrane.

Some materials used for the protection layer could accumulate water, which can be released to the vegetation during periods of drought.

2.1.4. Water storage and drainage layer

The drainage layer plays a crucial role in the correct development of a green roof. As most of the vegetation needs a ventilated and non-waterlogged substrate, this layer aims to drain the excess of water from the substrate, allowing a suitable equilibrium between air and water and providing adequate ventilation for the roots. In addition, by evacuating extra water, it decreases the load on the building structure and reduces the risks of a mechanical breakdown. Furthermore, the drainage layer defends the waterproof membrane and enhances the thermal performance.

Among all these roles, the aeration of the root apparatus is often penalized by incorrect green roof design, resulting in the failure of the entire technology. Therefore, under operating conditions, the drainage layer should be filled, at least 60%, with air, to preserve the vegetation and prevent deterioration. The draining and ventilation capacity of the drainage layer could decrease over time, influencing the development of the vegetation [50].

There are two main materials used for the drainage layer (Figure 2):

- Granular materials: These have a minimum thickness of 6 cm and a minimum density of 150 kg/m^3. If porous, they are also used as water storage. The main aggregates used in green roofs are pozzolana, pumice, lapilli, expanded clay, expanded pearlite, expanded slate, and crushed bricks;
- Modular panels: These have a thickness between 2.5–12 cm and a weight of about 20 kg/m^2. These panels are produced with high-strength synthetic or plastic materials (polyethylene or polystyrene) and cavities to store water while still allowing the removal of surplus water.

Figure 2. Green roof drainage materials: Modular panels (on the left) and granular materials (on the right).

For granular materials, the requirements are permeability (i>0.02), compressive strength (>1.5 N/mm^2), and thermal conductivity (λ<0.2 W/mK). For modular panels, the required characteristics are vertical draining capacity under operating loads (0.7 l/m^{2}s), compressive strength, having longitudinal tensile strength (>7.0 kN/m) and tensile strength (>7.0 kN/m to be applied only for green roofs with slope >30%), and resistance to aggressive agents. These panels are made with cavities to store water during rain and make it available during drought periods. From these cavities, the water evaporates and penetrates the filter layer where it condenses, reaching the root apparatus by capillarity.

The selection of a suitable drainage layer varies greatly according to the rainfall characteristics of the site, construction needs, structural requirements, costs, green roof size, roof slope, quantity and flow of discharges, and plant species. Moreover, the choice of the drainage layer depends on the hydraulic flow and the vertical load, since, during the operative phase, there is either a compaction (for granular materials) or a deformation (for plastic materials).

Generally, for small-scale green roofs, as in residential buildings, granular materials meet the requirements. Nevertheless, an important disadvantage of granular materials is that they can only be used on flat or slightly sloped roofs (<5°). In addition, limitations during installation and workmanship cannot be ignored. Modular panels are used for larger green roofs and, compared with granular material, they have higher performance thanks to their reduced thicknesses and weights, better management of the air/water ratio, ability to store more water in their cavities, greater mechanical resistance, and increased durability. In addition, transport, handling, installation, and maintenance (with the possibility of opening up the plastic modules as pieces) are simpler and quicker. On the other hand, cost and disposal are the major limitations of plastic drainage modules.

2.1.5. Filter layer

The key role of this layer is to separate the substrate from the drainage layer and to avoid smaller particles (for example fine soils and vegetation debris) entering and clogging the drainage layer, thus reducing its performance over time. This material, once penetrated, could favor the establishment of plants inside the drainage layer or obstruct the drains, causing infiltrations and blocking the entire greening system. The filter layer should have small holes to allow for high water permeability, at least 10 times higher than the substrate. Therefore, the performance to be monitored is the water permeability.

The two types currently used for the filter layer are:

- Granular materials, such as pozzolana, pumice, lapillus, expanded clay, expanded perlite, expanded slate, and crushed bricks, characterized by a water permeability greater than 0.3 m/s;
- Non-woven geotextiles with water permeability greater than 0.3 cm/sl x 10^{-3} m/s, able to absorb 1.5 L/m^2 of water.

Generally, geotextile materials are used for the filter layer.

The main parameters required for the filter layer are to withstand the weight overhead and punching resistance (>1.100 kN), longitudinal tensile strength (> 7.0 kN), transverse tensile strength (> 7.0 kN), deformation to the longitudinal operating load (< 60%), deformation to the transverse working load (< 60%), effective pore opening (0.10–0.20 mm), oscillation resistance (< 20%), and resistance to aggressive agents.

2.1.6. Substrate

The growing media should be designed to accomplish the numerous long-term advantages of a green roof, such as water quality improvement, peak flow decrease, and noise and thermal insulation, which are related to the substrate characteristics. The substrate plays an important role in the plant growth, as it guarantees establishment and stability, satisfying the control of the agronomic capacity; that is, the capacity to maintain the physical, chemical, and biological conditions for the correct vegetative development.

The thickness and weight of the substrate depend on the vegetation, roof geometry, climatic conditions, and irrigation strategy. In the rain, some substrates become saturated rapidly, increasing their weight. Generally, substrate weight varies from 12–14 kg/m^2 with a thickness of 8 cm for extensive green roofs to about 600 kg/m^2 with a thickness of 50–60 cm for intensive ones.

The substrate is characterized by two main sets of parameters:

- Physical parameters, such as density, particle size, water permeability, maximum water volume, and maximum air volume in saturated conditions;
- Chemical parameters, such as pH index, electrical conductivity, and quantity of organic matter.

In the case of a wrong choice of substrate, the consequences are compaction, imbalances between water and air, asphyxia of the root apparatus, increased weight, reduction in drainage, and the alteration of the nutrients.

2.1.6.1. Performance

The main characteristics required for the substrate in the development and maintenance of vegetation under different climate conditions are:

- High hydraulic conductivity and water retention capacity;
- High aeration and flow attributes;
- Poor leaching and high sorption capacity;
- Lightweight, locally available, and cost effective;
- Stability of the physical and chemical structure in severe climate conditions;
- Minimum organic content;
- Wide variety of vegetation;
- Improved water quality.

Optimization of the substrate performance is achieved through a mixture of materials with different characteristics and proportions. In this framework, it is very difficult to find or formulate a green roof substrate with all these beneficial attributes, since some qualities could be decreased to enhance others, depending on the performance required. For example, a low-bulk density attained by employing lightweight materials could compromise the stability of the substrate and vegetation anchorage. Furthermore, by reducing the particle size and increasing the organic matter content to improve water retention capacity could influence air-filled porosity and hydraulic conductivity. Therefore, enhancing these attributes through scientific investigation is necessary for long-term sustainability.

Green roof substrates should be characterized by low dry and wet bulk densities, as they represent the main load on the roof bearing structure, especially in old buildings where the roofs were not built to accommodate green roof systems [51]. One of the key approaches for decreasing the weight of the substrate is to utilize low-density inorganic materials. The bulk density of perlite was stated to be 9.4 times less than that of conventional garden soil. It should also be noted that the lower the density of the substrate, the thicker the substrate can be constructed, and the larger variety of vegetation that can be planted.

Concerning the hydraulic performance, water retention and permeability should be considered, guaranteeing a porosity not less than 58% and 48% for extensive and intensive green roofs, respectively. Schultz et al. [52] found that 125 mm and 75 mm vegetative roofs retained 32.9% and 23.2% of all precipitation by volume, respectively. Farrell et al. [53] tested whether two different water-retention additives (silicate granules and hydrogel) increased substrate water retention capacity and plant available water. Two substrates were compared, one based on scoria and the other based on crushed terracotta roof-tiles. Without additives both substrates had similar water holding capacity (40–43%). Furthermore, Vijayaraghavan, and Joshi [54] prepared a substrate using 30% perlite, 20% vermiculite, 10% sand, 20% crushed brick, 10% cocopeat and 10% *T. conoides* was found to have high water retention capacity (49.5%). However, Talebi et al. [55] revealed that the vegetation type had a greater impact on the water retention performance of green roofs than increases in substrate storage capacity associated with different substrate depth, porosity and wilting point over the range assumed in this study.

In addition, the substrate increases the thermal resistance of the green roof. However, the substrate is not considered to be an insulating material, due to the variability in the water content, which significantly influences the thermal conductivity. For this reason, the thermal performance of the green roof should be referred to at the maximum water saturation.

Numerous researchers examined the leaching tendency and sorption ability of green roof substrates, which affects the quality of the runoff. However, due to the percentage of inorganic components, the sorption ability of the substrate is reduced. For example, expanded perlite, a commonly-used substrate constituent, showed no more than 8.6 and 13.4 mg/g sorption abilities on Cu(II) and Pb(II) ions, respectively. An alternative broadly utilized substrate element, pumice, adsorbed only 3.5 and 1.6 mg/g of Cu(II) and Cr(III), respectively.

The water holding capacity (WHC) of the substrate components is essential for the endurance of the vegetation, since it delays the peak flow during storm events and helps the plants to withstand drought conditions. In addition, high WHC allows the use of non-succulent plant species. Forschungsgesellschaft Landschaftsentwicklung Landschaftsbau (FLL) [21] suggests WHC >20% for extensive green roofs. WHC can be improved by increasing the substrate volume, depth, and organic content. In recent years, some researchers have suggested the use of additives to maximize the water holding capacity of the growing media. Vijayaraghavan and Joshi [54] incorporated a brown seaweed (Turbinaria conoides) in the growth substrate to enhance the runoff quality of green roofs.

The ventilation and flow characteristics of the substrate are not only important for vegetative development, but in avoiding roof leakage and water overloading. For extensive roofs, FLL recommended an air-filled porosity >10% and hydraulic conductivity >3600 mm/h. Large-sized particles increase air-filled porosity and hydraulic conductivity, while small-sized particles and organic matters reduce air and flow features.

2.1.6.2.Composition

The common procedure is to blend various materials with different attributes at well-defined percentages to constitute the growth substrate. However, the substrate in green roofs differs from traditional garden soil, as traditional molds are mainly composed of organic materials, such as peat and compost. The substrates consist mainly of mineral materials (Figure 3), varying from 50% to 90% of the substrate volume and giving the green roof a lower density, higher porosity (75%), higher draining capacity in saturated conditions, and easier ventilation of the roots. The most used low-density inorganic materials for the substrate are pumice, zeolite, scoria, vermiculite, perlite, peat, and crushed brick. In particular, the particle size should have a high percentage of granules with a diameter between 2–4 mm. Some researchers recommended the use of more than 80% inorganic materials in the composition of the growing medium and, thus, the load of green roofs can be lowered.

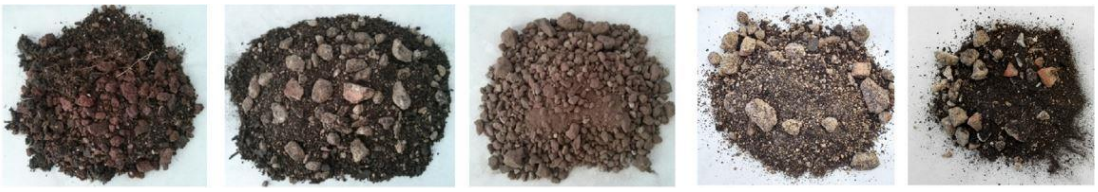

Figure 3. Commercial substrates analyzed by Coma et al. [56].

However, the growth medium is normally projected to incorporate nutrients to encourage vegetative development. Therefore, it is crucial to include organic components in the substrate to supply nutrients to the green roof. Some popular organic components used in the substrate are mulch, peat, and various other composts. Eksi et al. [57] quantified the optimal percentage of compost in a substrate for optimizing the growth and yield of cucumbers (*Cucumis sativus*) and peppers (*Capsicum annuum*). Cao et al. [58] examined the effects of adding one type of green waste, biochar, to two scoria-based substrates (with or without added organic matter) on bulk density. The results showed that biochar significantly reduced the bulk density, and substrates with 40% biochar had an additional 1.5 cm/m^2 of depth (compared to the same weight of scoria), further increasing the available water for the plants and rainfall retention.

When commercial substrates are prepared for the expected plant species, climate conditions, and maintenance levels, they may not work properly in different geographic regions. Ziogou et al. [59] used commercially-available materials for green roof layers (Bauder enterprise), focusing both on energy conservation and sustainability in two alternative solutions applied to a typical urban office building in representative climatic areas of Cyprus, in the Eastern Mediterranean. Vijayaraghavan et al. [60] used a commercial substrate (Daku enterprise) to assess the runoff quality from green roofs.

2.1.7. Vegetation

Most of the success of a green roof depends on how healthy the plants are, especially in meeting long-term client expectations. The benefits mainly depend on the plant species, as they enhance both water and air quality and thermal performance. In addition, the vegetation characterizes the visual aspect of the green roof, prevents the erosion of the substrate, and provides protection for various animal species, especially arthropods and birds.

In the choice of vegetation, the climate conditions, such as rainfall intensity, humidity, wind, and solar radiation, should be considered. Furthermore, the substrate mixture also affects the plant species that can be installed, especially in terms of pH, salinity, and nutrients.

In recent years, some authors have worked to identify suitable plant species based on the soil depth, defining the following plant species for extensive green roofs:

- 0–5 cm: Sedum, mosses, and lichens;
- 5–10 cm: Short wildflower meadows, long-growing, drought-tolerance, perennials, grasses, alpines, and small bulbs;
- 10–20 cm: A mixture of low or medium perennials, grasses, bulbs and annuals from dry habitats, wildflowers, and hardy sub-shrubs.

The roof installation site is important in optimizing the choice of plant species, as the emissions of hot/cold air and the chemical components in the air should be considered. Moreover, the shaded areas (due to surrounding buildings) alter the solar radiation and, consequently, the luminous flux and temperatures on the green roof. However, the roof of the building is not a natural ecosystem for the development of plants, as water is a restricting element and its availability varies between rain events. In addition, building load constraints limit the substrate weight and depth and, therefore, restrict the types of vegetation that can be used.

2.1.7.1.Performance

The favorable attributes of plants for extensive green roofs are good ground coverage, short and soft roots, phytoremediation, ability to survive in extreme climate conditions and under minimal nutrients conditions, limited maintenance, and fast development. Even if it is very difficult to find plant species with all these valuable qualities, a considerable improvement has been achieved for the choice of proper vegetation. Ground coverage is a key criterion for plant choice as it shields the substrate from direct sunlight and wind. Furthermore, ground cover plants delay unwanted plant growth and soil erosion when constructed on sloped rooftops. Plants with short, soft roots avoid the infiltration of the roots into the roof deck. The growth medium also requires only minimal nutrients to avoid wildflowers and the production of eutrophic runoff and, thus, only needs nutrient-poor inorganic recycled constituents as the main components of the green roof substrate.

A capacity for phytoremediation has never been a standard for choosing the green roof vegetation. Plants eliminate dissolved contaminants by phytoextraction and vaporous pollutants by phytovolatilization. While there have been numerous experiments on air and water quality improvements by green roofs, the role of vegetation on contamination management has rarely been examined. Baraldi et al. [61] evaluated the potential ability of fifteen species to mitigate carbon dioxide (CO_2) and urban pollutant concentrations, by analyzing the leaf-physiological traits (gas exchange) and morphological structures (stomata, trichomes, epicuticular waxes, and cuticular ornamentation) involved in pollutant removal. Their results suggested that the potential mitigation capacity, based on the investigated traits of the shrubs and herbaceous species, was species-specific. Speak et al. [62] quantified the effectiveness of four species, *Agrostis stolonifera*, *Festuca rubra*, *Plantago lanceolata*, and *Sedum albumat*, in capturing particulate matter smaller than 10 mm (PM10). The study found that the grasses, A. stolonifera and F. rubra, were more effective than *P. lanceolata* and *S. albumat* at PM10 capture.

In the Mediterranean climate, characterized by dry periods during the summer with high temperatures and solar radiation, it is necessary to provide an adequate quantity of water to the vegetation. It is necessary to know the response of the vegetation to conditions of water stress, thus identifying, in the substrate and in the drainage layer, the components capable of making water available to the vegetation without increasing the overall weight of the green roof. The ability of a plant species to withstand prolonged periods of water stress depends on their speed of transpiration, the water content in the substrate, and the resistance to the water transfer from the substrate to the vegetation. Savi et al. [63] analyzed the resistance to water stress of some plant species in the Mediterranean area, according to the indicator ψ_{50} that is the water potential of substrate. Water potential (ψ) is actually determined by taking into account two factors - osmotic (or solute) potential (ψ_S) and pressure potential (ψ_P). The formula for calculating water potential is:

$$\psi = \psi_S + \psi_P \tag{1}$$

higher values of this parameter correspond to a greater capacity of a species to withstand intense and prolonged water stresses. Currently, the parameter ψ_{50} is the most used, among physiological criteria, to select species suitable for green roofs. In the Mediterranean area, it is necessary to use species characterized by strongly negative critical values of ψ_{50}. These species use a greater quantity of water from the soil, enduring the increased transpiration, due to the high temperatures and increased solar radiation in the summer season.

2.1.7.2.Sedum species

Numerous researchers have identified succulent plants as the species with the highest performance for extensive green roofs. Among these, Sedum species are the most common because of their capacity to reduce transpiration and store additional water in leaves, allowing them to withstand drought conditions. In addition, Sedum species exhibit crassulacean acid metabolism (CAM), which improves their water-use efficiency by permitting stomatal opening and CO_2 storage during the night-time, when evaporation rates are lower than during the day. However, Sedum species are unable to exploit additional water.

The most used Sedum species are the following:

- *Sedum sediforme* [64–66]
- *Sedum album* [67–69]
- *Sedum kamtschaticum* [67,70]
- *Sedum lineare* [71,72]

Nektarios et al. [66] evaluated the growth capacity of native *Sedum sediforme* in extensive systems. It was found that *Sedum sediforme* was able to survive under minimal or no irrigation even at the shallow depth of 7.5 cm and proved to be a native plant species that could successfully be utilised in extensive systems in the Mediterranean and other semi-arid climatic regions.

Several studies underlined the potential of Sedum species to survive extended periods without water. Nagase and Dunnett [73] investigated plant survival, following an imposed drought. The authors concluded that the drought tolerance of Sedum species was superior to that in forbs and grasses. Lu et al. [71] highlighted that Sedum species survived through a five-week continuous drought treatment. With a restricted water supply, a deeper substrate (no less than 10 cm) was recommended by authors to ensure better drought tolerance performance of the plants in extensive green roofs. Additionally, Sedum species were demonstrated to be effective for a shallow substrate. Eksi et al. [74] analyzed a pre-vegetated mat of a mixture of sedum on shallow substrates, with a depth of 5 cm.

2.1.7.3. Other possible plant species

In humid tropical climates, *Portulaca grandiflora* has shown high performance, while, in warm and dry climates with long periods of drought, *Aptenia cordifolia* was proved to be suitable. Furthermore, upholstery plants offer greater performance, in terms of visual quality, compared to Sedum species, increasing the biodiversity in the greening. Synergy with succulent species is very significant, as upholstery plants can exploit an excess of humidity, without which they require additional irrigation, especially during the summer months. Blanusa et al. [75] used a range of contrasting plant types, such as a *Sedum mix*, *Stachys byzantina*, *Bergenia cordifolia*, and *Hedera hibernica*. The results showed that *Stachys* outperformed the other species, in terms of leaf surface cooling, substrate cooling below its canopy, and, even, cooling the air above its canopy. Gionannini et al. [76] compared the performance of plant communities with that of monocultures and compared the growth of natives to non-natives in a simulated green roof setting in a desert environment. Native plants selected were *Chrysactinia mexicana*, *Melampodium leucanthum*, *Euphorbia antisyphilitica*, and *Nassella tenuissima*, and non-natives were *Delosperma nubigenum*, *Stachys byzantina*, *Sedum kamtschiaticum* and *Festuca glauca*. The authors concluded that the lack of differences in plant performance regardless of assignment to monoculture or community would imply that communities and monocultures are equally suitable for an arid region.

Species mixtures have often been correlated to enhanced aesthetic value. Furthermore, plant variety could improve substrate cooling, prevent intrusive unwanted plants, and preserve water. Heim and Lundholm [77] tested three drought-tolerant, mat-forming species native to *Nova Scotia*, *Cladonia spp.* (lichen), *Polytrichum commune* (acrocarpous moss), and *Danthonia spicata* (bunchgrass). The results showed that the incorporation of functional diversity, especially varied growth forms, increases the diversity of green roofs, potentially improving the resilience and performance of these systems in the long term. Van Mechelen et al. [78] analyzed the initial plant composition of commercial extensive systems, in terms of functional diversity, and proposed two methods to compose species lists which maximize functional diversity. The authors believed that designing functionally diverse plant systems will support more sustainable urban planning and improve the quality of urban life.

2.1.8. Green roofs vs. conventional/traditional roofs

Vegetative roofs are gaining popularity, due to their many benefits compared to traditional roofs, since they absorb solar radiation and consequently waterproofing membrane is heated up by the sun during the day and cooled down at night. These daily temperature fluctuations could crack the roof membrane and reduce its durability. El Bachawati et al. [80] focused on characterizing and analyzing the temperature profile of a traditional roof mockup and two extensive green roof mockups with different substrate depths and composition in the winter season. The traditional roof mockup consisted of the following layers: Roof assembly, thermal insulation layer, waterproof membrane, filter sheet, and an exterior layer made of pebbles (Figure 4). The green roof mockups were each installed using the following layers: Roof assembly, thermal insulation layer, waterproof membrane, root resistant barrier, drainage layer, filter sheet, growing medium, and vegetation. As for the substrate, it entailed oil, peat, alumina, pumice, and organic fertilizer. The vegetation layer was pre-cultivated elements.

Results from [80] showed that during warmer days, the substrate temperature was lower than that of the traditional roof surface. During colder winter days, daily average substrate temperature values were similar to that of the traditional roof surface, mostly due to partial plant coverage. The highest recorded temperature values were 26.18 °C for air, 33.98 °C for traditional roof surface, 24.24 °C for 8 cm substrate, and 23.36 °C for 16 cm substrate. This indicated that the highest temperature values of air and on traditional roof surface were greater than that of under substrates.

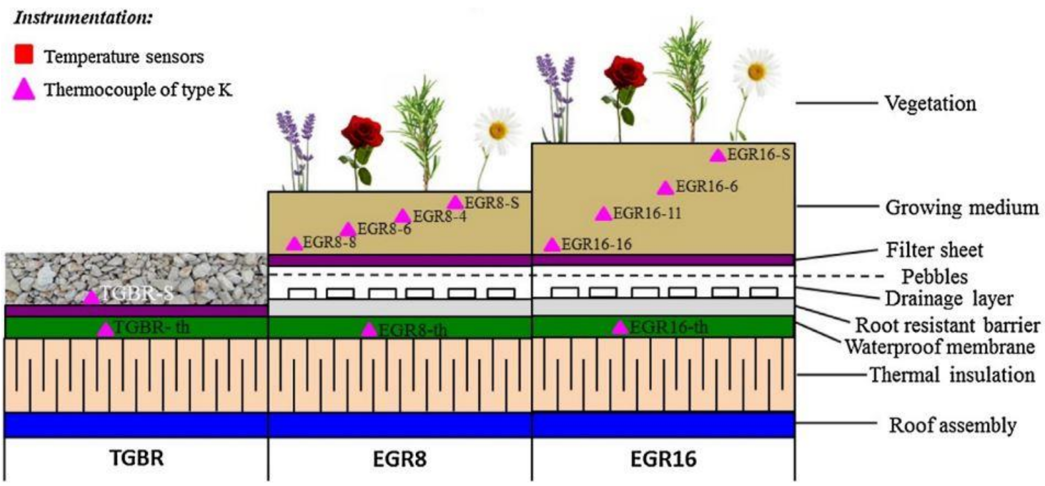

Figure 4. Comparison between traditional and green roof. (**a**) Traditional roof; (**b**) Extensive green roof (substrate thickness 8 cm); (**c**) Extensive green roof (substrate thickness 16 cm) [80].

In addition, Dos Santos et al. [81] indicated that the use of green roofs resulted in lower temperature variations throughout the day, decreased internal temperatures, and decreased thermal amplitude in relation to a conventional roof (with tiles). The reduction was 0.8 °C, 1.7 °C and 1.6, respectively. Theodosiou et al. [82] showed that in Mediterranean countries, a green roof can contribute substantially to building's energy conservation mainly during the warm period of the year, while its influence during the cold period is negligible.

Since roof finishing materials of non-vegetated roofs are most often rigid, there is a large potential to attenuate sound waves diffracting over the outer skin of the building and to enhance quiet facades, e.g., in road traffic applications. Due to their relatively large surface mass density, low stiffness and pronounced damping properties, green roofs increase the acoustic insulation on top of the basic roof [83]. Especially their performance in the low-frequency range could be interesting. Van Renterghem, and Botteldooren [84] demonstrated that green roofs lead to consistent and significant sound reduction at locations where only diffracted sound waves arrive relative to common, non-vegetated roofs. A single diffraction case with an acoustic improvement exceeding 10 dB was found for sound frequencies between 400 Hz and 1250 Hz, although the interaction path length was only 4.5 m.

In terms of cost, Sproul et al. [85] presented an economic perspective on roof color choice using a 50-year life-cycle cost analysis (LCCA) ND data collected from 22 flat roof projects in the U.S. The authors found that relative to black roofs, green roofs had negative net savings of \$71/m^2 (\$6.60/ft^2) because they cannot compensate for installation cost premium. However, owners concerned with local environmental benefits should choose green roofs.

2.2. Design optimization for Mediterranean climate

2.2.1. Influence of climate conditions

The majority of the regions with Mediterranean climates have relatively mild winters and very warm summers. Under the Köppen climate classification [86], "hot dry-summer" climates with average temperature in the warmest month above 22 °C (classified as Csa) and "cool dry-summer" climates with average temperature in the warmest month below 22 °C (classified as Csb) are often referred to as "Mediterranean". In many Mediterranean areas there is a strong diurnal character to daily temperatures in the warm summer months, due to strong heating during the day from sunlight and rapid cooling at night. As a result, areas with this climate receive almost all of their precipitation during their winter and spring seasons and may go anywhere from three to six months during the summer and early fall without having any significant precipitation [87].

Such conditions impose severe restrictions on plant growth and on plant survival and water is one of the most common limiting factors for the development of plants. Unfortunately, summer water shortages, a recurring problem in the Mediterranean region, are expected to increase according to climate change scenario forecasts. Yet irrigation is an unsatisfactory long-term option, both economically and ecologically. In Mediterranean regions high summer temperatures and prolonged seasonal drought make the installation of efficient and fully functional green roofs more difficult. Due to these climate restrictions, their design has been influenced; hence, new considerations about substrate characteristics and the plant species used are emerging in an adaptive approach to green roof construction in Mediterranean areas in contradistinction to the formalistic approach that is currently dominating the industry. It is therefore important to establish plant selection criteria prior to implementation. In the case of Mediterranean green roofs, the main criteria are drought tolerance, their indigenous nature, aesthetic characteristics (to ensure acceptance by the general public) and low maintenance requirements.

2.2.2. Possible material selection

Chenot et al. [88] assessed the role of substrate thickness and composition in maintaining the moisture necessary for good vegetation cover. The authors mixed fine elements (clays and silts) with coarse elements (pebbles of all sizes) with the aim of allowing typical pioneer Mediterranean vegetation communities to be maintained without human intervention (no watering, mechanical or chemical weeding). For the optimal colonization of the vegetation, the results showed that a substrate thickness of 15 cm composed mainly of clays and silt (75% clay-silt and 25% pebble-sand) would be recommended for the installation of green roofs with such substrates in a Mediterranean climate context. In two different papers, Monteiro et al. [89,90] tested the adequacy of different substrates for supporting aromatic plants. All experimental substrates proved to be adequate for vegetation growth, with the combination of 70% expanded clay, 15% organic matter and 15% crushed eggshell showing the best results regarding plant establishment and growth over time. These studies showed that selected aromatic plant species could be successfully used in green roofs in a Mediterranean climate. Ondoño et al. [91] studied the germination capacity and subsequent development of five Mediterranean species (*Silene vulgaris*, *Crithmum maritimum*, *Silene secundiflora*, *Lagurus ovatus*, *Asteriscus maritimus*, and *Lotus creticus*) on three different artificial substrates (green compost with crushed bricks, expanded clay and clay–loam soil, respectively). The result showed that crushed bricks and expanded clay substrates were more appropriate for every plant species tested than the clay–loam soil mixture. The authors strongly recommended the use of lightweight and highly porous substrates as the basis for Mediterranean plants growth, and the combined use of perennial and annual species, such as *S. vulgaris* and *L. ovatus*, which offered a permanent cover throughout the year. The same research group, in a different paper [92], investigated the ability of four different substrates to maintain and promote the growth of two Mediterranean plant species. The two plant species tested in the above-mentioned substrates were *Lotus creticus* and *Asteriscus maritimus*. The plant species selected are good candidates to be introduced in green roof systems located in Mediterranean cities because, as I have demonstrated, both are perfectly adapted for growth under harsh weather conditions with little irrigation and low organic matter inputs. Raimondo et al. [93] provided insights into the importance of species-specific drought resistance strategies and hydraulic properties for selecting Mediterranean native species best suited for specific technical functions and ecological requirements of green roofs. Experiments were performed using two Mediterranean shrub species: *Arbutus unedo* and *Salvia officinalis*. Both vegetation types were found to be suitable species in the Mediterranean area.

As concern the substrate depth, Savi et al. [94] investigated the performance of two sub-Mediterranean shrubs (*Cotinus coggygria and Prunus mahaleb*) grown over green roofs with extremely shallow substrate depths and identified the impact of substrate thickness on shrubs water status, survival, and growth in a sub-Mediterranean climate. The results confirmed the possibility to install extensive green roofs vegetated with stress-tolerant shrubs in sub-Mediterranean areas using 10 cm deep substrate.

Van Mechelen et al. [95] provided an overview of plant traits that are crucial for the survival of plants in areas where dry periods are prominent, especially in the

Mediterranean climate. The most important plant traits were incorporated in an easy to handle screening tool and it will be applied on a species list of a vegetation survey in Mediterranean southern France. The highest scoring species were Sedum album and Sedum acre, both already frequently used on green roofs. The authors highlighted that 35% of the species in the new potential species group recommended in the Mediterranean region are therophytes. Moreover, Caneva et al. [96] performed an extensive bibliographic search on plants proposed for extensive green roofs in Mediterranean countries, aimed at the creation of a wide database.

2.2.3. Comparison with Tropical climate

A tropical climate is characterized by hot-humid summer with frequent showers, thunderstorms and occasional typhoons. A limiting factor for tropical green roof implementation is plant survival. Plant selection and testing for applications have taken place mainly in the Mediterranean climate, with a set of conditions that are radically different from those of the hot-humid tropics.

Jim [97] evaluated vegetation effect on green roof thermal energy performance with reference to climate adaptation in the compact tropical city of Hong Kong. From the findings, practical recommendations have been distilled to inform design, installation and maintenance of a simple, durable and low-maintenance green roof on building rooftops in humid-tropical cities. The author concluded that:

- Vegetation: Peanut has been found to perform significantly better than Sedum;
- Substrate: A 5 cm layer of soil composed of completely decomposed granite amended with 20% fully mature compost and slow-release fertilizer was suitable for Peanut growth;
- Rockwool layer: The rockwool layer had the benefit of lightweight and exceptionally high-water storage capacity which can enhance water supply to plants.

In another study, Jim [98] evaluated green roofs of three vegetation types with different growth forms and biomass structure in comparison with a control plot in a field-based study in a humid, tropical environment. The findings showed that grass cooled the air more than groundcover and shrub indicated the key role played by biomass quantity and structural complexity in molding the passive cooling functions. Deng and Jim [99] established 94 voluntary vascular plant species from 26 families and 76 genera. They fall into three groups, namely dominant ruderal (herbaceous and sub-shrub) as a surrogate of early-stage local grassland ecosystem succession, arboreal (trees and shrubs), and hygrophilous herb. The results showed that local common ruderal plant species can be established and reproduced on a tropical extensive green roof.

2.3. Examples of products available in the international market

Table 3 shows the technologies provided by green roof enterprises in Italy. It should be noted that the selected companies are case studies and there are more and more into the market. Most of them have headquarters in Europe and they only send the materials in Northern Italy. Almost all these enterprises provide extensive and intensive green roofs. Concerning vehicular and sloped vegetative roof, some technical precautions need to be installed. In particular, the sloped one requires special pieces in order to avoid the slipping of the substrate during rains and the excess of water runoff.

The majority of existing buildings date back prior to the entry into force of the laws regulating building energy consumption. Green roof technologies could be used to reduce energy consumption and to increase sustainability in buildings. however, it is necessary to determine overloading in relation to different configurations and to compare it with the residual load bearing capacity of the building structures. To avoid an expensive structural upgrade, some companies developed lightweight systems to keep the weight below the load limit prescribed by law.

Table 3. Green roof technologies provided by enterprise case studies.

	Extensive	Intensive	Pedestrian Vehicular	PV	Sloped	Lightweight
Zinco	X	X	X	X		
Bauder	X	X			X	X
Daku	X	X				
Perlite	X	X				
Harpo	X	X				
Climagrun	X	X		X		
Optigrun			X	X	X	X

A brief description of the commercial technologies in Table 3 is provided:

- Extensive: They are lightweight and have a shallow build-up height. Suitable plants include various Sedum species, herbs and some grasses. After the establishment of the vegetation, the maintenance is limited to one or two inspections a year.
- Intensive: They are usually multifunctional and accessible. They require more weight and a deeper system build-up. The maintenance is regular and depends on the landscape design and the chosen plant material. Anything is possible from lawns, perennials, shrubs, trees, including other landscape options, such as ponds, pergolas and patios.
- Pedestrian/Vehicular: During the installation of the different build-up layers the waterproofing has to be protected from damage. It is possible to install a protection mat or a drainage layer which functions as a protective layer as well. Driveways on rooftops require both a stable construction and adequate load-

bearing capacity. Additionally, to the self-weight and imposed loads on driveways, horizontal forces and torsional movements may occur through acceleration, steering or breaking.

- Photovoltaic-green roof: The panels are covered with a prescribed amount of growing medium and the desired vegetation is then planted. The combined weight of the growing media and plants provides the ballast required by the solar energy system to deal with wind loads. Thanks to this ballast principle, roof membrane penetrations that would normally be necessary for anchoring standard solar energy systems are not required.
- Sloped: The plant selection has to be well adapted to the extreme conditions of steep pitched green roofs, where the solar radiation is the highest on the south facing roof side and the water runoff is much faster compared to a flat roof.
- Lightweight: It comprises mature sedum on 20 mm of extensive substrate and incorporating multifunctional water retention and filter layer. The system is suitable for both new build construction and retrofit refurbishment projects. In most instances an additional drainage layer is not required though on roofs up to 2° or in areas of high rainfall, its inclusion may be necessary.

The combination of green roofs with photovoltaic (PV) panels is a new tendency in the building sector because it provides synergistic benefits, such as the panel is cooled by the presence of the vegetation, and thus produces more electricity, while the solar panel enhances growing conditions for vegetation, and increases abiotic heterogeneity, resulting in higher plant diversity. In the Mediterranean area, where the annual average solar radiation and air temperature are high, several studies explored the possibility to combine the energy generation with extensive green roofs that are not walkable. Lamnatou and Chemisana [100] carried out a critical review about multiple factors which are related to PV-green roofing systems. These studies revealed that plant/PV interaction resulted in PV output increase depending on parameters, such as plant species, climatic conditions, evapotranspiration, albedo, etc. The same authors in another study [101] focused on the experimental evaluation of Photovoltaic (PV) – green roofs under Mediterranean climate summer conditions, demonstrating the benefits of this technology and filling the gap which existed in the literature in terms of the experimental evaluation of PV-green systems. The results obtained for a sunny, five-day time period revealed an average increase of the maximum power output of the PVs (ranging from 1.29% to 3.33% depending on the plant), verifying the positive synergy between the PVs and the plants. Schindler et al. [102] concluded that in a Mediterranean climate it would be appropriate to examine the use of irrigation in green roofs with PV panels, including effects on the plant community and on electricity production.

Table 4 compares materials and product used in green roof technology available into the international market.

Table 4. Materials and product available in the international market.

Anti-root membrane							
Parameters	N. 1	N. 2					
Thickness (mm)	1.1	0.36					
Surface mass (g/m^2)	1130	310					
Breaking strength (N/5cm)	80	20-47					
Breaking expansion (%)	>20	>400					
Drainage layer							
Parameters	N. 1	N. 2	N. 3	N. 4	N. 5	N. 6	N. 7
Height (mm)	45	19	25	40	60	75	25
Surface mass (kg/m^2)	2.0	19	1.7	2.0	2.2	1.0	5.0
Resistance (kN/m^2)	138	400	200	170-250	40-533	55	460
Water storage (l/m^2)	17	-	3.0	6.0	13	3.0	-
Runoff 1% slope (l/(s×m))	-	0.34	0.59	1.5	1.1	1.54	1.0
Runoff 2% slope (l/(s×m))	-	0.47	0.85	2.1	1.6	2.21	1.5
Runoff 3% slope (l/(s×m))	-	0.57	1.05	2.6	2.0	-	1.9
Filter layer							
Parameters	N. 1	N. 2	N. 3	N. 4	N. 5	N. 6	N. 7
Thickness (mm)	7.0	17-20	5.0	6.0	0.6	1.7	1.0
Surface mass (g/m^2)	650	1500	470	850	100	>300	>150
Water storage (l/m^2)	7.0	12	5.0	4.0	-	-	-
Breakthrough force (N)	-	2300	>2000	>3500	1100	4300	2250
Substrate							
Parameters	N. 1	N. 2	N. 3	N. 4	N. 5		
Dry Volumetric weight (g/l)	1000	1000	950	1000	1120		
Saturated Volumetric weight (g/l)	1500	1500	1400	1400	1400		
Maximum water capacity (%)	50	50	45	40	28		
Permeability (mm/min)	0.3-30	0.3-30	0.3-30	0.6-70	60-400		
pH ($CaCl_2$)	6.5-8.0	6.5-8.0	6.5-8.0	6.5-8.0	7.0-8.5		
Saline content (g/l)	<2	<2	<2.5	<2.5	<2.5		
Organic matter (g/l)	<90	<90	<90	<65	<40		
Compacting factor	1.3	1.25	1.25	1.2	1.12		

2.4. Irrigation systems in Mediterranean climate

The performance of a green roof is also measured in relation to the amount of irrigation it needs. In the southern European countries with Mediterranean climate, compared to those of northern Europe with continental climate where such coverage is experiencing a wide diffusion, it is necessary to install the irrigation system. Green roofs are generally seen as a desirable building element, providing numerous benefits where water availability does not restrict their implementation. However, most Mediterranean locations have long, dry summers, requiring irrigation to sustain vegetation throughout extended dry periods.

Numerous variables intervene in the availability of water for the vegetation survival, such as the average annual rainfall, the distribution of rains, the trend of daytime and nocturnal temperatures and the relative humidity of the air. It is necessary to make a strong irrigation in the initial period to allow the growth vegetation. After that, irrigation should be considerably decreased according to the type of green roof. The Rain Irrigation System is the oldest, simulating the rainfall through high-pressure water sprayers. This system is suitable for both large and small green roofs. A part of the water supplied evaporates, due to wind and heat, before it reaches the ground and the root apparatus. The Micro-irrigation System is more modern and based on providing small amounts of water with high frequency, near the plant roots. The driers located at the base of the stem allow the capillary distribution of water. This system reduces water losses, due to wind and evaporation.

Azeñas et al. [103] quantified the effect of irrigation water volume on the thermal capacity of a green roof system in a Mediterranean area. The modules with the 25% of potential evapotranspiration applied as limited irrigation reported lower heat flux values than the well-irrigated module (considered as 50% of potential evapotranspiration) in all seasons. Schweitzer and Erell [104] demonstrated that the water requirements of the plant species tested ranged from 2.6 to 9.0 L/m^2 per day. *Aptenia cordifolia* was the most efficient in its use of water, providing the highest cooling benefit per unit water required for irrigation. The authors concluded that it was hard to justify green roofs in such environments on the basis of their contribution to building energy conservation, although other benefits may nevertheless make them attractive.

2.5. Recycled materials for green roof layers

In recent years, the volume of recycled products has increased. Finding alternative uses for these materials in the construction sector represents one of the major challenges for the industries working in this sector. Therefore, it is always desirable to utilize local waste material for substrates, which can make the establishment of a green roof inexpensive.

Several studies have evaluated the performance of alternative recycled materials for substrates, in reducing the embodied energy required to construct a green roof and divert waste from landfills. Table 5 shows that crushed brick and construction waste are the most-used recycled material as an inorganic component in green roof substrates. Importantly, Chen et al. [105] tested a normal cultivated substrate with recycled glass. Recycled glass is a lightweight and porous material which improves pollutant absorption and water quality purification. This substrate performed well in the neutralization of acid rain, but did not significantly reduce the levels of other pollutants. The results showed that materials like recycled glass generally have higher performance than natural ones and have the advantage of increasing sustainability by recycling waste materials.

Table 5. Recycled materials in the green roof substrate.

Authors	Reference	Recycled material used	Main findings
Bisceglie et al.	[106]	Waste of granular Autoclaved Aerated Concrete	The pH value of the water extract was of 7.23; the organic matter was less than 4.08; the apparent density was 459.2 kg/m^2; the demand for high water retention capacity was completely satisfied by the value of 222.62% of the mass of water absorbed relative to the mass of the dry sample.
Chen et al.	[105]	Recycled glass	It performed well in the neutralization of acid rain, but did not significantly reduce the levels of other pollutants.
Matlock and Rowe	[107]	Crushed porcelain and foamed glass	Substrate volumetric moisture content was generally greater in shale than in foamed glass or porcelain.
Eksi and Rowe	[108]	Crushed porcelain and foamed glass	Total plant coverage in both porcelain and foamed glass was equivalent to expanded shale on five of the six dates measured over two growing seasons. Substrate moisture and temperature were observed during the second season. The moisture content of both the porcelain and foamed glass was either equivalent to or greater than that of the expanded shale throughout the season. Subsurface temperatures were cooler in the porcelain and foamed glass than the expanded shale during the daytime for the majority of the second season. Variation in daily temperatures in the porcelain was significantly lower than the expanded shale when plant coverage was below 50%.
Molineux et al.	[109]	Inert construction waste material	Some of the alternative substrates are comparable to the widely used crushed red brick aggregate (predominantly found in commercial green roof growing substrate) for supporting plant establishment. For some materials, such as clay pellets, there was increased plant coverage and a higher number of plant species than in any other substrate.

Bates et al.	[110]	Crushed brick, crushed demolition aggregate, and solid municipal waste incinerator ash aggregate	Treatments with a high proportion of crushed brick in the growth substrate supported richer assemblages, with more species able to seed, and a smaller amount of Sedum acre.
Mickovski et al.	[111]	Inert construction waste material	The substrate mix containing recycled construction waste materials was adequate in supporting plant growth, was resistant to erosion and slippage and capable of providing good drainage.
Molineux et al.	[112]	Clay and sewage sludge, paper ash, and carbonated limestone	Particle density and loose bulk density results have shown all substrates to be classed as lightweight aggregates and leaching analysis has confirmed that all substrates perform within legal leachate limits for drinking water.
Farias et al.	[113]	Sieved waste	The new aggregate had low bulk density and increased water absorption and porosity. The thermographic camera results provided evidence that new aggregates had significant insulating properties and were suitable for use on green roofs.

Only a few studies have assessed the performance of recycled materials used in the drainage layer of green roofs, mainly focusing on the performance and advantages of recycled rubber crumbs from tires in the drainage layer. A research group [114–116] at the University of Lleida (Spain) built three identical house-like cubicles, located in Puigverd de Lleida, where the only difference was the roof construction system. These researchers evaluated the energy consumption and thermal behavior of green roofs. The reference-case roof consisted of a conventional flat roof with thermal insulation while, in the other two cubicles, the insulation layer was replaced by a 9 cm deep layer of recycled rubber crumbs and pozzolana, respectively, as drainage layer materials of an extensive green roof. Both the cubicles showed less energy consumption (16.7% and 2.2%, respectively) than the reference case during warm periods, whereas they presented a higher energy consumption (6.1% and 11.1%, respectively), during heating periods. Furthermore, the insulating properties of rubber crumbs were tested and compared with the material performance of stone. A reduction of indoor temperatures between 2–5 °C during the summer and early autumn was found. Then, the hydrologic performance of the recycled rubber granules was studied and compared with that offered by stone materials. No significant differences were found in the hydraulic conductivity when pozzolana was replaced with rubber crumbs, especially when small and half-particulate sizes were used. Finally, a life cycle assessment (LCA) was applied to compare the environmental impact. Extensive green roof with recycled rubber had a significantly lower environmental impact, compared to the non-insulated conventional roof (7% reduction) and compared to the other vegetative roof, with pozzolana drainage layer (6.7% reduction), and had a similar environmental impact than a conventionally insulated roof (2% increase).

2.6. Discussion

In this section a comparison on the cited literature is performed, as suggested by Besir and Cuce [117]. Most of the previous studies focused on both selecting suitable substrate and vegetation. As concern the substrate, previous studies were classified into two big groups, depending on whether the aim was at analyzing the performance or the composition. Relating to substrate mixture, Eksi et al. [57] suggested that the addition of 60 or 80% compost resulted in the greatest plant growth and fruit yields. On the other hand, some studies suggested that the existence of organic material in the substrate was a cause of pollutants in the green roof runoff. In addition, organic components, such as coco-peat, were demonstrated to improve, by 5.2 times, their initial weight in the highest water content. The German guidelines FLL [21] for green roofs indicate that the substrate should include only 4–8% and 6–12% organic matter by volume for extensive and intensive green roofs, respectively. In countries where vegetative roof technologies are not commercially available, customers may use locally accessible materials for this assembly, such as garden soil and composts. However, normal garden soil is not suitable, being made by skilled gardeners more experienced in traditional gardens than in green roofs. Specific weaknesses related to the use of garden soil are poor water and nutrient retention, increased weight, and local wildflower growth. Furthermore, the use of 100% local mixtures should also be prevented, as this reduces support of the vegetation, encourages the development of unwarranted weeds, raises roof weight during rainfall events, and endangers the endurance of the entire roof. Therefore, the growth medium should be appropriately engineered to accomplish the advantages of green roofs and the features suitable for an ideal growth substrate.

Sedums were considered among the best plant species for use on extensive green roof types [71]. Contrary to the conventional logic that plants with high transpiration rates are superior, the authors established that, during the summer months, the Sedum species outperformed the herbaceous ones [74]. However, as Sedum species are not available in numerous areas of the world, investigations were also focused on testing further plant species suitable for green roofs and numerous studies have recommended the use of various kind of vegetation for increasing the efficiency of green roofs [75,76].

Several studies have been conducted on the temperature regime of green roofs compared to traditional roofs to prove that vegetative roofs protect the roof membrane from extreme temperature fluctuations [80–82]. Their results confirmed that green roof protected the roof membrane from high temperature fluctuations.

Among the layers analyzed, the drainage layer plays a fundamental role, because it ensures an optimal balance between air and water content in green roofs and creates the conditions for vegetation growth by storing water, allowing excess water runoff, and ensuring aeration of the substrate and root system. While several authors proposed and evaluated the performance of substrate using recycled materials (see Table 5), only a few studies considered innovative solutions (mainly rubber crumb [114–116]) for the drainage layer.

Because a green roof is a load on the roof structure, it is important to keep the weight below the load limit prescribed by law, i.e., 200 kg/m^2 (about 1.96 kN/m^2) is the load that can be applied on the flat roofs of residential buildings according to the European standard [118]. In a previous study [119], the authors compared the weights of three different granular drainage materials. Perlite and expanded clay represent commercial drainage solutions, while rubber crumb is an innovative solution in the green roof market. among the drainage materials investigated, rubber crumbs had the highest density values, as well as the highest values of thermal conductivity. Therefore, the main advantage of choosing rubber crumbs derives from their recycled origin.

2.7. Conclusions

This review thesis chapter analyzed the roles, requirements, performance, and materials of the layers of a green roof: The waterproof and anti-root membranes; the protection, filter, and drainage layers; the substrate; and the vegetation. In an engineered system, the role played by each component is well-defined and the optimal selection of each component depends on geographic location, in order to get the best outcomes from the green roof. A change in any of the mentioned components could alter its efficiency.

Future research on green technology should consider the peculiarities and availability of the materials in the area where the green roof is installed, replicating the same configuration in locations characterized by different climatic conditions can negate the positive effects of a green roof. These materials should come from the recycling of local agricultural waste to reduce costs and to improve performance and sustainability. Physical characteristics, such as thermal conductivity and inertia, maximum and minimum densities, specific gravity, hydraulic conductivity, and void index, of these recycled materials should be assessed. Finally, a life cycle analysis should be carried out to analyze the environmental impacts of these materials, also considering the recycling process.

References

[1] B.D. Solomon, K. Krishna, The coming sustainable energy transition: History, strategies, and outlook, Energy Policy. 39 (2011) 7422–7431. doi:10.1016/j.enpol.2011.09.009.

[2] M. Antrop, Landscape change and the urbanization process in Europe, Landsc. Urban Plan. 67 (2004) 9–26. doi:10.1016/S0169-2046(03)00026-4.

[3] Y. Dutil, D. Rousse, G. Quesada, Sustainable buildings: An ever evolving target, Sustain. 3 (2011) 443–464. doi:10.3390/su3020443.

[4] M. De Fino, A. Scioti, E. Cantatore, F. Fatiguso, Methodological framework for assessment of energy behavior of historic towns in Mediterranean climate, Energy Build. 144 (2017) 87–103. doi:10.1016/j.enbuild.2017.03.029.

[5] S. Cascone, G. Sciuto, Recovery and reuse of abandoned buildings for student housing: A case study in Catania, Italy, Front. Archit. Res. 7 (2018) 510–520. doi:10.1016/j.foar.2018.08.004.

[6] P. de Berardinis, M. Rotilio, L. Capannolo, Energy and sustainable strategies in the renovation of existing buildings: An Italian Case Study, Sustain. 9 (2017). doi:10.3390/su9081472.

[7] A. Ferrante, G. Mochi, G. Predari, L. Badini, A. Fotopoulou, R. Gulli, G. Semprini, A European project for safer and energy efficient buildings: Pro-GET-onE (proactive synergy of integrated efficient technologies on buildings' envelopes), Sustain. 10 (2018). doi:10.3390/su10030812.

[8] E. Quagliarini, A. Gianangeli, M. D'Orazio, B. Gregorini, A. Osimani, L. Aquilanti, F. Clementi, Effect of temperature and relative humidity on algae biofouling on different fired brick surfaces, Constr. Build. Mater. 199 (2019) 396–405. doi:10.1016/j.conbuildmat.2018.12.023.

[9] E. Di Giuseppe, M. D'Orazio, Assessment of the effectiveness of cool and green roofs for the mitigation of the Heat Island effect and for the improvement of thermal comfort in Nearly Zero Energy Building, Archit. Sci. Rev. 58 (2015) 134–143. doi:10.1080/00038628.2014.966050.

[10] S. Cascone, A. Gagliano, T. Poli, G. Sciuto, Thermal performance assessment of extensive green roofs investigating realistic vegetation-substrate configurations, Build. Simul. 12 (2019) 379–393. doi:10.1007/s12273-018-0488-y.

[11] J.C. Berndtsson, Green roof performance towards management of runoff water quantity and quality: A review, Ecol. Eng. 36 (2010) 351–360. doi:10.1016/j.ecoleng.2009.12.014.

[12] M. Akther, J. He, A. Chu, J. Huang, B. Van Duin, A Review of Green Roof Applications for Managing Urban Stormwater in Different Climatic Zones, Sustain. 10 (2018). doi:10.3390/su10082864.

[13] H.F. Castleton, V. Stovin, S.B.M. Beck, J.B. Davison, Green roofs; building energy savings and the potential for retrofit, Energy Build. 42 (2010) 1582–1591. doi:10.1016/j.enbuild.2010.05.004.

[14] O. Saadatian, K. Sopian, E. Salleh, C.H. Lim, S. Riffat, E. Saadatian, A. Toudeshki, M.Y. Sulaiman, A review of energy aspects of green roofs, Renew. Sustain. Energy Rev. 23 (2013) 155–168. doi:10.1016/j.rser.2013.02.022.

[15] U. Berardi, A. Ghaffarianhoseini, A. Ghaffarianhoseini, State-of-the-art analysis of the environmental benefits of green roofs, Appl. Energy. 115 (2014) 411–428. doi:10.1016/j.apenergy.2013.10.047.

[16] S. Sadat, G. Hashemi, H. Bin, M. Aqeel, Performance of green roofs with respect to water quality and reduction of energy consumption in tropics : A review, Renew. Sustain. Energy Rev. 52 (2015) 669–679. doi:10.1016/j.rser.2015.07.163.

[17] M. Sha, R. Kim, M. Ra, Green roof benefits , opportunities and challenges – A review, Renew. Sustain. Energy Rev. 90 (2018) 757–773. doi:10.1016/j.rser.2018.04.006.

[18] S. Cascone, J. Coma, A. Gagliano, G. Pérez, The evapotranspiration process in green roofs : A review, Build. Environ. 147 (2019) 337–355. doi:10.1016/j.buildenv.2018.10.024.

[19] K. Vijayaraghavan, Green roofs : A critical review on the role of components , bene fi ts , limitations and trends, Renew. Sustain. Energy Rev. 57 (2016) 740–752. doi:10.1016/j.rser.2015.12.119.
[20] B. Dvorak, A. Volder, Landscape and Urban Planning Green roof vegetation for North American ecoregions : A literature review, Landsc. Urban Plan. 96 (2010) 197–213. doi:10.1016/j.landurbplan.2010.04.009.
[21] Guidelines for the Planning, Construction and Maintenance of Green Roofs, (2018). https://shop.fll.de/de/english-publications/green-roof-guidelines-2018-download.html.
[22] UNI 11235 - Istruzioni per la progettazione, l'esecuzione, il controllo e la manutenzione di coperture a verde (Criteria for design, execution, testing and maintenance of roof garden), (2015).
[23] D. Pearlmutter, S. Rosenfeld, Performance analysis of a simple roof cooling system with irrigated soil and two shading alternatives, Energy Build. 40 (2008) 855–864. doi:10.1016/j.enbuild.2007.06.004.
[24] N.S.G. Williams, J.P. Rayner, K.J. Raynor, Green roofs for a wide brown land: Opportunities and barriers for rooftop greening in Australia, Urban For. Urban Green. 9 (2010) 245–251. doi:10.1016/j.ufug.2010.01.005.
[25] A.M. Coutts, E. Daly, J. Beringer, N.J. Tapper, Assessing practical measures to reduce urban heat: Green and cool roofs, Build. Environ. 70 (2013) 266–276. doi:10.1016/j.buildenv.2013.08.021.
[26] T. Eisenman, Raising the bar on green roof design, Landsc. Archit. 96 (2006) 22–29.
[27] E. Oberndorfer, J. Lundholm, B. Bass, R.R. Coffman, H. Doshi, N. Dunnett, S. Gaffin, M. Köhler, K.K.Y. Liu, B. Rowe, Green Roofs as Urban Ecosystems: Ecological Structures, Functions, and Services, Bioscience. 57 (2007) 823–833. doi:10.1641/B571005.
[28] M. Manso, J. Castro-Gomes, Green wall systems: A review of their characteristics, Renew. Sustain. Energy Rev. 41 (2015) 863–871. doi:10.1016/j.rser.2014.07.203.
[29] White Paper, (2015).
[30] M. Santamouris, Cooling the cities - A review of reflective and green roof mitigation technologies to fight heat island and improve comfort in urban environments, Sol. Energy. 103 (2014) 682–703. doi:10.1016/j.solener.2012.07.003.
[31] J.C. Berndtsson, L. Bengtsson, K. Jinno, Runoff water quality from intensive and extensive vegetated roofs, Ecol. Eng. 35 (2009) 369–380. doi:10.1016/j.ecoleng.2008.09.020.
[32] H. Luo, N. Wang, J. Chen, X. Ye, Y. Sun, Study on the Thermal Effects and Air Quality Improvement of Green Roof, Sustain. 7 (2015) 2804–2817. doi:10.3390/su7032804.
[33] T. Van Renterghem, D. Botteldooren, Reducing the acoustical facade load from road traffic with green roofs, Build. Environ. 44 (2009) 1081–1087. doi:10.1016/j.buildenv.2008.07.013.
[34] A. Mahmoud, M. Asif, M. Hassanain, M. Babsail, M. Sanni-Anibire, Energy and Economic Evaluation of Green Roofs for Residential Buildings in Hot-Humid Climates, Buildings. 7 (2017) 30. doi:10.3390/buildings7020030.
[35] B.G. Gregoire, J.C. Clausen, Effect of a modular extensive green roof on stormwater runoff and water quality, Ecol. Eng. 37 (2011) 963–969. doi:10.1016/j.ecoleng.2011.02.004.
[36] T. Van Renterghem, Green roofs for acoustic insulation and noise reduction, in: Nat. Based Strateg. Urban Build. Sustain., Elsevier, Amsterdam, The Netherlands, 2018: pp. 167–179. doi:10.1016/B978-0-12-812150-4.00016-1.
[37] C. Fabiani, J. Coma, A.L. Pisello, G. Perez, F. Cotana, L.F. Cabeza, Thermo-acoustic performance of green roof substrates in dynamic hygrothermal conditions, Energy Build. 178 (2018) 140–153. doi:10.1016/j.enbuild.2018.08.024.
[38] P. Bevilacqua, D. Mazzeo, N. Arcuri, Thermal inertia assessment of an experimental extensive green roof in summer conditions, Build. Environ. 131 (2018) 264–276. doi:10.1016/j.buildenv.2017.11.033.

[39] P. Bevilacqua, D. Mazzeo, R. Bruno, N. Arcuri, Surface temperature analysis of an extensive green roof for the mitigation of urban heat island in southern mediterranean climate, Energy Build. 150 (2017) 318–327. doi:10.1016/j.enbuild.2017.05.081.

[40] L.L.H. Peng, C.Y. Jim, Seasonal and diurnal thermal performance of a subtropical extensive green roof: The impacts of background weather parameters, Sustain. 7 (2015) 11098–11113. doi:10.3390/su70811098.

[41] F. Olivieri, C. Di Perna, M. D'Orazio, L. Olivieri, J. Neila, Experimental measurements and numerical model for the summer performance assessment of extensive green roofs in a Mediterranean coastal climate, Energy Build. 63 (2013) 1–14. doi:10.1016/j.enbuild.2013.03.054.

[42] M. D'Orazio, C. Di Perna, E. Di Giuseppe, Green roof yearly performance: A case study in a highly insulated building under temperate climate, Energy Build. 55 (2012) 439–451. doi:10.1016/j.enbuild.2012.09.009.

[43] N. Tassicker, P. Rahnamayiezekavat, M. Sutrisna, An Insight into the Commercial Viability of Green Roofs in Australia, Sustain. 8 (2016). doi:10.3390/su8070603.

[44] L.L.H. Peng, C.Y. Jim, Green-roof effects on neighborhood microclimate and human thermal sensation, Energies. 6 (2013) 598–618. doi:10.3390/en6020598.

[45] X. Zhang, L. Shen, V.W.Y. Tam, W.W.Y. Lee, Barriers to implement extensive green roof systems: A Hong Kong study, Renew. Sustain. Energy Rev. 16 (2012) 314–319. doi:10.1016/j.rser.2011.07.157.

[46] D.B. Rowe, Green roofs as a means of pollution abatement, Environ. Pollut. 159 (2011) 2100–2110. doi:10.1016/j.envpol.2010.10.029.

[47] L. Kosareo, R. Ries, Comparative environmental life cycle assessment of green roofs, Build. Environ. 42 (2007) 2606–2613. doi:10.1016/j.buildenv.2006.06.019.

[48] J.S. MacIvor, L. Margolis, C.L. Puncher, B.J. Carver Matthews, Decoupling factors affecting plant diversity and cover on extensive green roofs, J. Environ. Manage. 130 (2013) 297–305. doi:10.1016/j.jenvman.2013.09.014.

[49] J. Coma, G. Pérez, C. Solé, A. Castell, L.F. Cabeza, Thermal assessment of extensive green roofs as passive tool for energy savings in buildings, Renew. Energy. 85 (2016) 1106–1115. doi:10.1016/j.renene.2015.07.074.

[50] L. Jiang, M. Tang, Thermal analysis of extensive green roofs combined with night ventilation for space cooling, Energy Build. 156 (2017) 238–249. doi:10.1016/j.enbuild.2017.09.080.

[51] S. Wilkinson, R.C. Feitosa, Retrofitting housing with lightweight green roof technology in Sydney, Australia, and Rio de Janeiro, Brazil, Sustain. 7 (2015) 1081–1098. doi:10.3390/su7011081.

[52] I. Schultz, D.J. Sailor, O. Starry, Effects of substrate depth and precipitation characteristics on stormwater retention by two green roofs in Portland OR, J. Hydrol. Reg. Stud. 18 (2018) 110–118. doi:10.1016/j.ejrh.2018.06.008.

[53] C. Farrell, X.Q. Ang, J.P. Rayner, Water-retention additives increase plant available water in green roof substrates, Ecol. Eng. 52 (2013) 112–118. doi:10.1016/j.ecoleng.2012.12.098.

[54] K. Vijayaraghavan, U.M. Joshi, Application of seaweed as substrate additive in green roofs: Enhancement of water retention and sorption capacity, Landsc. Urban Plan. 143 (2015) 25–32. doi:10.1016/j.landurbplan.2015.06.006.

[55] A. Talebi, S. Bagg, B.E. Sleep, D.M. O'Carroll, Water retention performance of green roof technology: A comparison of canadian climates, Ecol. Eng. 126 (2019) 1–15. doi:10.1016/j.ecoleng.2018.10.006.

[56] J. Coma, A. de Gracia, M. Chàfer, G. Pérez, L.F. Cabeza, Thermal characterization of different substrates under dried conditions for extensive green roofs, Energy Build. 144 (2017) 175–180. doi:10.1016/j.enbuild.2017.03.031.

[57] M. Eksi, D.B. Rowe, R. Fernández-ca, B.M. Cregg, Effect of substrate compost percentage on green roof vegetable production, Urban For. Urban Green. 14 (2015) 315–322. doi:10.1016/j.ufug.2015.03.006.

[58] C.T.N. Cao, C. Farrell, P.E. Kristiansen, J.P. Rayner, Biochar makes green roof

substrates lighter and improves water supply to plants, Ecol. Eng. 71 (2014) 368–374. doi:10.1016/j.ecoleng.2014.06.017.
[59] I. Ziogou, A. Michopoulos, V. Voulgari, T. Zachariadis, Energy, environmental and economic assessment of electricity savings from the operation of green roofs in urban office buildings of a warm Mediterranean region, J. Clean. Prod. 168 (2017) 346–356. doi:10.1016/j.jclepro.2017.08.217.
[60] K. Vijayaraghavan, U.M. Joshi, R. Balasubramanian, A field study to evaluate runoff quality from green roofs, Water Res. 46 (2012) 1337–1345. doi:10.1016/j.watres.2011.12.050.
[61] R. Baraldi, L. Neri, F. Costa, O. Facini, F. Rapparini, G. Carriero, Ecophysiological and micromorphological characterization of green roof vegetation for urban mitigation, Urban For. Urban Green. 37 (2019) 24–32. doi:10.1016/j.ufug.2018.03.002.
[62] A.F. Speak, J.J. Rothwell, S.J. Lindley, C.L. Smith, Urban particulate pollution reduction by four species of green roof vegetation in a UK city, Atmos. Environ. 61 (2012) 283–293. doi:10.1016/j.atmosenv.2012.07.043.
[63] T. Savi, S. Andri, A. Nardini, Impact of different green roof layering on plant water status and drought survival, Ecol. Eng. 57 (2013) 188–196. doi:10.1016/j.ecoleng.2013.04.048.
[64] A. Vasl, H. Shalom, G.J. Kadas, L. Blaustein, Sedum — Annual plant interactions on green roofs : Facilitation , competition and exclusion, Ecol. Eng. 108 (2017) 318–329. doi:10.1016/j.ecoleng.2017.07.034.
[65] B.Y. Schindler, L. Blaustein, A. Vasl, G.J. Kadas, M. Seifan, Cooling effect of Sedum sediforme and annual plants on green roofs in a Mediterranean climate, Urban For. Urban Green. 38 (2019) 392–396. doi:10.1016/j.ufug.2019.01.020.
[66] P.A. Nektarios, N. Ntoulas, E. Nydrioti, I. Kokkinou, E. Bali, I. Amountzias, Drought stress response of Sedum sediforme grown in extensive green roof systems with different substrate types and depths, Sci. Hortic. (Amsterdam). 181 (2015) 52–61. doi:10.1016/j.scienta.2014.10.047.
[67] O. Starry, J.D. Lea-cox, J. Kim, M.W. Van Iersel, Photosynthesis and water use by two Sedum species in green roof substrate, Environ. Exp. Bot. 107 (2014) 105–112. doi:10.1016/j.envexpbot.2014.05.014.
[68] E.L. Villarreal, L. Bengtsson, Response of a Sedum green-roof to individual rain events, Ecol. Eng. 25 (2005) 1–7. doi:10.1016/j.ecoleng.2004.11.008.
[69] C. Butler, C.M. Orians, Sedum cools soil and can improve neighboring plant performance during water deficit on a green roof, Ecol. Eng. 37 (2011) 1796–1803. doi:10.1016/j.ecoleng.2011.06.025.
[70] S. Moritani, T. Yamamoto, H. Andry, M. Inoue, K. Kato, H. Saito, Effect of combined water and salinity stress factors on evapotranspiration of Sedum kamtschaticum Fischer in relation to green roof irrigation, Urban For. Urban Green. 12 (2013) 338–343. doi:10.1016/j.ufug.2013.04.005.
[71] J. Lu, J. Yuan, J. Yang, A. Chen, Z. Yang, Effect of substrate depth on initial growth and drought tolerance of Sedum lineare in extensive green roof system, Ecol. Eng. 74 (2015) 408–414. doi:10.1016/j.ecoleng.2014.11.018.
[72] J. Lu, J. Yuan, J. Yang, Z. Yang, Responses of morphology and drought tolerance of Sedum lineare to watering regime in green roof system : A root perspective, Urban For. Urban Green. 13 (2014) 682–688. doi:10.1016/j.ufug.2014.08.003.
[73] A. Nagase, N. Dunnett, Drought tolerance in different vegetation types for extensive green roofs: Effects of watering and diversity, Landsc. Urban Plan. 97 (2010) 318–327. doi:10.1016/j.landurbplan.2010.07.005.
[74] M. Eksi, D.B. Rowe, I.S. Wichman, J.A. Andresen, Effect of substrate depth , vegetation type , and season on green roof thermal properties, Energy Build. 145 (2017) 174–187. doi:10.1016/j.enbuild.2017.04.017.
[75] T. Blanusa, M.M. Vaz Monteiro, F. Fantozzi, E. Vysini, Y. Li, R.W.F. Cameron, Alternatives to Sedum on green roofs: Can broad leaf perennial plants offer better “cooling service”?, Build. Environ. 59 (2013) 99–106.

doi:10.1016/j.buildenv.2012.08.011.
[76] R. Gioannini, M. Al-Ajlouni, R. Kile, D. VanLeeuwen, R.. Hilaire, Plant Communities Suitable for Green Roofs in Arid Regions, Sustain. 10 (2018). doi:10.3390/su10061755.
[77] A. Heim, J. Lundholm, Species interactions in green roof vegetation suggest complementary planting mixtures, Landsc. Urban Plan. 130 (2014) 125–133. doi:10.1016/j.landurbplan.2014.07.007.
[78] C. Van Mechelen, K. Van Meerbeek, T. Dutoit, M. Hermy, Functional diversity as a framework for novel ecosystem design : The example of extensive green roofs, Landsc. Urban Plan. 136 (2015) 165–173. doi:10.1016/j.landurbplan.2014.11.022.
[79] M. Vaz Monteiro, T. Blanuša, A. Verhoef, M. Richardson, P. Hadley, R.W.F. Cameron, Functional green roofs: Importance of plant choice in maximising summertime environmental cooling and substrate insulation potential, Energy Build. 141 (2017) 56–68. doi:10.1016/j.enbuild.2017.02.011.
[80] M. El Bachawati, R. Manneh, R. Belarbi, H. El Zakhem, Real-time temperature monitoring for Traditional gravel ballasted and Extensive green roofs: A Lebanese case study, Energy Build. 133 (2016) 197–205. doi:10.1016/j.enbuild.2016.09.056.
[81] S.M. dos Santos, J.F.F. Silva, G.C. dos Santos, P.M.T. de Macedo, S. Gavazza, Integrating conventional and green roofs for mitigating thermal discomfort and water scarcity in urban areas, J. Clean. Prod. 219 (2019) 639–648. doi:10.1016/j.jclepro.2019.01.068.
[82] T. Theodosiou, D. Aravantinos, K. Tsikaloudaki, Thermal behaviour of a green vs. a conventional roof under Mediterranean climate conditions, Int. J. Sustain. Energy. 33 (2014) 227–241. doi:10.1080/14786451.2013.772616.
[83] L. Galbrun, L. Scerri, Sound insulation of lightweight extensive green roofs, Build. Environ. 116 (2017) 130–139. doi:10.1016/j.buildenv.2017.02.008.
[84] T. Van Renterghem, D. Botteldooren, In-situ measurements of sound propagating over extensive green roofs, Build. Environ. 46 (2011) 729–738. doi:10.1016/j.buildenv.2010.10.006.
[85] J. Sproul, M. Pun, B.H. Mandel, A.H. Rosenfeld, Economic comparison of white , green , and black flat roofs in the United States, Energy Build. 71 (2014) 20–27. doi:10.1016/j.enbuild.2013.11.058.
[86] M. Kottek, J. Grieser, C. Beck, B. Rudolf, F. Rubel, World Map of the Köppen-Geiger climate classification updated, Meteorol. Zeitschrift. 15 (2006) 259–263. doi:doi:10.1127/0941-2948/2006/0130.
[87] M.C. Peel, B.L. Finlayson, T.A. Mcmahon, Updated world map of the Koppen-Geiger climate classification, Hydrol. Earth Syst. Sci. 4 (2007) 439–473.
[88] J. Chenot, E. Gaget, C. Moinardeau, R. Jaunatre, E. Buisson, T. Dutoit, Substrate composition and depth affect soil moisture behavior and plant-soil relationship on Mediterranean extensive green roofs, Water (Switzerland). 9 (2017) 1–16. doi:10.3390/w9110817.
[89] C.M. Monteiro, C.S.C. Calheiros, J.P. Martins, F.M. Costa, P. Palha, S. de Freitas, N.M.M. Ramos, P.M.L. Castro, Substrate influence on aromatic plant growth in extensive green roofs in a Mediterranean climate, Urban Ecosyst. 20 (2017) 1347–1357. doi:10.1007/s11252-017-0687-9.
[90] C.M. Monteiro, C.S.C. Calheiros, P. Palha, P.M.L. Castro, Growing substrates for aromatic plant species in green roofs and water runoff quality: Pilot experiments in a Mediterranean climate, Water Sci. Technol. 76 (2017) 1081–1089. doi:10.2166/wst.2017.276.
[91] S. Ondoño, J.J. Martínez-Sánchez, J.L. Moreno, Evaluating the growth of several Mediterranean endemic species in artificial substrates: Are these species suitable for their future use in green roofs?, Ecol. Eng. 81 (2015) 405–417. doi:10.1016/j.ecoleng.2015.04.079.
[92] S. Ondoño, J.J. Martínez-Sánchez, J.L. Moreno, The inorganic component of green roof substrates impacts the growth of Mediterranean plant species as well as the C and

N sequestration potential, Ecol. Indic. 61 (2015) 739–752. doi:10.1016/j.ecolind.2015.10.025.
[93] F. Raimondo, P. Trifilò, M.A. Lo Gullo, S. Andri, T. Savi, A. Nardini, Plant performance on Mediterranean green roofs: Interaction of species-specific hydraulic strategies and substrate water relations, AoB Plants. 7 (2015). doi:10.1093/aobpla/plv007.
[94] T. Savi, D. Boldrin, M. Marin, V.L. Love, S. Andri, M. Tretiach, A. Nardini, Does shallow substrate improve water status of plants growing on green roofs? Testing the paradox in two sub-Mediterranean shrubs, Ecol. Eng. 84 (2015) 292–300. doi:10.1016/j.ecoleng.2015.09.036.
[95] C. Van Mechelen, T. Dutoit, J. Kattge, M. Hermy, Plant trait analysis delivers an extensive list of potential green roof species for Mediterranean France, Ecol. Eng. 67 (2014) 48–59. doi:10.1016/j.ecoleng.2014.03.043.
[96] G. Caneva, A. Kumbaric, V. Savo, R. Casalini, Ecological approach in selecting extensive green roof plants: A data-set of Mediterranean plants, Plant Biosyst. 149 (2015) 374–383. doi:10.1080/11263504.2013.819819.
[97] C.Y. Jim, Assessing climate-adaptation effect of extensive tropical green roofs in cities, Landsc. Urban Plan. 138 (2015) 54–70. doi:10.1016/j.landurbplan.2015.02.014.
[98] C.Y. Jim, Effect of vegetation biomass structure on thermal performance of tropical green roof, Landsc. Ecol. Eng. 8 (2012) 173–187. doi:10.1007/s11355-011-0161-4.
[99] H. Deng, C.Y. Jim, Spontaneous plant colonization and bird visits of tropical extensive green roof, Urban Ecosyst. 20 (2017) 337–352. doi:10.1007/s11252-016-0596-3.
[100] C. Lamnatou, D. Chemisana, A critical analysis of factors affecting photovoltaic-green roof performance, Renew. Sustain. Energy Rev. 43 (2015) 264–280. doi:10.1016/j.rser.2014.11.048.
[101] D. Chemisana, C. Lamnatou, Photovoltaic-green roofs: An experimental evaluation of system performance, Appl. Energy. 119 (2014) 246–256. doi:10.1016/j.apenergy.2013.12.027.
[102] B.Y. Schindler, L. Blaustein, R. Lotan, H. Shalom, G.J. Kadas, M. Seifan, Green roof and photovoltaic panel integration: Effects on plant and arthropod diversity and electricity production, J. Environ. Manage. 225 (2018) 288–299. doi:10.1016/j.jenvman.2018.08.017.
[103] V. Azeñas, J. Cuxart, R. Picos, H. Medrano, G. Simó, A. López-grifol, J. Gulías, Thermal regulation capacity of a green roof system in the mediterranean region : The effects of vegetation and irrigation level, Energy Build. 164 (2018) 226–238. doi:10.1016/j.enbuild.2018.01.010.
[104] O. Schweitzer, E. Erell, Evaluation of the energy performance and irrigation requirements of extensive green roofs in a water-scarce Mediterranean climate, Energy Build. 68 (2014) 25–32. doi:10.1016/j.enbuild.2013.09.012.
[105] C.F. Chen, S.F. Kang, J.H. Lin, Effects of recycled glass and different substrate materials on the leachate quality and plant growth of green roofs, Ecol. Eng. 112 (2018) 10–20. doi:10.1016/j.ecoleng.2017.12.013.
[106] F. Bisceglie, E. Gigante, M. Bergonzoni, Utilization of waste Autoclaved Aerated Concrete as lighting material in the structure of a green roof, Constr. Build. Mater. 69 (2014) 351–361. doi:10.1016/j.conbuildmat.2014.07.083.
[107] M. Eksi, D.B. Rowe, Green roof substrates: Effect of recycled crushed porcelain and foamed glass on plant growth and water retention, Urban For. Urban Green. 20 (2016) 81–88. doi:10.1016/j.ufug.2016.08.008.
[108] J.M. Matlock, D.B. Rowe, The suitability of crushed porcelain and foamed glass as alternatives to heat-expanded shale in green roof substrates: An assessment of plant growth, substrate moisture, and thermal regulation, Ecol. Eng. 94 (2016) 244–254. doi:10.1016/j.ecoleng.2016.05.044.
[109] C.J. Molineux, A.C. Gange, S.P. Connop, D.J. Newport, Using recycled aggregates in green roof substrates for plant diversity, Ecol. Eng. 82 (2015) 596–604. doi:10.1016/j.ecoleng.2015.05.036.

[110] A.J. Bates, J.P. Sadler, R.B. Greswell, R. Mackay, Effects of recycled aggregate growth substrate on green roof vegetation development: A six year experiment, Landsc. Urban Plan. 135 (2015) 22–31. doi:10.1016/j.landurbplan.2014.11.010.
[111] S.B. Mickovski, K. Buss, B.M. McKenzie, B. Sökmener, Laboratory study on the potential use of recycled inert construction waste material in the substrate mix for extensive green roofs, Ecol. Eng. 61 (2013) 706–714. doi:10.1016/j.ecoleng.2013.02.015.
[112] C.J. Molineux, C.H. Fentiman, A.C. Gange, Characterising alternative recycled waste materials for use as green roof growing media in the U.K., Ecol. Eng. 35 (2009) 1507–1513. doi:10.1016/j.ecoleng.2009.06.010.
[113] R.D. Farias, C. Martinez Garcia, T. Palomino Cotes, M. Martinez Arellano, Effects of Wastes from the Brewing Industry in Lightweight Aggregates Manufactured with Clay for Green Roofs, Materials (Basel). 10 (2017). doi:10.3390/ma10050527.
[114] G. Pérez, A. Vila, L. Rincón, C. Solé, L.F. Cabeza, Use of rubber crumbs as drainage layer in green roofs as potential energy improvement material, Build. Environ. 97 (2012) 347–354. doi:10.1016/j.apenergy.2011.11.051.
[115] J. Coma, G. Pérez, A. Castell, C. Solé, L.F. Cabeza, Green roofs as passive system for energy savings in buildings during the cooling period: use of rubber crumbs as drainage layer, Energy Effic. 7 (2014) 841–849. doi:10.1007/s12053-014-9262-x.
[116] L. Rincón, J. Coma, G. Pérez, A. Castell, D. Boer, L.F. Cabeza, Environmental performance of recycled rubber as drainage layer in extensive green roofs. A comparative Life Cycle Assessment, Build. Environ. 74 (2014) 22–30. doi:10.1016/j.buildenv.2014.01.001.
[117] A.B. Besir, E. Cuce, Green roofs and facades: A comprehensive review, Renew. Sustain. Energy Rev. 82 (2018) 915–939. doi:10.1016/j.rser.2017.09.106.
[118] P. De Berardinis, C. Bartolomucci, L. Capannolo, M. De Vita, E. Laurini, C. Marchionni, Instruments for Assessing Historical Built Environments in Emergency Contexts: Non-Destructive Techniques for Sustainable Recovery, Buildings. 8 (2018) 27. doi:10.3390/buildings8020027.
[119] S. Cascone, F. Catania, A. Gagliano, G. Sciuto, A comprehensive study on green roof performance for retrofitting existing buildings, Build. Environ. 136 (2018) 227–239. doi:10.1016/j.buildenv.2018.03.052.

3. Thermal performance assessment of extensive green roofs investigating realistic vegetation-substrate configurations

3.1. Introduction

Many previous studies have evaluated reductions in energy consumption for building conditioning through the installation of green roofs by using EnergyPlus simulation software, which integrates a green roof model. However, most of these studies, did not characterize vegetation and substrates using data derived from an experimental survey, without specifying the plant species and substrate composition used in extensive green roof model. Therefore, the energy performance evaluated through the simulations are not referred to as an effective vegetation-substrate configuration. The importance of developing a precise account of vegetation and soil parameters, to assess green roof effects on the building's thermal and energy performance was highlighted by Peri et al. [1].

Table 1 and Table 2 show the input parameters used in previous studies for green roof vegetation and substrate, respectively.

Zhou et al. [2] proposed a method to integrate a seasonally variable LAI equation into a green roof model based on an improved Dickinson's equation. After verification with measured data, this equation had a more accurate temperature setting for calculating seasonally variable LAI, the average error and average relative error were improved from 0.34 to 0.09 and 39.3 to 7.1%, respectively. Sedum linear was applied to the EcoRoof model in EnergyPlus, while no information was provided by authors on the substrate composition used. It was also assumed that the maximum LAI was 5 and minimum LAI was 0. Yuan and Rim [3] investigated cooling energy savings associated with exterior greenery systems for the US Department of Energy (DOE) standard reference buildings. Results showed that latent heat transfer due to plant transpiration can dominate heat transfer through the exterior greenery systems. The plant and substrate properties were based on previous studies without specifying the vegetation and substrate type applied to the model. Dahanayake and Chow [4] explored the cooling load benefits of green roofs and green walls simultaneously for comparison. Results revealed that both green roofs and green walls can protect building envelop from reaching higher temperatures and of reducing cooling load. Common succulent plants were used with appropriate conditions in terms of plant height and substrate thickness for both green roofs and green walls. Morakinyo et al. [5] presented a parametric study on the effect of four green roof types on outdoor/indoor temperature and cooling demand. Results revealed an outdoor night-time warming effect of not more than 0.2 °C with semi-extensive green roof while the outdoor and indoor cooling effect ranged between 0.05–0.6 °C and 0.4–1.4 °C, respectively. Authors included in the simulations intensive green roof composed of 0.7 m soil thickness and extensive green roof composed of soil 0.3 m soil thickness, containing grass species. Vera et al. [6] performed a parametric analysis to evaluate the influence of the main green roof design parameters on the cooling and heating loads of a stand-alone retail building subjected to different climatic conditions. Four different leaf area index (LAI) levels (0.1, 1.0, 3.0, and 5.0) were studied, while substrate thermal properties were selected based on the ranges for dry (0.15–0.3 W/mK) and wet substrates (0.5–1.2 W/mK). The main result obtained by this study is that the higher the LAI, the greater the reduction in cooling loads due to the evapotranspiration of vegetation-substrate system and the canopy's shading effect. Boafo et al. [7] evaluated the evapotranspiration effect of an extensive green roof on annual energy consumption of an office building in relation to the humid continental climate of Republic of Korea. Due to the influence of the humid conditions on the evapotranspiration process, it was found that high leaf area index reduced cooling energy demand and somewhat reduced heating energy demand as well. No information was provided for vegetation and substrate used. Ziogou et al. [8] focussed both on energy conservation and sustainability related aspects of two alternative green roof solutions applied to a typical urban office building in representative climatic areas of Cyprus in the Eastern Mediterranean. The analysis showed a reduction in primary energy consumption up to 25% in heating and up to 20% in cooling operation, thanks to the use of green roofs, and a corresponding reduction in emissions. Differently from previous studies, the authors provided some suitable information on chosen vegetation coverings (Sedum sediforme and Helichrysum Orientale L.) and substrate (mixture of pumice (P), compost (C) and sand (S) in a proportion (%v/v) of 5P:1C:4S). However, most of the characteristics were not evaluated in laboratory set-up but reported in different previous studies. Silva et al. [9] quantified green roofs energy savings in Mediterranean climate with distinct heating and cooling seasons. The three green roof types lead to similar heating energy needs but extensive green roof solution showed higher cooling energy needs than semi-intensive and intensive ones, of 2.8 and 5.9 times more, respectively. Parameters "Height of plants" and "soil thickness" were measured on site. Leaf's reflectivity was chosen following the literature recommendations. All other vegetation and soil parameters were adopted from EnergyPlus standard values. Thermal conductivity, density and specific heat were defined for dry soil without indicating the values used. Chan and Chow [10] established an experimental setup of a green roof system on the rooftop of a commercial building for computer model validation. The findings showed that a combination of thicker soil layer, lower plant height and higher value of leaf area index (LAI) can provide a better thermal insulation effect in a green roof system. The authors only listed the physical properties of the soil filled on the green roof area and the planted vegetation.

In this study the thermophysical characteristics of extensive green roof materials were selected from previous research. Coma et al. [11] experimentally determined the physical properties of five different substrates of extensive green roofs commonly used in Mediterranean climates. The study revealed that the thermal conductivity of substrates is strongly related to their masses. Furthermore, substrates with lower organic content showed the highest rates of volumetric heat storage capacity and provided higher time lags. The authors concluded that when the aim is to evaluate the energy performance of extensive green roofs, it is not accurate to assume equal properties for different types of substrates or to consider them as a generic layer. Vaz Monteiro et al. [12] investigated the canopy properties of two succulent and four broad-leaved plant genotypes with contrasting plant traits, which were monitored alongside bare substrate, over two summers. Their results suggested that succulent plants were not the best suited to provide significant summertime environmental cooling or substrate insulation and that other types of plants are preferable where the delivery of such benefits is a priority.

Table 1. Input parameters used in previous studies for green roof vegetation

References	Green roof	Vegetation	Height of plants [m]	LAI [m^2/m^2]	Leaf reflectivity -	Leaf emissivity -	Stomatal resistance [s/m]
Zhou et al.	Extensive	Sedum linear	0.2	0.1 1.5 3.0 5.0	-	-	-
Yuan and Rim	Extensive	-	0.2	2.5	0.22	0.95	-
Dahanayake and Chow	Extensive	Succulent	0.3	3	0.2	0.9	-
Morakinyo et al.	Extensive Intensive	Grass	0.3 1.0	2	0.35	0.95	180
Vera et al.	Extensive	-	0.3	0.1 1.0 3.0 5.0	0.22	0.95	300
Boafo et al.	Extensive	-	0.05	1.0 2.0 5.0	0.22	0.95	80
Ziogou et al.	Extensive	Helichrysum. Sedum Sedif.	0.15 0.25	3.5 1.75	-	-	125 300
Silva et al.	Extensive Semi-	-	0.05 0.5 1.0	1.0 2.5 5.0	-	-	-

	intensive Intensive						
Chan and Chow	Extensive	-	0.035	2.2	0.29	-	-

Table 2. Input parameters used in previous studies for green roof substrate.

References	Green roof	Composition	Thickness [m]	Conductivity [W/mK]	Density [Kg/m^3]	Specific heat [J/kgK]
Zhou et al.	Extensive	-	0.1	0.35	1100	1200
Yuan and Rim	Extensive	-	0.1	0.35	1100	1200
Dahanayake and Chow	Extensive	-	0.1	0.4	-	-
Morakinyo et al.	Extensive Intensive	-	0.3 0.7	0.9	1850	850
Vera et al.	Extensive	Heavyweight Lightweight	0.15	0.85 0.280	1639 730	1800 1100
Boafo et al.	Extensive	-	0.08	0.4	641	1000
Ziogou et al.	Extensive	Pumice Compost Sand	0.75 0.15	0.2	1020	1093
Silva et al.	Extensive Semi-intensive Intensive	-	0.1 0.35 0.7	-	-	-
Chan and Chow	Extensive	-	0.2	0.25	1600	890

The proposed study aimed to identify among the 30 plant-substrate configurations which one optimized the energy performance of extensive green roofs in Mediterranean areas. This study provided a merit ranking based on three indexes to identify which extensive green roof packages offered the highest performance related to the urban heat island phenomenon, energy saving and temperature fluctuations on the waterproof membrane. This study, unlike many literature studies, characterizes vegetation and substrates using all the data derived from an experimental survey. Therefore, the simulations carried out are referred to as a realistic plant species and substrate types.

3.2. Materials and methods

The energy performance of each green roof package was calculated considering a simplified case study, commonly referred to as a test cell.

In particular, as the test cell (case study) chosen is rather simple to realize, it offers the opportunity to perform future experimental tests, which may allow to validate the simulation results.

In addition, it is necessary to highlight that such a “test cell” was already built and used in previous research presented in well-known references within the green roof literature.

The test cell allows for a comparison, in absolute values, of the results for different envelope solutions and a generalization of the results obtained. On the other hand, when choosing a real building as a case study, energy performance depends largely on the constructive characteristics of the building envelope, building occupancy, endogenous charges, the type of equipment, etc.

3.2.1. The test cell

To evaluate the thermal and energy performance of different types of extensive green roofs, a test cell used in previous studies was modeled in EnergyPlus [13,14] (Figure 1).

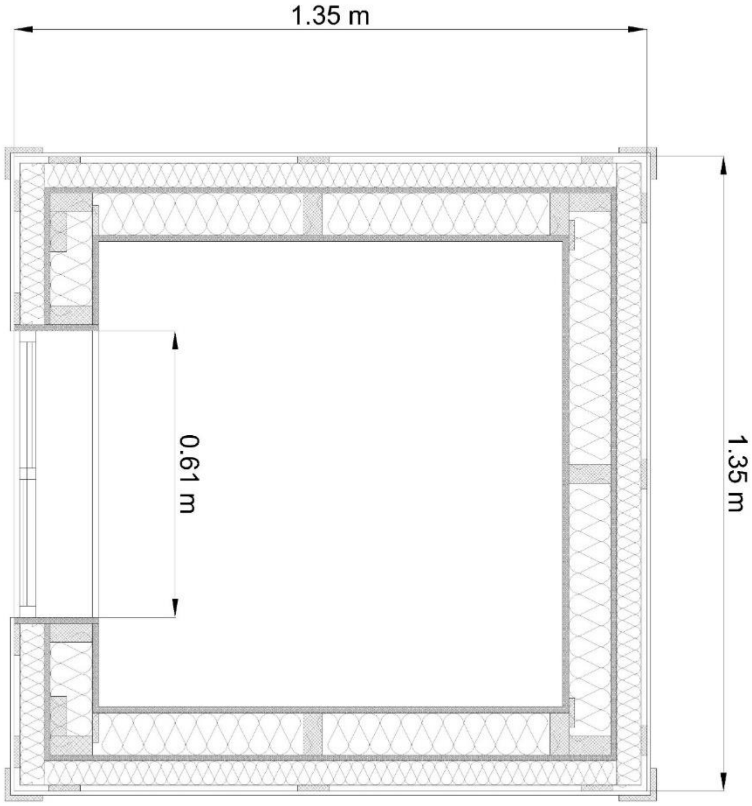

Figure 1. The test cell [13,14].

The test cell is 1.35×1.35×1.35 m, with one window in the south facing wall (610×610 mm and U-value of 1.960 W/m^{2}K). The walls and bare roof of the test cell are described in Table 3. The floor of the cell was composed of OSB boards and XPS insulation. The U-value of the test cell envelope is reported in Table 4.

Regarding the test cell used, I must note that although the U-value of the components of the building envelope is comparable to that of a standard building, due to its low volume (1.35×1.35×1.35 m), indoor temperatures may reach values significantly different from those of a real environment.

Table 3. Wall and Bare Roof section of test cell.

Wall							
	Drywall	Glass Wool	OSB	Vapor Barrier	XPS	Air Space	Plywood

s [mm]	10.0	89.0	11.0	0.50	51.0	13.0	5.0
λ [W/mK]	0.180	0.044	0.130	-	0.043	0.079	0.130
ρ [kg/m³]	950.0	12.0	650.0	-	35.0	1.23	560.0
Cp [J/kgK]	840.0	840.0	1700.0	-	1400.0	1000.0	2500.0
Bare Roof							
	Metal Sheet	Water Membrane	OSB	Air Space	XPS	Drywall	-
s [mm]	1.0	1.0	11.0	38.0	140.0	11.0	-
λ [W/mK]	44.000	0.210	0.130	0.233	0.0430	0.1800	-
ρ [kg/m³]	7824.0	1300.0	650.0	1.23	35.0	950.0	-
Cp [J/kgK]	500.0	1800.0	1700.0	1000.0	1400.0	840.0	-

Table 4. U-value of the test cell envelope.

	Wall	Window	Bare roof	Floor
U-value [W/m²K]	0.308	1.960	0.306	0.299

3.2.2. The plant species

The six plant species used as a vegetation layer in the extensive green roofs were modeled in EnergyPlus after defining the height of plants, leaf area index (LAI), leaf reflectivity, leaf emissivity and minimum stomatal resistance. The six species used (Figure 2) were selected due to their prevalence in the Mediterranean area. Moreover, they were chosen because all thermophysical parameters necessary for complete characterization through the simulation software were available for these species. The six species selected are suitable for extensive green roofs.

Table 5 shows the data used, which were obtained from a previous experimental study [12].

The following plants were used (with key leaf characteristics shown in parentheseses):

- *Heuchera ‘Obsidian’* (nonpubescent, purple)
- *Heuchera ‘Electra’* (nonpubescent, yellow)

- *Salvia officinalis 'Berggarten'* (pubescent with a gray-green hue)
- *Stachys byzantina* (pubescent with a pale gray hue)
- *Sempervivum 'Reinhard'* (nonpubescent, succulent, light to dark green hue)
- *Sedum mix* (nonpubescent, succulent leaves, light-green in color).

All plants used in the experiment were herbaceous/subshrub forms with the potential to be integrated into extensive green roofs, particularly if additional irrigation is provided during times of prolonged water deficit.

Figure 2. Photographs of plant canopies used in the experiment [12]. A. Heuchera 'Obsidian', B. Heuchera 'Electra', C. Salvia officinalis 'Berggarten', D. Stachys byzantina, E. Sempervivum 'Reinhard' and F. Sedum mix.

Table 5. Plant parameters utilized [12].

Plant species	Height of plants [m]	LAI [m^2/m^2]	Leaf reflectivity -	Leaf emissivity -	Stomatal resistance [$mmol/m^2s$]
Sedum mix*	0.125	2.80	0.180	0.97	105.0
Heuchera "Obsidian" Purple	0.250	5.00	0.200	0.97	170.0
Heuchera "Electra" Yellow	0.150	4.50	0.205	0.97	195.0

Stachys byzantina	0.375	4.25	0.195	0.97	255.0
Sempervivum "Reinhard"	0.050	3.25	0.155	0.97	105.0
Salvia officinalis "Berggarten"	0.475	5.00	0.220	0.97	300.0

* A mat of Sedum species used as an industry standard

3.2.3. The substrates

The parameters required for modeling substrates in EnergyPlus are thermal conductivity, density and specific heat, depending on the composition of the substrates. These data, shown in Table 6, were collected from a previous study [11]. The substrates selected were chosen using the same criteria reported for the plant species.

The composition of the substrates analyzed is also reported in Table 6. These commercial substrates are characterized by different material compositions. In particular, Substrate 1 is composed of compost, pozzolana and sand. Substrate 5 mainly consists of coco peat with a lower percentage of compost, crushed building waste and sand. Substrates 2 and 4 are characterized by homogeneous percentages of different materials. Due to their different compositions, the substrates analyzed vary in terms of thermal performance. Finally, the composition of Substrate 3 is characterized by a low percentage of compost. The substrate thickness used in the simulations was 15 cm, such that the roof could be classified as an extensive green roof.

Generally, the layers making up the green roof, from top to bottom, consist of vegetation, soil substrate, a filter, a drainage layer, and waterproof and antiroot membranes [15]. The drainage layer, filter and water storage felts were not included in the energy balance of the green roofs. This choice is based on the EnergyPlus limitations in considering the role of the drainage and filter layer and the reduced influence of these layers on the surface temperatures analyzed in this study.

Table 6. Substrate parameters utilized and composition *[11]*.

Sample	Coco peat	Compost	Crushed wastes	Sand	Pozzolana	Conductivity	Density	Specific heat
	%	%	%	%	%	[W/mK]	[Kg/m^3]	[J/kgK]
Substrate 1	0	40	0	20	40	0.2	873.2	788
Substrate 2	25	25	40	10	0	0.21	759.6	923
Substrate 3	N/A	6	N/A	N/A	N/A	0.284	772.7	1360
Substrate 4	25	40	30	5	0	0.288	748.4	546
Substrate 5	60	15	20	5	0	0.229	724.0	375

3.2.4. The simulation settings

Thermal building simulations were performed in EnergyPlus using the “Ecoroof” module, which allows one to define the outer layer of a building roof as a green roof, specifying various features including the height of plants, LAI, leaf reflectivity, thickness/density/thermal conductivity and specific heat of soil.

The simulations were developed using the features of the test cell previously described since it is located in the city of Catania (Lat. 37°30.3'N, Long. 15°05.2'E) in southern Italy. During summer, the air temperature reaches high values, with peaks of over 35 °C and air temperature fluctuations between the daily maximum and minimum reach values of over 15 °C. All the simulations were performed for a period of one typical year, from the 1st of January to the 31st of December. Moreover, for the climatic conditions typical of the Mediterranean area, it is necessary to guarantee a minimum period of daily green roof irrigation to allow the survival and proper growth of the vegetation. In fact, many Mediterranean countries are characterized by temperate climatic conditions with dry and hot summers, as defined by the Köppen Classification [16] “Csa.” Thus, in such areas, the reduction in the cooling energy needs of the building is one of the main issues faced by designers. Therefore, in this study, the irrigation period was set between 8 and 9 p.m., when the sun has set, to minimize the loss of water through evaporation and to reduce water consumption. A maximum saturation moisture content of 0.50, minimum residual moisture content of 0.01 and initial moisture content of 0.15 were held constant across the different types of substrate used.

The simulations were thus conducted under free running conditions to allow the air temperature inside the test cell to oscillate freely. The internal (below all the roof layers) and external (on the substrate, below the vegetation) surface temperatures of the test cell were obtained as results for each selected scenario.

The heating and cooling system was subsequently inserted into the test cell to assess the energy demand used for air conditioning. Temperature set point values were set to 20 °C for the heating period from the 1st of December to the 31st of March and to 26 °C for the cooling period from the 1st of June to the 30th of September. The same type of heating/cooling system was used throughout the simulations to analyze the energy performance only in relation to the type of extensive green roof used.

3.2.5. Indexes of performance

Indexes of performance as a function of external surface temperature were used based on the relevant works of Bevilacqua et al. [17] and Teemusk and Mander [18]. These indexes may be used to characterize the behaviors of green roofs in relation to the urban heat island phenomenon and energy savings. Moreover, these indexes have the advantage of being validated by high-precision experimental measurements of the surface temperatures of green roofs, allowing a direct comparison of different extensive green roof packages.

The first index, known as surface temperature reduction (STR), evaluates the reduction in surface temperatures of green roofs compared to bare roofs in terms of average daily temperatures. This index is defined as the ratio of the external surface temperature of a green roof to the external surface temperature of a bare roof. STR is evaluated in terms of average values (Eq. 1):

$$STR_{av} = \frac{T_{av}}{T_{av,bare}} \tag{1}$$

This index is representative of the sensible heat flow through the extensive green roof and, therefore, of the consumption of energy for heating and cooling.

The second index, the external temperature ratio (ETR), is defined as the ratio of the maximum external surface temperature of a green roof to the average temperature of surrounding air (Eq. 2):

$$ETR_{max} = \frac{T_{max}}{T_{av,air}} \tag{2}$$

This index represents the mitigation of the effect of the urban heat island due to the installation of the extensive green roof. Consequently, reduced ETR values correspond to greater reductions in the effect of the urban heat island.

The third index, temperature excursion reduction (TER), is representative of the fluctuation in the daily external surface temperature. This index is defined as the ratio of the temperature fluctuation of the green roof's external surface to the temperature fluctuation of the bare roof's external surface (Eq. 3):

$$TER = \frac{T_{max} - T_{min}}{T_{max,bare} - T_{min,bare}} \tag{3}$$

The fluctuation of surface temperatures (thermal stress) influences the durability of roof materials, in particular that of the watertight membrane. In fact, reductions in surface temperature fluctuations decrease the dilatation and contraction of materials and increase their useful life.

To compare the energy performance of the different plant-substrate green roof configurations, a ranking was developed summing the scores obtained for each of the abovementioned indexes, during both the heating and cooling periods. Specifically, the score of each of the 30 plant-substrate configurations was assigned based on the values of each index. Thus, the package with the lowest performance was given a score of 0, while the configuration with the highest performance was assigned a score equal to 30. The scores of the intermediate packages vary linearly between the maximum and minimum values, based on equations 4 and 5 for summer and winter conditions, respectively:

$$SCORE_{cooling,i} = 30 \times (1 - \frac{x_{max} - \mathrm{x_i}}{\mathrm{x_{max}} - \mathrm{x_{min}}}) \quad (4)$$

$$SCORE_{heating,i} = 30 \times \frac{x_{max} - \mathrm{x_i}}{\mathrm{x_{max}} - \mathrm{x_{min}}} \quad (5)$$

where x_{max} and x_{min} are the maximum and minimum values of the index considered (STR, ETR, and TER), while x_i is the value obtained from the i-th green roof package for the specific index considered. Moreover, considering the benefits of green roofs, the least important relative to energy savings and the mitigation of urban heat island effects is the reduction in temperature fluctuations of the waterproof membrane, and thus a maximum score of 6 points was assigned to the TER index for each extensive green roof package analyzed. Thus, the TER index was characterized by a weight of 0.20 in comparison with the other two indexes.

Overall, each green roof package (substrate and plants) is characterized by different levels of performance in terms of energy savings, urban heat island mitigation and roof material durability. Therefore, a comparison among different extensive green roof packages can be performed using a combination of the abovementioned performance indexes. Moreover, the analysis of each index provides information about specific energy performance. For example, it is possible to identify the extensive green roof package that optimizes urban heat island mitigation based on values obtained from the ETR index; in fact, the lower the roof surface temperatures are, the lower the overheating of the air in cities due to the buildings' roofs is.

To assess the influence of the different types of extensive green roofs examined on daily surface temperatures, representative days with the most severe climatic conditions were chosen, namely, the summer day with a maximum air temperature of approximately 34 °C (12^{th} of August) and a winter day with a minimum air temperature of approximately -2 °C (29^{th} of January).

While it is advisable during the summer to install plant species that reduce external surface temperatures to optimize energy performance, during the winter, it is preferable to use plant species that increase surface temperatures to maximize heat gains generated by direct solar radiation. In light of these considerations, during the summer period, the maximum score was found for the green roof package with the lowest index values, while the minimum score was given found for the green roof package characterized by the highest index values. The opposite criterion was used for the indexes assessing energy performance during the heating period. Therefore, for each index, the score assigned to each extensive green roof package depends on its ranking across the thirty configurations tested. This methodology made it possible to identify the plant-substrate configurations that optimized the energy performance of the green roof.

3.3. Results and discussion

3.3.1. Green roofs with different plant species

The first group of simulations was conducted maintaining constant thermophysical properties of the substrate and varying the plant species used.

3.3.1.1.Internal and external surface temperature

In particular, Figure 3 shows the results of the internal and external surface temperatures of the test cell during the summer reference day. These results show that, with regard to external surface temperatures, Sedum and Sempervivum increase temperatures the most, to over 40 °C, while Salvia reduces external surface temperatures to approximately 36 °C. Purple Heuchera, Stachys and yellow Heuchera exhibit intermediate behavior.

The internal surface temperatures, on the other hand, do not depend greatly on the different plant species that constitute the green roofs; in fact, as is shown in Figure 3, they overlap. This overlap is due to the particular technical and constructive features of the envelope, which are characterized by a high thermal insulation level and low thermal inertia, and to the reduced size of the indoor environment. Indeed, internal surface temperatures are more heavily affected by the thermophysical properties of the test cell envelope used and especially by the thickness of the thermal insulation. The maximum surface internal temperatures, approximately 36 °C, are reached at 4.00 p.m., with a delay of approximately three hours compared to the peak in external surface temperature. This time delay, generally termed “thermal lag”, does not vary across the different plant species analyzed. Moreover, no significant difference in the external surface temperatures of the different plant species was observed at night.

Figure 4 shows the results of the surface temperatures for the selected reference day during the heating period (29th of January). Compared to the results obtained on the summer day, the differences in the external surface temperature among the different plant species are less evident. Salvia is still the species with the lowest external surface temperatures, with a maximum of 9.5° C, while Sempervivum and Sedum increase temperatures, by approximately 11° C.

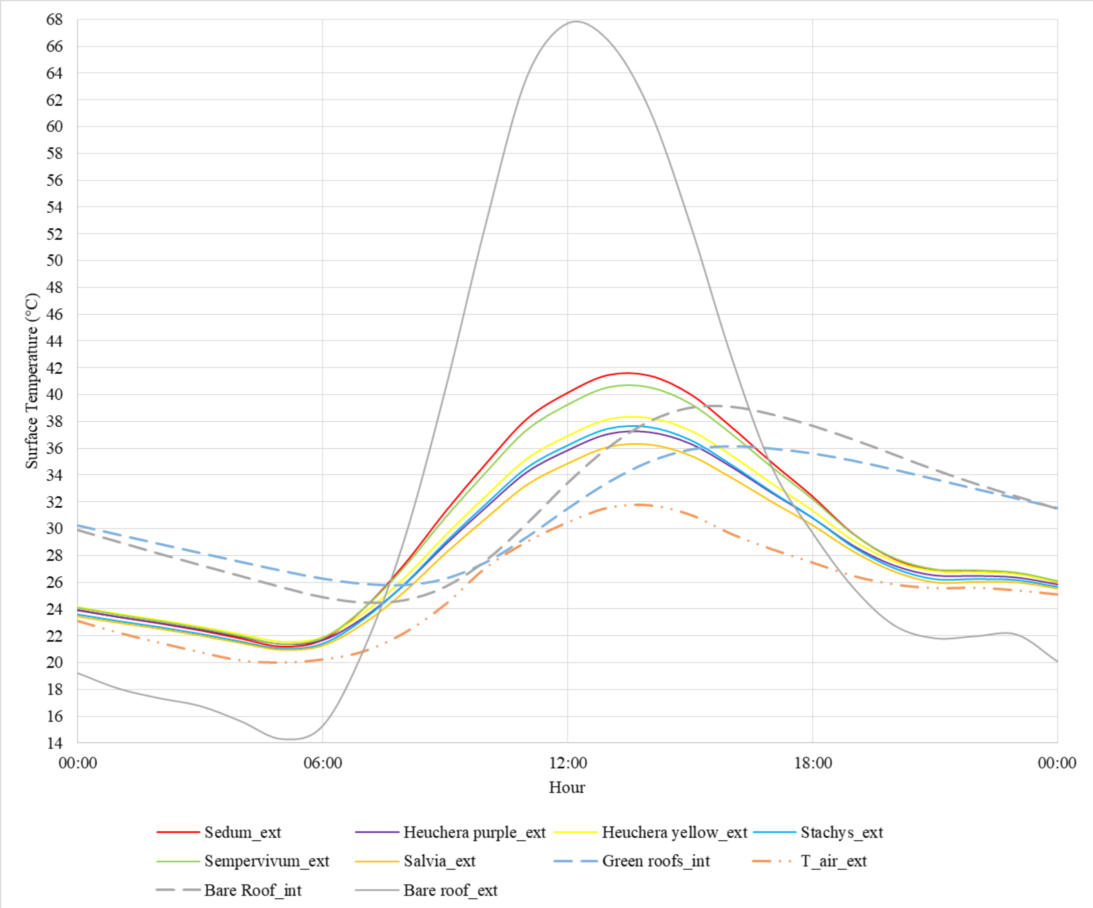

Figure 3. Internal and external surface temperatures of the test cell during the reference day in August

As a result, Salvia supports the lowest external surface temperatures, while Sedum and Sempervivum support the highest external surface temperatures. These results are in agreement with the experimental tests performed in [12], where the authors investigated whether certain plants cool summertime temperatures more than others during the day. In particular, the authors found that Salvia or Stachys supported the lowest external surface temperature, whereas Sempervivum presented the greatest differences in mean values across the monitoring period.

These results show that the major differences in terms of surface temperatures of the test cell are between Salvia and Sedum/Sempervivum. These differences are due to the specific features of the various plant species, as shown in Table 5. In particular, Salvia is the plant species with the highest values for height (0.475 m), LAI (5.00 m^2/m^2), leaf reflectivity (0.220) and minimum stomatal resistance (300 $mmol/m^2s$). Vice versa, Sedum and Sempervivum are the plants with the lowest values for these parameters

(0.125 and 0.050 m (height), 2.80 and 3.25 m^2/m^2 (LAI), 0.180 and 0.155 (leaf reflectivity), and 105.0 $mmol/m^2s$ (minimum stomatal resistance), respectively).

All of the green roof configurations examined permit a reduction in the external surface temperatures of over 40% compared to the bare roof, and all the minimum surface temperatures achieved by the green roof types are over 30% higher than those of the bare roof. In particular, Salvia reduces the maximum and minimum surface temperatures compared to the bare roof by 46.22% and 31.79%, respectively, and Sedum did so by 38.76% and 32.56%, respectively.

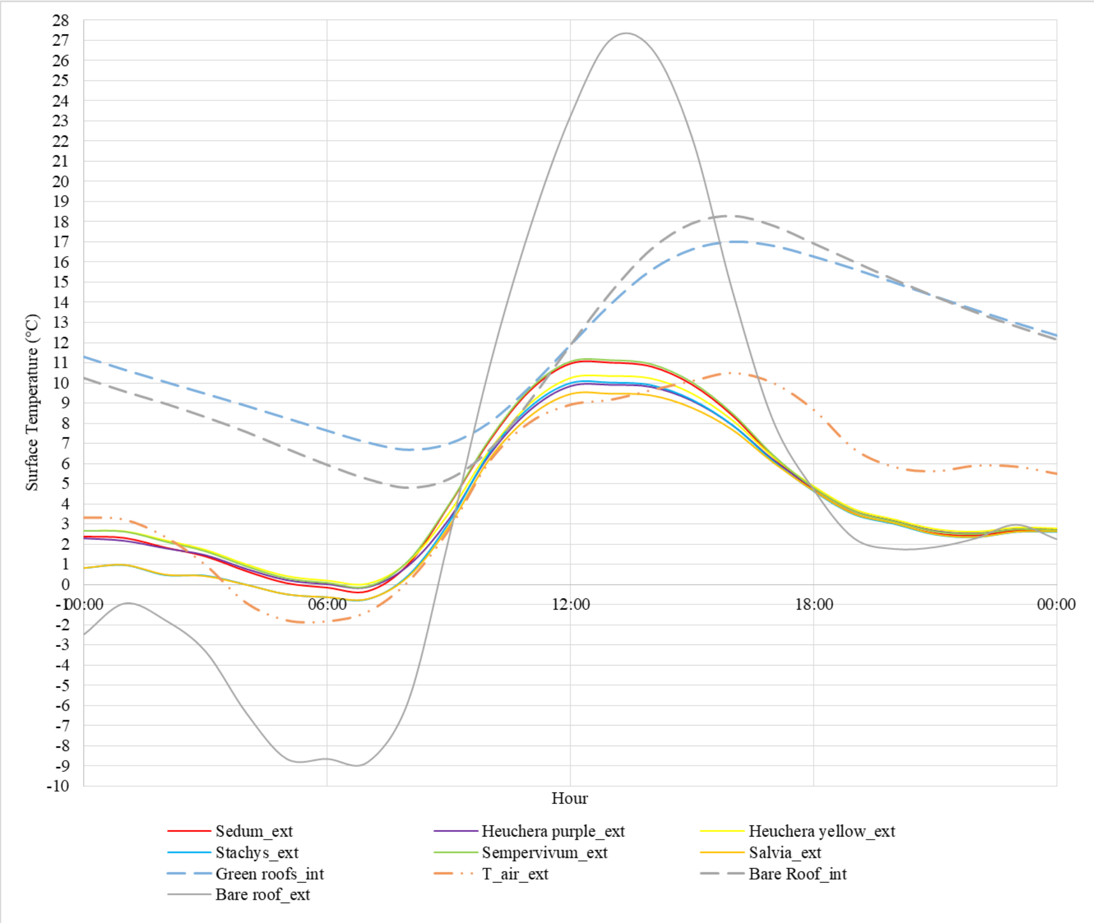

Figure 4. Internal and external surface temperatures of the test cell during the reference day in January.

Table 7 shows the variation in maximum and minimum external surface temperatures (maximum daily temperature minus minimum daily temperature) reached during the summer reference day for the different types of green roofs. The reduction in the percentage temperature fluctuations in comparison with the bare roof is also calculated. All the plant species were found to reduce temperature fluctuations between the minimum and maximum values by over 60%.

3.3.1.2. Annual energy consumption

Finally, Table 7 also shows the annual energy consumption of the bare roof and of the different types of green roofs and the annual energy savings of the various green roof types compared to the bare roof. The greater energy savings correspond to the lowest temperature fluctuations, as shown in Figure 3. Furthermore, based on summing the cooling and heating energy savings presented in Table 7, under Mediterranean climatic conditions, the highest energy savings are reached by choosing the vegetation with the highest energy performance during the summer, such as Salvia, and not the succulent plants (i.e., Sedum and Sempervivum), enhancing energy performance during the heating period.

In particular, in accordance with the findings for surface temperatures, Sedum reduces energy consumption during the winter by 8.41% compared to the bare roof, while Salvia maximizes energy savings during the summer by 23.53% compared to the bare roof.

The results show, both for surface temperatures and for energy savings, that for climatic conditions characteristic of the Mediterranean area, Salvia is the plant species with the highest energy performance, while Sedum and Sempervivum, which are widely used in northern European regions, are characterized by the lowest energy performance.

Table 7. Surface temperature comparison and annual energy consumption and saving of bare roof and green roof compared during summer and winter period.

Roof type	T_{ext_max}-T_{ext_min}	Δ	T_{ext_max}-T_{ext_min}	Δ	Cooling energy consumption	Cooling energy saving	Heating energy consumption	Heating energy saving
	[°C]	[%]	[°C]	[%]	[Wh/m^2]	[%]	[Wh/m^2]	[%]
Bare roof	53.42	-	35.87	-	43606	-	49860	-
Sedum	20.28	62.05	11.34	68.38	34603	20.65	45668	8.41
Purple Heuchera	15.81	70.4	10.04	72.02	33761	22.58	46214	7.31
Yellow Heuchera	16.69	68.75	10.3	71.27	34126	21.74	45991	7.76
Stachys	16.54	69.04	10.75	70.03	33621	22.9	46363	7.01
Sempervivum	19.16	64.14	11.23	68.7	34583	20.69	45674	8.4
Salvia	15.33	71.31	10.18	71.61	33345	23.53	46529	6.68

3.3.2. Performance evaluation

In this section of the study, the performances of 30 configurations of green roofs derived from combinations of the different plant species and substrates are evaluated.

3.3.2.1.STR, ETR and TER indexes

Figure 5 shows the STR_{av} index, while Figure 6 depicts the ETR_{max} index for the different plant species and substrates analyzed during the summer and winter reference days.

Since these indexes are a function of the external surface temperature, during the summer season, the lower their values are, the higher the energy performance of the plant-substrate configuration used is.

During the summer, all the types of green roofs achieve STR_{av} values lower than 1.0, signifying that both maximum and average external surface temperatures are lower than those of the bare roof. The values of STR_{av} range from 0.854 to 0.928. The values of ETR_{max}, on the other hand, are constantly higher than 1.0, ranging from 1.175 to 1.455; this denotes that all the plant-substrate configurations reach surface temperatures higher than the outside air temperature. Furthermore, the greater variability of the ETR_{max} shows that properly choosing the green roof package mainly can affect this index.

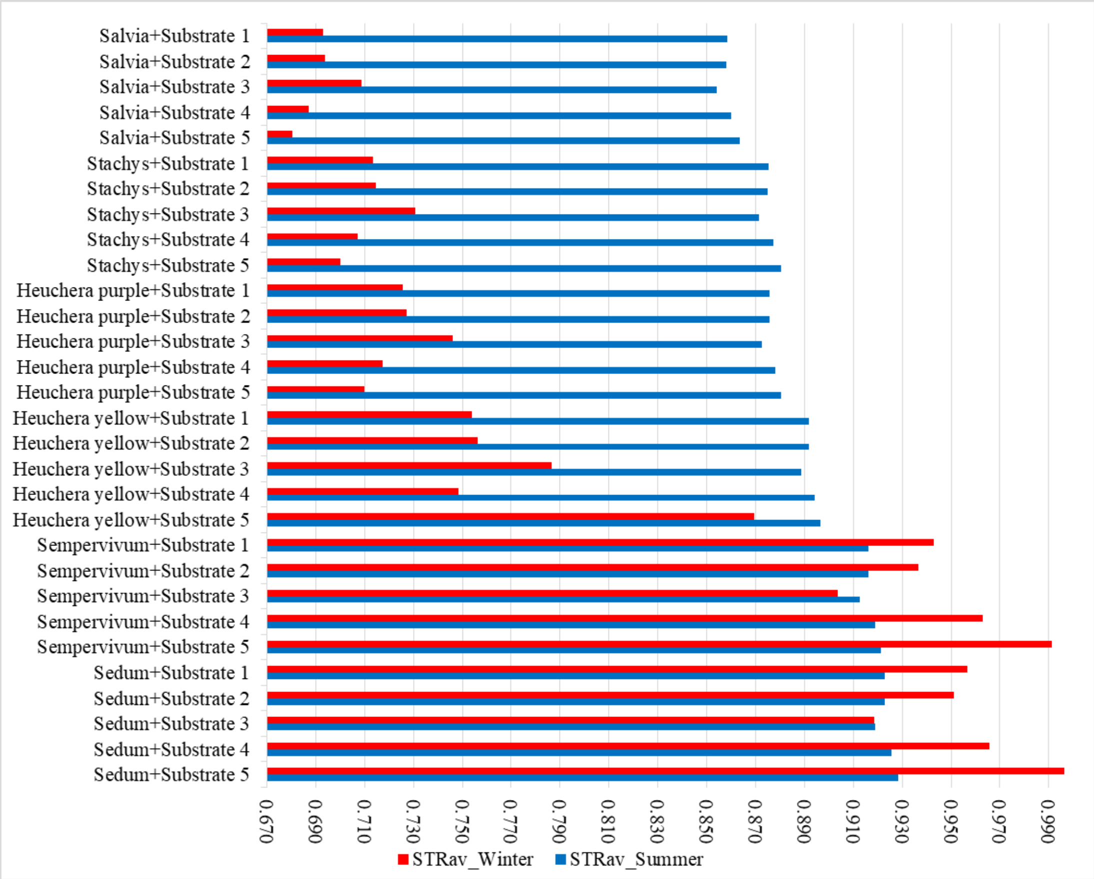

Figure 5. STR_{av} index in the summer and winter reference day for different green roof packages.

Regarding these two indexes, the green roof packages that use Salvia achieve the best performance during the summer (lowest index values), regardless of the type of substrate used. Stachys and purple Heuchera attain a slightly lower energy performance than Salvia. Among the different soil layers examined, the green roofs that include Substrate 3 perform the best (lowest index values). Furthermore, the use of yellow Heuchera with Substrate 5 offers better performance compared to the use of yellow Heuchera with the other substrate, during both the winter and summer. During the winter, Sedum and Sempervivum perform best when they are combined with Substrates 1, 2, 4 and 5 and not with Substrate 3 to enhance the cooling energy performance of all the green roof packages. These considerations highlight the importance of choosing an appropriate substrate during green roof design.

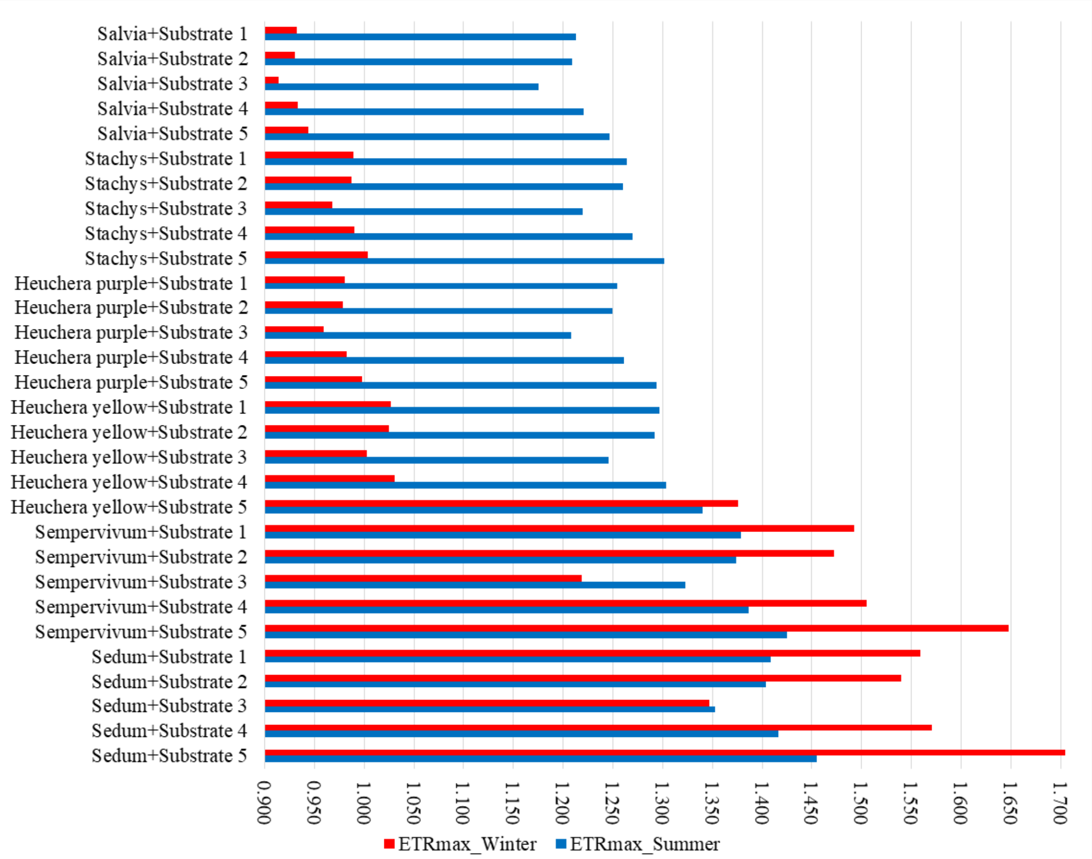

Figure 6. ETR_{max} index in the summer and winter reference day for the different green roof packages.

ETR_{max} depends more on the substrate type than on STR_{av}. Purple Heuchera and Stachys are characterized by a lower energy performance than Salvia during the summer; however, when used with Substrate 3, they achieve values of 1.208 and 1.219, respectively, for ETR_{max}, which are lower than those achieved by some configurations using Salvia as the plant species. Similarly, Sempervivum, which is generally characterized by a lower performance during the winter compared to Sedum, has a higher energy performance than Sedum when used with substrate 5, but not when Sedum is used with Substrate 5.

Unlike patterns observed for the summer period, during the winter, the higher the index values are, the higher the energy performance of the different plant-substrate configurations becomes. Even during the winter period, STR_{av} attains values lower than 1.0, signifying external surface temperatures lower than those of the bare roof. The plant-substrate configurations perform in a similar way for the winter season as they do for the summer season. Salvia was found to be the plant with the lowest index values, while Sedum achieved the highest index values, and thus, Sedum achieves better energy performance during the heating period. The different configurations exhibit significant variations in index values. In this way, the plant-substrate configuration that best optimizes the energy performance of the green roof during the winter season is found, i.e., Sedum and Sempervivum, regardless of the substrate type used.

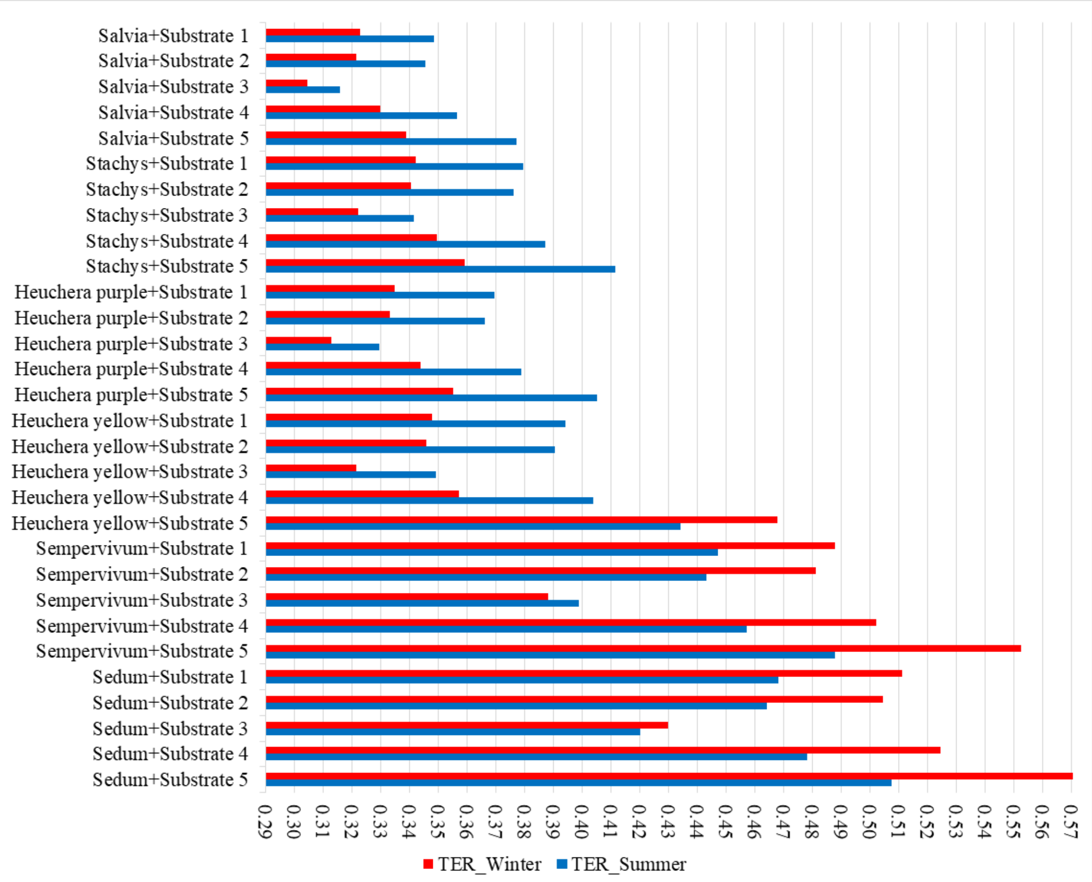

Figure 7. TER index in the summer and winter reference day for the different green roof packages.

Finally, in Figure 7, the TER index is shown for the summer and winter days. All the analyzed plant-substrate configurations decrease temperature fluctuations compared to the bare roof. In particular, during the summer cooling period, TER varies between 0.316 and 0.507, while during the winter period, it is between 0.304 and 0.571.
The conclusions drawn for the previous indexes also apply to the TER indexes. In particular, the TER values are affected by the substrate and vary in a fairly continuous way during the cooling period.

3.3.2.2.Comparison of index results with previous research

Bevilacqua et al. [17] used the previously defined indexes to provide a very concise description and comparison of the surface thermal behavior of the investigated green and traditional roofs. Therefore, a comparison of the results obtained was carried out.
In Bevilacqua et al. [17], STR_{av} varied between 0.72 and 0.92 and between 0.8 and 1.10 during the summer and winter periods, respectively. In the present study, this index varied from 0.85 to 0.93 during the summer and from 0.70 to 1.0 during the winter.
Bevilacqua et al. [17] found that ETR_{max} varied between 1.08 and 1.17 and between 1.0 and 2.40 during the summer and winter periods, respectively. In the present study, this index varied from 1.17 to 1.45 during the summer period and from 0.95 to 1.70 during the winter.
Finally, the TER index varied between 0.46 and 0.53 during the summer and between 0.43 and 0.61 during the winter in the previous study [17], while in this research, it varied from 0.33 to 0.51 and from 0.31 to 0.57.
As this comparison shows, the values of the different indexes obtained previously are close to those obtained by the previous study. However, the aforementioned indexes were evaluated at a monthly scale in Bevilacqua et al. [17], while in this study, the indexes are shown daily for the extreme climatic conditions during both summer and winter periods. Thus, the climatic conditions considered differ.

3.3.2.3.Ranking results

To compare the energy performance of the various plant-substrate configurations, a ranking was developed summing the scores obtained for each of the abovementioned indexes, during both the heating and cooling periods. The results are reported in Table 8. In particular, the plant-substrate configurations with the best energy performance are Sempervivum with Substrate 5 (69.62 points), Salvia with Substrate 3 (68.67 points) and yellow Heuchera with Substrate 5 (66.66 points).

Table 8. Results of the effect of the different plant-substrate configurations on the energy performance of green roofs

Legend	25-30 High Cooling		25-30 High Heating		20-25 Medium-high		15-20 Medium	
Green roof Package	STR_{av} Cooling	STR_{av} Heating	ETR_{max} Cooling	ETR_{max} Heating	TER Cooling	TER Heating	**Score**	**Rank**
Salvia + Substrate 1	28.23	1.19	25.91	0.70	4.97	0.41	**61.41**	**13**
Salvia + Substrate 2	28.40	1.27	26.32	0.64	5.07	0.38	**62.08**	**12**
Salvia + Substrate 3	30.00	2.67	30.00	0.00	6.00	0.00	**68.67**	**2**
Salvia + Substrate 4	27.65	0.61	25.11	0.72	4.72	0.57	**59.37**	**15**
Salvia + Substrate 5	26.29	0.00	22.31	1.15	4.08	0.77	**54.60**	**20**
Stachys + Substrate 1	21.40	3.12	20.46	2.85	4.00	0.85	**52.68**	**23**
Stachys + Substrate 2	21.55	3.22	20.91	2.78	4.10	0.82	**53.38**	**22**
Stachys + Substrate 3	23.12	4.78	25.23	2.06	5.19	0.40	**60.78**	**14**
Stachys + Substrate 4	20.68	2.52	19.82	2.88	3.76	1.02	**50.67**	**25**
Stachys + Substrate 5	19.34	1.85	16.45	3.39	3.00	1.24	**45.26**	**30**
Purple Heuchera + Substrate 1	21.24	4.29	21.53	2.54	4.31	0.69	**54.60**	**21**
Purple Heuchera + Substrate 2	21.35	4.42	21.99	2.45	4.42	0.65	**55.29**	**19**
Purple Heuchera + Substrate 3	22.65	6.23	26.40	1.71	5.57	0.19	**62.75**	**11**
Purple Heuchera + Substrate 4	20.34	3.51	20.72	2.59	4.02	0.89	**52.07**	**24**
Purple Heuchera + Substrate 5	19.34	2.78	17.28	3.19	3.20	1.15	**46.94**	**28**
Yellow Heuchera + Substrate 1	14.76	6.98	16.95	4.30	3.54	0.98	**47.51**	**27**
Yellow Heuchera + Substrate 2	14.86	7.19	17.46	4.23	3.66	0.93	**48.33**	**26**
Yellow Heuchera + Substrate 3	16.10	10.06	22.44	3.39	4.95	0.38	**57.32**	**18**
Yellow Heuchera + Substrate 4	13.77	6.45	16.20	4.42	3.24	1.19	**45.27**	**29**
Yellow Heuchera + Substrate 5	12.92	17.96	12.27	17.54	2.29	3.68	**66.66**	**3**
Sempervivum + Substrate 1	4.85	24.93	8.15	21.94	1.88	4.13	**65.89**	**6**
Sempervivum + Substrate 2	4.96	24.35	8.67	21.19	2.01	3.98	**65.16**	**7**
Sempervivum + Substrate 3	6.31	21.20	14.20	11.55	3.40	1.88	**58.53**	**17**
Sempervivum + Substrate 4	3.84	26.83	7.38	22.41	1.57	4.46	**66.49**	**4**
Sempervivum + Substrate 5	2.83	29.53	3.21	27.85	0.61	5.59	**69.62**	**1**
Sedum + Substrate 1	2.15	26.25	4.92	24.47	1.23	4.66	**63.69**	**8**
Sedum + Substrate 2	2.28	25.70	5.44	23.75	1.35	4.51	**63.04**	**10**
Sedum + Substrate 3	3.76	22.61	10.99	16.43	2.73	2.82	**59.34**	**16**
Sedum + Substrate 4	1.18	27.12	4.10	24.90	0.92	4.96	**63.19**	**9**
Sedum + Substrate 5	0.00	30.00	0.00	30.00	0.00	6.00	**66.00**	**5**

In addition, the data in Table 8 offer further useful information related to the ability of each package to perform better during the winter or summer period. With this aim, the cells in Table 8 are highlighted with different colors. Specifically, the packages performing better during the summer period are highlighted in blue, while the packages performing better during the winter period are colored in red. Packages with intermediate performance in both the winter and summer are highlighted in green, with a range of 24-20. The packages with acceptable performances are highlighted in orange, with a range of 19-15. As an example, if performance during the cooling period is emphasized, the plant species with the highest energy performance is Salvia, which does not have adequate thermophysical properties during the heating period. Furthermore, purple Heuchera and Stachys are characterized by medium-high performance during the cooling period. In contrast, Sempervivum and Sedum have the highest performance during the winter period. Finally, yellow Heuchera offers more balanced performance during both the heating and cooling periods.

It is interesting to highlight the role of the characteristics of the substrate on green roof energy performance. The prominence of the substrate is confirmed, given that the best configurations involve Substrate 5 when used with Sedum and Sempervivum and Substrate 3 when used with Salvia and yellow Heuchera. As a result, substrate and vegetation selection are strictly correlated. In addition, the same plant species used with different substrate types attains heterogeneous performances.

3.4. Implications and limitations

The present study made it possible to identify among the 30 plant-substrate configurations the one that optimized the energy performance of extensive green roofs in a Mediterranean climate.

Researchers and designers could apply the same methodology to evaluate the energy performance of green roofs under different climatic conditions and identify which green roof packages offer the highest performance. In fact, because climatic conditions affect the energy performance of green roofs, other substrate-plant combinations may enhance green roof performance under other climatic conditions, regardless of whether heating or cooling periods dominate. The indexes and methodology proposed for comparing the performances of different green roof packages have general validity; therefore, they can be applied to different climates.

Further analysis may be carried out to investigate the performance of additional substrate types and plant species, for which thermal and physical parameters determined through experimentation have to be used. Furthermore, future trials and simulation may use “innovative” materials in the extensive green roof packages, e.g., products derived from waste or recycling processes. In addition, future research should include the drainage and filter layers in simulations.

Although EnergyPlus is one of the most advanced energy simulation software using an advanced vegetation model, the results obtained may be affected by some imprecisions depending by the assumptions and simplifications of the model. Thus, the results of this study, even if they are based on realistic values of plant and substrate characteristics, need to be compared and validated by experimental measurements to define their rate of precision.

3.5. Conclusions

The present study assessed the effect of plant-substrate combinations on the energy performance of extensive green roofs by using realistic values to characterize the vegetation and substrate. The methodology defined involves a comparison among 30 different green roof types by means of indexes, which made it possible to identify the extensive green roof packages with the highest energy performance, and a ranking was developed summing the scores obtained for each of the indexes. These indexes are used to characterize the behavior of the green roofs in relation to the urban heat island phenomenon, energy savings and temperature fluctuations on the waterproof membrane.

The analysis carried out reveals Salvia as the plant species with the highest ranking during the summer period in the Mediterranean climate, due to its high values for height, (0.475 m), LAI (5.00 m^2/m^2), leaf reflectivity (0.220) and minimum stomatal resistance (300 $mmol/m^2s$).

However, in Mediterranean regions, succulent plants such as Sedum and Sempervivum, which are widely used in extensive green roofs, have the best ranking when year-round performance is considered. Purple Heuchera, yellow Heuchera and Stachys exhibit poorer energy performance than the other plant species analyzed. Finally, it was found that the performance of extensive green roofs depends largely on the thermophysical properties of the substrate used. In fact, the same plant species combined with different substrate types attain heterogeneous performances.

References

[1] G. Peri, G. Rizzo, G. Scaccianoce, M. La Gennusa, P. Jones, Vegetation and soil – related parameters for computing solar radiation exchanges within green roofs: Are the available values adequate for an easy modeling of their thermal behavior?, Energy Build. 129 (2016) 535–548. doi:10.1016/j.enbuild.2016.08.018.

[2] L.W. Zhou, Q. Wang, Y. Li, M. Liu, R.Z. Wang, Green roof simulation with a seasonally variable leaf area index, Energy Build. 174 (2018) 156–167. doi:10.1016/j.enbuild.2018.06.020.

[3] S. Yuan, D. Rim, Cooling energy saving associated with exterior greenery systems for three US Department of Energy (DOE) standard reference buildings, Build. Simul. 11 (2018) 625–631. doi:10.1007/s12273-018-0427-y.

[4] K.C. Dahanayake, C.L. Chow, Comparing reduction of building cooling load through green roofs and green walls by EnergyPlus simulations, Build. Simul. 11 (2018) 421–

434. doi:10.1007/s12273-017-0415-7.
[5] T.E. Morakinyo, K.W.D. Kalani, C. Dahanayake, E. Ng, C.L. Chow, Temperature and cooling demand reduction by green-roof types in different climates and urban densities: A co-simulation parametric study, Energy Build. 145 (2017) 226–237. doi:10.1016/j.enbuild.2017.03.066.
[6] S. Vera, C. Pinto, P.C. Tabares-Velasco, W. Bustamante, F. Victorero, J. Gironás, C.A. Bonilla, Influence of vegetation, substrate, and thermal insulation of an extensive vegetated roof on the thermal performance of retail stores in semiarid and marine climates, Energy Build. 146 (2017) 312–321. doi:10.1016/j.enbuild.2017.04.037.
[7] F.E. Boafo, J.T. Kim, J.H. Kim, Evaluating the impact of green roof evapotranspiration on annual building energy performance, Int. J. Green Energy. 14 (2017) 479–489. doi:10.1080/15435075.2016.1278375.
[8] I. Ziogou, A. Michopoulos, V. Voulgari, T. Zachariadis, Energy, environmental and economic assessment of electricity savings from the operation of green roofs in urban office buildings of a warm Mediterranean region, J. Clean. Prod. 168 (2017) 346–356. doi:10.1016/j.jclepro.2017.08.217.
[9] C.M. Silva, M.G. Gomes, M. Silva, Green roofs energy performance in Mediterranean climate, Energy Build. 116 (2016) 318–325. doi:10.1016/j.enbuild.2016.01.012.
[10] A.L.S. Chan, T.T. Chow, Energy and economic performance of green roof system under future climatic conditions in Hong Kong, Energy Build. 64 (2013) 182–198. doi:10.1016/j.enbuild.2013.05.015.
[11] J. Coma, A. de Gracia, M. Chàfer, G. Pérez, L.F. Cabeza, Thermal characterization of different substrates under dried conditions for extensive green roofs, Energy Build. 144 (2017) 175–180. doi:10.1016/j.enbuild.2017.03.031.
[12] M. Vaz Monteiro, T. Blanuša, A. Verhoef, M. Richardson, P. Hadley, R.W.F. Cameron, Functional green roofs: Importance of plant choice in maximising summertime environmental cooling and substrate insulation potential, Energy Build. 141 (2017) 56–68. doi:10.1016/j.enbuild.2017.02.011.
[13] D. Yeom, P. La Roche, Investigation on the cooling performance of a green roof with a radiant cooling system, Energy Build. 149 (2017) 26–37. doi:10.1016/j.enbuild.2017.05.035.
[14] U. Berardi, P. La Roche, J.M. Almodovar, Water-to-air-heat exchanger and indirect evaporative cooling in buildings with green roofs, Energy Build. 151 (2017) 406–417. doi:10.1016/j.enbuild.2017.06.065.
[15] K. Vijayaraghavan, Green roofs : A critical review on the role of components , bene fi ts , limitations and trends, Renew. Sustain. Energy Rev. 57 (2016) 740–752. doi:10.1016/j.rser.2015.12.119.
[16] M. Kottek, J. Grieser, C. Beck, B. Rudolf, F. Rubel, World map of the Köppen-Geiger climate classification updated, Meteorol. Zeitschrift. 15 (2006) 259–263. doi:10.1127/0941-2948/2006/0130.
[17] P. Bevilacqua, D. Mazzeo, R. Bruno, N. Arcuri, Surface temperature analysis of an extensive green roof for the mitigation of urban heat island in southern mediterranean climate, Energy Build. 150 (2017) 318–327. doi:10.1016/j.enbuild.2017.05.081.
[18] A. Teemusk, Ü. Mander, Greenroof potential to reduce temperature fluctuations of a roof membrane: A case study from Estonia, Build. Environ. 44 (2009) 643–650. doi:10.1016/j.buildenv.2008.05.011.

4. A comprehensive study on green roof performance for retrofitting existing buildings

4.1. Introduction

The increase in the number of green roof installations is related to a growing interest from the international scientific community, but only a few studies have analyzed the energy performance of green roofs installed on existing buildings. These show that the benefits of green roofs are reduced when the roof has a thick layer of thermal insulation [1]. In these studies, the use of green roofs for the retrofitting of existing buildings, built prior to the entry into force of energy-saving standards and therefore, those with little thermal insulation, proved to optimize energy saving and economic benefits. In addition, many studies have found that the energy advantages of green roofs are greater in warm climates than in cold ones, thanks to a reduction in surface temperatures due to the shading effect [2] and to the evapotranspiration phenomenon [3,4].

The majority of existing buildings, in fact, date back prior to the entry into force of the laws regulating building energy consumption; moreover, in many cities, only limited areas are available for the construction of new buildings [5]. In 2010, Castleton et al. [6] reviewed the potential of green roof installation on existing buildings. Following a literature review, the authors identified the costs and the structural implications of green roofs when they were used to retrofit existing buildings. Berardi [7] analyzed the benefits of green roof retrofits on the energy and microclimate of a case study located on a university campus in Toronto. The results of the microclimate analysis proved that a green roof retrofit had high impact on the rooftop microclimate, between 1.1 and 2.0 °C, while it resulted in a slight cooling effect at the pedestrian level, between 0.4 and 0.7 °C. Furthermore, it was found that green roof retrofits reduced the building energy consumption, with annual energy savings of 10 $kWh \cdot m^{-2} \cdot y^{-1}$. Silva et al. [8] revealed that 79% of Lisbon is suitable for incorporating green roofs and 52% have high potential for green roof retrofits.

In recent years, the thermal and physical performance of different materials used in green roof technology has been assessed in a number of studies, regarding both the substrate [9–11] and the drainage layer [12–14]. Also evaluated was the environmental performance of green roofs by means of Life Cycle Analysis (LCA) [15,16] and a quantitative estimate of the reduction in CO_2 emission [17]. However, no studies have verified whether these materials are suitable to be used on existing buildings. Other studies [6] have focused on the weight of some commercial green roof systems. In these, the authors found that the weight of a saturated green roof planted with Sedum varies between 0.49 and 0.96 kN/m^2.

From the economic point of view, several studies assessed the convenience of green roofs by comparing them with roofs made of traditional materials [18,19]. Sproul et al. [20] used a life-cycle cost analysis (LCCA) to determine the net savings for green, white, and black roofs over a 50 year life cycle. Cool roofs provided 50 year net savings of USD 25/m^2 and green roofs had negative net savings of USD 71/m^2, compared to black roofs, due to their higher installation cost. This was despite their lasting at least twice as long as white or black roofs. Furthermore, Niu et al. [21] estimated positive externalities of green roofs considering both sequestration of nitrogen oxides and storm water reduction.

Previous studies focused mainly on assessing the benefits associated with the installation of green roofs on existing buildings. However, no study has verified whether commercial and experimental green roof solutions, made up of different substrate and drainage materials for which the thermal and physical characteristics have been assessed experimentally, are suitable for use in the retrofitting of existing buildings, based on analysis of their structural, thermal, economic, and environmental compatibility.

In the present thesis chapter, a broad analysis of green roof performance for the retrofitting of existing buildings was carried out. In particular, a variety of extensive green roofs were considered, using different materials for the substrate and drainage layer. All the possible solutions were applied to an existing multi-story residential building located in the city of Catania (Italy), which is characterized by a Mediterranean climate. The overload derived from each solution, considering the worst scenarios (which occur when the substrates are water saturated) was evaluated and compared with the load limit prescribed by law for the retrofitting of existing buildings. Furthermore, energy performance in terms of surface temperatures and energy savings were analyzed and compared to the existing roof performance. Finally, following the installation of each green roof, an evaluation was done of both the economic costs and the environmental benefits, such as CO_2 and NO_x reduction, storm water management, etc.

4.2. Material and methods

4.2.1. Evaluation of additional load on the roof structure

The first phase in retrofitting a building with a green roof is to determine the existing load-bearing capacity. Because a green roof adds to the load on the roof structure, it is necessary to determine overloading in relation to different green roof configurations and to compare it with the residual load bearing capacity of the building structures. To avoid an expensive structural upgrade, it is important to keep the green roof weight below the load limit prescribed by law. Designers evaluating the overloading on existing structures, usually take into account the specific weight of the materials and the thickness of the layers used in the green roof system, but evaluate them under dry conditions. This does not consider the substantial increase in the green roof weight due to the amount of water contained in the substrate. In fact, the soil layer receives water from irrigation and precipitation, and loses water from runoff and evapotranspiration [22]. Following abundant rainfall, the substrate is saturated and the green roof reaches its maximum weight.

The load that can be applied on the flat roofs of residential buildings is 200 kg/m^2 (about 1.96 kN/m^2), according to the European standard [6]. This value corresponds to flat roofs of which the load bearing structure was considered usable during the design phase of the building structure. However, not all of the 200 kg/m^2 load margin is available for green roof installation. This is because a residual load of 0.5 kN/m^2 is considered necessary for maintenance. Therefore, the maximum additional load allowed for installation of a green roof on an existing building is 1.46 kN/m^2.

In this study, the weights of seventeen commercial substrates and three different granular drainage materials were compared (Table 1). The weight of these materials depends on their state of compaction (i.e., void ratio, porosity); however, for normal green roof laying procedures, this value is almost constant.

Table 1. Composition of different substrates analyzed.

Sample identifier	Coco peat %	Compost %	Crushed wastes %	Sand %	Pozzolana %	Porous silica %	Expanded slate %	Expanded clay %
Sub1	0	40	0	20	40	0	0	0
Sub2	25	25	40	10	0	0	0	0
Sub3	N/A	6	N/A	N/A	N/A	0	0	0
Sub4	25	40	30	5	0	0	0	0
Sub5	60	15	20	5	0	0	0	0
Sub6	0	10	0	40	0	50	0	0
Sub7	0	0	0	50	0	50	0	0
Sub8	0	0	0	25	0	75	0	0
Sub9	0	10	0	15	0	75	0	0
Sub10	0	10	0	40	0	0	50	0
Sub11	0	0	0	50	0	0	50	0
Sub12	0	0	0	25	0	0	75	0
Sub13	0	10	0	15	0	0	75	0
Sub14	0	10	0	40	0	0	0	50
Sub15	0	0	0	50	0	0	0	50
Sub16	0	0	0	25	0	0	0	75
Sub17	0	10	0	15	0	0	0	75

The thermal and physical characteristics of these commercial substrates had been assessed in previous experimental studies [23,24]. The properties analyzed, however, did not include the substrate weight when water saturated; so this was calculated (according to [25]) using the following equation to correlate the dry density γ_d with the saturated density γ_s of the substrate:

$$\gamma_s = \gamma_d + n\gamma_w \qquad (1)$$

where γ_w is the density of water (1000 kg/m^3) and n is the porosity of the substrate expressed as a pore volume percentage.

Table 2 shows the different types of drainage used in this study. Perlite and expanded clay represent commercial drainage solutions, while rubber crumb is an innovative solution in the green roof market, resulting from the recycling of tires and guaranteeing low environmental impact. The thermal performance and physical characteristics of these commercial drainage materials had been evaluated using a market survey, while the performance of the rubber crumbs had been assessed in previous experimental studies [13].

Table 2. Physical and thermal characteristics of the drainage layers analyzed.

Drainage material	Density [kg/m^3]	Thermal Conductivity [W/mK]
Perlite	100	0.066
Expanded clay	300	0.10
Rubber crumb	480	0.15

Because the weight of the rubber crumbs depends on the particle size of the material, the lower-density material was chosen. This choice could be the most suitable for building retrofitting to increase the overload on the existing roof as little as possible. However, among the drainage materials investigated, rubber crumbs had the highest density values, as well as the highest values of thermal conductivity. Therefore, the main advantage from choosing rubber crumbs derives from their recycled origin. To evaluate the thermal behavior under dynamic conditions of the different materials used for the drainage layer of the green roofs, the thermal lag was calculated. The thermal lag of the existing roof was evaluated according to the EN ISO 13786 standard. The substrates and drainages were combined to compare the additional loads determined for the different green roof solutions. It was thus possible to identify the combinations most suitable for the retrofitting of existing buildings.

4.2.2. Thermal performance of green roofs

Thermal building simulations were performed using EnergyPlus [26]. The energy budget analysis follows the Fast All Season Soil Strength (FASST) model developed by Frankenstein and Koenig for the US Army Corps of Engineers [27]. It is a one-dimensional model that draws heavily from other plant canopy models including BATS [28] and SiB [29].

The Ecoroof module allows the user to define as "green roof" the outer layer of a rooftop construction. The user can specify various features of the green roof construction including height of plants, leaf area index (LAI), leaf reflectivity, as well as the thickness, density, thermal conductivity, and specific heat of the soil. With this Ecoroof model, EnergyPlus can simulate and evaluate the thermal and energy performance of a building constructed with a green roof system.

To compare the energy performance of the green roof solutions analyzed, with those of an existing roof, a building constructed in the early 1970s was chosen as representative of typical multi-story residential buildings in European cities. This study was developed in the city of Catania in southern Italy (37.52° N, 15.07° E). The Mediterranean climate typical of this geographical area is characterized by hot summers and mild winters (Csa according to the Köppen climate classification [30]). The energy performance of green roofs is enhanced when temperature peaks exceed 35 °C and the monthly average daily direct solar radiation exceeds 6.0 kWh/m^2. To consider these climatic conditions during the simulations, the Weather File available in EnergyPlus was used.

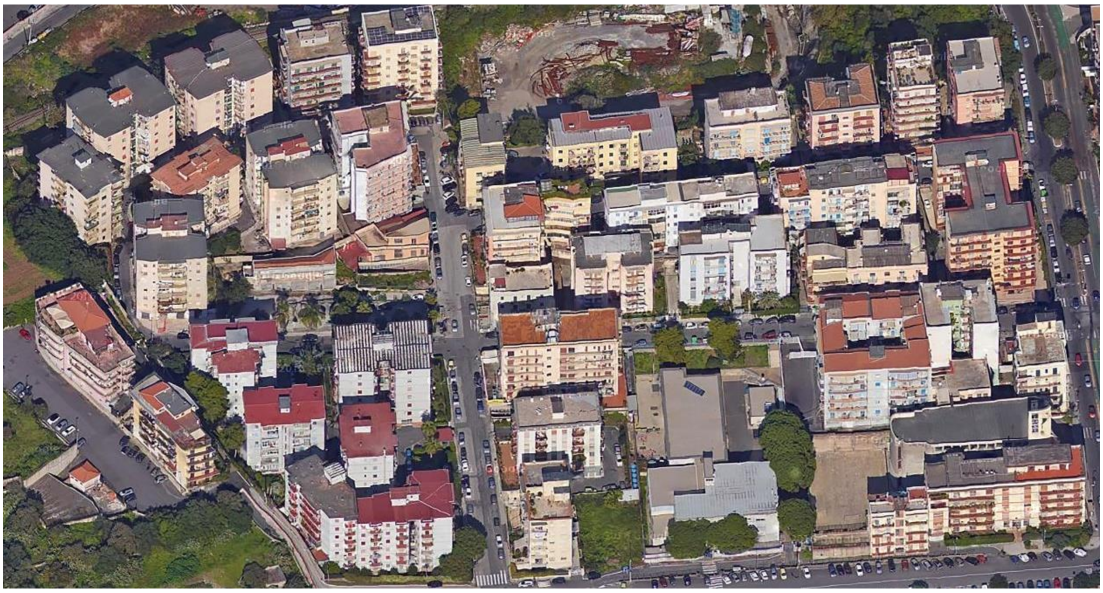

Figure 1. Aerial view of the urban area where the reference building is located (Catania, Italy).

The case study used as the reference consisted of a seven-floor multi-story building that is of a type widespread in the densely urbanized area close to the city center of Catania (Figure 1). All the useful roof area, therefore, was considered for the installation of the green roof (equal to about 270 m^2). There were two residential apartments on each floor. The structure of the building was reinforced concrete, while the floors were reinforced concrete with hollow bricks.

Thermal analyses were carried out for the top floor of the building, which was directly below the green roof. It was found, in fact, that the benefits ensuing from the installation of the green roof on the building, in terms of reduction of energy consumption for air conditioning and decrease in surface temperatures, were reduced to zero on the floors not located directly below the green roof. In most cases, moreover, the owner of the top floor of a multi-story residential building also owns the terrace, and consequently, is the most interested in the green roof installation.

The building walls are described in Table 3. This type of vertical envelope, widespread in buildings belonging to the same period, is characterized by low thermal performance (U-value 0.975 $W \cdot m^{-2} \cdot K^{-1}$). Single transparent panes of glass were used with a thickness of 3 mm and thermal transmittance $U_g = 5.89\ W \cdot m^{-2} \cdot K^{-1}$. The window frame was aluminum without a thermal break and with a thermal transmittance of $U_F = 5.88\ W \cdot m^{-2} \cdot K^{-1}$. The difference between the existing flat roof and the green roof mainly consisted of the presence of the drainage layer and the substrate above the existing roof layers. The overall thermal transmittance U of the existing flat roof was 1.12 $W \cdot m^{-2} \cdot K^{-1}$. Table 4 shows the roof stratigraphy after the green roof installation, where the thermal and physical characteristics of the substrate and drainage (layers 1 and 2 in Table 4) were varied for each case, in line with the purpose of this study to analyze different green roof solutions.

Table 3. Stratigraphy of the existing external wall in the case study building.

N.	Material	Thickness [mm]	Oven Dry Density [kg/m^3]	Thermal Conductivity	Specific Heat [$J \cdot kg^{-1} \cdot K^{-1}$]	Thermal transmittance [$W \cdot m^{-2} \cdot K^{-1}$]	Ref.
1	Plaster	20	1860	$\lambda = 0.72$ [W/mK]	840	36.00	CIBSE
2	Hollow brick	120	-	R = 0.31 [$m^2 \cdot K \cdot W^{-1}$]	-	3.23	UNI 10355
3	Air gap	60	-	R = 0.18 [$m^2 \cdot K \cdot W^{-1}$]	-	5.55	ISO 6946
4	Hollow brick	120	-	R = 0.31 [$m^2 \cdot K \cdot W^{-1}$]	-	3.23	UNI 10355

5	Plaster	20	1860	λ = 0.72 [W/mK]	840	36.00	CIBSE

Table 4. Stratigraphy of the roof after green retrofitting.

N.	Material	Thickness [mm]	Oven Dry Density [kg/m^3]	Thermal Conductivity [W/mK]	Specific Heat [J·kg^{-1}·K^{-1}]	Thermal transmittance [W·m^{-2}·K^{-1}]	Ref.
1	Substrate	Variable	Variable	Variable	Variable	Variable	-
2	Drainage layer	Variable	Variable	Variable	Variable	Variable	-
3	Bitumen sheet	10	1100	0.23	1000	23.00	ISO 6946
4	Lightweight concrete	50	500	0.17	840	3.40	CIBSE
5	Structural slab	250		R = 0.39 [m^2·K·W^{-1}]		2.56	UNI 10355
6	Plaster	20	1860	0.72	840	36.00	UNI 10355

After the most suitable green roof configurations were identified, their energy performance was assessed and compared to the existing roof performance. In addition, the energy performance of different plant species was evaluated. Table 5 reports the thermal and physical characteristics of the species of genera Salvia and Sedum obtained from previous studies in the literature [31].

The results of the various green roof solutions are shown in terms of external and internal surface temperature and energy consumption for heating and cooling of the apartment. These results were compared to those obtained without installation of the green roof.

Table 5. Properties of the two types of vegetation analyzed.

Properties	Sedum	Salvia
Height of plants [m]	0.10	0.35
Leaf Area Index (LAI) [m^2/m^2]	3.00	5.50
Leaf reflectivity α	0.19	0.21
Leaf emissivity ε	0.97	0.97
Min. stomatal resistance [mmol·m^{-2}·s^{-1}]	120	380
Max. volumetric moisture content	0.5	0.5
Min. residual volumetric content	0.01	0.01
Initial volumetric moisture content	0.15	0.15

4.2.3. Simulation settings

A generic template for residential use with an occupancy level of 0.0188 person/m^2 and a metabolic rate of 110 W/person was used for the simulation. This template defines the endogenous loads due to human activity and from the presence of electrical equipment. In climatic conditions typical of the Mediterranean area, it is necessary to establish an irrigation system to ensure the survival of the plants. Therefore, 1 h of irrigation, from 20:00 to 21:00, was set in summer, and half an hour, from 18:30 to 19:00, during winter.

The thickness of the layers was 10.0 and 6.0 cm respectively for substrate and drainage. These values are typical of extensive green roofs: in particular, a thinner substrate could impede the proper growth of vegetation, while a less thick drainage layer would decrease the water flow capacity of the green roof.

The internal and external surface temperatures of the building were obtained under free floating conditions, in order to allow the air temperature inside the building to fluctuate freely. The heating and cooling system was switched on in the building when the purpose was to assess the energy demand. The temperature values were set at 20 °C for the heating period, from December 1st to March 31st, and at 26 °C for the cooling period, from June 1st to September 30th. The type of heating/cooling system used remained constant during the simulations, to analyze the energy performance according to the type of green roof used, without considering the variability of technical features of the heating and cooling system.

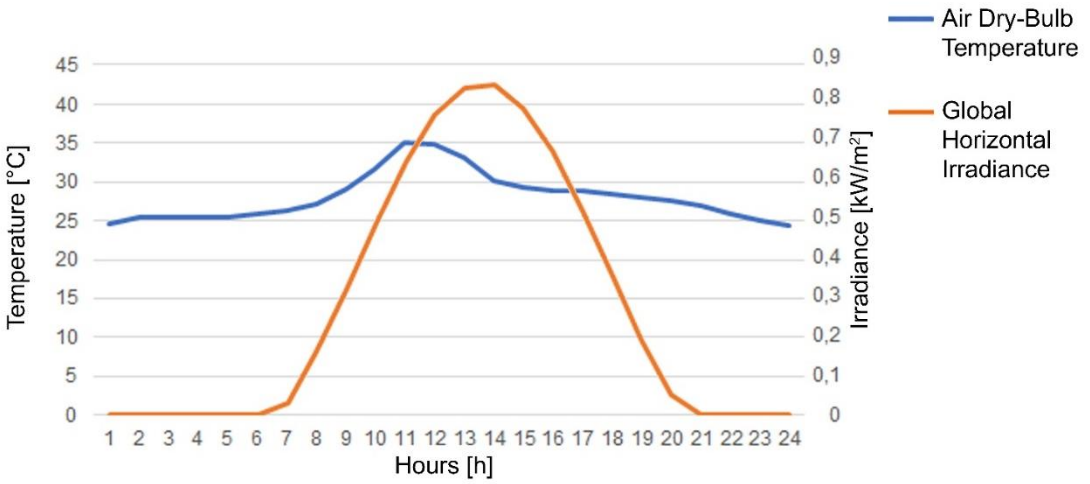

Figure 2. Air temperature and solar radiation during the reference summer day.

To assess the effect of the different types of green roof on the daily surface temperatures, representative days of the most severe climatic conditions were chosen. Specifically, the summer day selected, with the maximum air temperature of about 34 °C, was August 9th, and the winter day, with the minimum air temperature of about −2

°C, was January 21st. The air temperature and solar radiation during these reference days are shown in Figure 2 and Figure 3. Data from existing weather files such as EnergyPlus Weather File (EPW) as the meteorological boundary conditions were used.

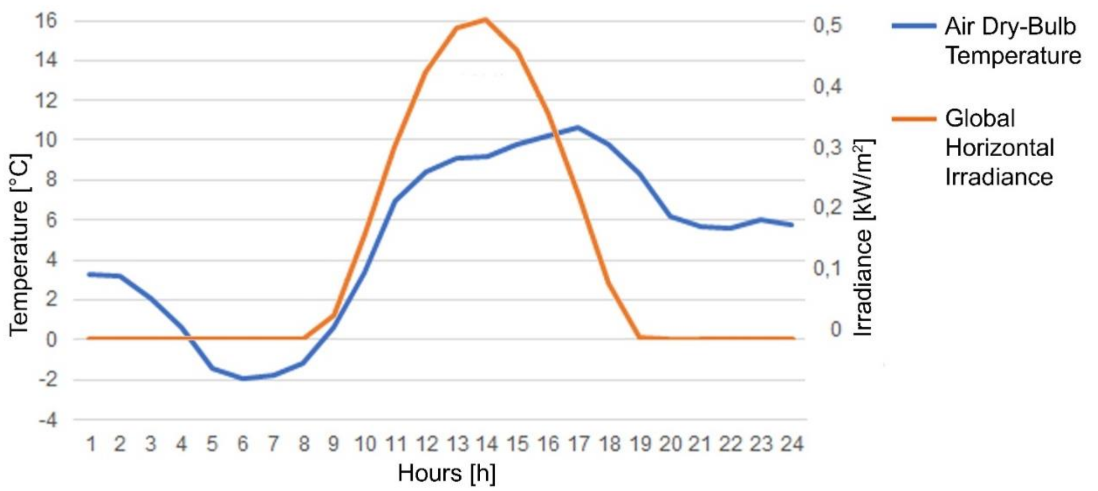

Figure 3. Air temperature and solar radiation during the reference winter day.

4.2.4. Economic and environmental assessment

After considering the green roof solutions suitable for the retrofitting of existing buildings from the structural point of view and analyzing the energy performance in terms of surface temperatures and energy consumption, the economic aspects and environmental benefits of green roofs for building retrofitting were also evaluated. A complete assessment of the real advantages of green roofs installed on existing buildings, in fact, cannot take into account only the aspects linked to a reduction in energy consumption, but should also consider the installation costs and the environmental benefits of a green roof.

The costs of different green roof solutions were assessed using market surveys. Subsequently, the time to return on investment was defined by comparing the installation costs with the reduction in energy consumption.

Different economic parameters were considered to evaluate the effectiveness of the investment made. In all cases, a constant net cash inflow value for each annual period was used, corresponding to the economic value in euros due to energy savings.

The payback period method, however, did not take into account the variation of money value over time. To avoid overly optimistic and non-realistic results, a discounted payback period was introduced, which is used to calculate the length of time needed to recover an investment based on the investment's discounted cash flows.

First, the cash flow of a project must be estimated and divided into periods. These cash flows are then reduced by their present value factor to reflect the discounting using the following equation:

$$\text{Discounted Cash Inflow} = \frac{\text{Actual Cash Inflow}}{(1+r)^n} \quad (2)$$

where *r* is the discount rate (1%) and *n* is the period to which the cash inflow relates. The discount rate was recently used to carry out the economic analysis of green roofs [32]. This value was chosen by approximating the current guidelines of the Italian Ministry of Economic Development, which set the value at 0.82% for economic assessments during the year 2018. In recent years, moreover, this value has always been around 1%. The discounted payback period was calculated when the inflows were equal to the outflows.

The Net Present Value (NPV), which is the sum of the discounted values of incoming and outgoing cash flows (i.e., revenues (R) and costs (C), over the whole lifespan, taking into account the discount rate r) was calculated by:

$$NPV = \sum_{t=0}^{T} \frac{R_t - C_t}{(1+r)^t} \quad (3)$$

These economic parameters were calculated for each of the different green roof solutions.

Nevertheless, green roofs offer a number of environmental benefits that cannot be directly quantified in energy savings, but which must be taken into account when assessing whether or not to install such roofs on existing buildings.

Through innovative policies, the inclusion of air pollution mitigation (CO_2 and NO_x) and the reduction of urban storm water infrastructure costs in an economic assessment of the environmental benefits of green roofs, can reduce the cost gap that currently hinders investment in green roof technology [33].

The reduction in CO_2 emission following the installation of a green roof on an existing building is estimated on the basis of the energy saving achieved. The impact on air quality due to the mitigation of nitrogen oxide (NO_x) was also evaluated in this study. To quantify nitrogen oxide uptake by plants per unit area, data from Morikawa, et al. [34] were used. The annual uptake of NO_x can be translated into health benefits in terms of fewer premature deaths and fewer cases of chronic bronchitis. Another research study has evaluated the level of air pollution reduced by green roofs in terms of O_3, NO_2, PM10, and SO_2 [35].

4.3. Results

4.3.1. Load analysis

Table 6 shows the dry and saturated density of the different substrates analyzed. Significant differences emerged between the dry density and the density calculated under saturated conditions. This difference is due to the substrate composition shown in Table 1. In fact, lighter substrates, such as Sub4 and Sub5, consist mainly of coco peat and compost, which are materials with lower dry density values (0.07 and 0.24 g/cm^3, respectively), while heavier substrates, such as Sub1 and Sub2, had a large percentage of crushed building wastes (dry density of 0.494 g/cm^3), sand (dry density of 0.457 g/cm^3), and Pozzolana. Furthermore, light substrates such as Sub8 and Sub9 exhibited high percentages of porous silica.

Table 6. Dry and saturated density of substrates.

Sample identifier	Dry density [kg/m^3]	Saturated density [kg/m^3]
Sub1	788	1490
Sub2	923	1560
Sub3	1360	2010
Sub4	546	1320
Sub5	375	1220
Sub6	1050	1750
Sub7	1020	1720
Sub8	730	1430
Sub9	680	1380
Sub10	1430	2130
Sub11	1490	2190
Sub12	1240	1940
Sub13	1250	1950
Sub14	1290	1990
Sub15	1410	2110
Sub16	1280	1980
Sub17	1150	1850

On the basis of the previously mentioned thicknesses for both drainage and substrate, the additional load of the different green roof configurations was calculated (see Table 7). The results reveal that, considering the load limit on the roof of existing buildings (1.46 kN/m^2) only a few green roof solutions, as colored in Table 7, are suitable for the retrofitting of existing buildings. Specifically, four of the substrates combined with perlite as drainage layer, two substrates with the expanded clay, and one substrate with rubber crumb, are acceptable. However, expanded clay and perlite, unlike rubber crumbs, are hygroscopic materials so they absorb water by increasing the weight in saturated conditions. Moreover, if the thickness of the substrate is increased from 10 to 15 cm, none of the green roof solutions can be installed on existing buildings without allowing for structural interventions.

Table 7. Weight of additional load from different green roof combinations (substrate + drainage layer).

Sample identifier	Substrate load	Total load (Substrate +Drainage)		
		Perlite	Expanded clay	Rubber Crumb
	[kN/m^2]	[kN/m^2]	[kN/m^2]	[kN/m^2]
Sub1	1.46	1.52	1.64	1.74
Sub2	1.53	1.58	1.70	1.80
Sub3	1.97	2.03	2.14	2.25
Sub4	1.29	**1.35**	**1.47**	1.57
Sub5	1.20	**1.25**	**1.37**	**1.47**
Sub6	1.72	1.78	1.89	2.00
Sub7	1.69	1.75	1.86	1.97
Sub8	1.40	**1.46**	1.58	1.68
Sub9	1.35	**1.41**	1.53	1.63
Sub10	2.09	2.15	2.27	2.37
Sub11	2.15	2.21	2.32	2.43
Sub12	1.90	1.96	208	2.18
Sub13	1.91	1.97	2.09	2.19
Sub14	1.95	2.01	2.13	2.23
Sub15	2.07	2.13	2.25	2.35
Sub16	1.94	2.00	2.12	2.22
Sub17	1.81	1.87	1.99	2.09

4.3.2. Thermal performance

Once the most appropriate green roof solutions for installation on existing buildings were determined, their energy performance was analyzed in terms of surface temperature and energy consumption for heating and cooling. These values were obtained for Sub4 and Sub5 combined with perlite, expanded clay, and rubber crumb. The results show that the internal and external surface temperatures of the building were not affected by the different type of substrate and drainage material used in the green roof, while they did vary according to the plant species installed. Therefore, in order to evaluate the influence of the plant species on the energy performance of the green roof, the surface temperatures of Salvia and Sedum were analyzed, while the type of substrate (Sub4) and the drainage layer (expanded clay) remained unchanged. During summer, both analyzed green roof solutions effected reductions in external surface temperatures of 34.5 and 36.3% for Sedum and Salvia, respectively, compared to those registered using the traditional roof (Figure 4). Moreover, a reduction of about 20.5% in the average daily external surface temperature was noted for both types of green roof (Table 8). In particular, Salvia proved to have a lower surface temperature than Sedum. These results are in agreement with the findings of a previous experimental study [31], in which Salvia was found to be the plant species with the highest energy performance of the species analyzed and Sedum with the lowest. Moreover, due to the evapotranspiration process, which allows the heat accumulated during the day to be lost, the surface temperature of the green roof proved lower than that of the traditional roof during the night.

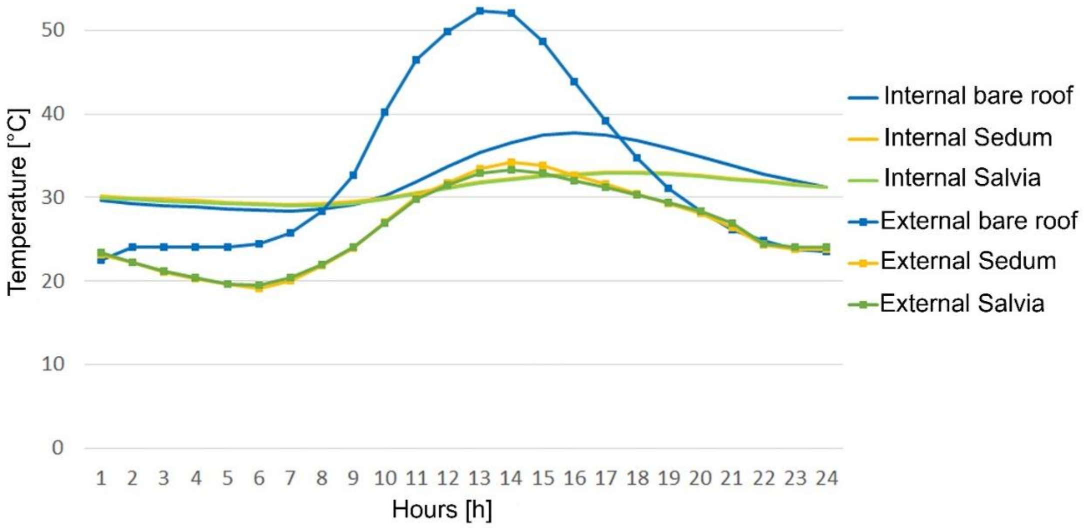

Figure 4. Surface temperatures during the hottest day in summer.

Table 8. Maximum and mean external surface temperatures during summer.

	Max External [°C]	Δ %	Mean external [°C]	Δ %
Bare roof	52.26	-	33.11	-
Green roof Sedum	34.21	34.5	26.32	20.5
Green roof Salvia	33.27	36.3	26.27	20.7

During winter (Figure 5), when it is preferable to have higher external surface temperatures, the roof made with traditional materials reaches higher temperatures during the day. However, owing to the greater thermal inertia created by the presence of the substrate and drainage layers, during the night the green roof presents higher temperatures than the traditional roof, reducing the daily temperature fluctuations.

During both summer and winter, it was found that the internal surface temperatures of the green roof were lower than the surface temperatures of the traditional roof. Maximum values during the summer daytime were 33.04 and 37.72 °C for green roof and traditional roof, respectively. Furthermore, Figures 4 and 5 show that there is little difference between the internal surface temperatures of the different green roof solutions analyzed, because the thermal inertia of the existing floor structure has the predominant role.

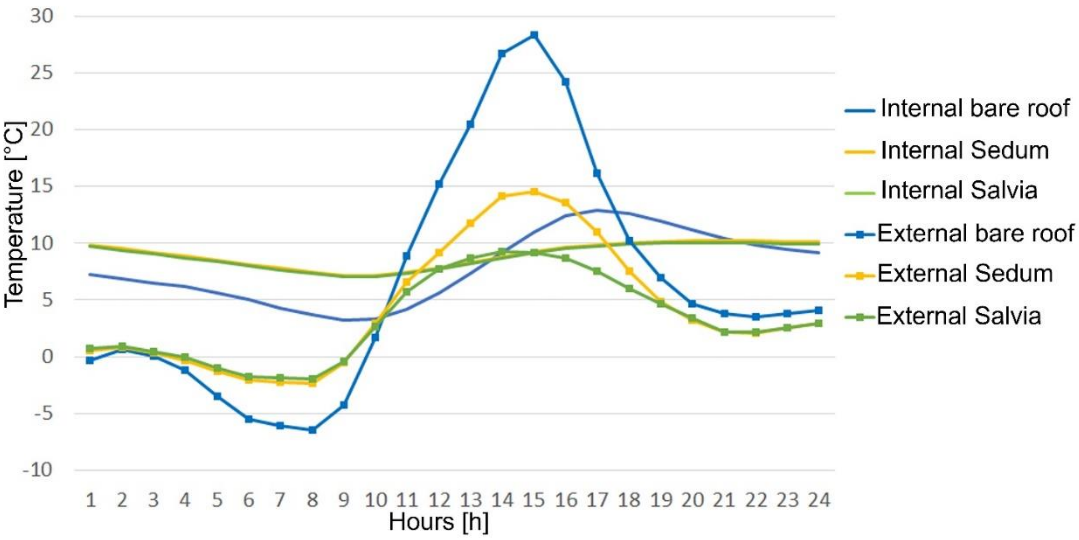

Figure 5. Surface temperatures during the coldest day in winter.

Table 9 shows, for the various substrates (Sub4 and Sub5), drainage layers (perlite, expanded clay, and rubber crumb), and plants (Salvia and Sedum) analyzed; the annual energy consumption for heating and cooling, and compares these values with those obtained with the roof before retrofitting. These results show that the green roof gives better energy performance during both summer and winter (Figure 6). During summer, in fact, consumption for cooling is reduced by between 31 and 35% for all the types of green roof analyzed; while during winter, the energy savings for heating are between 2 and 10%, compared to the same building without a green roof. In addition, the annual energy reduction for air conditioning is between 20 and 24% for all the green roofs analyzed.

Table 9. Annual energy consumption for heating and cooling.

Substrate	Drainage layer	Vegetation	Heating [kWh]	Δ [%]	Cooling [kWh]	Δ [%]	Total [kWh]	Δ [%]
Bare roof			7136.03	-	-10303.19	-	17439.22	-
Substrate 4	Perlite	Sedum	6482.73	**-9.16**	-6991.74	**-32.14**	13474.47	**-22.73**
		Salvia	6526.21	**-8.55**	-6838.02	**-33.63**	13364.22	**-23.37**
	Expanded clay	Sedum	6742.81	**-5.51**	-6913.68	**-32.90**	13656.49	**-21.69**
		Salvia	6783.53	**-4.94**	-6763.06	**-34.36**	13546.60	**-22.32**
	Rubber Crumb	Sedum	6951.52	**-2.59**	-6846.76	**-33.55**	13798.28	**-20.88**
		Salvia	7008.97	**-1.78**	-6668.45	**-35.28**	13677.42	**-21.57**
Substrate 5	Perlite	Sedum	6455.63	**-9.53**	-7026.05	**-31.81**	13481.68	**-22.69**
		Salvia	6511.07	**-8.76**	-6864.09	**-33.38**	13375.16	**-23.30**

	Expanded clay	Sedum	6720.42	**-5.82**	-6945.67	**-32.59**	13666.10	**-21.64**
		Salvia	6511.07	**-8.76**	-6864.09	**-33.38**	13375.16	**-23.30**
	Rubber Crumb	Sedum	6933.55	**-2.84**	-6876.93	**-33.25**	13810.47	**-20.81**
		Salvia	6995.98	**-1.96**	-6687.79	**-35.09**	13683.77	**-21.53**

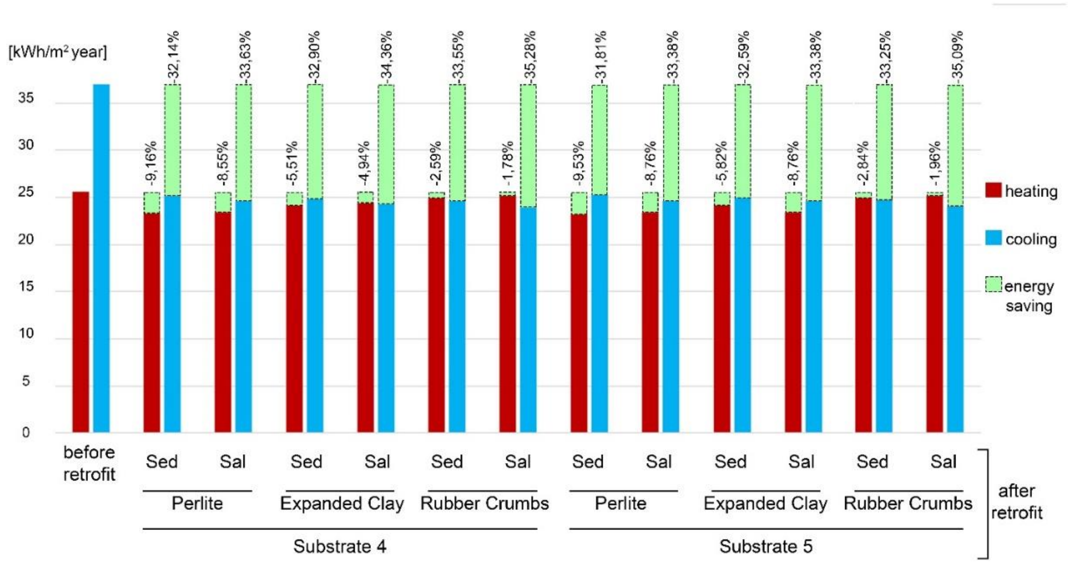

Figure 6. Energy savings for the different solutions analyzed

In particular, during winter, the solution with the highest energy performance was Sub5 + Perlite + Sedum, while the solution with the lowest performance was Sub4 + Rubber + Salvia. Conversely, during summer the best green roof configuration was Sub4 + Rubber + Salvia while the worst was Sub5 + Perlite + Sedum. Accordingly, depending on the climatic conditions of the area where the green roof is installed, some solutions give better energy performance than others, demonstrating the high sensitivity to climatic conditions of the green roof.

The thermal lag calculated for the existing roof was 7.69 h. With Sub5, the thermal lag of the green roof reached 11.83, 12.40, and 12.59 h for perlite, expanded clay, and rubber crumbs, respectively. Installation of the green roof increased the thermal lag, as found in previous studies [36].

4.3.3. Cost assessment

An analysis was performed of the costs of a green roof installed on an existing building, to assess the real economic benefits. The law currently in force in Italy encourages energy retrofitting by means of interventions on the existing building envelope. This law provides for a tax deduction equal to 65% of the cost for green roof installation on existing buildings.

Table 10 shows that a green roof can reduce the annual costs for air conditioning by between 14 and 19% compared to the existing roof. This energy saving will automatically increase with increase in energy costs.

Table 10. Costs of energy consumption for annual air conditioning.

Substrate	Drainage	Vegetation	Heating [€]	Cooling [€]	Total [€]	Δ [%]
Bare roof			713.6	453.3	1166.9	-
Substrate 4	Perlite	Sedum	648.2	307.6	955.9	**-18.08**
		Salvia	652.6	300.8	953.4	**-18.29**
	Expanded clay	Sedum	674.2	304.2	978.4	**-16.15**
		Salvia	678.3	297.5	975.9	**-16.37**
	Rubber Crumb	Sedum	695.1	301.2	996.4	**-14.61**
		Salvia	700.9	293.4	994.3	**-14.79**
Substrate 5	Perlite	Sedum	645.5	309.1	954.7	**-18.19**
		Salvia	651.1	302.0	953.1	**-18.32**
	Expanded clay	Sedum	672.0	305.6	977.6	**-16.22**
		Salvia	651.1	302.0	953.1	**-18.32**
	Rubber Crumb	Sedum	693.3	302.5	995.9	**-14.65**
		Salvia	699.6	294.2	993.8	**-14.83**

Some other economic benefits could be taken into account. For example, nitrogen oxide emission allowances are currently traded in the U.S.; and market-based economic valuations for 2005–2006 ranged from 798 to 3800 €/mg. Considering therefore an average value of 2300 €/mg of NO_2 and that green roofs have an uptake capacity of 0.27 $kg{\cdot}m^{-2}{\cdot}y^{-1}$ of NO_2, it is concluded that for 270 m^2 of green roof there is a saving of 167.67 €/y.

Moreover, the reduction of storm water volume by green roofs benefits municipalities; therefore local water authorities could pass the economic savings on to the owner of the green roof. Clark [33] indicated that a potential fee reduction for green roofs resulted in a mean storm water fee of about 0.06 €/m^2. For a roof with a surface conversion of 270 m^2, as in the present case study, a saving of 16.2 €/y is therefore achieved.

To perform the economic analysis and calculate the payback periods, both the savings achieved in terms of energy costs and the quantified environmental benefits were taken into account. It was supposed that the extra cost for maintenance of the green roof are equal to the cost reduction the maintenance of the reference roof due to the increase in useful life of waterproofing membrane because green roof protects it from the direct solar radiation.

Table 11 shows the unit costs of the materials analyzed and considers the real thickness of the materials used for the green roof. From the market investigation carried out, it was found that the cost of the substrate did not vary considerably among the different types analyzed (unit cost about 30.00–35.00 €/m^3). Sub4 had a slightly lower cost because it contained more crushed waste and less coco peat than Sub5 did.

Table 11. Costs of vegetation, drainage, and substrate.

Material	Thickness	Cost	Cost
	[m]	[€/m^3]	[€/m^2]
Sedum	-	-	15.20
Salvia	-	-	24.30
Substrate 4	0.10	-	30.00
Substrate 5	0.10	-	35.00
Perlite	0.06	100	6.00
Expanded clay	0.06	80	4.80
Rubber Crumb	0.06	140	8.40

Among the different types of drainage analyzed, expanded clay was the cheapest, while rubber crumb was the most expensive, owing to the high cost of collection, transport, and recycling.

Table 12 shows the total installation costs and those obtained using the 65% tax deduction provided by the standard. The savings obtained as the difference between the energy consumed before and after the installation of the green roof, were added to the economic and environmental benefits.

Table 12. Costs of 270.00 m^2 of the six different packages of green roof with Sub5.

	Green roof	Costs	Total Costs	Cost with Tax Reduction	Savings	Payback period	Discounted Payback Period	Net Present Value (20 years)
		[€/m^2]	[€]	[€]	[€/year]	[year]	[year]	[€]
SEDUM	Perlite	56,20	15,174	5,310.9	394.9	13.4	14.5	1815.3
	Expanded clay	55,00	14,850	5,197.5	372.4	13.9	15.1	1522.7
	Rubber Crumb	58,60	15,822	5,537.7	354.4	15.6	17.1	857.7
SALVI	Perlite	65,30	17,631	6,170.85	397.4	15.5	16.9	1000.0
	Expanded clay	64,10	17,307	6,057.45	374.9	16.1	17.7	707.8

Rubber Crumb	67,70	18,279	6,397.65	356.5	17.9	19.9	35.6

The payback time of the investment varied between 13.4 years for perlite with Sedum, to as long as 17.9 years for rubber crumb with Salvia. Observing the values of the discounted payback period, there was a slight lengthening of the times of payback. They varied between 14.5 years for perlite with Sedum, to as long as 19.9 years for rubber crumb with Salvia. The Net Present Value calculated over a period of 20 years shows how the current value of the investment is decidedly low, especially in the case of solutions that have longer payback periods. Figure 7 shows the annual cash flow over a period of 20 years and the cumulative discounted cash flow for the green roof with Sedum and perlite, taking into account the value of the initial investment. However, private individuals, not being companies, do not have the goal of reducing the time of return on economic investment.

To reduce these return times, future research into green roofs must be aimed at reducing the costs of green roof materials, especially for the substrate and drainage layers.

Recent studies [32] have also evaluated the increase in the economic value of buildings on which a green roof is installed. This value cannot be directly quantified and depends on both the geographical area and the intended use of the building. In the case of residential buildings, the economic value of the apartments increased following installation of the green roof, which improved energy efficiency and at the same time the attractiveness and environmental sustainability of the entire building.

If the entire terrace is not affected by the installation of the green roof, the remaining surface does not use the residual load of the supporting structures for the installation of the green roof and, therefore, remains walkable and utilizable by people who can use it to spend their moments of leisure. This benefit associated with the installation of the green roof is even more evident when the roofing of the building is owned by the condominium and not by the private individual who lives on the building floor below the terrace.

Finally, the green roof, from a life cycle perspective, represents a perfectly reversible solution. In fact, although it is necessary to consider its load on the load-bearing structure of the building as permanent, following its disposal, the terrace is available to be used for other purposes.

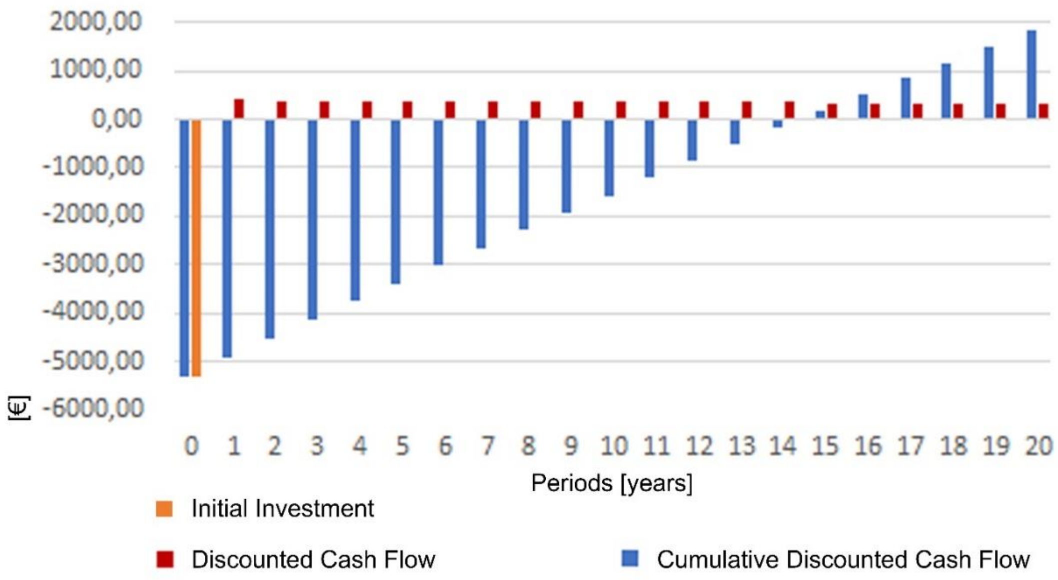

Figure 7. Annual cash flow for a green roof package.

4.3.4. Air pollution mitigation

In addition to the benefits from previous analyses, green roofs contribute to mitigation of air pollution. In this section, the benefits related with CO_2 and NO_X deriving from green roofs installation are described.

Green roofs reduce CO_2 emission into the atmosphere, adding to the reduction due to energy saving, a reduction caused by the presence of a larger green surface absorbing carbon dioxide during its life cycle. Yang et al. [37] tested the capacity of the green roof to remove CO_2, stating that the annual rate of CO_2 removal by green roofs is 85 kg/ha. Furthermore, as demonstrated by Jeong [38], one kWh of energy for heating produces 0.06 kg of CO_2 if using natural gas.

In the present study, the retrofit intervention removed 229 kg of CO_2 per year. The area of the roof surface affected by the retrofit was 270 m^2. Thus, it absorbed the emissions generated by the use of approximately 3816 kWh for building heating. As Table 9 shows, the energy consumption for heating before the retrofitting is about 7100 kWh, so the green roof is not able to absorb all the carbon dioxide produced in winter for the heating of the apartments placed below. Nevertheless, after the retrofit intervention, a reduction in energy consumption during winter of about 8% due to the green roof installation leads to a reduction of 340 kg of CO_2 into the atmosphere.

In summer, CO_2 emissions depend on the cooling system used. However, as another study demonstrated [39], the difference in CO_2 input per kWh from a natural gas system and a heat pump system was small, although the heat pump systems produced less greenhouse gases. The higher the Coefficient of Performance of the heat pump, the lower the CO_2 emission. By using 0.06 kg of CO_2 per kWh, in summer and in winter, with a reduction of around 33% of the annual consumption with the green roof and 10 300 kWh used for cooling, there is a reduction of 203.4 t of CO_2.

Over the course of a year, taking into account the carbon dioxide values due to the reduction in energy consumption, there was a reduction of 240 kg of the CO_2 released into the atmosphere. To this value, it is necessary to add the quantity of CO_2 directly absorbed by the green roof vegetation; however, in general this is negligible compared to the reduction due to energy saving.

With the climatic conditions of Catania, therefore, each square meter of green roof eliminates 0.88 kg of CO_2 from the atmosphere. These data only concern the air-conditioned environments underneath the green roof, but the entire building considered consists of seven floors, so only a small portion of the heated volume contributes to reducing environmental impacts.

The emission of NO_X in urban areas is mainly due to vehicles and power plants. Combination of nitrogen oxides (NO_X) with other air pollutants such as ozone, sulfur oxides, and particulate materials (PM) can cause respiratory diseases and increase the risk of heart attacks.

Damage from NO_X can extend to plants as well, reducing growth, respiration, photosynthesis, stomatal conductance, and enzyme activities. The effect of the removal of nitrogen oxides by green roofs may be quantified using data from [34], who determined that 217 plant taxa had a mean uptake capacity of 0.27 $kg \cdot m^{-2} \cdot y^{-1}$ of NO_2. The installed green roof could therefore guarantee an uptake capacity of 58.59 kg of NO_2 per year. This uptake capacity is sufficient to balance the NO_X emissions attributable to energy consumption for 316.000 kWh. An emission factor of 50 g/GJ was used [40]. The annual uptake of NO_X can be translated into health benefits in terms of fewer premature deaths and fewer cases of chronic bronchitis.

Finally, when rubber crumb is used as a drainage layer, the GHG emissions avoided by the recycling of source-segregated waste materials may be taken into account. Turner et al. proposed a GHG emission factor of −636 net kg/t of CO_2 eq. [41]. Coupling a green roof with green facade for the retrofitting of existing buildings, a greater value of energy is saved and the vegetation can absorb more CO_2.

4.4. Discussion

As regard the load analysis, a significant difference between dry density and saturated density was noted between the substrates analyzed. The results revealed that, considering the load limit on the roof of existing buildings (1.46 kN/m^2), only a few green roof solutions are suitable for the retrofitting of existing buildings. In particular, the saturated density of the materials analyzed was about 15% more than the dry density. Therefore, considering saturated conditions, expanded clay and perlite could lose their characteristics as light materials, reducing the range of green roof packages suitable for installation on existing buildings. Thus, if the thickness of the substrate is increased from 10 to 15 cm, none of the green roof solutions can be installed on existing buildings without allowing for structural interventions.

These results establish one of the novelty as, previous literature studies focused did not evaluate if the extra load of commercial or experimental green roof solutions are suitable for use in the retrofitting of existing buildings.

The following are the main suggestions that designers should take into consideration to make the practical installation of green roofs on existing buildings possible. In addition to the use of lighter substrates and drainage materials, many weight-saving strategies could be adopted to reduce the load on the existing roof and, therefore, increase the load margin available for the installation of green roofs. These include removing the existing flooring, often made of heavy material, marble grit tile, light concrete screed, as well as heavy old roofing systems, and replacing them with newer lighter ones. For example, a built-up roof with aggregates weighs from 20 to 25 kg/m^2, while a single-ply membrane (e.g., ethylene propylene diene monomer) weighs less than 2.0 kg/m^2. Such a weight reduction would contribute to the wider loading margin needed to add a green roof.

Furthermore, to increase the number of green roof solutions suitable for the redevelopment of existing buildings, it is possible to reduce the saturated density of the substrates, which mainly depends on the dry density of the material; this can be achieved by using lighter materials or reducing the index of voids. In fact, the more voids present in the material, the greater the amount of water contained in the substrate when it is saturated. As a result, reducing the void index decreases the weight of the saturated substrate. To reduce the number of voids, machines suitable for compacting the material should be used during installation. However, by compacting the substrate, at the same thickness, both the quantity of material used and the weight of the system increase; therefore, it is necessary to use a higher percentage of light inert material inside the substrate, to reduce the void index without increasing the weight of the green roof. In addition, in normal applications of the green roof, both the substrate and the drainage layer are installed "by hand" and without the use of special compacting machinery, which use, moreover, would have the disadvantage of increasing both the production costs and the complexity of the processing.

Globally, the analysis carried out show that only a few solutions are currently suitable for energy retrofitting.

As a consequence, it is clear that new types of substrates for green roofs must be created. These should be from natural or from recycled materials, but also should be light materials, such as coco peat and porous silica, to be used for the energy retrofitting of existing buildings. It is fundamental, moreover, that the designers take the saturated density into account during the design phase of the green roof on existing buildings. Future research on new green roof materials should be carried out to develop solutions more suitable for application on existing buildings, considering their density under both dry and saturated conditions.

From the economic and environmental point of view, this research proposes a complete assessment of the real advantages of green roofs installed on existing buildings, considering the costs for both installation and environmental benefits, such as air pollution mitigation and reduction of urban storm water infrastructure costs.

This approach enlarges the economic viability of the green roof respect to many existing studies that considered only the aspects linked to a reduction in energy consumption when used for the retrofitting of existing buildings. As result, the economic assessment of the environmental benefits of green roofs allow to reduce the payback time that is one of the constrains that currently hinders investment in green roof technology.

4.5. Conclusions

The research carried out, highlighted the current structural limits for adopting green roofs for the retrofitting of existing buildings, and the adequacy of the materials used, giving specific information about different green roof packages.

Moreover, the economic analysis carried out has taken into account not only the money savings coming from the decrease in energy consumption, but also includes the benefits due to the income derived from the reduction in storm water and air pollution. Thereby, this research provided a much more comprehensive economic analysis than the majority of literature studies did.

Finally, the results of the study suggested the recommendation to allow the appropriate choice of materials and thicknesses relative to the various layers constituting the green roof. This should be done in relation to the maximum applicable load on the flat roof of an existing building, and by providing useful information to the building designers concerning the constraints and the perspectives when adopting a green roof system for a building retrofit.

In the present study, the payback time of the investment was calculated taking into account only the financially quantifiable benefits obtainable with the construction of a green roof. Most of the benefits of the green roof are not economically quantifiable (reduction of CO_2 in the atmosphere, mitigation of the heat island effect, improvement of the microclimate, psychological well-being of the residents); although they can provide orientation to justify the choice of this intervention.

References

[1] M.M. Liu, Probabilistic prediction of green roof energy performance under parameter uncertainty, Energy. 77 (2014) 667–674. doi:10.1016/j.energy.2014.09.043.
[2] R. Kumar, S.C. Kaushik, Performance evaluation of green roof and shading for thermal protection of buildings, Build. Environ. 40 (2005) 1505–1511. doi:10.1016/j.buildenv.2004.11.015.
[3] A.M. Coutts, E. Daly, J. Beringer, N.J. Tapper, Assessing practical measures to reduce urban heat: Green and cool roofs, Build. Environ. 70 (2013) 266–276. doi:10.1016/j.buildenv.2013.08.021.
[4] P. Bevilacqua, J. Coma, G. Pérez, C. Chocarro, A. Juárez, C. Solé, M. De Simone, L.F. Cabeza, Plant cover and floristic composition effect on thermal behaviour of extensive green roofs, Build. Environ. 92 (2015) 305–316. doi:10.1016/j.buildenv.2015.04.026.
[5] G. Verbeeck, H. Hens, Energy savings in retrofitted dwellings: Economically viable?, Energy Build. 37 (2005) 747–754. doi:10.1016/j.enbuild.2004.10.003.
[6] H.F. Castleton, V. Stovin, S.B.M. Beck, J.B. Davison, Green roofs; Building energy savings and the potential for retrofit, Energy Build. 42 (2010) 1582–1591. doi:10.1016/j.enbuild.2010.05.004.
[7] U. Berardi, The outdoor microclimate benefits and energy saving resulting from green roofs retrofits, Energy Build. 121 (2016) 217–229. doi:10.1016/j.enbuild.2016.03.021.
[8] C.M. Silva, I. Flores-Colen, M. Antunes, Step-by-step approach to ranking green roof retrofit potential in urban areas: A case study of Lisbon, Portugal, Urban For. Urban Green. 25 (2017) 120–129. doi:10.1016/j.ufug.2017.04.018.
[9] D.J. Sailor, D. Hutchinson, L. Bokovoy, Thermal property measurements for ecoroof soils common in the western U.S., Energy Build. 40 (2008) 1246–1251. doi:10.1016/j.enbuild.2007.11.004.
[10] S.E. Ouldboukhitine, R. Belarbi, R. Djedjig, Characterization of green roof components: Measurements of thermal and hydrological properties, Build. Environ. 56 (2012) 78–85. doi:10.1016/j.buildenv.2012.02.024.
[11] A. Pianella, R.E. Clarke, N.S.G. Williams, Z. Chen, L. Aye, Steady-state and transient thermal measurements of green roof substrates, Energy Build. 131 (2016) 123–131. doi:10.1016/j.enbuild.2016.09.024.
[12] J. Coma, G. Pérez, A. Castell, C. Solé, L.F. Cabeza, Green roofs as passive system for energy savings in buildings during the cooling period: use of rubber crumbs as drainage layer, Energy Effic. 7 (2014) 841–849. doi:10.1007/s12053-014-9262-x.
[13] G. Pérez, A. Vila, L. Rincón, C. Solé, L.F. Cabeza, Use of rubber crumbs as drainage layer in green roofs as potential energy improvement material, Build. Environ. 97 (2012) 347–354. doi:10.1016/j.apenergy.2011.11.051.
[14] L. Rincón, J. Coma, G. Pérez, A. Castell, D. Boer, L.F. Cabeza, Environmental performance of recycled rubber as drainage layer in extensive green roofs. A comparative Life Cycle Assessment, Build. Environ. 74 (2014) 22–30. doi:10.1016/j.buildenv.2014.01.001.
[15] N.H. Wong, S.F. Tay, R. Wong, C.L. Ong, A. Sia, Life cycle cost analysis of rooftop gardens in Singapore, Build. Environ. 38 (2003) 499–509. doi:10.1016/S0360-1323(02)00131-2.
[16] F. Bianchini, K. Hewage, How “green” are the green roofs? Lifecycle analysis of green roof materials, Build. Environ. 48 (2012) 57–65. doi:10.1016/j.buildenv.2011.08.019.
[17] J. Li, O.W.H. Wai, Y.S. Li, J. Zhan, Y.A. Ho, J. Li, E. Lam, Effect of green roof on ambient CO2 concentration, Build. Environ. 45 (2010) 2644–2651. doi:10.1016/j.buildenv.2010.05.025.
[18] T. Carter, A. Keeler, Life-cycle cost-benefit analysis of extensive vegetated roof

systems, J. Environ. Manage. 87 (2008) 350–363. doi:10.1016/j.jenvman.2007.01.024.
[19] L. Kosareo, R. Ries, Comparative environmental life cycle assessment of green roofs, Build. Environ. 42 (2007) 2606–2613. doi:10.1016/j.buildenv.2006.06.019.
[20] J. Sproul, M.P. Wan, B.H. Mandel, A.H. Rosenfeld, Economic comparison of white, green, and black flat roofs in the United States, Energy Build. 71 (2014) 20–27. doi:10.1016/j.enbuild.2013.11.058.
[21] H. Niu, C. Clark, J. Zhou, P. Adriaens, Scaling of Economic Benefits from Green Roof Implementation in Washington, DC, Environ. Sci. Technol. 44 (2010) 4302–4308. doi:10.1021/es902456x.
[22] S.E. Ouldboukhitine, G. Spolek, R. Belarbi, Impact of plants transpiration, grey and clean water irrigation on the thermal resistance of green roofs, Ecol. Eng. 67 (2014) 60–66. doi:10.1016/j.ecoleng.2014.03.052.
[23] J. Coma, A. de Gracia, M. Chàfer, G. Pérez, L.F. Cabeza, Thermal characterization of different substrates under dried conditions for extensive green roofs, Energy Build. 144 (2017) 175–180. doi:10.1016/j.enbuild.2017.03.031.
[24] D.J. Sailor, M. Hagos, An updated and expanded set of thermal property data for green roof growing media, Energy Build. 43 (2011) 2298–2303. doi:10.1016/j.enbuild.2011.05.014.
[25] C. Farrell, X.Q. Ang, J.P. Rayner, Water-retention additives increase plant available water in green roof substrates, Ecol. Eng. 52 (2013) 112–118. doi:10.1016/j.ecoleng.2012.12.098.
[26] U.S.D. of E. (DOE) B.T.O. (BTO) managed by the N.R.E.L. (NREL), EnergyPlus, (n.d.).
[27] S. Frankenstein, G. Koenig, Fast All-Season Soil STrength (FASST) Cold Regions Research and Engineering Laboratory, (2004).
[28] E. Dickinson, A. Henderson-Sellers, J. Kennedy, Biosphere-atmosphere Transfer Scheme (BATS) Version 1e as Coupled to the NCAR Community Climate Model, NCAR Tech. Rep. NCAR/TN-3871STR, 72. (1993) 77. doi:10.5065/D67W6959.
[29] P.J. Sellers, Y. Mintz, Y.C. Sud, a. Dalcher, A simple biosphere model (SiB) for use within general circulation models, J. Atmos. Sci. 43 (1986) 505–531. doi:10.1175/1520-0469(1986)043<0505:ASBMFU>2.0.CO;2.
[30] M. Kottek, J. Grieser, C. Beck, B. Rudolf, F. Rubel, World map of the Köppen-Geiger climate classification updated, Meteorol. Zeitschrift. 15 (2006) 259–263. doi:10.1127/0941-2948/2006/0130.
[31] M. Vaz Monteiro, T. Blanuša, A. Verhoef, M. Richardson, P. Hadley, R.W.F. Cameron, Functional green roofs: Importance of plant choice in maximising summertime environmental cooling and substrate insulation potential, Energy Build. 141 (2017) 56–68. doi:10.1016/j.enbuild.2017.02.011.
[32] R. Berto, C.A. Stival, P. Rosato, Enhancing the environmental performance of industrial settlements : An economic evaluation of extensive green roof competitiveness, Build. Environ. 127 (2018) 58–68. doi:10.1016/j.buildenv.2017.10.032.
[33] C. Clark, P. Adriaens, F.B. Talbot, Green roof valuation: A probabilistic economic analysis of environmental benefits, Environ. Sci. Technol. 42 (2008) 2155–2161. doi:10.1021/es0706652.
[34] H. Morikawa, A. Higaki, M. Nohno, M. Takahashi, M. Kamada, M. Nakata, G. Toyohara, Y. Okamura, K. Matsui, S. Kitani, K. Fujita, K. Irifune, N. Goshima, More than a 600-fold variation in nitrogen dioxide assimilation among 217 plant taxa, Plant, Cell Environ. 21 (1998) 180–190. doi:10.1046/j.1365-3040.1998.00255.x.
[35] J. Yang, Q. Yu, P. Gong, Quantifying air pollution removal by green roofs in Chicago, Atmos. Environ. 42 (2008) 7266–7273. doi:10.1016/j.atmosenv.2008.07.003.
[36] T. Theodosiou, D. Aravantinos, K. Tsikaloudaki, Thermal behaviour of a green vs. conventional roof under Mediterranean climate, Int. J. Sustain. Energy. 33 (2014) 227–241. doi:10.1080/14786451.2013.772616.
[37] J. Yang, Q. Yu, P. Gong, Quantifying air pollution removal by green roofs in Chicago,

Atmos. Environ. 42 (2008) 7266–7273. doi:10.1016/j.atmosenv.2008.07.003.
[38] K. Jeong, T. Hong, J. Kim, Development of a CO 2 emission benchmark for achieving the national CO 2 emission reduction target by 2030, Energy Build. 158 (2018) 86–94. doi:10.1016/j.enbuild.2017.10.015.
[39] S. Liu, Z. Li, B. Dai, Energy, Economic and Environmental Analyses of the CO 2 Heat Pump System Compared with Boiler Heating System in China, Energy Procedia. 105 (2017) 3895–3902. doi:10.1016/j.egypro.2017.03.803.
[40] M. Könings, Emission trading – why State aid is involved : NOx trading scheme, Eu Compet. Policy Newsl. 3 (2003) 77–80.
[41] D.A. Turner, I.D. Williams, S. Kemp, Greenhouse gas emission factors for recycling of source-segregated waste materials, Resour. Conserv. Recycl. 105 (2015) 186–197. doi:10.1016/j.resconrec.2015.10.026.

5. Energy and environmental assessment of plastic granule production from recycled greenhouse covering films in a circular economy perspective

5.1. Introduction

Plastic films are utilized in greenhouse cultivation system as covering materials, in the form of transparent sheets for under-tarp moisture collection or as black sheets for crops mulching [1]. With regard to covering materials in greenhouse cultivation system, usage of plastic films has been increasing since the middle of the twentieth century due to several benefits such as: increase in crop yield; earlier harvest; reduced consumption of both herbicides and pesticides; frost protection; and water conservation. By analyzing official statistical data, a large amount of plastic films was found as being utilized in the Mediterranean countries where protected crops are widely cultivated [2]. In detail, the consumption of plastic films as greenhouse and low tunnel covering material is about 72,000 and 75,000 tons per year, respectively. Because of direct exposure to both solar radiation and wind, greenhouse plastic coverings are replaced every 6 to 45 months [2–4]. At the end of their useful life, these covers are taken off and treated as waste in two different ways: one is about disposing them of in landfills, often equipped with energy recovery systems; while the other regards recycling them into secondary raw materials for a wide range of applications, including rubbish bags and boxes, so contributing to reduction of the environmental impact overall associated with the film life cycle [5,6]. Unfortunately, to-date, around 50% of plastic wastes generated by agricultural activities is treated in landfills, so emphasizing upon the urgent need to find and follow alternative, more sustainable routes [7].

In Italy, each year, more than 350,000 t of agricultural plastic materials are utilized with a consequent post-consumption material flow of about 200,000 t [8]. With regard to protected cultivation areas, more than 2 million hectares are covered by greenhouses, i.e. approximately 21% of the whole cultivated surface.

In this context, given the relevance of plastic film amount to be collected and recycled, evaluations would be desirable to check upon energy-efficiency and sustainability related issues of raw materials obtained from recycled greenhouse covering films: Life Cycle Assessment (LCA) could be one valid tool for such a purpose. As a matter of fact, it has been used by authors like Horodytska et al. [9], to identify and pursue the best environmentally performing waste treatments among a set of alternatives. In details, the authors reviewed previously published LCAs on waste management. While several LCA studies were carried out in different countries to assess the municipal solid waste management, only few LCAs were focused upon flexible plastic film waste management. According to the authors, this can be attributed - even only in part - to a lower degree of sorting and recycling technologies development as compared with rigid plastics and the modelling of e.g. shredding, washing, and drying operations is required to better understand and improve the plastic films recycling processes. Gu et al. [10] presented a detailed LCA investigation on plastic from various sources, such as agricultural wastes, by analyzing a recycling company in China. The results demonstrated that the extrusion process was the primary process in determining the overall impacts of recycled plastic production, while the introduction of fillers and additives contributed the most significant part in the environmental impacts associated with recycled composite production. Finally, Hottle et al. [11] explored the impacts associated with the production and disposal of biopolymers compared to fossil-based plastics by means of LCA. The authors found that recycling resulted in significant life cycle impact reductions.

Although the topic of plastic waste management and recycling is an important environmental issue at the global level, the review conducted highlighted a gap in the literature of LCAs on the production or recycling process of flexible film used for agricultural purposes. Moreover, another gap stays in the fact that, though mechanical recycling of agricultural post-consumer films is highly recommended because of the high amount of homogenous, single polymer waste available [12], to the authors' knowledge, no research studies have been conducted thus far to assess the environmental impact deriving from such recycling process.

This research was designed to contribute filling those two gaps, with the final objectives of stimulating creation of cleaner paths for plastic waste disposal, as well as of enriching the current specialized literature with findings obtained and lessons learned.

It reports upon a combined evaluation of environmental issues, like consumption of water and energy, and resultant emissions of Greenhouse Gases (GHGs), arising from manufacturing plastic granules by utilizing Agricultural Plastic Waste (APW) as a zero-burden material input.

A Sicilian firm operating in the sector was positively involved in giving all technical support to this author team as needed for development of the study. The latter addresses energy and environmental issues related to the reuse of plastic covering films for producing recycled granules as a secondary raw material. To this end, a Life Cycle Assessment (LCA) approach was adopted according to the specific International Standards 14040-44:2006 (ISO, 2006a, ISO, 2006b) and applied to a Sicilian firm, representative of the agricultural plastic waste (APW) collection and recycling.

Apart from the above-reported introduction, the study was conducted through the framework depicted in Figure 1.

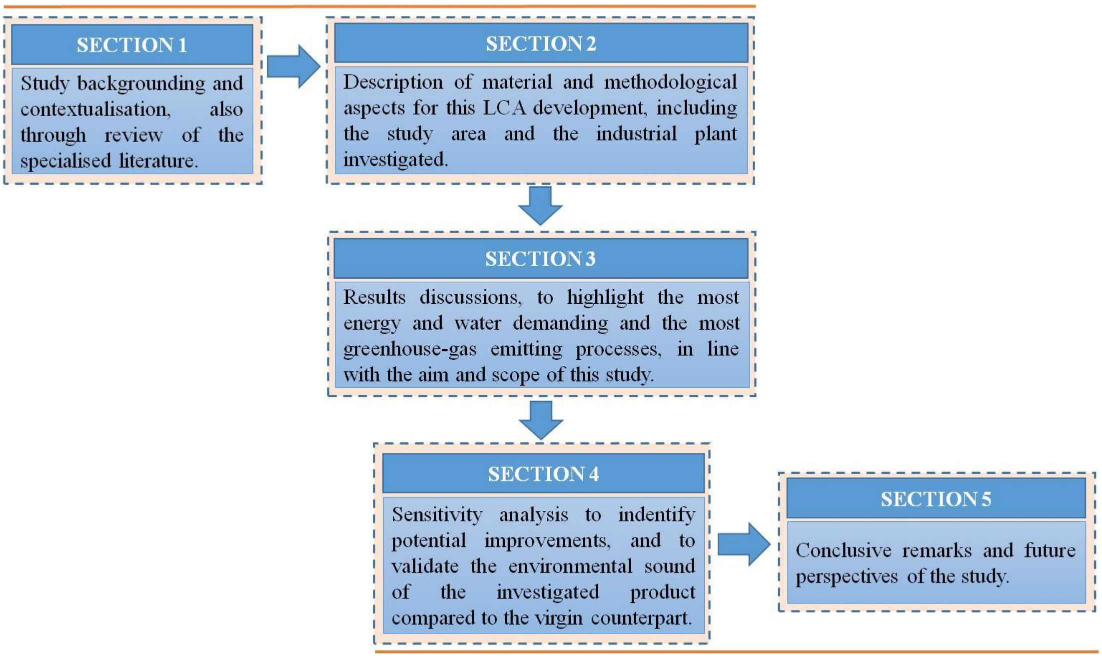

Figure 1. Study content framework.

5.2. Materials and methods

5.2.1. <u>Study area</u>

Sicily is the Italian region with the highest percentage (76.1%) of greenhouse surface (GHS) among the total cultivated surface (TCS), followed by Campania e Lazio (Table 1).

Within Sicily, Ragusa is the province with the largest protected cultivation area [13], which covers about 470,000 ha and is nearly 68% of the protected cultivation of the whole region. In particular, that area is invested as follows: 58.7%, for tomatoes; 33.6%, for other vegetables; and the remaining 6.7%, for flowers and ornamental plants.

Table 1. Cultivated and greenhouse surfaces in Italy.

Italian regions	**Cultivated surface (TCS) [ha]**	**Greenhouse surface (GHS) [ha]**	**[GHS/TCS]**
Abruzzo	481,043.2	22,588.5	4.7%
Apulia	855,847.2	125,094.5	14.6%
Basilicata	471,100.2	45,793.0	9.7%
Calabria	507,203.0	55,737.0	11.0%
Campania	479,295.2	355,096.0	74.1%
Emilia-Romagna	783,905.2	49,697.4	6.3%
Friuli-Venezia Giulia	94,425.7	5,891.0	6.2%

Lazio	666,610.3	312,409.0	46.9%
Liguria	58,921.2	58,336.0	99.0%
Lombardy	498,982.2	72,525.0	14.5%
Marche	366,105.0	13,492.9	3.7%
Molise	148,728.0	1,665.4	1.1%
Piedmont	505,085.5	45,426.0	9.0%
Sardinia	994,106.2	64,779.5	6.5%
Sicily	902,429.3	686,758.0	76.1%
Trentino Alto Adige	541,410.6	4,541.0	0.8%
Tuscany	846,496.7	69,648.7	8.2%
Umbria	354,323.1	5,562.0	1.6%
Valle d'Aosta	34,393.4	130.0	0.4%
Veneto	551,923.1	169,525.7	30.7%
Total	10142,334.2	2164,696.6	21.3%

This has led increase in supply chains being implemented for manufacturing and distribution of plastic covering films, especially in those parts of Sicily (e.g., the province of Ragusa) where protected crop production was documented to be significant. However, to meet the necessary demand for those films to be treated as waste after usage, those chains are increasingly expanding to incorporate industrial plants for sustainable treatment of those films at the end of their service life, so reducing harmful consequences to the environment and to the health of humans. As the result of this, several firms have been founded over last thirty years or so, to deal with recycling of post-use covering films, so to convert them into value-added material commodities in line with the principle of circular economy. One of those firms was involved to technical support this study development: its geographical position within the province of Ragusa was depicted in Figure 2. It collects and recycles Agricultural Plastic Waste (APW) to obtain Low-Density Polyethylene (LDPE) granules, which find application as a secondary raw material in a wide range of sectors. These recycled granules are generally characterized by quality rates that are highly comparable to the virgin counterparts and, therefore, are suitable for manufacturing of printed materials, pipes and bituminous membranes, and new films [6].

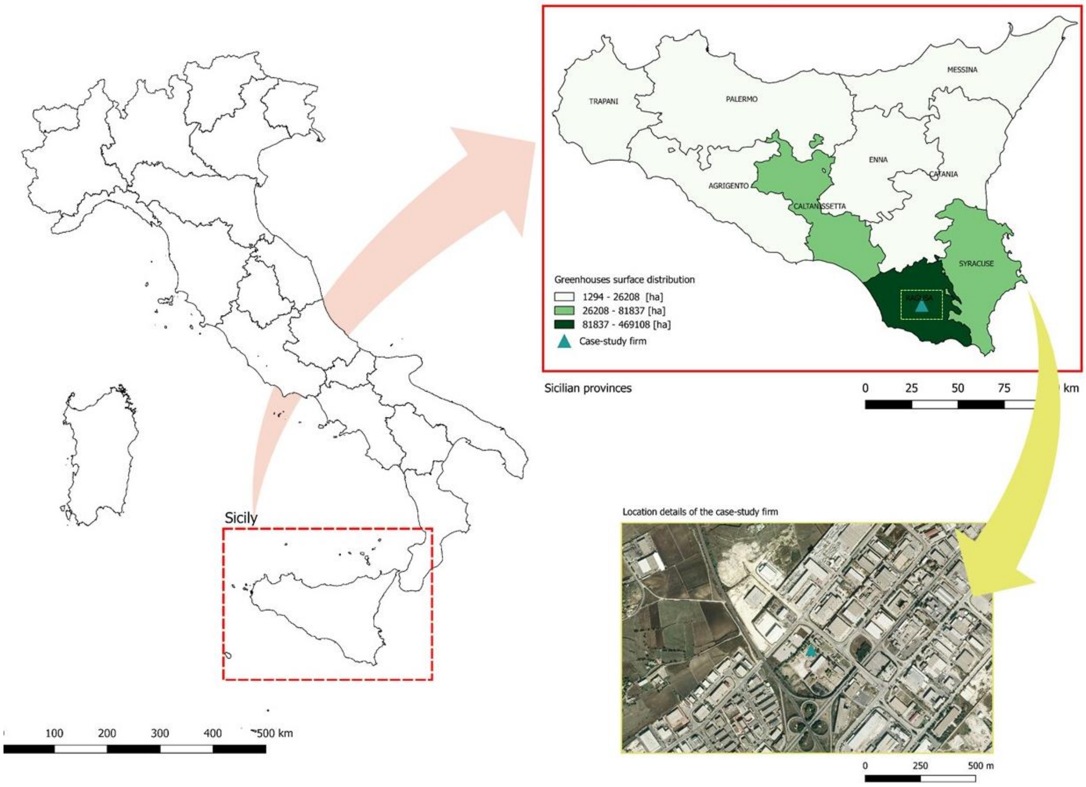

Figure 2. Geographic position of the study area and the firm considered in the case study.

5.2.2. Description of the analyzed industrial process

The production process of the considered firm starts with supply of APWs, which is entirely collected from the surrounding areas and stored before being processed (Figure 3). APW is initially subjected to grinding and to a first phase of pre-washing and spinning. After these phases, all macroscopic impurities are eliminated through decantation in a water tank. The post-use water is treated in an adjacent plant and stored in tanks before being pumped back to the LDPE-granule production process, so it continuously feeds the recycling process.

The sludge resulting from the wastewater treatment is decanted and extracted from the bottom of the tanks for the dehydration process on drying beds. Next, the APW goes through a subsequence of processes to eliminate all the impurities and humidity within the material by washing, drying, and milling. During the final step of the entire transformation chain, material (in small pieces) is melted, extruded and stored in silos before marketing and distribution.

5.2.3. Assessment of energy and environmental issues

To estimate energy and environmental impacts of the production process of recycled LDPE granules above-described, an LCA approach was developed according to the specific International Standards 14040-44:2006 and organized in the standard phases, i.e. Goal and Scope Definition, Life Cycle Inventory (LCI), Life Cycle Impact

Assessment (LCIA), and Life Cycle Interpretation. The development of each of these phases was discussed in the sections below.

5.2.3.1.Goal and scope definition

The study was developed by following the LCA standard framework and the LCIA phase was focused upon single issues, such as water consumption, primary-energy sources exploitation, and GHG emissions. In fact, based upon the inventory analysis, they were found to be both highly representative of the analyzed process and a priority in the EU agricultural policy for their impact reduction [14]. To this end, Carbon Footprint (CF), Cumulative Energy Demand (CED) and Water Footprint (WF) were applied as they are worldwide known as key indicators for the assessment of energy and environmental performance.

The Functional Unit (FU) and the system boundaries were defined by following the International Standards, in order to best represent the investigated process and be consistent with the aim of the study. The FU represents the unit of product and provides a reference through which inputs are linked to outputs and to the resulting impacts and damages: in this case study, the FU was chosen to be 1 ton of produced LDPE-granules.

As regards the system boundaries (see Figure 3), they were defined to include: 1) APW acquisition, pre-treatment and transformation into the reference finished-product (1t recycled-LDPE); 2) preparation and acquisition of auxiliaries, oils, and energy; 3) the treatments of all waste materials as generated by the recycling process; and 4) the annexed plant for treatment and recirculation of the APW-cleaning water.

Those boundaries were designed based upon information provided by the supporting firm to clearly highlight the material and energy flows throughout the investigated chain, which enabled connecting the up-stream processes to the down-stream ones. Furthermore, as emerges from Figure 3, all transports for input material supply and for delivery of the wastes generated by the process to treatment were considered in the assessment. Only the recycled-LDPE distribution was excluded because it was considered as pertaining to the utilization phase and, therefore, the downstream border of the system was set at the firm exit gate. All transport flows considered were detailed in the following section, together with the related diesel consumptions and Ecoinvent modules used for the system assessment based upon information provided by the firm.

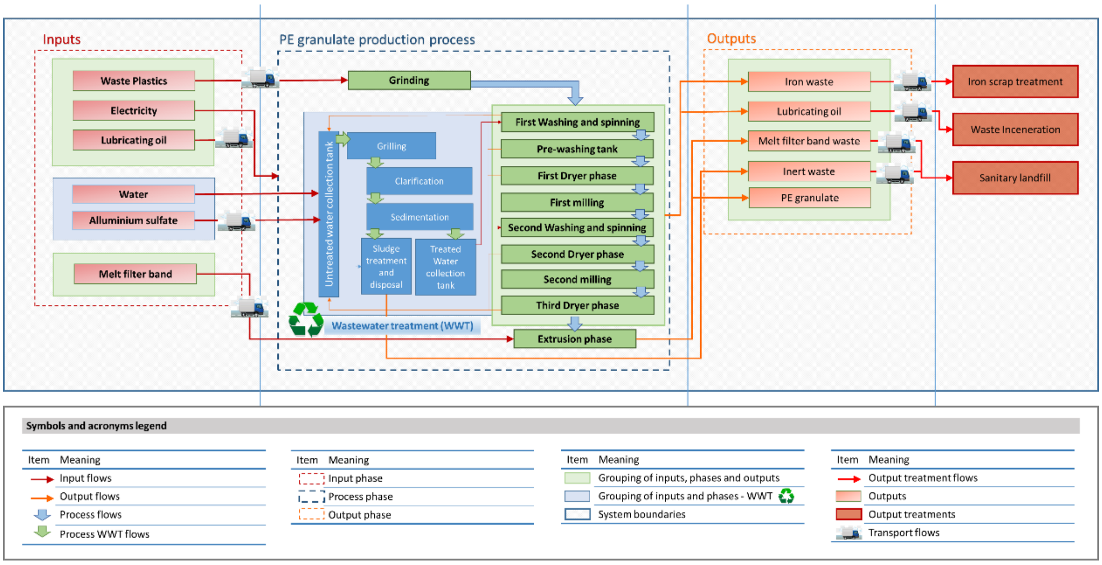

Figure 3. Boundaries of the system investigated.

5.2.3.2. Life cycle inventory (LCI)

This is the key phase of any LCA since it deals with compilation, qualification and quantification of all input and output streams, as needed for the goal achievement. The inputs considered are the resources, materials, fuels, and energies, while the outputs are the material emissions in air, water and soil, as well as the exploitation of natural and primary-energy resources [15].

In this context, since it comes to investigation of a system being highly interconnected with the local territory, the LCI was centered upon collection of site-specific data (primary data), regarding typologies and amounts of both inputs and outputs. A specific questionnaire was developed to be filled in through interviews with technicians and to gather firm-management related information, like main structural and economic features; production system; the product obtained (i.e., the recycled granule), and the wastes to be treated [16].

The questionnaire was organized into five different parts: i) a general section containing questions aimed at getting information about the input materials, such as water and covering plastic films (the amount of product to be processed); ii) the second section, ‘electricity consumption’, for acquiring information on the type of process and its electricity consumption, the techniques and the machinery utilized; iii) the third section aimed to acquire data related to the production process, i.e. the type and amount of the obtained products and which kind of auxiliary materials were adopted during the process; iv) the waste disposal section was aimed to collect information about typologies and quantities of by-products and wastes obtained during the production and which kind of disposal processes was adopted; v) the last section, ‘supplying section’, contained information related to the logistics phases, before, during and after process production. In detail, in this section of the questionnaire, information about distances in kilometers were required to detail as much as possible the logistics phase with regard the transport flows, which often in Sicily region represent a key factor for managing sustainable processes.

Primary data were combined with background ones extrapolated from the database of acknowledged scientific value and relevance, like Ecoinvent v.3 as available in SimaPro 8.1. This database was used because it is recognized worldwide as accommodating most of the background materials and processes often used in LCAs [17], which contributes making it suitable for the modelling of industrial systems like the one investigated in this study.

Data collection regarded a 3-year campaign between 2015 and 2017 and information used for the LCI were reported in Table 2 and Table 3. In detail, Table 2 shows that data related on LDPE granules production differ only about 5% during the three years analyzed, confirming the standardization of the process. Therefore, the LCA developed in this study is representative of the production process of LDPE granules from recycled greenhouse covering films.

Table 2. Data collected at the LDPE granules production site from 3-year campaign and the annual average base. All data reported are referred to the annual production.

Outputs				
Items	***Amount***			***UM***
	2015	**2016**	**2017**	
Products				
LDPE granules	11445	11536	12359	ton
Waste streams				
Inert	5923	6213	6988	ton
Exhausted mineral oil	3778	4000	4889	kg
Steel	11000	21800	24290	kg
Inputs				
Items	***Amount***			***UM***
	2015	**2016**	**2017**	
Material and energy commodities				
Underground water without treatment (production and distribution)	43051	51617	45528	ton
Aluminium sulphate	24600	29760	20860	kg
Mineral oil	3778	4000	4889	kg
Steel	11000	21800	24290	kg

Diesel*	34500	37000	35000	l
Electricity	1.115E7	1.094E7	1.011E7	kWh
Melt filter band	15000	18000	24000	m

*All emissions related to Diesel combustion were extrapolated from Ecoinvent and referred to the Diesel consumption volume

Table 3. Transport flows related to the system investigated, calculated from average values.

Transport	Raw material	Waste	Flow (kgkm)	Diesel consumption (kg)	Ecoinvent module
T1	Aluminum sulphate	-	219.39	23.91	Transport, freight, lorry 3.5-7.5 metric ton, EURO5 {RoW}| transport, freight, lorry 3.5-7.5 metric ton, EURO5 | Alloc Def, S
T2	Plastic waste	-	8.649E4	9.43E3	Transport, freight, lorry 3.5-7.5 metric ton, EURO4 {RoW}| transport, freight, lorry 3.5-7.5 metric ton, EURO4 | Alloc Def, S
T3	Mineral oil	-	39.38	4.29	Transport, freight, lorry 7.5-16 metric ton, EURO5 {RoW}| transport, freight, lorry 7.5-16 metric ton, EURO5 | Alloc Def, S
	-	Exhausted oil	132.82	14.48	
T4	Steel wire	-	2.75	0.30	Transport, freight, lorry 16-32 metric ton, EURO5 {RoW}| transport, freight, lorry 16-32 metric ton, EURO5 | Alloc Def, S
	-	Iron waste	4.893	0.53	

For the assessment, the collected data were averaged to obtain a yearly LDPE-granule production of about 11780 tons and an electricity consumption of about 1.11E7 kWh, i.e. approximately 950 kWh are required to produce 1 ton of LDPE-granules. In Table 3, forward and reverse transport flows were detailed and the chosen Ecoinvent modules were reported. All the data recorded and averaged (Table 2 and Table 3) were then elaborated to be referred to the system FU, namely 1 ton of recycled LDPE, and reported in Table 4.

Table 4. Average data from Tables 2 and 3 referred to the system FU, namely 1 ton recycled LDPE

Outputs		
Items	**Average U.M/ton$_{LDPE}$**	***UM***
Products		
LDPE granules	1.000	ton
Waste streams		
Inert	0.521	ton

Exhausted mineral oil	0.358	kg
Steel	1.615	kg
Inputs		
Items	**Average U.M/ton$_{LDPE}$**	***UM***
Material and energy commodities		
Underground water without treatment (production and distribution)	3.882	ton
Aluminium sulphate	2.128	kg
Mineral oil	0.358	kg
Steel	1.615	kg
Diesel	3.014	l
Electricity	942.275	kWh
Melt filter band	1.613	m
Total of transports (as sum of values in Table3)		
Raw material supply	7.364	kgkm
Waste to treatment	0.012	kgkm

Considering the uncertainty and variability in LCA studies, it is important to determine both the validity of the collected data and the reliability and robustness of the results [18]. As reported by [19], the different types of uncertainties can be distinguished in: parameter uncertainties, model uncertainty and uncertainty linked with choices.
The robustness of data and modelling of this study should be considered very high since the analysis is based on real acquired data, during a 3-years campaign.

5.2.3.3.Life cycle impact assessment (LCIA)

Within the LCIA step, two approaches of characterization, i.e. mid-point and end-point, can take place along the pathway of an impact indicator. According to De Benedetto and Klemes [20], LCIA phase was carried out by aggregating the output flows, previously quantified in the LCI phase, in a limited set of Impact Categories (ICs), by adopting a mid-point approach. Then, the study was extended to the damage assessment as part of the end-point approach, and the ICs were grouped into Damage Categories (DCs) which are the environmental compartments that suffer the damage caused by the LDPE granule production during its life cycle.
To this aim, the authors accessed and used the classification/characterization framework provided by three single-issue impact assessments i.e., CF, CED, WF, available in Simapro 8.1, to evaluate the created inventory dataset (Table 4).

<u>Carbon Footprint (CF)</u>

The CF is one of the most popular ‘impact category indicators’, for the climate change category. The emissions of different greenhouse gases are weighted based on their global warming potential (GWP) relative to carbon dioxide (e.g., one kg of methane has a much greater GWP than one kg of carbon dioxide). The weighting is technically called ‘characterization’ of the inventory results, and the GWPs of different greenhouse gases are the characterization factors. The resultant CF is expressed in terms of CO_2 equivalent (CO_{2eq}) [21].

In this study, among the mid-point approaches the IPCC 2013 GWP 100a method was used, which was developed by the Intergovernmental Panel on Climate Change and it contains the climate change factors of IPCC with a timeframe of 100 years.

According to eq. (1) by [21]:

$$CF_i = \sum_j GWP_j * e_j \quad (1)$$

where:

- e_j is the emission (in mass unit) of the j-th GHG associated with the given process;
- GWP_j is the Global Warming Potential of the j-th GHG for a 100-year temporal horizon (GWP100), which is required for any CF assessment.

Table 5 reports the GWP100 of the GHGs that were considered by the authors as the most representative of the investigated system and extrapolated by Simapro 8.1.

Table 5. Global Warming Potential of relevant GHGs. Conversion factors from IPCC (2013).

GHG	Formula	GWP_{100} [gCO_{2eq}/gGHG]
Carbon dioxide	CO_2	1
Methane	CH_4	28
Nitrous oxide	N_2O	265

At the end-point approach, the computed impacts were transformed into damages using conversion factors based upon the classification scheme provided by ‘ReCiPe Endpoint’ in the Egalitarian perspective (E/E) for the CF. ReCiPe method was used, in particular, for quantification of environmental damages that the emissions of the most significant GHGs generate -upon the DCs, i.e. Climate Change (CC), Human Health (HH) and Ecosystem Quality (EQ).

Cumulative Energy Demand (CED)

The CED is an impact indicator that expresses the energy utilization throughout the life cycle of a product or a service. So, it can be considered as an indicator of environmental impacts with regard to the energy resource depletion [22].

According to Wiesen and Wirges [23], CED was calculated based upon the ‘Cumulative Energy Demand’ method described in the Ecoinvent database. The aim of the method is both to calculate the direct and indirect energy used throughout the life cycle of the LDPE--granules and differentiate among renewable and non-renewable energy sources [24]. Therefore, this method allows the evaluation of environmental effects related to both the emissions and energy consumption [25]. In detail, the method includes the direct and indirect uses of energy and it is organized in eight different impact categories. Normalization or weighting data are not included in the method. In this study, the CED was calculated by including both non-renewable (from fossil fuels, nuclear, and non-renewable biomass) and renewable (from wind, solar, geothermal, and water) energy sources, associated to each input considered in the LDPE granules production process.

Water Footprint (WF)

Among the methods involved in LCA-based water footprint, the Water Footprint Assessment (WFA) was adopted, according to Pfister et al. [26]. This method is centered upon computation of the Water Stress Index (WSI), which calculates the water impact on the consumption-to-availability perspective of freshwater deprivation, corresponding to the ‘blue water’ in the WFA methodology. The Water Stress Index was used as a general screening indicator or characterization factor for the freshwater consumption at the mid-point approach for all three areas of protection: Resources, Ecosystems and Human Health. Then, at the end-point approach, the damages using conversion factors based upon the classification scheme provided by Eco-indicator 99 were computed. In detail, Eco-indicator-99 was used for estimating the environmental damages as the consequence of water consumption upon DCs, i.e. Resources (Re), Human Health (HH) and Ecosystem Quality (EQ).

5.3. Results and discussion

5.3.1. Carbon Footprint assessment

The assessment showed that CO_2, CH_4 and N_2O are the most significant GHGs since they represent the 94.87% of the CF associated to the system investigated. In particular, CO_2 is characterized by the highest GWP_{100}, as shown in Table 6, and it is the most emitted GHG, as reported in Figure 4.

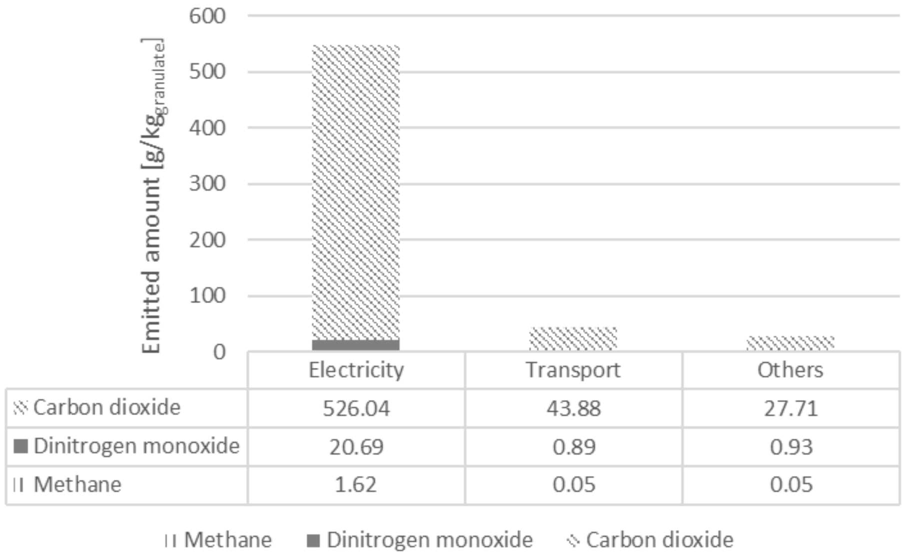

	Electricity	Transport	Others
Carbon dioxide	526.04	43.88	27.71
Dinitrogen monoxide	20.69	0.89	0.93
Methane	1.62	0.05	0.05

Figure 4. Emitted GHGs, with aggregated and disaggregated values.

Two different results can be gathered from Figure 4: one per emitted GHG by taking into account the considered phases (horizontal sum); and the other one per each considered phase by taking into account the three selected gases (vertical sum). Furthermore, the following materials, fuels and activities were grouped in the '*Others*' category since they contribute with less than 5% to the GHG emissions: production of diesel (and emissions from its combustion), tap water, aluminum sulphate, lubricating oil; manufacturing of steel wire and of filtering material; as well as treatment of inert waste, waste mineral oil, and steel waste pre-treatment.

From Figure 4 there is evidence that the most contributing phases are: the production and distribution of electricity required for the process working and the transports (Table 3). Electricity, in particular, is the largest contributor for each of GHG emissions, with percentage values (up to the total ones) equal to: 88.02% (CO_2); 91.90% (N_2O); and 94.63% (CH_4). Contribution from the transport section is far lower and ranges from 2.74% in the case of CH_4 to 7.34% as per CO_2-emission.

Mid-point results demonstrate that CF is equal to 655.46 kgCO_2, which, based upon results shown in Table 6, is due for the major percentage (91.18%) to CO_2. As anticipated in the methodological-approach discussion, the study was extended to incorporate the damages assessment phase as part of the end-point approach, so considering the environmental damage that each emitted GHG considered causes to CC, HH and EQ. The end-point categories affected by the three GHGs were reported in Table 6.

Table 6. Mid-point and end-point results per each GHG emitted considered in the assessment.

GHG	Mid-point analysis* Characterisation	Endpoint analysis Damages assessment		
	GWP_{100}	CC	HH**	EQ**
	$kgCO_2$ eq	$kgCO_2$ eq	DALY	species.yr
CO_2	597.63	597.63	2.10E-03	1.12E-05
CH_4	47.97	47.97	4.57E-05	2.43E-07
N_2O	5.97	5.97	1.21E-05	6.44E-08

* IPCC 2013

** values are referred to kg of emitted substance (ReCiPe Endpoint (E/E))

5.3.2. Cumulative Energy Demand assessment

The CED was found 12.015 GJ per kg of recycled-LDPE granules, with electricity contributing 88.72%, as evident from Figure 5. In addition, from this figure emerges that the electricity utilized in the recycling process is 76.17% of fossil origins.

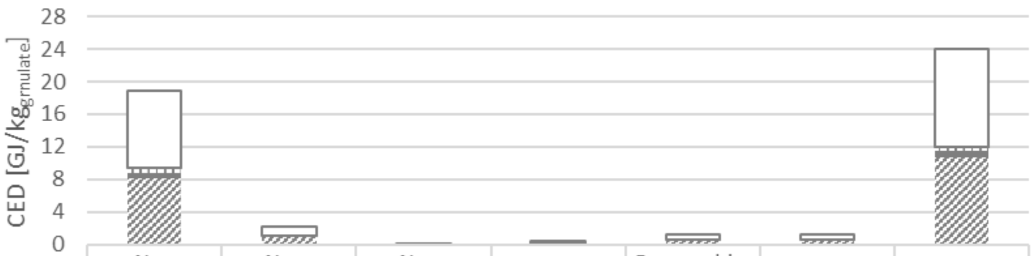

	Non renewable, fossil	Non-renewable, nuclear	Non-renewable, biomass	Renewable, biomass	Renewable, wind, solar, geothermy	Renewable, water	Total
Total	9.391	1.143	0.001	0.186	0.635	0.634	11.990
Others	0.595	0.020	0.000	0.008	0.001	0.008	0.633
Transport	0.699	0.012	0.000	0.005	0.001	0.005	0.722
Electricity	8.120	1.111	0.001	0.174	0.633	0.621	10.660

Electricity Transport Others Total

Figure 5. Primary-energy resources considered for CED estimation, with aggregated and disaggregated values.

As shown in Table 7, gas natural, crude oil, and hard coal represent 77.3% of the overall amount of fossil primary-energy resources, and so can be considered as the most consumed ones within the process.

Electricity is the most impacting item, with the aforementioned energy resources exhibiting comparable values in the range 90-98% as of Table 7, except for crude oil, with a far lower contribution rate being around 54%. This should be attributed to the transport issue showing – as expected - its greatest contribution (26.3%) in crude oil rather than in the other ones.

Table 7. Inventory and CED values for each of the most contributing fossil primary energy resources, with details on the contributions given by electricity, transports, all of the other processes, materials and phases

Primary Energy Resources	**Inventory**		**CED**	**Electricity**	**Transport**	**Others**
	Amount	**UM**	**GJ**	**[%]**		
Gas, natural	95.6	kg	5.41	97.9	0.9	1.2
Oil, crude	49.6	kg	2.27	53.7	26.3	20.0
Coal, hard	81.5	kg	1.56	93.9	3.0	3.1
Others (*)	66.6	kg	0.15	90.1	4.3	5.6

These are the resources that contribute far less than the others and are represented by coal brown, peat and gas mine. ‘Others’ represent 1.60 % of the total primary energy resources.

The same was found for ‘*Others’*, as they contribute a total of 20% to the CED associated with crude oil, which is far higher than that shown in the case of the other energy resources (1.2-5.6%). This should be attributed to materials, processes, and phases grouped in this category consuming, overall, more crude oil than gas natural or hard coal or other minor energy resources, as considered by the CED assessment method used in this study.

5.3.3. Water footprint assessment

At the mid-point approach, the WSI resulted equal to 4.15 m^3, and was significantly due to the cleaning steps as operational water and to the consumption of electricity as virtual water. With regard to the damage assessment step, Table 8 shows the DCs affected by the overall consumption of water. In detail, ‘*water*’, ‘*electricity*’, ‘*transportation*’ and ‘*others*’ columns refer to water consumption due to the recycling-process and water consumption embodied in the electricity consumed as well as in the transports and in all the other materials, processes, grouped under the ‘*others*’.

As for the CF assessment, it was not possible to weigh the three DCs and identify the most affected one, because each of them is assigned a specific damage indicator, which is established by Eco-Indicator 99. However, from Table 8, it is possible to assert that for each DCs the most damaging issue is the consumption of operational water with contribution around 65%, followed by electricity with a 25.15% average contribution.

Table 8. Results from the WF-related damages assessment (endpoint approach), with percentages for the most contributing items within the system investigated.

Damage categories (DCs)	Damages assessment		Water	Electricity	Transport	Others
	UM	Amount	[%]			
Resources	MJ surplus	1.24E+01	69.29	21.07	2.07	7.57
Ecosystem Quality	PAF*m2yr	3.69E+00	61.97	29.05	1.95	7.03
Human Health	DALY	4.45E-06	65.32	25.33	2.03	7.31

5.4. Interpretation and improvements

This study highlighted that the electricity required by the process for 1 ton of recycled-LDPE production (942.75 kWh) is the largest contributor to both the CF and CED, so emphasizing upon the importance to search for potential improvements. In agreement with the firm technicians, it was understood that no solutions are viable at the plant level by improving the technical quality and energy efficiency of machineries used in the production process. Therefore, electricity consumption is with no doubt the major energy and environmental issue of the whole system. Nonetheless, the energy/environmental burden associated with the electricity consumption may be reduced through a change in the energy source, by shifting it from fossil to renewable. A valid solution could be to install a wind power plant to cover the whole energy demand. In this regard, a first sensitivity analysis conducted for the purpose highlighted significant reductions for all the three indicators that have been addressed in this study, with CED and GWP_{100} showing the greatest reduction of about 56% and 85%, respectively, as they are clearly most affected by electricity use (Figure 6). It should be observed that this is just a preliminary evaluation that must be checked in terms of technical and economic feasibility.

By contrast, no solutions were found to be viable for reduction of the water consumption demanded by the process in the cleaning steps.

Finally, to validate the energy and environmental sound of the recycled-LDPE granule, another sensitivity analysis was conducted with the virgin counterpart of the LDPE granule, on the same base of FU and system boundaries. In addition, a comparable quality level was assumed between the two differently produced LDPE granules. It was found that, for all indicators considered in the study, i.e. CF, CED and WF, production of LDPE from APW is far more sustainable than the virgin counterpart (Figure 7), mainly because the recycled-LDPE granules is produced from a zero-burden resource, like the AWP utilized, rather than crude oil as happens for the virgin equivalent. In detail, the considered indicators decreased of about 85% (CED), 69% (GWP_{100}) and 32% (WSI). Such a result contributes validating processes like this as viable for production of comparable-quality secondary raw materials for application in the market.

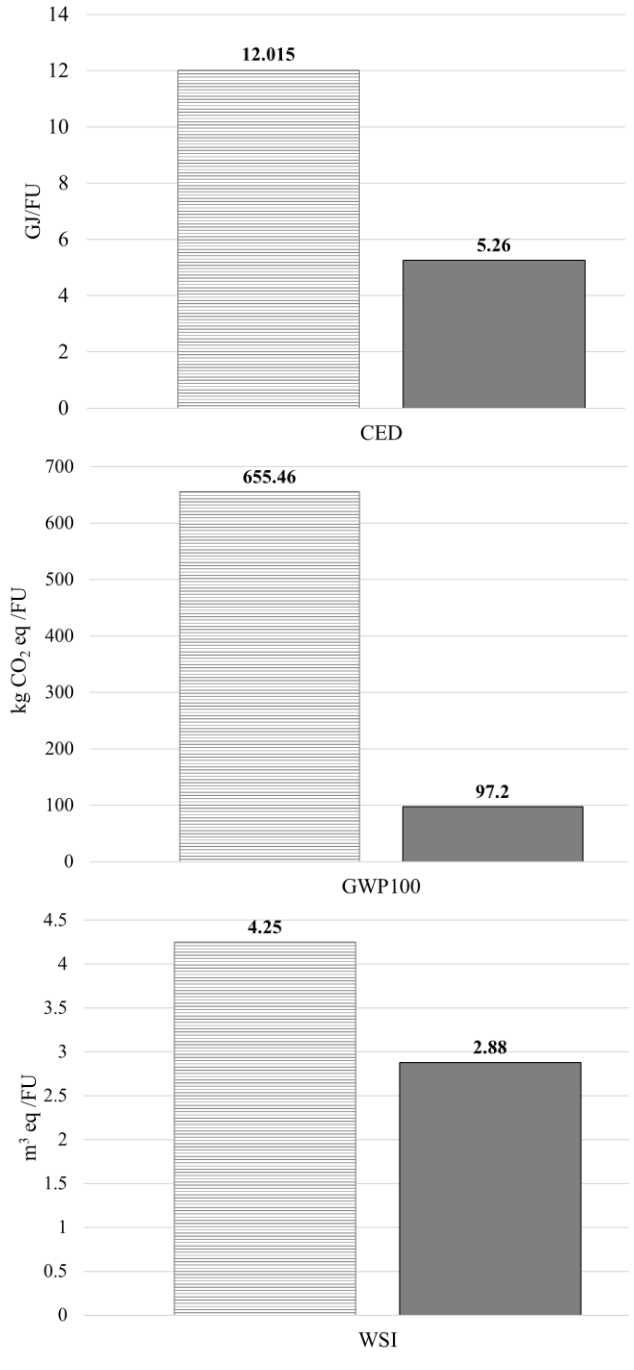

Figure 6. Comparison based upon application of the wind power based solution. The horizontal lines-column is referred to results from the first study, while the grey column reports results from the improved study.

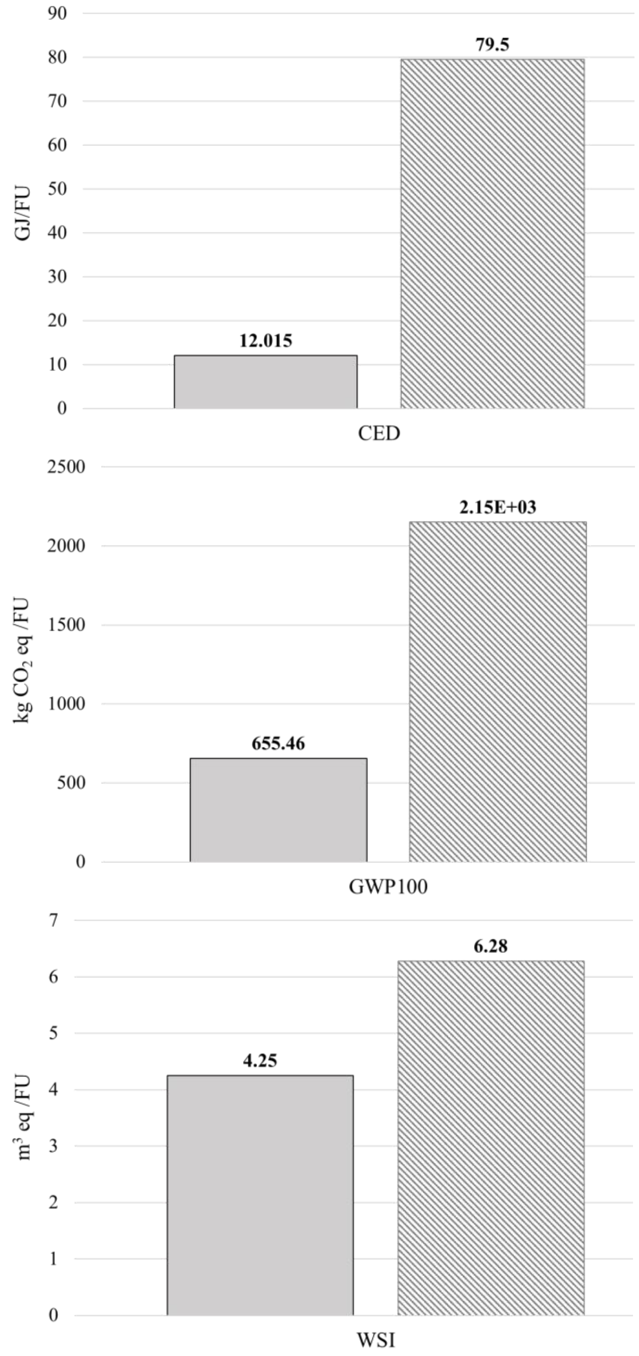

Figure 7. Comparison between the recycled-LDPE (light grey column) and the virgin counterpart (diagonal lines-column).

5.5. Conclusion

The study attained the proposed goal of evaluating the environmental impacts generated from the recycling of plastic films used for greenhouse cultivation system. To this end, a Life Cycle Assessment (LCA) approach was adopted and applied to an Italian firm located in Sicily, representative of the agricultural plastic waste (APW) collection and recycling.

The main conclusions related to the key indicators for the assessment of energy and environmental performance are the following:

- The CF was equal to 655.46 $kgCO_2$, showing that CO_2, CH4 and N_2O are the most significant GHGs emitted, since they represent the 94.87%, and electricity was the largest contributor for each of these GHGs.
- The CED was found 12.015 GJ per kg of recycled LDPE granules, with electricity contributing 88.72% produced from fossil origins for 76.17%. Gas natural, crude oil, and hard coal represented 77.3% of the fossil primary-energy resources.
- The WSI was 4.15 m^3, with significant contributions coming from the cleaning steps of the process as operational water, and from the consumption of electricity as virtual water.

Other important lessons were learned through the two sensitivity analyses that were incorporated in this study. The first showed that the energy and environmental impacts associated with the electricity consumption could be reduced through the installation of a wind power plant, resulting in significant reductions in all the three indicators addressed. While, the second allowed to understand that, despite the huge consumption of energy and water and the resultant GHG emissions characterizing the recycling process, the production of recycled-LDPE resulted as far more sustainable than the virgin counterpart, mainly because it is produced from a zero-burden resource rather than crude oil as happens for the virgin equivalent.

Such recycled granules can be considered as intermediate products for the manufacture of bags, pipes, and other products for several applications. Such transformations generally take place in industries outside Sicily, resulting in potentially high environmental impacts, mainly related to transport. For example, using polyethylene granules for construction applications, such as for the drainage layer in green roofs, is an innovative way of using this material, transforming it from an unfinished product into a finished product. The polyethylene granule as drainage material could be a cost-effective solution compared to those used for green roofs, from an environmental, economic and social point of view.

Furthermore, by considering the widespread diffusion of the eco-industrial technology, hydroponics, polyethylene granules could be used as an alternative substrate. In detail, this could contribute to reduce the use of inert substrates made of natural non-renewable materials and improve the environmental sustainability of the soilless crops production process in a circular economy perspective.

References

[1] M.R. Granadosa, S. Bonachela, J. Hernández, J.C. López, J.J. Magán, E.J. Baeza, J.C. Gázquez, J.J. Pérez-Parra, Soil temperatures in a mediterranean greenhouse with different solarization strategies, Acta Hortic. 927 (2012) 747–754.

[2] G. Scarascia-Mugnozza, C. Sica, G. Russo, Plastic materials in european agriculture: actual use and perspectives, J. Agric. Eng. Res. 42 (2012) 15–28.

[3] D.K. Barnes, F. Galgani, R.C. Thompson, M. Barlaz, Accumulation and fragmentation of plastic debris in global environments, Philos. Trans. R. Soc. B. 364 (2009) 1985–1998.

[4] M. Nanna, M.T. Batista, F.J. Baptista, E. Schettini, G. Vox, Mapping greenhouse plastic wastes in the west region of Portugal, Acta Hortic. 1227 (2018) 257–263.

[5] J.I. Montero, J.C. López, M. Teitel, Developments in covering materials for intensive horticulture: Technical properties and recycling opportunities, Acta Hortic. 1015 (2014) 269–280.

[6] Y. Aryan, P. Yadav, S.R. Samadder, Life Cycle Assessment of the existing and proposed plastic waste management options in India : A case study, J. Clean. Prod. 211 (2019) 1268–1283. doi:10.1016/j.jclepro.2018.11.236.

[7] D. Briassoulis, E. Babou, M. Hiskakis, G. Scarascia, P. Picuno, D. Guarde, C. Dejean, Review , mapping and analysis of the agricultural plastic waste generation and consolidation in Europe, Waste Manag. Res. 31 (2013) 1262–1278. doi:10.1177/0734242X13507968.

[8] P. Picuno, C. Sica, R. Laviano, A. Dimitrijevi, G. Scarascia Mugnozza, Experimental tests and technical characteristics of regenerated fi lms from agricultural plastics, Polym. Degrad. Stab. 97 (2012) 1654–1661. doi:10.1016/j.polymdegradstab.2012.06.024.

[9] O. Horodytska, F.J. Valdés, A. Fullana, Plastic flexible films waste management – A state of art review, Waste Manag. 77 (2018) 413–425. doi:10.1016/j.wasman.2018.04.023.

[10] F. Gu, J. Guo, W. Zhang, P.A. Summers, P. Hall, From waste plastics to industrial raw materials: A life cycle assessment of mechanical plastic recycling practice based on a real-world case study, Sci. Total Environ. 601–602 (2017) 1192–1207. doi:10.1016/j.scitotenv.2017.05.278.

[11] T.A. Hottle, M.M. Bilec, A.E. Landis, Biopolymer production and end of life comparisons using life cycle assessment, Resour. Conserv. Recycl. 122 (2017) 295–306. doi:10.1016/j.resconrec.2017.03.002.

[12] S. Martínez-Lera, J. Torrico, J. Pallarés, A. Gil, Thermal valorization of post-consumer film waste in a bubbling bed gasifier, Waste Manag. 33 (2013) 1640–1647.

[13] C. Arcidiacono, S.M.C. Porto, A model to manage crop-shelter spatial development by multi-temporal coverage analysis and spatial indicators, Biosyst. Eng. 107 (2010) 107–122.

[14] K.R. Caffrey, M.W. Veal, Conducting an Agricultural Life Cycle Assessment: Challenges and Perspectives, Sci. World J. 2013 (2013) 1–13.

[15] C. Ingrao, F. Licciardello, B. Pecorino, G. Muratore, A. Zerbo, A. Messineo, Energy and environmental assessment of a traditional durum-wheat bread, J. Clean. Prod. 171 (2018) 1494–1509. doi:10.1016/j.jclepro.2017.09.283.

[16] F. Valenti, S.M.C. Porto, G. Chinnici, G. Cascone, C. Arcidiacono, A GIS-based model to estimate citrus pulp availability for biogas production: an application to a region of the Mediterranean Basin, Biofuels, Bioprod. Biorefining. 10 (2016) 710–727.

[17] R. Frischknecht, G. Rebitzer, The ecoinvent database system: A comprehensive web-based LCA database, J. Clean. Prod. 13 (2005) 1337–1343.

[18] B. Notarnicola, G. Tassielli, P.A. Renzulli, F. Monforti, Energy fl ows and greenhouses gases of EU (European Union) national breads using an LCA (Life Cycle Assessment) approach, J. Clean. Prod. 140 (2017) 455–469. doi:10.1016/j.jclepro.2016.05.150.

[19] M.A.J. Huijbregts, Application of uncertainty and variability in LCA, Int. J. Life Cycle Assess. 3 (1998) 273–280.

[20] L. De Benedetto, J. Klemeš, The environmental bill of material and technology routing: An integrated LCA approach, Clean Technol. Environ. Policy. (2010) 191–196.
[21] C. Maalouf, C. Ingrao, F. Scrucca, T. Moussa, A. Bourdot, C. Tricase, A. Presciutti, F. Asdrubali, An energy and Carbon Footprint assessment upon the usage of hemp-lime concrete and recycled-PET façades for office facilities in France and Italy, J. Clean. Prod. 170 (2018) 1640–1653.
[22] D. Gürzenich, J. Mathur, N.K. Bansal, H.J. Wagner, Cumulative energy demand for selected renewable energy technologies, Int. J. Life Cycle Assess. 4 (1999) 143–149.
[23] K. Wiesen, M. Wirges, From cumulated energy demand to cumulated raw material demand: the material footprint as a sum parameter in life cycle assessment, Energy. Sustain. Soc. 7 (2017) 1–13.
[24] M.A.J. Huijbregts, L.J.A. Rombouts, S. Hellweg, R. Frischknecht, A.J. Hendriks, D. Van De Meent, A.M.I. Ragas, L. Reijnders, J. Struijs, Is cumulative fossil energy demand a useful indicator for the environmental performance of products?, Environ. Sci. Technol. 40 (2006) 641–648.
[25] V. Girgenti, C. Peano, M. Bounous, C. Baudino, Science of the Total Environment A life cycle assessment of non-renewable energy use and greenhouse gas emissions associated with blueberry and raspberry production in northern Italy, Sci. Total Environ. 458–460 (2013) 414–418. doi:10.1016/j.scitotenv.2013.04.060.
[26] S. Pfister, A. Koehler, S. Hellweg, Assessing the environmental impacts of freshwater consumption in LCA, Environ. Sci. Technol. 43 (2009) 4098–4104.

6. Thermal behavior comparison between innovative and commercial green roofs in Mediterranean summer conditions

6.1. Introduction

In recent year, several studies analyzed the thermal performance of green roofs during summer in Mediterranean climate. Olivieri et al. [1] analyzed the impact of vegetation density on the energy performance of a green roof by monitoring the surface temperatures and the thermal fluxes through a roof in three periods of time characterized by similar climate conditions but by a different degree of vegetation density. From the results it was deduced that when the roof had dense vegetation the thermal gain entering the roof went down by about 60% compared with the roof with no vegetation. Moreover, the roof with vegetation acted as a passive cooling system, as the outgoing energy throughout the summer was about 9% greater than the incoming energy during the same period. Bevilacqua et al. [2] evaluated the temperature levels and the thermal performances of different layering solutions compared to a reference configuration representing the original configuration of the roof surface before the installation of the green roof. The results showed that in summer the green roof was able to maintain a noticeable lower temperature at the base of the additional green stratigraphy. The plots were able to produce a temperature approximately 12 °C lower than the average surface temperature of the reference roof at the interface with the structural roof. The presence of the green roof determined also a reduction of the internal environment temperature on average of 2.3 °C in the investigated summer period, demonstrating the quality of this solution to decrease the cooling demand for the building air-conditioning. The green roof plots generated negative heat fluxes during the investigated summer period, producing a passive cooling of the building room through the structural roof, and provided a reduction of the ingoing thermal energy of 100% in summer when compared to the ingoing energy into the reference room. Azeñas et al. [3] quantified the contribution of vegetation to the thermal regulation capacity in a green roof system, evaluated the effect of two different plant types and canopy architectures (grasses and succulents) on thermal regulation capacity and assessed the effect of irrigation treatment on thermal regulation capacity. The results showed that the presence of vegetation improved the thermal insulation capacity of the green roof by reducing the total transferred heat between 48% and 86% along the different seasons. Moreover, important differences between plant species were observed. *Sedum sediforme*, despite having been reported as a low water consumer, increased the thermal insulation capacity of the green roof between 82% and 86%. Similarly, water-limited irrigation treatment was shown to increase the thermal insulation capacity when compared to complete well-watered irrigation treatment, by reducing the total transferred heat between 25% and 71% along the different seasons of the year, suggesting that the air/water substrate content has a greater effect on insulation than evapotranspiration.

Some studies analyzed the thermal performance of green roof using innovative materials. Coma et al. evaluated and compared two extensive green roofs solutions without insulation layer, where the only difference lies in the drainage layer material (one of them with pozzolana and the other with recycled rubber from waste tires) with a conventional flat roof. The two extensive green roofs reduced the cumulative electrical energy consumption in 16.7% and 2.2% respectively, compared to the cumulative electrical energy consumed by conventional flat roof during representative periods of cooling demand. Therefore, extensive green roofs, especially with rubber crumbs as drainage layer, can be a good tool for passive energy savings during summer periods in dry Mediterranean continental climate. Almeida et al. [4] assessed the thermal behavior of a green roof system containing insulation cork board used as water drainage and storage layer. It was found that this layer has the better insulation capacity, although adding layers led to improved thermal insulation. When the green roof was subjected to wetting, the temperatures across the system were influenced by the temperature of the water penetrating the layers and by the variation of the thermal conductivity coefficients of the materials. Just after the wetting period the system started to recover its dry values. The cork board layer was found to recover its performance more quickly than the substrate layer.

Finally, only few researches determined the dynamic parameters of green roofs in summer conditions. Porcaro et al. [5] determined the thermal performance of three green roofs with different substrates for the retrofitting of existing buildings, compared to a traditional gravel ballasted roof. Hence, several dynamic parameters were studied for each roof, such as decrement factor, DF, time lag, TL, sol-air temperature, T_{sa}, cooling potential, CP, and annual reduction of energy demand in $kWhm^{-2}$. The experimental results showed that the three plots with green roofs achieved high reduction of DF and high increases of CP, compared to the reference roof for warm and dry climate, with a weekly average reduction of DF equal to 0.24 and a weekly average increase of CP equal to 16.3 °C. Significant increases of TL for the green roofs were obtained, up to 6:08 h and 6:34 h during the hot and cold periods considered, respectively, compared to the reference roof. Finally, significant reductions of energy gains during the hot period and energy losses during the cold period were obtained in the three green roofs, compared to the reference roof. The annual average reductions in energy gains and losses of the three green roofs were 66% and 63%, respectively.

Bevilacqua et al. [6] performed a comprehensive experimental dynamic characterization in summer condition of an extensive green roof with the aim of assessing thermal inertia properties. The analysis of the experimental daily values of dynamic parameters for the three green roof solutions implemented in the experimental site showed that the decrement factor can be considered to have a quite stable trend, as confirmed by the low values of standard deviations that in the whole period of analysis were 0.019, 0.026 and 0.022. The time lag that showed a more variable trend in every Plots around the mean seasonal values of 7.2 h in two plots and 8.50 in one plot.

In this thesis chapter, the thermal performance of a green roof using the recycled polyethylene granule as drainage layer and the substrate consisting of a high percentage of organic matter have been determined in order to increase retention water supply and reduce the water to be supplied. The thermal performance of the proposed system is compared with those of two commercial green roofs and those of the existing roof. To this end, a set-up was installed at the University of Catania having the goal of assessing the thermal performance of different green roof technologies. The analysis of thermal behavior involved both thermo-physical parameters (surface temperatures and heat flows) and dynamic parameters (decrement factor and time lag).

6.2. Materials and methods

6.2.1. The existing roof and the sample structure

The experimental set-up was made on the flat cover of the Department of Agriculture, Food and Environment (Di3A) of the University of Catania (37°32'07.76"N; 15°04'05.96"E) which does not have relevant shading throughout the day and is easily accessible via an elevator (Figure 1). Catania is characterized by a Mediterranean climate (Csa according to the Koppen-Geiger classification), with mild winter and warm and dry summer. During the summer, maximum air temperatures exceed 40 °C, with high daily thermal excursions between day and night.

The existing roof, named "Reference", consists of the following layers, from the bottom to the top: plaster (s=0.02 m), brick (s=0.20 m), concrete (s=0.07 m), lightened concrete screed (s=0.06 m), waterproofing membrane (s=0.01 m). This stratigraphy can be considered representative of the buildings built in the 1970s and 1980s in Catania.

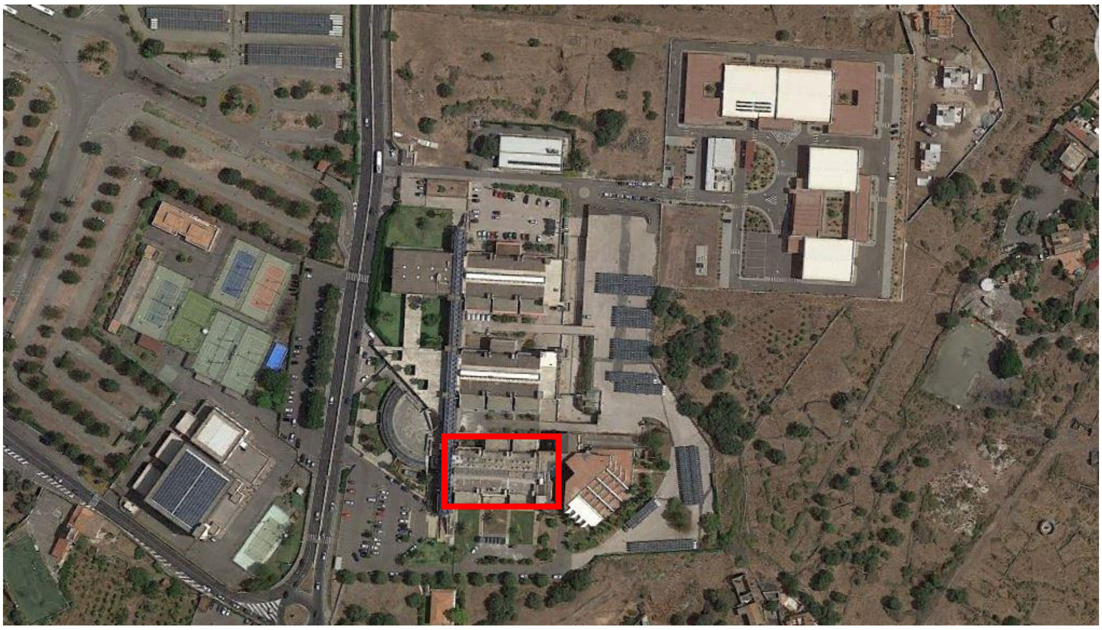

Figure 1. Position of the building case-study.

The set-up consists of three samples (2.50×2.50 m) allowing to assess the thermal performance of green roofs at a near-real scale, reducing the edge effect due to the small size of the samples (Figure 2). Two green roofs are conventional solutions available on the market while one is innovative as it was made from local materials.

Figure 2. Experimental set-up.

The structure of the samples to contain the materials of the green roof was made of phenolic fir wood (length 2.50 m, height 0.25 m and 0.018 m thick). Given that wood is a hygroscopic material, it has been treated to prevent the absorption of rainwater, resulting in an increase in durability. The wooden boards were connected in the corners by "L"-shaped stainless steel plates and threaded wood screws.

In addition, a tap connected to the building's water supply was built to power the irrigation system. Several researches have defined that in areas with Mediterranean climate the irrigation system must be installed to ensure the survival of vegetation due to prolonged summer periods of drought, unlike the rainy regions of northern Europe where extensive green roofs do not require irrigation. The irrigation system consists of a main flow pipe to which are connected a series of dripping wings placed at a distance of 33 cm for a total of 7 for each green roof sample. In each dripping wing are placed holes (drips) for the leakage of water, at 33 cm. In this way, 33 cm square meshes were created between two drips of a dripping wing and those of the adjacent dripping wing. During the installation phase of the irrigation system, it was checked that each dripper provides 1.15 l/h, for a total of about 9 l/(h×m^2) for each sample.

6.2.2. Common features of green roofs

The three green roof samples consist of the following materials, from bottom to top: drainage layer, filter layer, substrate and vegetation. For a detailed analysis of each layer and the materials currently used, refer to a previous review carried out by Cascone [7]. Given that the finishing layer of the existing roof consists of a reinforced waterproofing membrane, neither a new waterproofing membrane for the green roof nor the anti-root layer had to be installed.

The green roofs installed have a thickness of the substrate less than 15-20 cm, therefore they are extensive. For a detailed description of the typological characteristics of extensive green roofs and differences with intensive ones, refer to the review conducted by Cascone [7]. In the set-up installed, the thicknesses of the drainage layer and the substrate are 5 and 10 cm, respectively. The filter layer, in non-woven geotextile of grilled polypropylene with a mass of 100 g/m^2 and permeability greater than 3.5×10^{-3} m/sec, is placed between the drainage layer and the substrate.

In order to compare the thermal performance of the innovative green roof with those of the two commercial green roofs and the reference roof by varying the materials used for the drainage layer and the substrate, the vegetation remained unchanged between the different green roof samples. A pre-cultivated *Agropyrum* lawn has been installed to facilitate the installation phase and reduce the time of growth and development of vegetation. In addition, this lawn is suitable for Mediterranean climatic conditions as it can withstand prolonged periods of drought.

6.2.3. Materials used for commercial samples

In the first commercial green roof, named "Perlite", the drainage and water storage layer is made with expanded perlite, granules 1-3 mm, packaged in bags of non-woven geotextile. The dimensions of these bags are 70×130 cm and weigh 160 g/m^2. In addition, they were placed well-juxtaposed in order to obtain a thickness as uniform as possible (about 5 cm) and were wet before the substrate was laid, as suggested by the manufacturer. Given the reduced slope of the roof, the perlite bags were combined with a hot joined net with non-woven geotextile, 5 mm thick, placed between the existing waterproof membrane and the perlite, in order to facilitate water drainage. The substrate consists of natural components, namely a mixture of lapilli, pumice, peat and organic fertilizers. This substrate is suitable for extensive green roofs with roll grass carpet and has been packaged in 1500 liter per bags.

The second commercial system, named "Daku", consists of expanded polystyrene panels as layer of drainage and water storage, produced with unrecycled virgin raw material, 125 × 100 cm size. The top of the panel has a series of cells that store water, with a maximum capacity of about 5 l/m^2. The bottom of the panel has supports with a diameter of 36 mm and 20 mm high that allow the outflow of water that cannot be stored inside the cells. The substrate consists of a mix of volcanic mineral materials mixed with organic substances, i.e. lava lapilli and pumice stone in different grains, as well as a peat finer. Like the substrate used in Perlite, this substrate is also weed-free and has been packaged in a 1 m^3 big bag.

The characteristics of the materials used for the drainage layer and the substrate are summarized in Table 1 and Table 2, respectively.

Table 1. Characteristics of the commercial green roof drainage layer.

Features	**Perlite**	**Daku**
Panel size	-	1250 x 1000 (mm)
Granulometry	1 ÷ 3 (mm)	-
Dry density	110 ± 20% (kg/m^3)	25 ± 10% (kg/m^3)
Compacted density		-
Water storage capacity	27,5 (l/m^2)	5,0 (l/m^2)
Dry thermal conductivity	0,050 (W/mK)	0,034 (W/mK)
Free air volume with maximum water storage	-	18,8 (l/m^2)
Total porosity	>95% v/v	-

Table 2. Characteristics of the commercial green roof substrate.

Features	**Perlite**	**Daku**	**UNI 11235**
Dry density	950 ±5 % kg/m^3	650-750 kg/m^3	350-1000 kg/m^3
Density in saturation	1350 kg/m^3	1072 Kg/m^3	-
Water storage capacity	40 l/m^2	N/A	-
Total porosity	>60 %	≥ 70 %	>60 %
Air volume at pF1	>18 %	30-40 %	≥ 15 %
Water volume at pF1	>40 %	> 30 %	≥ 10 %

Vertical permeability	> 6 (mm/min)	> 30 mm/min	≥ 10 mm/min
pH	6 ÷ 7	7 ÷ 8	4.0 ÷ 8.5
Electrical conductivity	< 40 mS/m	24 mS/m	≤ 50 mS/m
Cationic Exchange Capacity	>12 meq/100 g	16,3 meq/100g	≥ 8 meq/100g
Organic matter	< 5%	41 g/litro s.s.	≤ 60 g/litro s.s.
Degree of volume reduction	20%	< 7 %	-
Dry thermal conductivity	0,141 W/mK	N/A	N/A
Thermal saturation pipelines	0,441 W/mK	N/A	N/A

6.2.4. Innovative green roof solution

The third sample, named "Unict", uses materials from local companies, thereby reducing transport costs and increasing the sustainability of green roofs. In the previous thesis chapter 5, the environmental impacts of the low-density polyethylene granule (LDPE) production process from recycling plastic sheets used to cover agricultural greenhouses were analyzed. In particular, the company in the province of Ragusa that provided the material for this research was examined as a case study. Results showed that recycling polyethylene granules significantly reduces environmental impacts compared to the production process of virgin polyethylene granules and the environmental impact of the recycling process is mainly related to significant amount of electricity used.

In this research, recycled polyethylene granule was used as an innovative material for green roof drainage. This material has been placed within micro-drilled plastic nets used to shade and protect agricultural crops from hail. The small size of the holes allows the drainage of the water. In addition, these micro-drilled bags, 1.25x1.25 m in size to cover the entire area with a total of 4 bags, reduced the time of laying the drainage layer and prevented the dispersion of the granules. The recycled granule has density 0.92-0.94 g/cm^3 e apparent density 500 kg/m^3, as certified by the manufacturer. The substrate has been specially formulated for this research and is composed of the following materials: 30% perlite, 30% peat and 40% volcanic material. Compared to the commercial substrates described above and used in the other two green roof samples, this substrate has a higher content of organic matter. In fact, the state-of-the-art review on the materials used in green roofs [...] has shown that, in rainy regions, such as those in northern Europe, a high percentage of inorganic material is required in the substrate as it is necessary to drain the high amount of rainwater to reduce the weight on the roof. On the contrary, in areas characterized by warm and dry climates, it is necessary to store water in the substrate during rain and irrigation, in order to make it available to vegetation through evapotranspiration. This substrate was formulated at the Department of Agriculture, Food and Environment of the University of Catania using local components from a farm.

6.2.5. Sensor characteristics and location

In order to assess the thermal behaviour of green roofs, sensors were installed to monitor the following parameters: thermal flow; surface temperature between layers; water content in the substrate (VWC); surface temperature of the substrate. The list of sensors and their characteristics is indicated in Table 3. In addition, a weather station located on the roof of the Department of Electrical, Electronic and Computer Engineering was used for monitoring weather conditions (Table 3).

Table 3. Sensor characteristics.

	Model	**Principle**	**Range**	**Uncertainty**	**Resolution**
Green roof sensors					
Thermal flow	DPE240	Termopila	-2000÷+2000 W/m^2	5% su 12 h	50 µV/W/m^{-2}
Surface contact temperature	DLE124	Pt100 1/3 DIN B	-50÷70°C	0.1°C	0,01°C
Water content	DQA340	Time domain reflectometry	0÷100%	0÷40%: ± 1% 40÷70%: ± 2%	0,1%
Substrate surface temperature	DLE041	Pt100 1/2 DIN B	N/A	N/A	0,15°C
Weather station					
	Model	**Principle**	**Range**	**Uncertainty**	**Resolution**
Temperature	DMA672.1	Pt100 1/3 DIN B	-50÷+70°C	0,1°C (0°C)	0,01°C
Relative humidity	DMA672.1	Capacitive	0-100%	±1,5% RH (5-95%)	-
Wind speed	DNA202	Relay Ree	0÷75 m/s	2,5%	0,5 m/s
Wind direction	DNA212	No contact Hall effect sensor	0÷360°	5°	0,25 m/s
Radiation	DPA053	Thermopila	305÷2800 nm	10% daily	-
Rain	HD2015	-	-	-	0.5 mm

The surface temperature of the substrate, temperature between the substrate and the drainage layer, temperature between the drainage layer and existing waterproofing membrane, water content in the substrate (at the base), thermal flow between the substrate and drainage layer and thermal flow between the drainage layer and waterproofing membrane (positive thermal flows are incoming while negatives are outgoing) have been monitored (Figure 3). A thermal flow sensor was placed on the surface of the substrate. In addition, a surface temperature sensor was placed inside the room located below the green roof Unict.

In order to compare the thermal performance of the green roofs with those of the reference roof, a surface temperature sensor was placed both on the existing waterproofing membrane and inside the room below (Figure 3). Both the sensors below the green roof and those below the reference roof are placed inside the same room, in order to reduce the uncertainties related to the different use and exposure. This room is intended for office and has been regularly used during the monitoring period.

The sensors listed above have been connected to a data logger (ELO305-ELO105 model, 22 inputs including 16 analog, 4 impulsive and 2 on-off) recording data every 10 minutes.

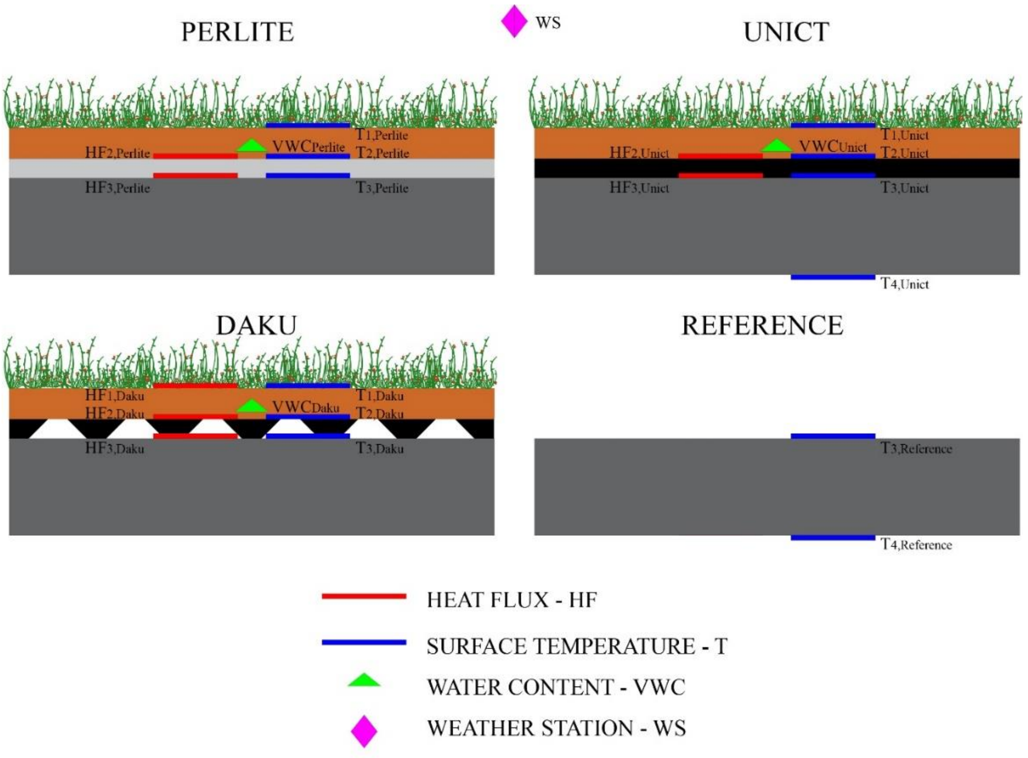

Figure 3. Sensor position.

6.2.6. Data analysis

The construction of green roofs, including vegetation, ended in May 2019, therefore, the monitoring period began on 1 June 2019. Irrigation has been set to provide water three times per day (1.00 p.m., 8:00 p.m. and 8:00 a.m.) for 20 minutes each. The week between 01/07/2019 and 06/07/2019 was chosen as representative of the typical summer conditions in the Mediterranean climate, with high solar radiation and no rains.

Figure 4 shows the air temperature and solar radiation measured by the weather station during the monitoring period.

First, the evolution of temperatures, thermal flows and water content in the substrate was analyzed. In addition, a statistical temperature analysis was carried out, counting how many values fall within temperatures ranges between 22 and 30 °C with steps 0.5 °C. In addition, the cumulative function was calculated.

Finally, the experimental green roof analysis was evaluated according to several dynamic parameters used in previous studies. The dynamic parameters evaluated were the following:

- Decrement factor, DF, is defined as the ratio between the maximum daily excursions of the internal and external temperature fluctuations, expressed by Eq. (1).

$$DF = \frac{T_{i,max} - T_{i,min}}{T_{e,max} - T_{e,min}} \quad (1)$$

- Time lag, TL, is defined as the time difference between the maximum peak of the internal temperature and the maximum peak of the external temperature for summer climatic conditions, expressed by Eq. (2):

$$TL = \tau_{Ti,max} - \tau_{Te,max} \quad (2)$$

  DF and TL were evaluated considering the substrate surface temperature as the external boundary temperature for all the plots and the temperature between the existing waterproof membrane and the drainage layer (i.e. below green roof layers) as the internal boundary temperature.

- Cooling potential, CP, is defined according to Eq. (3).

$$CP = U \times A \times \sum(T_{1,Ref,day} - T_{1,GRi,day}) \quad (3)$$

  where A is the surface (1 m^2) and U is the thermal transmittance that is supposed unchanged varying the time. Therefore, per each day considered, this index represents the energy through the green roof.

The above parameters were determined daily and then averaged to define a single value for each green roof.

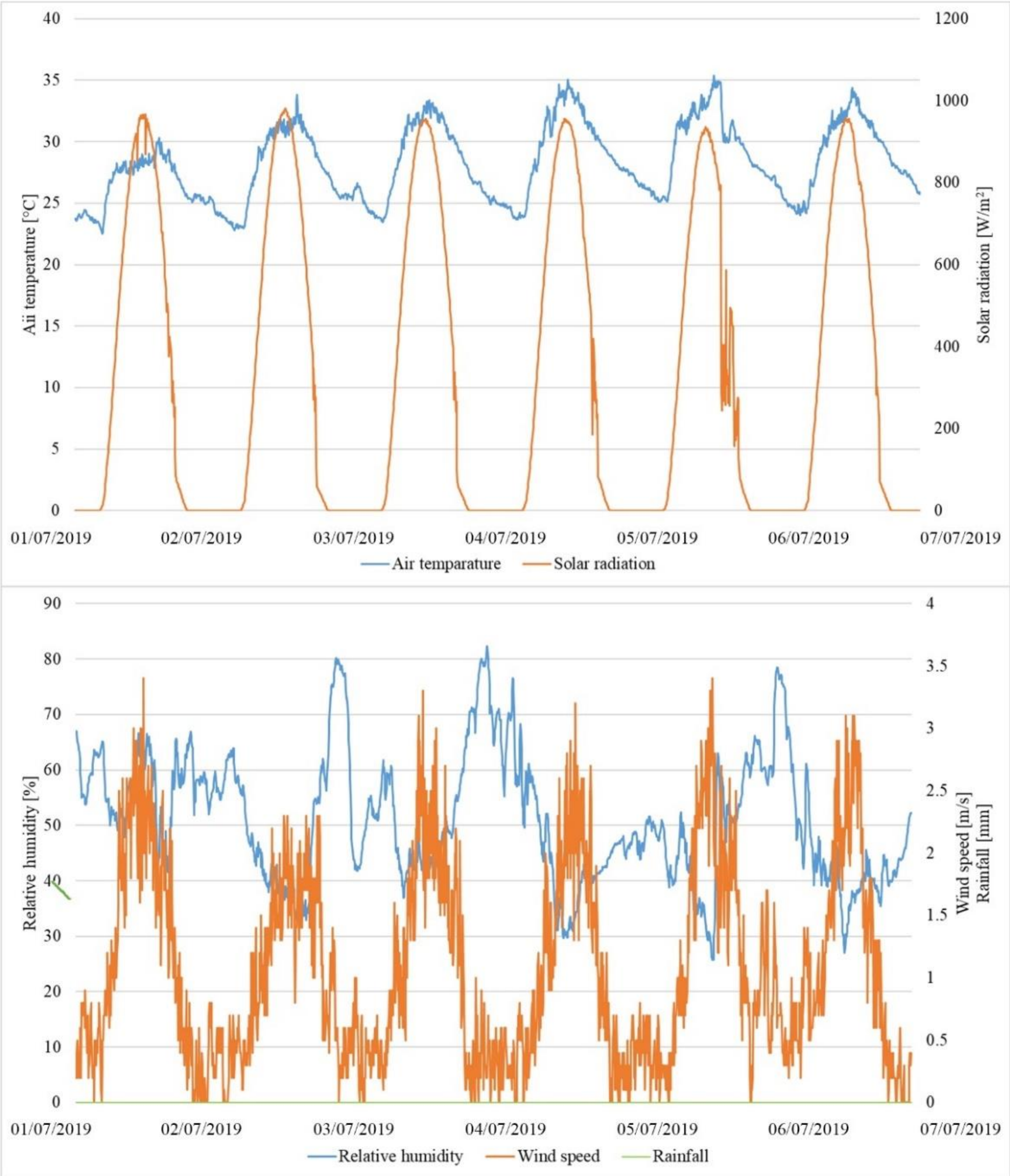

Figure 4. Wheater condition during the monitored period.

6.3. Results and Discussion

6.3.1. Thermal behavior of green roofs

The measured VWC showed significant differences in the green roofs analyzed (Figure 5). The VWC of the Perlite and Daku substrates follows the pattern of the irrigation regime, with a rapid increase when irrigation is on and a rapid decrease when irrigation is off. This variation in the VWC is significantly reduced in the Unict substrate. Perlite had the highest VWC (about 20%) throughout the monitoring period, as both the substrate and the drainage layer consist mainly of materials that are able to absorb significant amounts of water, allowing to keep moisture in the substrate high. The VWC of Daku substrate shows the widest variations (between 10 and 20%). Table

2 shows that Perlite and Daku substrates have similar characteristics and, therefore, this variation is mainly due to the different drainage layer. In fact, the drainage layer of the Daku system is made of plastic panels that can store water in the cavities, evaporating rapidly due to high solar radiation. These results show that, in the Mediterranean climate, water storage and drainage panels, widely used in other regions, have a reduced ability to maintain high VWC and, therefore, unsuitable in warm and dry climates. Finally, the VWC of Unict substrate remained almost unchanged (around 13%) despite irrigation. This substrate has a higher percentage of organic material than the others, in order to ensure a higher accumulation of water and, therefore, the water reaching the sensor is less than the other two substrates (mainly made of high-draining materials), as the VWC is measured at the base of the substrate. In addition, during the monitoring period, Unict vegetation developed better than other green roofs and, therefore, more water was used by vegetation for transpiration, reducing VWC in the substrate. Finally, the drainage layer made of the recycled polyethylene granule, being a plastic material, has no water retention capacity (unlike perlite) and, therefore, is not able to store water and provide it by evaporation to the substrate.

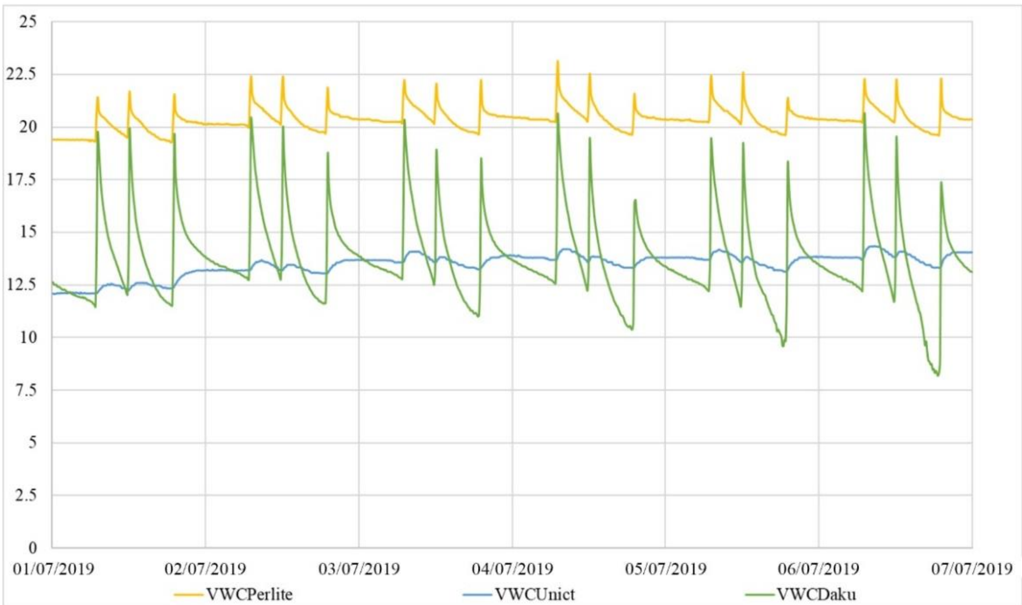

Figure 5. Volumetric water content.

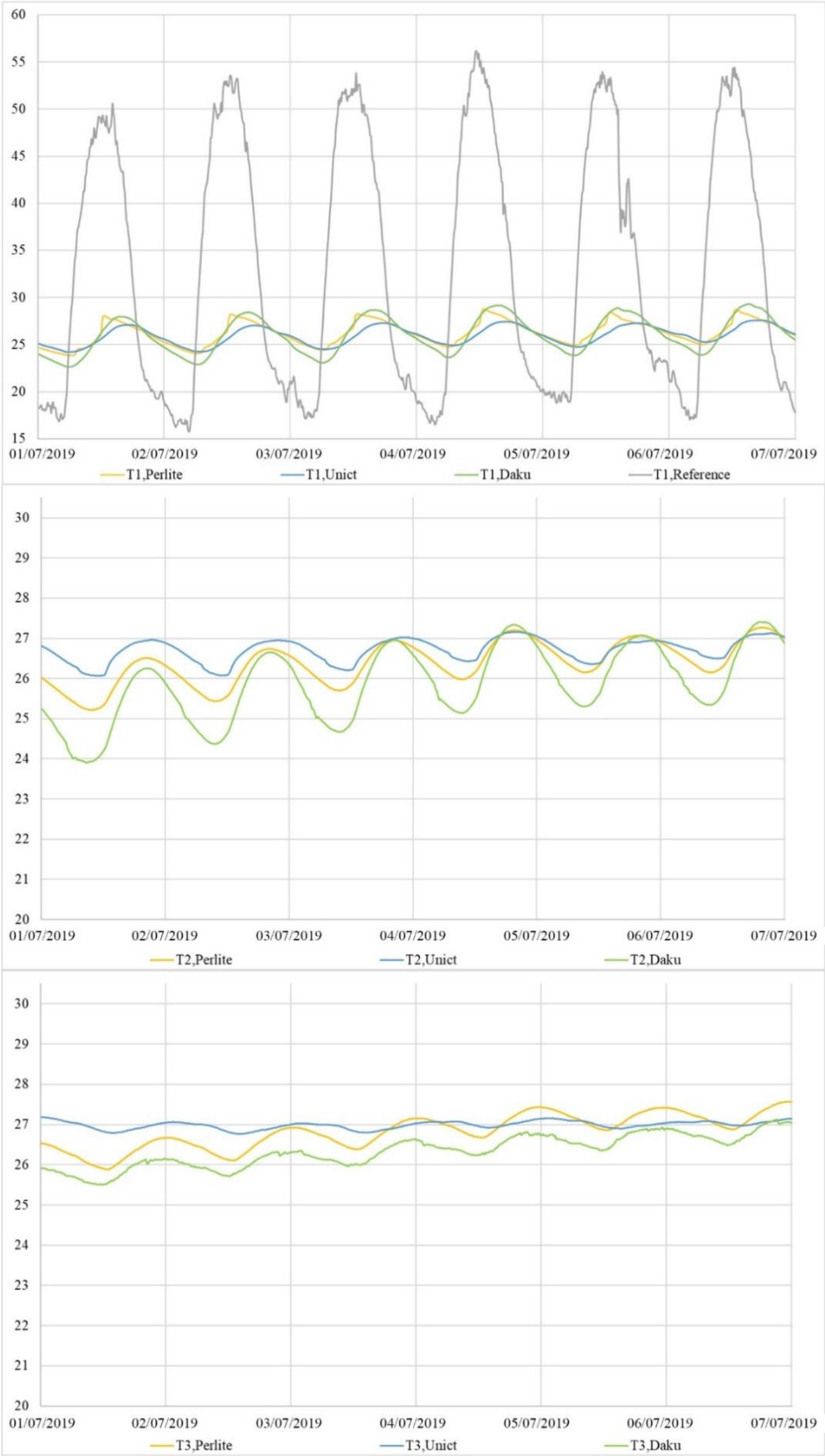

Figure 6. Surface temperatures (at the top), temperatures between the substrate and drainage layer (in the middle) and temperatures between the drainage layer and existing membrane.

Figure 6 shows the evolution of temperatures in the different layers of green roofs. In particular, the surface temperatures of the green roofs (measured below the vegetation and 2 cm of the substrate to avoid the influence of direct solar radiation) are considerably lower than the Reference roof, which reaches maximum temperatures of more than 50 °C, while green roofs reach maximum surface temperatures between 25 and 30 °C (graph at the top in Figure 6). This high reduction in surface temperatures is in line with several previous studies that highlighted the ability of green roofs to mitigate the urban heat island. The maximum surface temperatures of Perlite and Daku are similar while the Unict reaches lower surface temperatures. This reduction is mainly related to the better development of vegetation that has covered the substrate entirely, reducing its surface overheating.

Temperatures between the substrate and the drainage layer (graph in the middle of Figure 6) are lower in Daku and Perlite, due to the higher water content. However, their temperatures show significant daily fluctuations between maximum and minimum temperatures. The highest temperatures were measured in Unict. However, the latter has significantly reduced temperature fluctuations due to its ability to accumulate heat and the high amount of organic matter in the substrate. Similar comments can be made for temperatures between the drainage layer and the waterproofing membrane (graph at the bottom in Figure 6). The reduction in temperature fluctuations in Unict is even more evident (almost constant temperatures around 27 °C). In the days between 04/07/2019 and 07/07/2019, this reduction leads to lower temperatures in Unict than in Perlite.

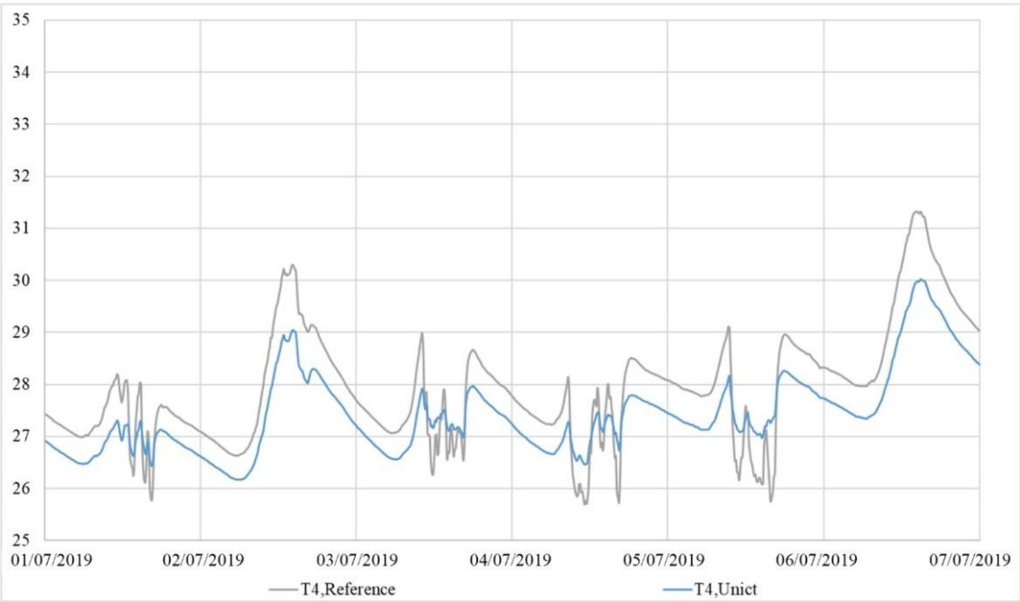

Figure 7. Internal surface temperatures.

Figure 7 shows the internal surface temperatures. In order to reduce the uncertainties related to the different use of the rooms, the probes were installed in the same room (covered for about half by the green roof and for the other half by the reference roof) and, therefore, must be considered a mutual influence on monitored internal surface temperatures, despite the sensors being placed at an appropriate distance (about 2 m) to reduce boundary effects. In addition, fluctuations in surface temperature on some days of the monitoring period are due to the ignition and shutdown of the cooling system.

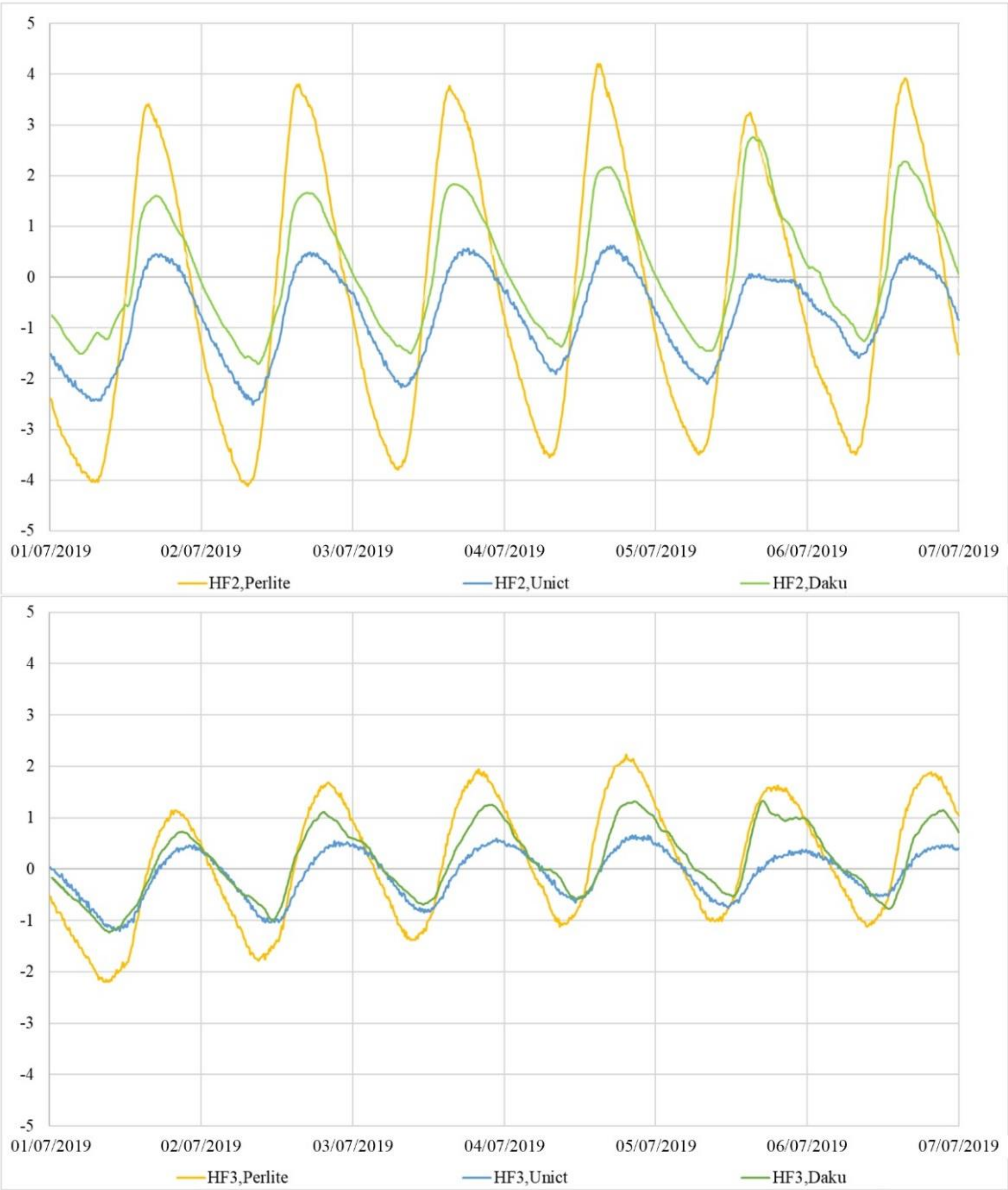

Figure 8. Heat flow between the substrate and drainage layer (at the top) and heat flow between the drainage layer and existing waterproof membrane (at the bottom).

Considering the days when the office was not used (02/07/2019 and 07/07/2019) and the air conditioning system was turned off, surface temperatures below the green roof are about 2 °C lower than the temperatures measured below the reference roof, resulting in a passive cooling effect due to the green roof and a reduction in energy consumption.

Finally, Figure 8 shows the heat flows below the substrates (graph above) and drainage layers (graph below). Positive heat flows are entering the roof while negatives are coming out of the roof.

Although Perlite and Daku had lower temperatures, Unict reduced heat flows across the green roof and enter the building, due to reduced temperature fluctuations. For example, the maximum heat flow for Unict is approximately 0.5 W/m^2 while the heat flow for Perlite is approximately 2 W/m^2.

Figure 9. Temperature distributions and cumulative function.

The temperature distribution analysis allowed to determine how many values fall within the temperature ranges with a 0.5 °C amplitude (Figure 9). Results show that the distribution of temperatures is less wide going from the surface layers to the innermost ones. In addition, Unict has a much higher temperature concentration than other samples that have a wider distribution. In fact, in Unict, both temperatures below the substrate and below the drainage layer are located for about 60% between 26.5 and 27 °C and between 27 and 27.5 °C, respectively. The cumulative temperature functions (graphs on the right in Figure 9) show that the Unict reaches the highest temperatures as the cumulative is shifted to the right. However, given that Unict reduces temperature fluctuations, the cumulative is more vertical than those of other green roofs.

6.3.2. Dynamic parameters

Figure 10 shows the daily and average weekly decrement factor for green roofs. Lower is the decrement factor, higher is the reduction in cyclical temperature on the inside surface compared to the outside surface. Perlite has the highest decrement factor while Unict is the green roof with the lowest decrement factor, with a weekly average of 0.19 and 0.10, respectively. The best dynamic thermal performance is mainly due to the substrate, made with a higher content of organic matter than commercial substrates.

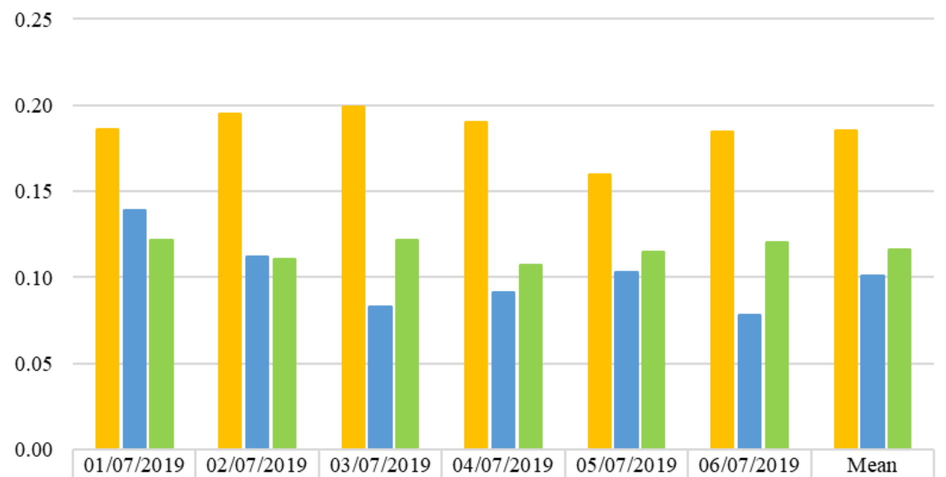

	01/07/2019	02/07/2019	03/07/2019	04/07/2019	05/07/2019	06/07/2019	Mean
Perlite	0.19	0.19	0.20	0.19	0.16	0.18	0.19
Unict	0.14	0.11	0.08	0.09	0.10	0.08	0.10
Daku	0.12	0.11	0.12	0.11	0.12	0.12	0.12

Figure 10. Daily and weekly average decrement factor.

Figure 11 (above) shows time lag determined using daily minimum and maximum temperature values. Perlite has the largest time lag (11.3 h) while Daku is the green roof with the lowest time lag (7.7 h). However, as shown in Figure 6, surface temperatures already have a time lag compared to the time when there is maximum solar radiation, at 1 p.m. This delay is due to the position of the surface temperature sensor, located below 2 cm of substrate. In addition, the biggest delay occurs in Unict, as there is also the contribution of vegetation that further protects the sensor, reducing the surface temperature and delaying the effect of solar radiation. Therefore, time lag was also determined by considering as a boundary condition the time in which there is maximum solar radiation (1 p.m.) (graph at the bottom of Figure 11), by modifying Eq. 2 as follows:

$$TL_{1p.m.} = \tau_{Ti,max} - \tau_{=1p.m.} \tag{4}$$

This parameter allowed comparing the performance of green roof by excluding the time lag due to only vegetation while accounting all green roof layers.
In such conditions, the green roof with the largest time lag is Unict (13.4 h) while the one with the lowest time lag remains Daku (9.9 h).
Results for decrement factor and time lag show small variations between days (except time lag for Unict on 05/07/2019), demonstrating the reliability of temperatures measured during the monitoring period with similar weather conditions in the seleted days.

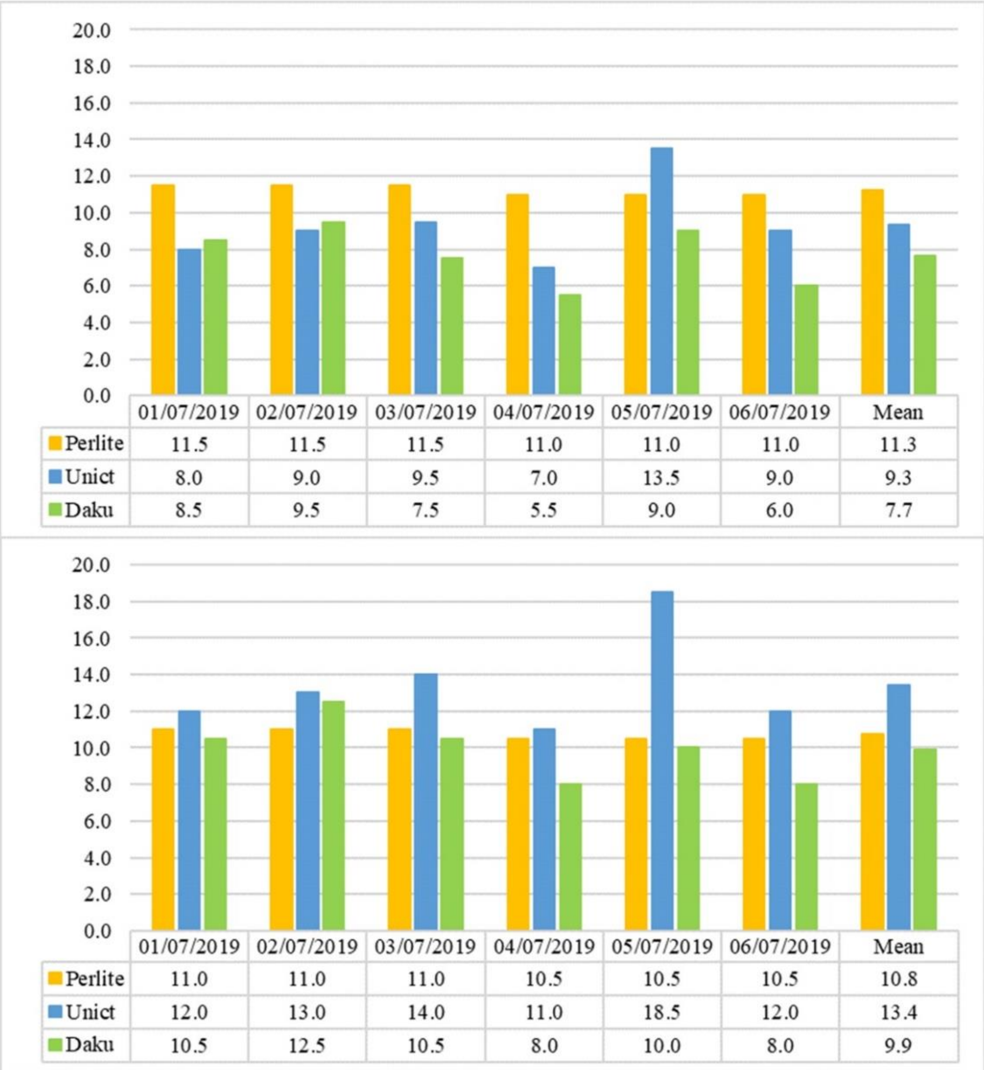

	01/07/2019	02/07/2019	03/07/2019	04/07/2019	05/07/2019	06/07/2019	Mean
Perlite	11.5	11.5	11.5	11.0	11.0	11.0	11.3
Unict	8.0	9.0	9.5	7.0	13.5	9.0	9.3
Daku	8.5	9.5	7.5	5.5	9.0	6.0	7.7

	01/07/2019	02/07/2019	03/07/2019	04/07/2019	05/07/2019	06/07/2019	Mean
Perlite	11.0	11.0	11.0	10.5	10.5	10.5	10.8
Unict	12.0	13.0	14.0	11.0	18.5	12.0	13.4
Daku	10.5	12.5	10.5	8.0	10.0	8.0	9.9

Figure 11. Time lag with the maximum surface temperature time as boundary conditions (at the top) and with the maximum solar radiation time (1 p.m).

Figure 12 shows the cooling potential, which is the energy savings (Wh×day^{-1}×m^{-2}) that green roofs reach compared to the Reference. Unict allows for a greater reduction in daily energy through the roof (876 Wh×day^{-1}×m^{-2}) than Perlite and Daku, 900 and 970 Wh×day^{-1}×m^{-2}, respectively.

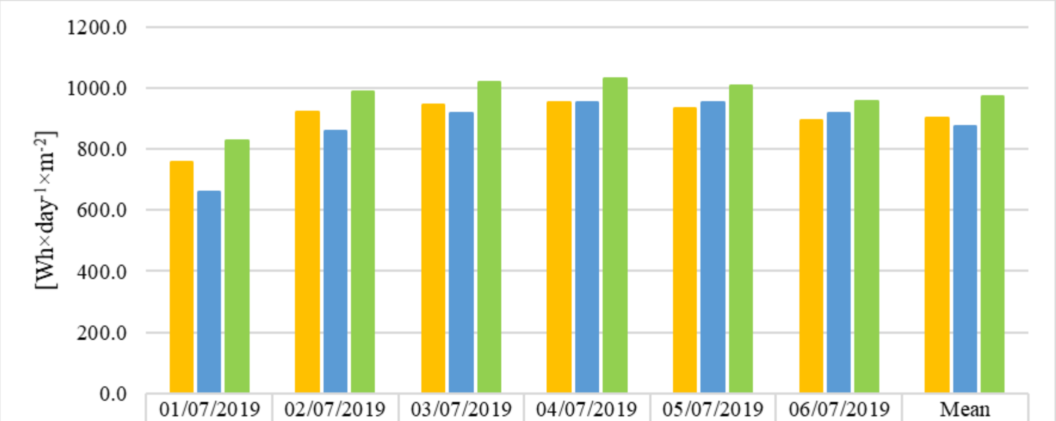

	01/07/2019	02/07/2019	03/07/2019	04/07/2019	05/07/2019	06/07/2019	Mean
Perlite	758.3	920.3	945.5	953.1	931.8	894.0	900.5
Unict	657.8	857.5	918.5	952.0	953.4	918.0	876.2
Daku	825.9	988.5	1017.6	1030.0	1007.2	955.4	970.8

Figure 12. Cooling potential (Wh×day^{-1}×m^{-2}).

6.4. Conclusions

In this thesis chapter, the thermal performance of different green roof solutions has been compared. An innovative solution was proposed by using recycled polyethylene granules for green roof drainage and a substrate formulated with local components. In addition, the substrate contains a higher content of organic matter than conventional solutions used in green roofs. The performance of this system was compared with those of two commercial green roofs.

The main results are as follows:

- The green roof that uses perlite as drainage layer has a higher water content in the substrate due to its ability to absorb water
- All green roofs reduce surface temperatures compared to the reference roof by about 25 °C
- The innovative green roof has higher temperatures than commercial solutions, however, it reduces daily fluctuations between minimum and maximum temperatures
- The innovative green roof reduces the surface temperatures inside the building by about 2 °C compared to the reference roof
- The reduction in temperature fluctuations in the innovative green roof resulted in less thermal flow through the green roof

- Innovative green roof has better dynamic thermal performance (decrement factor and time lag) than commercial green roofs

Overall, the innovative green roof has optimized thermal performance in the Mediterranean climate. Future studies should be carried out in the laboratory to analyze the thermal conductivity and physical characteristics (permeability, index of voids, density, etc.) of the materials studied (recycled polyethylene granule and local substrate), in order to be able to compare them with commercial materials. Finally, data from this study could be used to validate numerical simulations using green roofs.

References

[1] F. Olivieri, C. Di Perna, M. D'Orazio, L. Olivieri, J. Neila, Experimental measurements and numerical model for the summer performance assessment of extensive green roofs in a Mediterranean coastal climate, Energy Build. 63 (2013) 1–14. doi:10.1016/j.enbuild.2013.03.054.

[2] P. Bevilacqua, D. Mazzeo, R. Bruno, N. Arcuri, Experimental investigation of the thermal performances of an extensive green roof in the Mediterranean area, Energy Build. 122 (2016) 63–69. doi:10.1016/j.enbuild.2016.03.062.

[3] V. Azeñas, J. Cuxart, R. Picos, H. Medrano, G. Simó, A. López-grifol, J. Gulías, Thermal regulation capacity of a green roof system in the mediterranean region : The effects of vegetation and irrigation level, Energy Build. 164 (2018) 226–238. doi:10.1016/j.enbuild.2018.01.010.

[4] R. Almeida, N. Simões, A. Tadeu, P. Palha, J. Almeida, Thermal behaviour of a green roof containing insulation cork board . An experimental characterization using a bioclimatic chamber, Build. Environ. 160 (2019) 106179. doi:10.1016/j.buildenv.2019.106179.

[5] M. Porcaro, M.R. De Adana, F. Comino, A. Peña, E. Martín-consuegra, Long term experimental analysis of thermal performance of extensive green roofs with different substrates in Mediterranean climate, Energy Build. 197 (2019) 18–33. doi:10.1016/j.enbuild.2019.05.041.

[6] P. Bevilacqua, D. Mazzeo, N. Arcuri, Thermal inertia assessment of an experimental extensive green roof in summer conditions, Build. Environ. 131 (2018) 264–276. doi:10.1016/j.buildenv.2017.11.033.

[7] S. Cascone, Green Roof Design: State of the Art on Technology and Materials, Sustain. 11 (2019) 3020.

7. The evapotranspiration process in green roofs: a review

7.1. Introduction

In recent years, the continued growth of high-density urban areas, characterized by extensive paved areas, have increased the overwarming and energy needs within the cities [1,2]. Furthermore, these areas often have higher air temperatures than their rural surroundings which is commonly called urban heat island (UHI) effect [3,4]. Engineers, researchers, and designers are committed to develop sustainable solutions to reduce both energy consumption and pollutant emissions by using innovative materials and technologies [5,6]. One of the most effective solutions adopted in the field of bioclimatic architecture is the replacement of materials traditionally used in flat roofs, which comprise around 25% of the total horizontal surfaces in urban areas, with green roof technologies [7].

Green roofs provide several benefits at both building and city level. The following are the most commonly observed at urban scale: mitigation of urban heat island effect [8–10]; decrease in storm water runoff [11,12]; enhancement of biodiversity in densely urban areas [13]; purification of air and water runoff [14]. At building scale, green roofs reduce the sensible heat flux due to the cooling effect [15,16] thus decreasing the heating and cooling demand of a building [17–19], and improving human thermal comfort [20,21]. This effect may vary depending on the climate conditions [22–24], and the level of insulation specially in cases of building retrofitting [25,26]. Most of these multiple benefits are linked to the cooling effect due to the evapotranspiration process (ET) that humidifies the external ambient air, reduces the surface temperature of the roof [27], and mitigates the urban heat island phenomenon [28].

Previous studies have considered the cooling effect due to the evapotranspiration process among the major energy benefits of green roofs [29,30]. The importance of evapotranspiration in energy transfer models was also highlighted in previous studies [31] in which the authors analysed the vegetation effect on horizontal surfaces in urban, suburban and agricultural environments. However, the existent literature is scarce and controversial in evaluating the physical-mathematical models and dynamic simulation software for calculating ET, the main influencing parameters that have to be considered, and the suitable equipment and methodologies for the measurement in urban contexts.

To fill these gaps in the literature, the present study carried out a wide analysis of the cooling effect due to the evapotranspiration process on green roofs. The scope of this thesis chapter includes the analysis and discussion of the following topics: the main equipment and methodologies used to measure the ET in green roofs, the correlation between evapotranspiration and the energy performance of green roofs, the main experimental results from the literature and the physical-mathematical models used to calculate the latent heat flux on green roofs. Furthermore, this thesis chapter provides an exhaustive review of the main influencing parameters of ET in green roofs and their classification according to the potential evapotranspiration capacity.

However, due to the high number of studies carried out on green roofs, this review is focused on the research that expressly evaluate experimentally or analytically the evapotranspiration process in green roofs. Therefore, all researches examining performance and benefits of green roofs without directly correlating them with evapotranspiration is out of the scope of this study. In addition, the previous studies that have evaluated the role of evapotranspiration in the hydraulic performance and water balance of green roofs, in terms of storm water management and runoff of these systems, are not included in this review.

In order to organize the reviewed data and to facilitate the understanding thereof, thesis chapter is structured in seven sections as follows: Section 7.2 provides a general description of evapotranspiration process, how it is defined, what does it depends on and how it can be determined. Section 7.3 and 7.4 show the main climatological parameters and characteristics of vegetation and substrate that influence the ET of green roofs, respectively. Section 7.5 describes the principal experimental measurement methods used to evaluate the evapotranspiration of green roofs, the results obtained from them and a summary of the different units of measurement used. Section 7.6 describes the mathematical models that take into account the latent heat within a green roof energy balance and their main outcomes. In section 7.7, the main findings derived from research performed using dynamic simulation software are reported. Finally, Section 7.8 presents the sensitivity analysis conducted by previous studies to determine the influence of the different parameters (volumetric water content, solar radiation, wind velocity, relative humidity, soil thickness, etc.) on the evapotranspiration effect.

7.2. An overview of evapotranspiration in green roofs

During recent years, evapotranspiration (ET) has received a growing interest from the green roof research community because of its impact on heat and mass transfer. This phenomenon is a combination of the water transpired by plants during their growth or retained in the plant tissue (transpiration) plus the moisture evaporated from the soil surface and vegetation (evaporation). On one hand, transpiration is the process by which moisture is carried through plants from roots to small pores on the underside and upper side of leaves, where it changes to vapour and is released to the atmosphere.

Transpiration is essentially evaporation of water from plant leaves. Transpiration also includes a process called guttation, which is the loss of water in liquid form from the uninjured leaf or stem of the plant, principally through water stomata. On the other hand, evaporation is the process whereby liquid water is converted into water vapour and is removed from the soil surface. It is the only form of moisture transfer from land and oceans into the atmosphere. These processes are mainly determined by solar irradiation reaching the soil surface as it supplies the necessary energy.

The level of the plant development has a considerable influence on the rate of water consumption and in the final energy balance of a green roof system. During the development of complete vegetative cover, the water consumption rate increases rapidly from low to high values. When plants are small, water is mainly lost by evaporation from the soil; later, once the vegetation is well developed and completely covers the soil surface, transpiration becomes the main process. However, the experimental data revealed that ET has a dynamic and complex behaviour that depends on both climatological parameters and soil and vegetation characteristics [32,33].

The principal climatological parameters to assess the ET process are: the solar radiation, the wind speed, the air temperature, the relative humidity, and the sky conditions. In addition, ET also depends on the characteristics of both vegetation and soil, principally the degree of shading of the canopy (leaf area and density, LAI) and the amount of water available at the soil surface. In particular, the characteristic of the vegetation that is most important from the standpoint of impacts on the heat transfer through the roof is the leaf area index (LAI). LAI is established as the one-sided green leaf area per unit ground surface area (LAI = leaf area/ground area, m^2/m^2) in broadleaf canòpies. The LAI value depends on the type and the growth phase of the plant (crop), usually ranging from 0 to 10.. E.g., if the average parcel of roof surface is beneath two leaves, the corresponding LAI is 2. Values of LAI for green roofs vary depending upon plant type, but are typically in the range of 0.5–5.0 [34]. Moreover, the stomatal resistance, the plant height, the development of the vegetation and the transpiration rate of each plant species, determine the aptitude to transfer moisture near to the surface roots and canopy, consequently, these characteristics have also influence on the ET rate.

When rain and irrigation are scarce, the water content in the substrate drops and the soil surface dries out. Thereby, in the absence of water supply the evapotranspiration decreases rapidly and may cease almost completely within a few days.

Table 1 summarizes the climatological and green roof parameters affecting evapotranspiration.

Table 1. Climatological and green roof parameters affecting ET.

Climatological	Canopy	Soil	Management practice
Solar radiation	Degree of shading	Water content	Irrigation regime
Air temperature	Canopy characteristics	Soil characteristics	Cultivation practice
Air humidity	Canopy development		
Wind speed			
Rain			
Sky condition			
Season			

The evapotranspiration rate can be obtained by experimental measurements or by means of modelling approaches. Specific devices and accurate measurements of various physical parameters, or the soil water balance, are required to determine evapotranspiration.

The lysimeter is one of the most widely used equipment to measure evapotranspiration. Such device is made of a soil volume covered by plants placed in a container hydrologically separated by the surrounding soil. Lysimeters can be classified as non-weighing and weighing type. The weighing lysimeter is based on the principle of the mass continuity. The evapotranspiration (ET), expressed in mm, is calculated by Eq. 1 as the difference among precipitation (P), drainage (D), superficial runoff (O) and the variations in soil water storage (ΔS) (Figure 1).

$$ET = P - D - O \pm \Delta S \qquad (1)$$

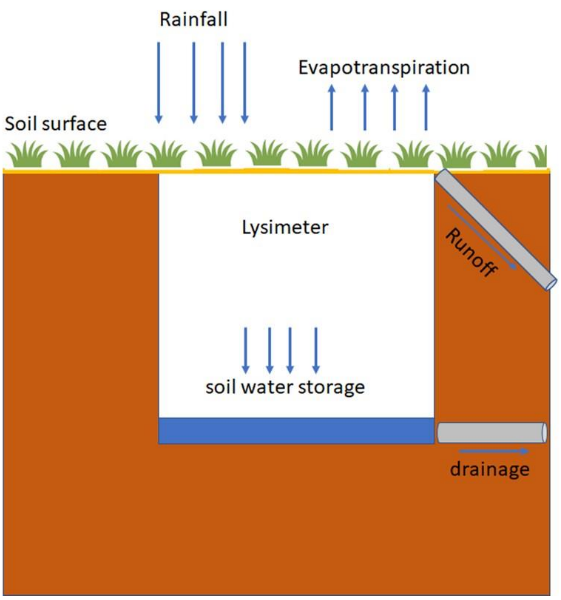

Figure 1. Schematic representation of the soil water balance in weighing lysimeter.

Weighing lysimeters provide the direct measurements of evapotranspiration over time by monitoring the evolution of the tray weights (change of mass) due to the water losses. As regard the variation of water stored (ΔS), it is determined through measurement of the weight change of the soil column over time, with an accuracy of few hundredths of millimeters. Usually the following equivalence is assumed: 1 kg ≈ 1 L m^{-2} = 1 mm.

Non-weighing lysimeters allow determining the evapotranspiration, during a given time period, subtracting the drainage water collected at the bottom of the lysimeters from the total water input. Actually, few studies directly quantified ET by measuring the rate of water loss [35], since such method is often expensive and demanding in terms of accuracy of measurements.

In order to predict the evapotranspiration, therefore, numerous numerical methods have been developed based on climatological data (e.g. temperature, day length, humidity, wind, and solar irradiance) [36]. These numerical models, such as those of Hargreaves and Allen [37], Priestley and Taylor [38], Penman [39], and Penman–Monteith [40,41], estimate the so called “potential evapotranspiration” (PET or ET_0) over bare soil surface or vegetation.

Penman defined PET as the ET from actively growing short green vegetation, completely shading the ground and never suffering scarcity of moisture availability. Consequently, PET models neglect factors that, conversely, are decisive in the actual evapotranspiration (AET) that occurs under natural field conditions (i.e., variable soil water contents).

Table 2 summarizes the most common models used to evaluate ET. All these previous models are characterized by a daily time step.

Table 2. Models for estimating evapotranspiration.

Name	Function	Reference
Penman-Monteith (1965)	$ET = \frac{0.408\,\Delta(R_n - G) + \frac{\gamma 900}{T_a + 273} u_2 (e_s - e_a)}{\Delta + \gamma\,(1 + 0.34 u_2)}$	[39]
Priestley-Taylor (1972)	$ET = \alpha\,\Delta(R_n - G) / (\Delta + \gamma)$	[38]
Hargreaves (1975)	$ET_0 = 0.0075 R_s T_F$	[37]
Hargreaves (1985)	$ET_0 = 0.0022 R_s (T_a + 17.8) TD^{0.5}$	[37]
FAO-56 Penman-Monteith (1998)	$ET_0 = \frac{0.408\Delta\,(R_n - G) + \gamma \frac{\gamma 900}{T_a + 273} u_2 (e_s - e_a)}{\Delta + \gamma\,(1 + 0.34 u_2)}$	[41]

Penman-Monteith ASCE (2005)	$ET_{sz} = \frac{0.408\Delta(R_n - G) + \gamma(\frac{C_n}{T_a + 273})\, u_2(e_s - e_a)}{\Delta + \gamma(1 + C_d u_2)}$	[40]

The most known PET model is the Penman-Monteith, which allow estimating the latent heat fluxes at the vegetation layer that achieve the daily evapotranspiration in a time step, taking into account numerous physical phenomena and some characteristics of the plants [42]. However, existing evapotranspiration models have substantial errors for hourly ET predictions over a range of moisture conditions to assess the hydrological performance of the green roofs during storm events. Therefore, Jahanfar et al. [43] developed a modified Penman-Monteith equation to provide improved prediction of hourly evapotranspiration specifically for green roof applications.

Alternatively, the indirect methods calculate the ET through the energy and mass balance equations [44,45]. The energy budget method (EBM) is based primarily on the concept that ET is function of the availability of energy to evaporate water (Q_{ET}), under the hypothesis that the moisture supply is not restricted.

7.3. Climatological parameters influencing ET

The principal meteo-climatic parameters affect the ET by removing water from the plants and soil surface are solar radiation, wind speed, relative humidity and air temperature, and sky conditions (e.g. cloudy, sunny). These climatic features have both seasonal and geographic variations.

7.3.1. <u>Solar radiation and seasonal variation</u>

The water depletion rate of soil reflects the solar radiation input that sustains the evapotranspiration. Tabares-Velasco and Srebric [46] performed a sensitivity analysis in order to understand which parameters greatly affect ET. Among all the environmental variables, solar radiation was the one with the strongest influence on ET. However, ET intensity varies due to the combined effect of solar radiation with the other meteo-climatic parameters.

Jim and Tsang [47] found that the transpiration rate peaked in autumn due to the high level of solar radiation and the low relative humidity. The actual solar radiation reaching the earth surface depends by the turbidity of the atmosphere and the presence of clouds, which reflect and absorb a large percentage of the radiation. Therefore, sky conditions affect ET, since they modify the energy balance of the evaporating surface. Coutts et al. [48] evaluated the advancement of ET for both a green roof and a bare soil measuring the volumetric water content during four clear sunny summer days. In both vegetated and bare soil, the ET was rather modest, with values of about 50 W/m^2, suggesting that during the monitored summer period there was scarcity of water available in the soil to support evapotranspiration. Consequently, the cooling effect of the green roofs was significantly restricted. Jim and Peng [49] differentiated the sky conditions into three types: sunny, cloudy and rainy. Overall, sunny days registered progressive water loss from the substrate due to evapotranspiration, while during cloudy days the evapotranspiration was low so the water was maintained in the substrate. Moreover, the ET was correlated with the volume of water contained in the substrate, distinguishing between moist and dry substrates. For each weather type, wet means that the moisture content is at or near the maximum daily initial moisture level; moist means at or near the average daily initial moisture level; and dry means at or near the minimal daily initial moisture level. Thus during cloudy days both moist and dry substrate recorded similar evapotranspiration, while during sunny days the dry substrate recorded an even higher evapotranspiration than the moist.

Otherwise, Lazzarin et al. [50] compared the ET in dry and wet soil in summer and observed that the wet soil gave rise to higher evapotranspiration whereas in dry conditions that contribution was limited. In winter, despite the considerably lower solar irradiance in comparison to the summer season, the evapotranspiration flux was also appreciable. During summer, with the soil in almost dry conditions the green roof allowed an attenuation of the thermal gain entering the underneath room of about 60% with respect to a traditional roofing with an insulating layer. During the winter the evapotranspiration process was driven above all by the air vapour pressure deficit; it is not negligible weight produced an outgoing thermal flux from the roof that was 40% higher than the corresponding one of a high solar absorbing and insulated roofing.

Jim and Tsang [47] found that the seasonal transpiration rates on sunny days were, in descending sequence: autumn, summer, winter and spring. They suggested that the relatively high transpiration rate observed in summer sunny days occurs because high solar radiation and air temperatures promote photosynthesis. In winter sunny days, the transpiration rate was lower than in autumn and summer because of the solar radiation is less intense. Such result was confirmed by the modest transpiration rate observed in spring, the lowest recorded in this study, which were due to weak solar radiation and low temperatures characterizing this season.

In the study performed by Lee and Jim [51], the progressive dropping of air and green roof surface temperatures in the course of the sunny day was explained by the effective cooling brought by evapotranspiration fuelled by solar radiation input. Even though irradiance at the green roof surface was limited, the ambient warmth and relatively low surface temperature did not require a lot of latent heat absorption to cool down.

As shown in Table 3, most of the analyzed studies evaluated ET during summer periods when it is expected to be higher in comparison to winter periods, due to the influence of solar radiation and relative humidity. Since sky conditions influence on the final ET process, it is important to highlight the scarce literature (6 over 21) that provide a proper description of the weather conditions.

Table 3. Classification of the studies reviewed according to the season, sky conditions and climate classification.

References	Köppen classification	Weather	Season	Type of study
Feng et al. [52]	Cfa	-	Summer	Modelling
Jim and Peng [49]	Cwa	Sunny-cloudy-rainy	Summer	Experimental
Jim and Tsang [47]	Cwa	Sunny-cloudy-rainy	Whole year	-
Lazzarin et al. [50]	Cfa	-	Summer-winter	Modelling
He et al. [53]	Cfa	Clear-cloudy-rainy	Summer	Modelling
Tabares-Velasco and Srebric [54]	-	-	Summer	Experimental
Tabares-Velasco and Srebric [46]	-	-	Summer	Modelling
Ouldboukhitine et al. [55]	Cfb	-	Summer	Experimental
Coutts et al. [48]	Cfb	Sunny	Summer	Experimental
Schweitzer and Erell [56]	Csa	-	Summer-winter	Experimental
Ouldboukhitine et al. [57]	Cfb	-	Summer	Experimental
Tan et al. [58]	Af	-	Summer-winter	Experimental
Tian et al. [59]	Cfa	-	Summer	Modelling
Hodo-Abalo et al. [60]	-	Sunny	-	Modelling
Tsang and Jim [61]	Cwa	Sunny-cloudy	Summer	Modelling
Ouldboukhitine et al. [62]	-	Sunny	Summer	Modelling
Boafo et al. [63]	Dwa	-	Summer-winter	Simulation
Silva et al. [64]	Csa	-	Summer-winter	Simulation

Vera et al. [65]	Bsk Csc Cfb	-	Summer	Simulation
Lee and Jim [51]	Cwa	Sunny-cloudy-rainy	Summer	Experimental

The previous survey indicates that the solar radiation is the climatic data with the strongest correlation with evapotranspiration [49]. Such correlation will be further analysed in Section 8, assessing previous sensitivity analyses.

Otherwise, since the ET phenomena depends also by the whole meteo-climatic features, future studies have to include as much possible complete meteo-climatic description in order to correlate the ET with the main climatic conditions (e.g. sunny, cloudy and rainy days). Furthermore, because of the lack of studies that cover the ET during an entire year, further experimental studies should include a whole year analysis in order to evaluate the ET in the different seasons and in different weather conditions.

7.3.2. Wind speed

The process of vapour removal also depends by the air turbulence, which increase the convective heat fluxes between the atmosphere and the soil surface, as well as the airflow over the soil surface. Continuous vaporization of water by means of ET leads the air above the soil surface to become gradually saturated. If this vapour is not continuously replaced with drier air, the driving force for water vapour removal and ET decrease. Intense wind improved the transport not only of heat but also of water vapour, increasing the evapotranspiration fluxes.

Schweitzer and Erell [56] compared the total daily evapotranspiration for four plant species during days with weak (2 $m \cdot s^{-1}$) and strong wind (5 $m \cdot s^{-1}$). The authors concluded that there were substantial differences among the plant species, i.e. the vegetated roof with *Aptenia* losing less than half as much water as the vegetated roof with *Halimione*, about 3.0 $L \cdot m^{-2} \cdot day^{-1}$ compared to 7.5 $L \cdot m^{-2} \cdot day^{-1}$ under low wind conditions (2 $m \cdot s^{-1}$). This rate was even less than for exposed moist soil, i.e. without plants, about 3.8 $L \cdot m^{-2} \cdot day^{-1}$. The other two species analysed, *Pennisetum* and *Sesuvium*, reached intermediate value, about 7.0 $L \cdot m^{-2} \cdot day^{-1}$. In windy conditions (5 $m\ s^{-1}$), the maximum hourly loss for *Pennisetum* was nearly 2.0 $L \cdot m^{-2} \cdot h^{-1}$, and the daily total was over 9.0 $L \cdot m^{-2} \cdot day^{-1}$. *Sesuvium*, moist soil, *Aptenia* and *Halimione* reached lower values of evapotranspiration, 8.8, 6.0, 5.8 and 4.0 $L \cdot m^{-2} \cdot day^{-1}$, respectively. In this study, high wind speed enhanced the ET.

In another experiment, Tabares-Velasco and Srebric [54] found that when the wind speed varied from 0.1 $m \cdot s^{-1}$ to 1.0 $m \cdot s^{-1}$ the evapotranspiration rate increased from 10%

to 30%. This result confirm that air convection effectively brings water vapour from the soil or foliage to the atmosphere increasing the evapotranspiration rate.
For instance, an increase of the convection coefficient, which has a direct correlation with wind velocity, from 12.0 to 16.0 W/m^{2}K reduce the heat storage by 24% and 45% for bare and green roofs, respectively [61].
Jim and Tsang [47] found a rather modest correlation between the wind above the canopy and transpiration, so the wind should not play a major role in facilitating the transpiration rate. Figure 2 shows the sunny and rainy wind speed measured at canopy top in [47]. The wind speed was relatively higher on rainy days than on sunny ones.

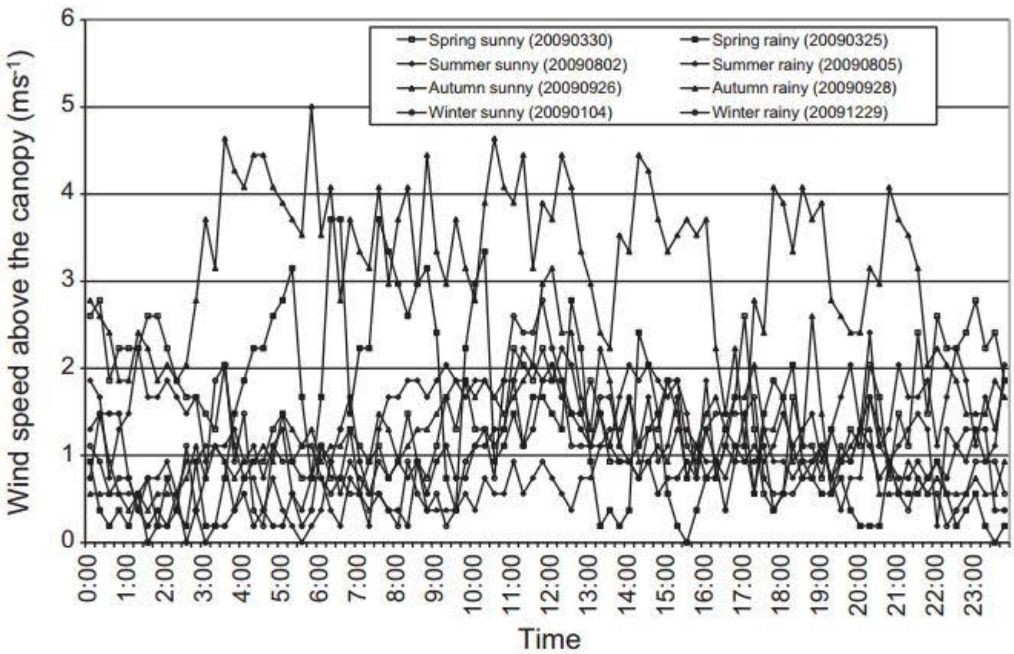

Figure 2. Seasonal and diurnal wind speed above the canopy of the sky woodland [47].

7.3.3. Relative humidity and air temperature

Even if the energy supplied by the solar radiation is the main driving force for the vaporization of water, the difference between the water vapour pressure at the soil and plants surface, and the surrounding air are other important factors that also determine the vapour removal.
High temperatures combined with lower relative humidity (RH) enhance the evapotranspiration process [66]. Tabares-Velasco and Srebric [46] stated that ET was strongly influenced by the environmental conditions, in terms of air temperature and relative humidity in the vicinity of the green roof.
Generally, during night-time the outdoor air reach low temperatures that conversely cause the increase of RH until 100%, so reducing the ET process. On the contrary,

during day-time the higher air temperature induces a fall of RH so allowing the evaporative process to take place [49].

In a Cwa climatic area where the relative humidity and the air temperature varied between 50%, 23 °C in autumn, and 80%, 36 °C in summer, Jim and Tsang [47] found that the highest transpiration rate is observed in autumn rather than in summer, because of low relative humidity and mild air temperature. According to this study, evapotranspiration is minimized in a humid environment and the high relative humidity is the crucial factor that dampens the transpiration rate.

Unlike the green roof in the temperate region, the experiment carried out by Jim and Tsang [47] showed that the transpiration rate of an intensive green roof in the humid-subtropical region, dominated by the Monsoon climate system, depends mainly on photosynthetically active radiation and relative humidity.

As with all the other processes that take advantage of evaporation, planted roofs do not have much to offer in terms of ET rate in a humid environment compared with an arid one [50].

7.3.4. Irrigation regime

Azeñas et al. [67] analyzed the relationship between irrigation regime and heat flux through green roofs. In particular, the authors considered well-watered and water-limited condition. Surface drip irrigation at 50% and 25% of potential evapotranspiration (ET_0) was applied twice a week during the calculated time according to the nominal drippers flow (2 l h^{-1} for each dripper) and considering the number of drippers (9 drippers for each module). Results showed lower heat flux in water-limited than in well-watered treatments in both non-vegetated and vegetated modules, suggesting that the lower heat transfer with air in comparison to water would counteract the cooling effect of evapotranspiration that is supposed to be higher in the well-watered modules, where the volumetric water content is higher. In particular, water-limited irrigation treatment was shown to increase the thermal insulation capacity when compared to complete well-watered irrigation treatment, by reducing the total transferred heat between 25% and 71% along the different seasons of the year, suggesting that the air/water substrate content has a greater effect on insulation than evapotranspiration.

7.3.5. The geographic area

The review conducted by Pérez et al. [68] concluded that the Köppen climate classification is the most suitable reference to compare research results about green infrastructures. In order to provide a continuous framework in the literature, this review used the same climate classification for all the reviewed papers (Table 4).

Table 4. Climate classification of experimental, modelling and simulation studies.

Ref	Authors	Year	Location		Climate according to the author	Köppen classification
[49]	Jim and Peng	2012	Hong Kong	Hong Kong	Humid-subtropical	Cwa
[69]	Takebayashi and Moriyama	2007	Japan	Kobe	-	Cfa
[54]	Tabares-Velasco and Srebric	2011	USA	Pennsylvania	-	Dfb
[46]	Tabares-Velasco and Srebric	2012	USA	Pennsylvania	-	Dfb
[55]	Ouldboukhitine et al.	2012	France	La Rochelle	-	Cfb
[48]	Coutts et al.	2013	Australia	Melbourne	-	Cfb
[56]	Schweitzer and Erell	2014	Israel	Tel Aviv	Mediterranean	Csa
[57]	Ouldboukhitine et al.	2014	France	La Rochelle	-	Cfb
[58]	Tan et al.	2017	Singapore	Singapore	-	Af
[52]	Feng et al.	2010	China	Guangzhou	-	Cfa
[70]	Djedjig et al.	2012	France	La Rochelle	-	Cfb
[69]	Takebayashi and Moriyama	2007	Japan	Kobe	-	Cfa
[50]	Lazzarin et al.	2005	Italy	Vicenza	-	Cfa
[53]	He et al.	2016	China	Shanghai	North subtropical monsoon	Cfa
[46]	Tabares-Velasco and Srebric	2012	USA	Pennsylvania	-	Dfb
[59]	Tian et al.	2017	China	Chongqing	Humid subtropical monsoon	Cfa
[60]	Hodo-Abalo et al.	2012	Togo	-	-	Aw
[61]	Tsang and Jim	2011	Hong Kong	Hong Kong	-	Cwa
[62]	Ouldboukhitine et al.	2011	France	La Rochelle	-	Cfb
[63]	Boafo et al.	2017	Republic of Korea	Incheon	Humid continental	Dwa
[64]	Silva et al.	2016	Portugal	Lisbon	Mediterranean	Csa
			USA	Albuquerque	Semi-arid	Bsk
[65]	Vera et al.	2017	Chile	Santiago	Semi-arid	Csc
			Australia	Melbourne	Marine	Cfb

Most of the studies reviewed in this thesis chapter (71%) were carried out considering temperate climatic conditions, first letter C according to the Köppen classification. About 17%, 8% and 4% of the studies were developed in tropical (D), arid (A) and cold climates (B), respectively.

The 71% of the studies performed in temperate climates are located in areas without dry seasons (Cf according to the Köppen classification). About 17% of these studies were performed in climates with dry summers, second letter s (Cs according to the Köppen classification). Finally, only a few of the studies analysed, about 12%, are located in climates with dry winters, second letter w (Cw according to the Köppen classification).

Figure 3 shows the analysed studies located on the world evapotranspiration map. The Water Holding Capacity is the total amount of water available for plants that is held against gravity in a soil and is usually estimated as the amount present at -0.03 MPa average water potential minus the amount present at -1.5 MPa water potential. In [71], the authors stated that it is a very important soil characteristic strongly and positively correlated to the inherent productivity of soils.

Most of the studies were performed in the western part of the world under temperate climatic conditions (Figure 3). However, other regions could allow achieving high rates of ET that have not yet deeply explored or at least there is a lack of data in literature. Consequently, future studies should encompass experimental study in tropical and arid climates where green roofs could enhance the cooling effect on buildings thanks the potential high ET rates.

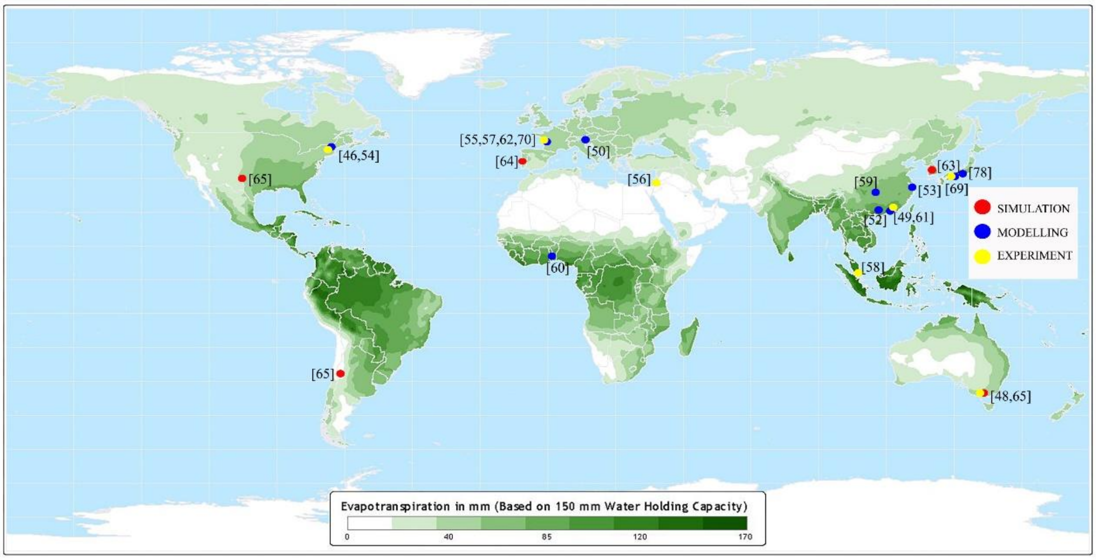

Figure 3. Location of simulation, modelling and experiment studies in the world Evapotranspiration map [72].

However, it has to be underlined as in hot arid regions green roofs need to be well watered, due to the abundance of solar energy and dry air, consequently they consume large amounts of water. On the other hand, in humid tropical regions, since the air is frequently close to saturation, less additional water can be transferred from the green roof to the atmosphere, and hence the evapotranspiration rate is lower than in arid regions.

The world evapotranspiration map presented in Figure 3 is obtained by considering all the environmental parameters of a specific geographic area affecting natural evapotranspiration, such as solar radiation, relative humidity, annual average temperatures and annual average precipitation, which are the most important parameters for the vegetation development.

In some geographic areas of the world presented in Figure 3, such as in the African desert area, where potential evapotranspiration is high due to solar radiation and air temperatures, there is no evapotranspiration due to the lack of water. Therefore, if there were enough amounts of natural water (e.g. rain and water wells), these geographic areas could be enabled to take advantage of the cooling effect of green roofs.

An analysis of Figure 3 underlines that further experimental studies about ET should be carried out in regions of the world that have not been yet deeply investigated.

It is worth mentioning that the ET in green roofs differs from the phenomenon of natural evapotranspiration since, in addition to the above-mentioned climatic variables, it is also affected by the inherent properties of a green roof system. Some of these properties are; type of plants, substrate characteristics (thickness and composition), and irrigation regime that provides water for evapotranspiration in the absence of precipitation.

7.4. Plant-substrate parameters influencing ET

7.4.1. Volumetric water content

The cooling performance of a green roof depends on the water content of the substrate that determines the availability of water for evapotranspiration. Volumetric water content in the soil is related to the green-roof hydrological cycle because the green roof gains water from rainfall and irrigation, and loses it through evapotranspiration, surface runoff and drainage.

Djedjig et al. [70] found that when the green roof was characterized by a VWC in the soil of 10% of the maximum value, evapotranspiration was reduced to its minimum. On the contrary, evapotranspiration increased when the substrate had high water content.

Jim and Peng [49] found that during rainy days, antecedent VWC in the soil reduces the infiltration rate, thus increasing the runoff quantity. On successive sunny or cloudy days when drainage and run-off are negligible, the water stored in the substrate depends by irrigation and evapotranspiration. Previous studies [27,73,74] identified volumetric water content in the soil as the key factor for the evapotranspiration process, especially when irrigation is not present. In Bevilacqua et al. [75] even though the environmental conditions would allow evapotranspiration to take place, no considerable ET was found due to the limited water content in the substrate.

In the research conducted by Tan et al. [58] on conventional garden soil and artificial substrates, consisting mainly of perlite, the evapotranspiration rates exhibited strong positive correlations with the volumetric water content. In fact, when volumetric water content in the soil decreased gradually, the plant evapotranspiration rate was restricted. In addition, the ET decreased because of the low plant transpiration activity due to the lack of available water even if high solar irradiance occurred.

The use of a water retention layer below the green roof substrate makes it possible to maintain the VWC consistently higher. The water retention layer, therefore, sustains plant life by providing an additional availability of moisture, i.e. a liquid such as water in the form of very small drops, either in the air, in a substance, or on a surface. In green roof systems planted with *Sedum mexicanum* and *Disphyma austral*, Voyde et al. [35] observed a rapid water loss via latent heat flux in the days after watering. This water loss gradually decreased because the water available was reduced until plants stopped transpiring to preserve water.

The sensitivity test performed by Feng et al. [52] has shown that an increase from 30% to 60% in volumetric water content in the soil showed a reduction of 24% the heat stored within the green roofs, thanks to the increasing latent heat. On the contrary, Tabares-Velasco and Srebric [46] found that the water content in the substrate did not have the most significant impact on ET. However, a change in substrate conditions from the driest to the wettest led to a decrease in the substrate temperature of about 10.0 °C and a reduction in the incoming heat flux by 40%. This reduction was mainly due to an increase in the evapotranspiration rate (from 8.0 to 230.0 W/m^2) despite of an increase of 70% in substrate thermal conductivity and a decrease of 50% in substrate reflectivity, measured with a Portable Spectroradiometer using a calibrated lamp different that the fluorescent lamps directly above plants. Soil reflectivity depends on soil type and water content that typically varies from 0.10 for wet soil to 0.35 for dry soil.

He et al. [76] found that a higher water ratio helped to increase the evapotranspiration intensity while it decreased the thermal resistance of soil layer. As it was evaluated in some studies, the relation between the increment in the substrate volumetric water content and the increment of ET was not linear [49,54].

As Figure 4 shows, evapotranspiration-substrate water content curves have an elongated ‘‘S’’ shape with low evapotranspiration rates when water is scarce in the substrate and high evapotranspiration rates when water is abundant. In the middle of the substrate water content range, the relationship is approximately linear. Refer to [54] for more information about the experiment 1 to 8 carried out. Experimental data revealed that samples with higher water content provided higher latent fluxes and lower convective fluxes [52].

As result this section highlight that substrate water content plays an important role in decreasing temperatures on the green roof surface and the total incoming heat flux through the roof.

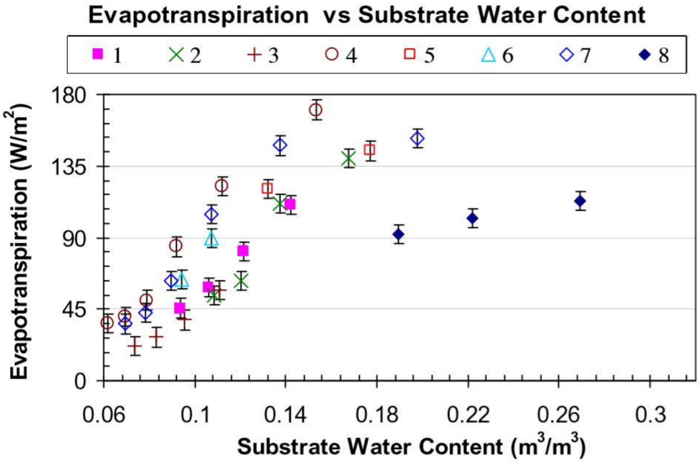

Figure 4. Relationship between evapotranspiration and substrate water content [54].

7.4.2. Vegetation

The transpiration process of plants contributes to the evaporation from the substrate, moreover the plant layer shades the roof surface and further reduces the heat fluxes incoming into the roof.

The species of plants, their physiology and growth typology, influence the green roof cooling effect by means of the ET process. Succulent plants, which store excess water in their thick leaves, are generally well adapted to extreme climates, and particularly in dry conditions. The *Sedum* family, capable of activating *Crassulacean Acid Metabolism* (CAM) photosynthesis, is recommended for extensive roofs where the depth of the soil layer is very shallow [77]. Under dry soil conditions, the evapotranspiration in a green roof with *Sedum* may be mostly evaporation from soil, with little transpiration from plants. Voyde et al. [35] found that planted treatments of *Sedum mexicanum* and *Disphyma australe* attained a latent heat flux of 2.19 mm/day and 2.21 mm/day, respectively, when the plants were not water stressed. Irrigated green roofs showed a latent heat flux higher than 200 $W \cdot m^{-2}$, suggesting that despite the presence of drought-tolerant *Sedum*, irrigation increased evapotranspiration when water was available.

Schweitzer and Erell [56] compared a well-watered roof covered with and without plants and observed that ET was the least effective cooling mechanism without the shade provided by plants. *Aptenia* lost less than half as much water as *Pennisetum*, about 3 L $m^{-2}day^{-1}$ and 7 L m^{-2} day^{-1} respectively. The *Pennisetum* loss rate was even less than in bare moist soil, about 3.8 L m^{-2} day^{-1}. Coutts et al. [48] evidenced that soil without plants may deliver greater latent heat fluxes, as the resistance to water loss from the vegetation surface is not present. The peaks of latent heat flux afterwards a cycle of irrigation are lower on the green roofs than the bare soil, this because the green roofs retained water in the substrate and vegetation over a longer period. The samples with plants consistently show an average reduction of the heat flux transferred into the spaces beneath the roof of about 25% compared to samples without plants. This is because plants provide extra shading to the roof, additional water storage, and a better water control by means of evapotranspiration and photosynthesis [54].

It was found that the Leaf Area Index (LAI) factor and the amount of evapotranspiration from the top surface have a large effect on the heat flow transferred into the spaces beneath the roof [78]. In a Mediterranean climate, results have shown that the LAI greatly influences the thermal performance of the vegetated roof since it enhances shading, convective heat transfer, and evapotranspiration. Higher LAI values allow to achieve higher cooling effect due to the increase of evapotranspiration [79,80].

Tabares-Velasco and Srebric [46] pointed out that among the green roof design variables, the most significant factor that allowed a reduction in temperature and heat flux through the substrate was the LAI.

In agreement with the findings obtained by Tabares-Velasco and Srebric [62], Hodo-Abalo et al. [60] found that evapotranspiration is more intense when the foliage is sufficiently dense. In addition, the LAI has important effects on the energy phenomena in the vegetation layer, thanks to the shading and transpiration that it provides, reducing solar flux penetration, stabilizing fluctuating values and reducing the indoor temperature.

Theodosiou [66] revealed large heat flows from the substrate surface to the atmosphere for surfaces on sunny days and relatively small flows on cloudy days, when the value of LAI was up to 3.0. Therefore, under such operative conditions there was a significant increase the cooling effect on the room space. It was an office building. The floor beneath the planted roof had an area of 70 m^2, internal gains of 1.10 kWh during working hours (08:00–16:0 h) and 0.1 kWh during the rest of the day. The air conditioning functions during the 8 h period with a thermostat set at 26 ºC and.

Lee and Jim [51] concluded that the dense foliage of the woodland vegetation should have provided greater shading and evapotranspirative cooling than an Indian green roof with herbaceous vegetation but 0.4 m-deep substrate used by Kumar and Kaushik [81]. The green roof used in [51] achieved only half the maximum air temperature of 12 °C on the Indian intensive green roof. The authors concluded that such disparity could be caused by variations in vegetation characteristics.

7.4.3. Stomatal resistance

Plant transpiration or latent heat flux depends on the physiological properties of the plants and their stomatal resistance or conductance that controls water loss. Stomatal resistance is opposed to the transport of water vapor and carbon dioxide to or from the stomata on the leaves of plants, the lower the value of stomatal resistance, the greater the ET. It depends by the water content in the interior of the stomata cavity and on the exterior surface of the leaf, but also by air density and moisture flux.

The dimension of stomatal resistance is time over distance that is the inverse of velocity, its values depend on plant selection. Grass plants with stomatal resistance of 60 $s \cdot m^{-1}$ produce evapotranspiration fluxes that are 3-4 times higher than those produced by succulent plants (e.g. *Sedum*) [46].

Generally, plant species with low values of stomatal resistance allow achieving higher ET if there is sufficient water in the soil.

7.4.4. Stomatal conductance

Otherwise, the stomatal conductance gives an estimation of the rate of exchange of gases and transpiration through the stomata of the plants, which depends by solar radiation, temperature, humidity and water availability. Higher stomatal conductance tends to correspond to higher evapotranspiration rates. The stomatal conductance is usual measured in $mmol \cdot mo^{-2 \cdot} s^{-1}$.

Tan et al. [58] have studied the variation of the stomatal conductance of *Cyathula prostrata* in function of both the cycle of irrigations and the type of soil (i.e. artificial soil, consisting mainly of perlite, and normal garden soil), which is a commercially available soil mix commonly used in urban landscapes. It was observed that during periods of regular irrigation, average stomatal conductance of *Cyathula prostrata*, which is a creeping shrub, was about 600.0 $mmol \cdot m^{-2} \cdot s^{-1}$. When irrigation was withheld, the stomatal conductance of *Cyathula prostrata* planted into the artificial soil was reduced to around 100.0 $mmol \cdot m^{-2 \cdot} s^{-1}$, while in a normal garden soil the stomatal conductance was reduced to 50.0 $mmol\ m^{-\ 2} s^{-1}$. For the case of the artificial soil equipped with a water retention layer, when irrigation was withheld the stomatal conductance slightly reduced to 425 $mmol \cdot m^{-2} \cdot s\text{–}^{1}$. When irrigation was resumed, stomatal conductance levels increased to 375.0 mmol· m−2· s−1[1] both in the case of artificial and normal garden soil.

This section has highlighted that the choice of the type of plants entails to different stomatal conductance, which in turns affects the ET.

7.4.5. The substrate and drainage layer

Several studies [33,82,83] have revealed that the characteristics of the substrate and drainage layer affect the evapotranspiration phenomena in the green roof.

The characteristics of the substrates that influence evapotranspiration are porosity, size of the soil particles, compaction of the material and permeability (or hydraulic conductivity), as well as the thickness of the material. Several studies have investigated the thermo-physical and hydrological properties of different types of substrate [84,85], which could be constituted of both organic and inorganic material.

However, less attention was paid in assessing the impact of the drainage layer on the green roof evapotranspiration, although the evapotranspiration varies considerably depending on the type of solution adopted for the drainage layer. The most common solutions used as drainage layers in green roofs are constituted by modular plastic panels with a water retention layer, or in alternative by natural granular materials such as expanded clay, pumice, natural pozzolana, perlite, etc. Recently new granular materials deriving, in whole or in part, from the recycling of materials have been proposed as drainage layer [86,87]. The benefits derived by the use of such materials are their low environmental impact, in terms of reduction of natural resource consumptions in comparison to traditional drainage layer materials [88].

Regarding different types of substrates for green roofs, Tan et al. [67] have analyzed the performance of an artificial substrate characterized by a higher porosity compared to a garden soil, which drain water faster than topsoil (natural soil). Hence, when irrigation was being withheld, less water was available for transpiration or evaporation from the substrate. As consequences, lower volumetric water content and evapotranspiration rates were experimented in this artificial soil compared to a normal garden soil.

Getter et al. [89] suggested that increasing substrate depth would allow the use of plants with greater biomass and leaf area, leading to a higher latent heat flux. In the thin substrate of common extensive green roofs, due to the limited substrate mass effect, solar energy heating the whole substrate increasing its temperature, which in turn increase the evapotranspiration and the water depletion [49].

However, it has to be reminded that when the VWC decreases below specific threshold also the ET is reduced.

This section has highlighted how the substrate and the drainage layers affects the ET. Generally, artificial soil characterized by higher porosity drain water faster than topsoil (natural soil). Hence, when irrigation is withheld less water is available for transpiration or evaporation from the substrate.

7.5. Equipment used in the reviewed green roof set-ups

Evapotranspiration is difficult to measure in a direct way, since it is a complex physical-physiological phenomenon that depends on both the phase change of the water contained in the substrate and the physiological processes occurring in the plant species used in green roofs.

As a result, several studies [47,49,52,69,70] have estimated the evapotranspiration rate from plants and soil through data derived from the substrate water content ("indirect" measurements). Sensors located at different depths of the soil layer measured the volumetric water content (VWC). Other studies carried out by Lazzarin et al. [50], and He et al. [53] have used the volumetric water content in the soil to calculate the heat transfer model of green roofs.

Table 5 summarizes the main equipment used to evaluate ET and the monitoring periods adopted in literature studies reviewed. On one hand, the "indirect" measurements presented within this table refer to ET estimation using data derived from the substrate water content. In this case, the water content variation is assumed equal to the ET. On the other hand, "direct" measurements refer to ET estimation using data collected by a lysimeter or load cells, monitoring the evolution of sample weight and not the water content variation in the substrate.

Table 5. Summary of the main instrumentation used in the reviewed set-ups and the length of monitoring periods.

Ref.	VWC sensor	Load balance	Portable closed chamber	Indoor test	Outdoor test	Monitoring period	Type of measurements
[52]	X	-	-	-	X	11 days	Indirect
[49]	X	-	-	-	X	2 months	Indirect
[70]	X	-	-	-	X	3 weeks	Indirect
[69]	X	-	-	-	X	1 month	Indirect
[47]	X	-	-	-	X	1 day	Indirect
[50]	X	-	-	-	X	2 months	Indirect
[53]	X	-	-	-	X	2 weeks	Indirect
[90]	X	-	-	X	-	6 days	Indirect
[54]	X	X	-	X	-	2-6 days	Direct and indirect
[46]	X	X	-	X	-	2-6 days	Direct and indirect
[55]	-	X	-	X	-	7 days	Direct
[48]	X	-	X	-	X	4 days	Direct and indirect

[56]	-	X	-	X	-	1 day	Direct
[57]	-	X	-	X	-	Two days	Direct
[58]	X	X	-	-	X	2 months	Direct and indirect

The devices used for evaluating ET depend on the aim of the research. In fact, if the objective is to validate an energy and mass balance model, researchers have frequently used volumetric water content sensors. On the other hand, when the aim of the research consists in estimating the rate of evapotranspiration, high precision scales combined with volumetric water content sensors are commonly used.

Most of the studies that used load cells were carried out in a laboratory (indoor test) set-up installing samples with reduced size, while only a few studies evaluated ET directly in-situ (outdoor test)[48,58]. Finally, the monitoring period varied widely, from one day to two months (see in Table 5). An important gap in the literature review is detected since the duration of almost all experimental studies (12 over 16) do not provide long periods of measurement (shorter than one month) that include the ET behaviour within the different seasons of a specific climate. Only four studies [49,50,58,69] overcome the duration of a month period monitoring. Besides the experimental set-ups of the following studies [46,50,52,70] were basically used for validating numerical models, they also contributed in providing methodologies to evaluate ET at both levels, theoretical and experimental.

In the following, a brief description of the different sensors and devices used for the ET measurement in previous experimental studies is given.

Schweitzer and Erell [56] associated the water consumption in extensive green roofs to the ET process, using mini-lysimeters. Ouldboukhitine et al. [57] evaluated the amount of water transpired by the plants using wind tunnel to control the wind speed. The hydrologic transfer was measured using a load cell installed under two green roof tray to track the weight loss due to water evapotranspired during the test. The only difference between the two samples was that one of them was planted with vegetation and the other without. While water was evapotranspired by the test trays with vegetation, it was only evaporated by the tray without vegetation. The difference between the two trays allowed an estimation of the quantity of water transpired by the plants. Ouldboukhitine et al. [55] measured the amount of water lost by evapotranspiration and its impact on the prediction of water content variations using a setup to measure the weight of trays suspended on the traction-compression sensor balance.

Liang Tan et al. [58] evaluated ET by using both direct (with load cell) and indirect methods (with volumetric water content sensors). In such study, the authors divided green roof plots into three treatment combinations characterized by different substrate type as well as the adoption of the water retention layer or not. Sensors were embedded at 0.1 m depth in the middle planters in order to monitor volumetric water content in the soil for each of the set-ups; then, evapotranspiration was measured by weighing the middle planter box. Coutts et al. [48] used a portable closed-chamber to measure evapotranspiration rates from green roof and soil without vegetation. With this method, chambers restrict the volume of air available for the exchange between the surface and the atmosphere and the net emission or uptake of gases can be measured as a change of water concentration. The latent heat flux, therefore, was determined from the change in the mass concentration of water over time. Green roof samples were also instrumented with volumetric water content into the soil probe at a depth of 0.08 m.

Ayata et al. [90], Tabares-Velasco and Srebric [46,54] evaluated evapotranspiration rates by tracking continuously both, the variations in weight of the green roof sample with high-resolution load cells, and the changes in the volumetric water content of the substrate. In these studies, the total water loss measured with the water balance method were 10–20% larger than the load cell. Thus, the authors used evapotranspiration data measured directly from the load cell to validate the heat transfer model proposed.

At the end of this survey, it is possible to observe that load cell is the most widely used device for assessing in a direct way the evapotranspiration in green roofs. Thus, such equipment could be recommended in future studies on ET.

7.5.1. Units of measurement for expressing the evapotranspiration rate

The evapotranspiration rate is frequently expressed in millimetres (mm) per unit time. The rate expresses the amount of water lost from a cropped surface in units of water depth. Furthermore, the time unit has large variability, it can be assumed equal to an hour, day, ten-day period, month or even an entire growing period.

The evapotranspiration rate can be stated or in terms of the energy necessary for the water evaporation, namely the latent heat of vaporization (L_e), expressed in MJ m^{-2} day^{-1}, or, using the lysimeter (load cell) to evaluate evapotranspiration by monitoring the evolution of the tray weights due to water loss over time, expressed the evapotranspiration in kg m^{-2} day^{-1}.

Thus, a plethora of units of measurement are used to express evapotranspiration (mm, kg, W/m^2, etc.), so it becomes rather complicate to compare the results obtained from different studies. Therefore, it could be useful to provide the conversion factors among the units of measurements used to characterize the evapotranspiration process in green roof.

Table 6 summarizes the conversion factors among the units of measurements used to express the evapotranspiration rate.

Table 6. Conversion factors for evapotranspiration process measurement.

	Depth	**Volume per unit area**		**Energy per unit area**	**Mass per unit area**	**Power per unit area**
To / From	mm day^{-1}	m^3 ha^{-1} day^{-1}	L m^{-2} day^{-1}	MJ m^{-2} day^{-1}	kg m^{-2} day^{-1}	W m^{-2}
mm day^{-1}	1	10	1	2.45	1	28.36
m^3 ha^{-1} day^{-1}	0.1	1	0.1	0.245	0.1	2.836
L m^{-2} day^{-1}	1	10	1	2.45	1	28.36
MJ m^{-2} day^{-1}	0.408	4.082	0.408	1	0.408	11.57
kg m^{-2} day^{-1}	1	10	1	2.45	1	28.36
W m^{-2}	0.035	0.35	0.035	0.0864	0.035	1

7.5.2. Evapotranspiration rate carried out by literature studies

Besides providing valuable technical details regarding the methods for measuring ET, experimental set-up tests also offer useful information on the real quantification of the ET process.

Liang Tan et al. [58] developed a study on both conventional garden soil, which is a commercially available soil mix commonly used in urban landscapes, and K-soil, which is a proprietary lightweight soilless media, consisting mainly of perlite and organic matter. They found that evapotranspiration ranged between 2.0 and 7.0 kg m^{-2} d^{-1}. Moreover, the authors also observed that plant evapotranspiration decreased gradually in a similar manner to the corresponding soil water content, to approximately 2.0 kg m^{-2} d^{-1} in both conventional garden soil and K-soil. On the contrary, evapotranspiration was around 4 kg m^{-2} d^{-1} when an artificial soil, consisting mainly of perlite, was tested.

Other studies demonstrated that the evapotranspiration for trays with plants was always higher than the evaporation of trays without vegetation [57], especially for trays using periwinkle (leafy plant) than for ryegrass. In the periwinkle test, the water lost by evapotranspiration after 48 hours was 5.2 kg, about twice as much as that lost only by evaporation that was about 3.0 kg. While the water loss was 3.5 kg after 48 hours for the ryegrass sample.

A substantial variation of water loss among some plant species was found also in other literature studies. In the tests performed by Schweitzer and Erell [56], *Aptenia* lost less than half as much water as *Pennisetum*, about 3 L $m^{-2}day^{-1}$ and 7 L m^{-2} day^{-1} respectively. The *Pennisetum* loss rate was even less than in bare moist soil, about 3.8 L m^{-2} day^{-1}. Ouldboukhitine et al. [55] measured that daily evapotranspiration with a grass tray (2.34 mm) was greater than that with a *Sedum* tray (1.42 mm). The cumulative evapotranspiration over three days was around 8.0 mm, 5.0 mm, and 4.0 mm for grass, *Sedum*, and bare soil, respectively. These results are in contrast with those found by Coutts et al. in [48], where the plants limited the ET. In addition, the daily evapotranspiration measured for grass (2.53 mm) is greater than that calculated by the Penman-Monteith equation (1.66 mm). This difference is probably due to the “tray factor”, as defined by Ouldboukhitine et al. in [55], and to the input parameters taken in the Penman-Monteith equation such as temperature, aerodynamic resistance, and vapour pressure.

Some studies calculated the latent heat flux after measuring the quantity of water lost. In Coutts et al. [48], the higher latent heat flux on soil (with maximum value about 280 W m^{-2}) compared to green roof (with maximum value about 210 W m^{-2}) suggested that wet soil freely evaporated while evapotranspiration from the green roof was limited by the lower surface temperatures and water uptake by vegetation. After irrigation, there was a substantial increase in latent heat flux for both green roof and bare soil. Maximum rates of latent heat flux increased on green roof and soil a mean of 100 W m^{-2} and 90 W m^{-2}, respectively.

Other studies analyzed the relationship between ET and different weather conditions. Jim and Peng [49] evaluated both different typical days (sunny, cloudy, and rainy) and different substrate water content. The authors found that for a sunny day with moist soil, about 4.0 mm of water is extracted from the substrate to satisfy evapotranspiration (9.3 mm considering 5 mm due to irrigation). The water depletion during a sunny day with dry soil was 13.1 mm and it was notably higher in comparison to a sunny day with moist soil, despite the lower water content in the substrate. On the contrary, a cloudy day with limited solar gains and dry soil notably suffered a subdued depletion, at merely 5.8 mm.

Tabares-Velasco and Srebric concluded in their study [46] that the latent heat flux due to ET reached maximum values during the experiment with high wind speed, around 170 W m^{-2}, while minimum values occurred when there was low solar radiation, around 20 W m^{-2}. Takebayashi and Moriyama [69] found that the quantity of evaporation from the green surface in November, with maximum value of 0.06 g m^{-2} s^{-1}, was higher than in August with maximum value of 0.02 g m^{-2} s^{-1}.

In the study conducted by Tabares-Velasco and Srebric in [54], they observed that latent heat rates vary the substrate water content. The green roof sample achieved the largest and nearly constant evapotranspiration rates over 135 Wm^{-2} when VWC was above 0.14 m^3 m^{-3}. Evapotranspiration decreased linearly with the VWC up to approximately 0.07 m^3 m^{-3}, showing values between 135 and 45 Wm^{-2}. Evapotranspiration rates dropped in a nonlinear way when VWC was lower than 0.07 m^3m^{-3} with values below 45.0 W m^{-2}. The daily evapotranspiration ratio was about 3.0 when the substrate was wet, with 20.0 and 60.0 W m^{-2} latent heat flux during night and day respectively, while the day/night ratio was about 5.0 when the substrate is dry, with 50.0 and 150.0 W m^{-2} latent heat flux during night and day, respectively.

Since the presented results about evapotranspiration rates make difficult to perform a comparative analysis because of the different units of measurement used by authors, Table 7 shows all data summarized and converted into kg/m^2 to facilitate the cross-comparison of the findings.

Table 7. Summary of the minimum and maximum values obtained from the parameters reviewed in experimental studies.

Ref.	Parameter	Description	Minimum value	Maximum value	Unit	Climatic condition	Minimum value kg m^{-2} day^{-1}	Maximum value kg m^{-2} day^{-1}
[49]	Sky conditions Moisture soil	Sunny day+wet soil	-	9.3	mm	Hong Kong (Cwa)	-	9.3
		Sunny day+moist soil	-	9.0			-	9.0
		Sunny day+dry soil	-	13.1			-	13.1
		Cloudy day+wet soil	-	8.1			-	8.1
		Cloudy day+moist soil	-	5.0			-	5.0
		Cloudy day+dry soil	-	5.8			-	5.8
[69]	Season Vegetation	August	-	0.08	g m^{-2} s^{-1}	Kobe (Cfa)	-	6.9
		November	-	0.02			-	1.72
		Bare soil	-	0.05			-	4.3
[46,54]	Solar radiation Relative humidity Wind speed Air temperature	**Soil UVA.** Solar radiation simulated with UVA lamps for the experiment with a green roof sample without plants.	30	130	W m^{-2}	Pennsylvania (Dfb)	1.1	4.6
		Soil Day. Solar radiation simulated with Fluorescent Daylighting VHO lamps for the experiment with	40	100			1.4	3.6

green roof sample without plants.				
UVA plants. Solar radiation simulated with UVA lamps for the experiment with a green roof sample with S. spurium	95	115	3.3	4.0
Base. Solar radiation simulated with Fluorescent Daylighting VHO lamps for the experiment with green roof sample with Delosperma nubigenum.	45	120	1.6	4.2
Humidity. Conditions equal to 'Base' experiment, except that relative humidity was set to 50%.	50	140	1.8	4.9
Solar. Conditions equal to 'Base' experiment, except solar radiation decreased by 50%.	25	55	0.9	1.9
Wind. Conditions equal to 'Base' experiment, except wind speed increased to 1 m/s.	40	170	1.4	6.0
Temperature. Conditions equal to 'Base' experiment, except air temperature changed to 26 °C.	60	140	2.1	4.9
Base II. Conditions equal to 'Base' experiment in order	40	150	1.4	5.3

		to duplicate the measurements.						
[55]	Vegetation	Sedum	-	5.0	mm	La Rochelle (Cfb)	-	5.0
		Grass	-	8.0			-	8.0
		Bare soil	-	4.2			-	4.2
[48]	Vegetation	Sedum	20	210	W m^{-2}	Melbourne (Cfb)	0.7	7.4
		Bare soil	20	280			0.7	9.9
[56]	Vegetation	Soil moist	4.0	6.0	L m^{-2} day^{-1}	Tel Aviv (Csa)	4.0	6.0
		Pennisetum	7.0	9.0			7.0	9.0
		Aptenia	3.0	6.0			3.0	6.0
		Sesuvium	6.5	7.5			6.5	7.5
		Halimione	7.5	4.0			7.5	4.0
[57]	Vegetation	Periwinkle	0.5	5.0	kg m^{-2} day^{-1}	La Rochelle (Cfb)	0.5	5.0
		Grass	0.5	3.5			0.5	3.5
		Soil bare	0.5	3.0			0.5	3.0
[58]	Substrate	Normal soil	2.0	6.0	kg m^{-2} day^{-1}	Singapore (Af)	2.0	6.0
		Artificial soil	2.0	6.0			2.0	6.0
		Artificial soil + water retention	4.0	7.0			4.0	7.0

The variability of the results depends on both the instrumentation and the parameters (plant species, substrate type, climatic conditions, etc.) influencing the ET process.
In terms of weight, the ET maximum values were 7.0 kg m^{-2} day^{-1} and 3.0 kg m^{-2} day^{-1} respectively, using artificial soil with water retention layer below the substrate and bare soil. In terms of water lost by evapotranspiration, the maximum values during a sunny day were 13.1 mm with dry soil and 8.0 mm using grass. Latent heat flux reached the maximum value with high wind speed conditions (170 W m^{-2}) and using bare soil (280 W m^{-2}) compared to *Sedum* (210 W m^{-2}).
Most of the analyzed studies performed a comparison between green roof evapotranspiration (plants + substrate) and bare soil evaporation (only substrate). However, few of them evaluated ET when different solutions of green roof layer were alternated and compared, and/or varying the plant species [55–57]. Moreover, only Tan et al. [58] measured evapotranspiration rates varying the substrate type.
Few studies evaluated the evapotranspiration under different environmental boundary conditions. In particular, in [49], the weather was differentiated into three types: sunny, cloudy and rainy. Interestingly, Jim and Peng [49] claim that the dry soil reached 13.1 kg m^{-2} day^{-1} and the wet soil 9.3 kg m^{-2} day^{-1} during sunny days. This assumption underlines the importance in evaluating, not only the substrate water content, but also the climatic conditions. Because the limited substrate-moisture effect on ET and

associated cooling that could be explained due to sufficient water supply by occasional rainfall events and regular irrigation confined soil moisture variations to a small range during the summer period and to the relatively weak capability of the substrate to hold water tightly during the dry state to resist ET water extraction.

This survey has highlighted a lack of studies concerning the effect of the drainage layer on ET. This could be an interesting field for future studies considering that the drainage layer is particularly important since it has the aim of ensuring an optimal balance between air and water within green roof system.

Further researches also should focus on optimizing green roof technology with a water retention layer inside the drainage layer in order to increase ET.

7.6. Mathematical models to characterize ET on green roofs

7.6.1. Heat and mass transfer models for ET in green roofs

Due to the heat and mass transfer through the roof resulting from shading, insulation, cooling (evapotranspiration) and wind effects, modelling the latent heat flux of green roofs is not a simple process. Many researchers have explored the heat exchange between green roofs and the environment in which the heat and mass transfer in soil were mostly taken as a quasi-steady-state process.

The energy exchanged between the green roof surface and the outside environment consists of latent and/or sensible heat. Latent heat is the heat loss by evapotranspiration that involves soil surface evaporation and vegetation transpiration. Evapotranspiration affects the net heat flux by modulating incoming/outgoing heat transfer mechanisms, depending on the plant species and on environmental conditions. An increase in the evapotranspiration rate decreases the convection heat flux related to sensible heat and storage [61]. Several studies obtained numerical results of each heat flux in order to quantify the latent heat flux.

Most of the studies used the following equations to evaluate latent heat flux on the plant canopy (L_F) and the soil surface (L_G) [91]:

$$L_F = LAI \frac{\rho_{af} c_{pa}}{\gamma(r_a + r_{sto})}(q_c - q_{af}) \tag{2}$$

$$L_G = \frac{\rho_{af} c_{pa}}{\gamma(r_g + r_a)}(q_g - q_{af}) \tag{3}$$

Stomatal resistance for transpiration r_{sto} is influenced by factors including solar radiation and vapor pressure difference, volume water content, temperature of soil. Air resistance for transpiration r_a is associated with plant height and wind speed [92].

The evapotranspiration rate from plant canopy and soil surface can be calculated by the following equations:

$$E_c = L_c/\mu \quad (4)$$

$$E_g = L_g/\mu \quad (5)$$

Feng et al. [52] simplified heat losses by transpiration (L_c) and evaporation (L_g) in one equation, so the heat loss by evapotranspiration is given by:

$$L_{et} = L_c + L_g = E_{et}\mu \quad (6)$$

where, E_{et} is the evapotranspiration rate and is given by $E_{et} = E_c + E_g$. Evapotranspiration rates can be measured by weighing or by using soil hygrometers, as explained above. This approach was used by Quezada-Garcia et al. [93] to develop a heterogeneous model of heat transfer for green roofs.

Table 8 summarizes all the references regarding the ET phenomenon within green roofs studies. This table reports that a heat transfer model for green roofs is based on different approaches and equations to evaluate the required parameters for the calculation of latent heat flux.

Table 8. Equations and/or models adopted in heat transfer models for green roofs and their validation parameters.

References	Previous equation utilized	Input parameters	Validation parameters
[70]	-	Meteorological data Substrate temperature	Temperature at 2 cm below soil Degree of saturation in substrate
[50]	Rana-Katerji [94]	-	-
[46]	-	Air temperature Air relative humidity Air speed Sky temperature Incoming solar radiation Substrate water content LAI Substrate temperature	Evapotranspiration Incident incoming short-wave radiation Incident incoming long-wave radiation Outgoing long-wave radiation Heat fluxes through green roofs Convective heat transfer fluxes Substrate top and bottom layer temperatures Substrate thermal conductivity Plant temperatures Average substrate volumetric water contents Air velocities Room air relative humidity levels and temperatures

			Spectral reflectivity of green roof samples Leaf Area Index (LAI)
[93]	Feng et al. [52]	-	Green layer temperature
[59]	Diedjig et al. [70]	Weather data Characteristics of vegetation Characteristics of soil	Soil surface temperature Temperature at 2 - 8 cm below soil
[60]	Banna [95]	-	-
[61]	Levallius [96]	-	-
[62]	Deardoff [97]	Weather data Characteristics of vegetation Characteristics of soil	Soil surface temperature
[76]	Choudhury and Monteith [98] Philip and De Vries [99]	Height of plant Minimum stomata resistance Average LAI Soil thermal capacity Soil depth Soil conductivity Reflectivity of leaves Soil water conductivity Soil water capacity	Temperature Moist distribution Heat flux

Most of the developed mathematical models that analyze the energy performance of green roofs were then validated through experimental analysis. Table 8 also shows the principal parameters used to validate the green roof models.

Unlike the models presented in section 2, which were developed to evaluate evapotranspiration on bare and/or vegetated soils, the models listed in Table 8 concern green roofs were developed to analyze the energy performance of green roofs. They considered latent heat and not having the ultimate aim of evaluating the phenomenon of evapotranspiration.

Among all the models, only Tabares-Velasco and Srebric [46] measured evapotranspiration in a laboratory set-up to validate the model. Most of the models used soil and/or plant temperatures measured in-situ to validate the proposed models. Some studies, around 35% of the literature reviewed, adopted simplified energy balance models because of the complex structures of green roofs that include canopy and soil. In particular, Tian et al. [59] analyzed the loss of water in the soil through evapotranspiration considering that it occurred only on the surface of soil while He et al. [53] assumed that the change of soil water content is equal to water loss through evapotranspiration.

Hodo-Abalo et al. [60] developed a model for evaluating the cooling potential of green roofs. The authors solved the heat transfer equations using a finite difference scheme and Thomas algorithm. The authors developed a numerical model based on an implicit finite difference method for discretizing time-average Navier-Stokes equations and for calculating evapotranspiration variations. Evapotranspiration was obtained by summing the hourly values of local latent heat flux from different layers within the canopy, added to the hourly value of soil evaporation.

Djedjig et al. [70] developed a thermo-hydric model considering the thermal inertia of the whole green roof system. This model allowed an explicit calculation of the evapotranspiration, and the thermo-physical properties of the substrate were calculated according to the volumetric water content. The results demonstrate the effectiveness of the explicit calculation of evapotranspiration, unlike the Penman–Monteith equation, which does not incorporate water stress.

Tabares-Velasco and Srebric [46] included a complete validation of heat transfer fluxes, such as evapotranspiration rates. The study had laboratory-rated acquisition equipment for the detailed measurement of evapotranspiration rates by the gravimetric method, while simultaneously measuring the total energy balance on the green roof sample. Thus, the authors used the experimental data to calibrate the green roof evapotranspiration model.

The study conducted by Tsang and Jim [61] modelled a quadratic-like relation between evapotranspiration and the water content in green roofs that allowed an analysis of the latent heat flux of green roofs in terms of volumetric water content in the soil and the relative humidity. This model considers the combined effect of evaporation and transpiration to reduce calculation complexities.

He et al. [76] analyzed energy balance of plant and soil layer using a coupled hydro-thermal transfer model validated by field experiments in Shanghai area. In particular, the authors assessed the effects of thickness of soil layer and leaf area index of plant layer on green roof energy and thermal performance. In the model, it was assumed that the water content variation of soil layer equals to the water loss through evapotranspiration.

All heat transfer models of green roofs take into account the latent heat flux due to evaporation of water from the substrate and transpiration of plants. However, only a few of them considered experimental data for their validation. Future models should include experimental measurements of ET rates for the validation process.

7.6.2. Latent heat flux results

This section describes the results found by the studies that used mathematical models to characterize ET on green roofs in order to evaluate the surface energy, focusing on the latent heat flux.

Evapotranspiration and net long wave radiation dominate the energy balance of the green roof. In particular, He et al. [53] found that, under both free-floating and air-conditioned scenarios, the evapotranspiration flux accounted for 58.15% and 63.93% respectively of all the dissipated heat by the green roof. When the moisture content of the soil is low, the proportion of evapotranspiration decreases greatly while heat convection rises. Similar results were obtained by Feng et al. [52], who found that the heat loss through the evapotranspiration of the plants–soil system accounted for 58.4% of the total energy flux and played the most important role. The net long-wave radiative exchange between the canopy and the atmosphere as sensible heat accounts for 30.9%, and the net photosynthesis of plants accounts for 9.5%. Only 1.2% was stored by plants and soil, or transferred into the room beneath. During the day, Tian et al. [59] found that most of the absorbed radiation (about 40%) is dissipated as latent heat on the canopy.

However, other studies found controversial results regarding the role of evapotranspiration in the green roof energy balance. Schweitzer and Erell [56] estimated that the contribution of evaporation was the least important of these mechanisms (about 4%). In addition, Coutts et al. [48], through an experimental analysis, evaluated the surface energy balance for green roof and bare soil, showing that only a small portion of the overall heat flux was partitioned into latent heat (0.15%) for green roof and for bare soil (0.13%). These results show that when succulent vegetation with coverage less than 100% and in absence of irrigation the evapotranspiration achieves modest benefits. The mean daytime evaporative fraction is strictly connected with the time of irrigation. It increased about 41% for green roof and 51% for bare soil immediately after the irrigation, while by the third day of having watered the latent heat flux was reduced by 26% in the green roof and by 38 % in the bare soil.

The study conducted by Lazzarin et al. in [50] evaluated the performance of a green roof system in summer in both dry and wet conditions. The wet soil gave rise to an evapotranspiration rate of about 25.0% of the overall heat flux, whereas in dry conditions that contribution was limited to 12.0%.

Tsang and Jim [61] observed that the peaks of latent heat flux (about 7 Wm^{-2}) were achieved when long period of high solar radiation occurred. Thus, solar radiation could expedite the evapotranspiration rate and increase the latent heat loss.

These results show the importance of evapotranspiration in reducing thermal loads in a green roof. As a general outcome of this section, it is possible to observe that the latent heat flux calculated through mathematical models showed a wide range of values on the overall heat flux in a green roof, depending on the mathematical model used and the boundary conditions assumed (climatic conditions).

7.7. Evaluation of ET through dynamic simulation

7.7.1. <u>EnergyPlus software</u>

This section shows the ET results obtained by using EnergyPlus [63–65] dynamic simulation software.

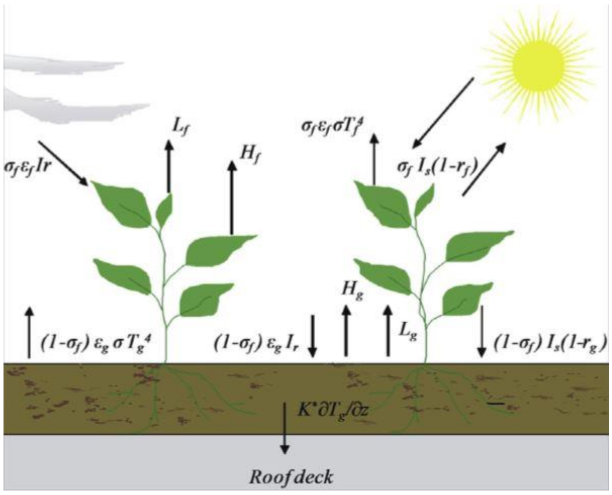

Figure 5. Energy balance of a green roof *[17]*.

EnergyPlus integrates a green roof model developed by Sailor [100] and based on an Army Corps of Engineers' FASST vegetation model [101]. This model considers simultaneously the foliage surface and soil temperatures at each time step. The "Ecoroof" module is a one-dimensional model containing energy budgets for both the foliage layer and the soil surface. It considers long and short wavelength radiation exchanges, the effects of vegetation on convective (sensible heat) thermal flux, evapotranspiration (latent heat), heat storage and transfer through the substrate (Figure 5).

The energy balance for the foliage is the following (Eq. 1):

$$F_f = \sigma_f\left[I_s\left(1-\alpha_f\right) + \varepsilon_f I_{ir} - \varepsilon_f \sigma T_f^4\right] + \frac{\sigma_f \varepsilon_f \varepsilon_g \sigma}{\varepsilon_1}\left(T_g^4 - T_f^4\right) + H_f + L_f \qquad (9)$$

where $\left[I_s\left(1-\alpha_f\right) + \varepsilon_f \sigma T_f^4\right], \frac{\sigma_f \varepsilon_f \varepsilon_g \sigma}{\varepsilon_1}\left(T_g^4 - T_f^4\right), H_f \text{ and } L_f$ are shortwave solar radiation, long wave radiation exchange between sky and foliage, convective heat transfer between air and foliage as sensible heat flux, and evapotranspiration on the foliage surface as latent heat flux, respectively.

The energy balance for the soil surface is the following (Eq. 2):

$$F_g = (1-\sigma_f)\left[I_s(1-\alpha_g) + \varepsilon_g I_{ir} - \varepsilon_g T_g^4\right] - \frac{\sigma_f \varepsilon_f \varepsilon_g \sigma}{\varepsilon_1}\left(T_g^4 - T_f^4\right) + H_g + L_g + k \times \frac{\delta T_g}{\delta z} \quad (10)$$

where all the terms have the same meaning as in Equation (1), but are referred to the soil layer. The last term represents the conductive heat transfer in the soil substrate.
The "Ecoroof" module allows to specify various features of the green roof, including height of plants, leaf area index (LAI), leaf reflectivity, thickness/density/thermal conductivity and specific heat of soil.
Table 9 provides input data for the green roof model in EnergyPlus reported by Peri et al. [79]. However, many previous studies assuming theoretical data for the features of substrate and plant species have already been developed. Therefore, the thermo-physical values used in the simulations not always may be confirmed through experimental test. As rule, it is necessary to use only realistic thermo-physical values, which have to be associated with specific plant and substrate types.

Table 9. Range of values provided by Peri et al. *[79]* for an EnergyPlus model.

Input Parameter	Range of values	
	Minimum	Maximum
LAI	0.1	5
σ_f	0	1
Canopy albedo	0.1	0.4
ρ_g	0.04	0.4
k_l	0.3	0.83
σ_t	0.11	0.5
τ_t	0.2	0.2

7.7.2. ET results using EnergyPlus

Boafo et al. [63] investigated the potential contribution of the evapotranspiration in green roofs on the annual energy consumption of an office building located in Incheon, Republic of Korea. So this study could be representative of the Dwa climate according with the Köppen classification [102]. The evapotranspiration flux was evaluated varying the LAI (from 1 to 5) as well the irrigation regime. They found that the average monthly evapotranspiration ranged from 1.80 mm·day^{-1} to 4.79 mm·day^{-1} for high LAI, from 0.31 mm·day^{-1} to 4.16 mm·day^{-1} for low LAI from 1.31 mm·day^{-1} to 4.28 mm·day^{-1} for high irrigation. For the scenarios without irrigation the ET varied from 1.31 mm · day^{-1} to 3.92 ·mm day^{-1}, in December and May respectively. As expected, the highest and lowest evapotranspiration fluxes were found during summer and winter, respectively. The latent heat flux, associated to the evapotranspiration, increasing the LAI from 1.0 to 5.0, was grown-up by 10.4% in summer and 80.2% in winter keeping soil thickness constant. Silva et al. [64] analyzed the thermal performance of intensive and extensive green roofs located in Lisbon, Csa climate according to the Köoppen classification. The evapotranspiration was significantly different in extensive green roofs (max value 2 mm·day^{-1}·10^{-4}) when compared to semi-intensive (max value 6 mm·day^{-1}·10^{-4}) and intensive roofs (max value 9 mm·day^{-1}·10^{-4}), particularly in summer when the solar radiation was higher. Vera et al. [65] investigated the effect of the variation of the LAI of the green applied over an uninsulated concrete slab and lightweight metal roofs, in different climate, i.e. Bsk (Albuquerque), Csc (Santiago) and Cfb (Melbourne) according to the Köppen classification. In this study, the LAI values were varied between 0.1 and 5.0 that represent the range of potential values for vegetated roofs. The results show that the cooling load of the room decreases when LAI increases because of the increase in the evapotranspiration that diverts incoming solar heat gains through the roof, for the three evaluated cities. A heat flux reduction of about 20.0 W/m^2 was calculated when a vegetated roof without plant was compared to a vegetated roof with plants having a LAI equal to 5.0. Finally, the highest evapotranspiration flux was achieved with a LAI of 4.79 mm·day^{-1}) and irrigation of 4.28 mm·day^{-1} during the summer period.

7.8. Sensitivity analysis of green roof ET

The above performed review have highlighted that there is a plethora of parameters, as well as their reciprocal meddling, that affect the evapotranspiration process. Thereby, several studies from the literature review have tried to perform sensitivity analysis to understand which parameter most affects ET.

Tsang and Jim [61] have investigated the influence of the volumetric water content and the air convection coefficient on the performance of the green roofs. Their sensitivity test showed that an increase from 30 to 60 % of VWC implies a reduction of heat stored in the green roofs by 24 %. While, the increase from 12 to 16 W·m-2·K-1 of the convection coefficient reduces the heat stored by 45 %.

Tabares-Velasco and Srebric [46] carried out a sensitivity analysis of the energy performance of the green roof, considering the effect of soil thickness, wind velocity, volumetric water content, solar radiation, and stomatal resistance. The results of this study provide, in function of the parameters and their range of variation analyzed, the evapotranspiration rate expressed as latent heat flux. Starting from these results, Figure 6 has been developed in this review study with the aim to synthetize and systemize the reading of the performed study by Tabares-Velasco and Srebric.

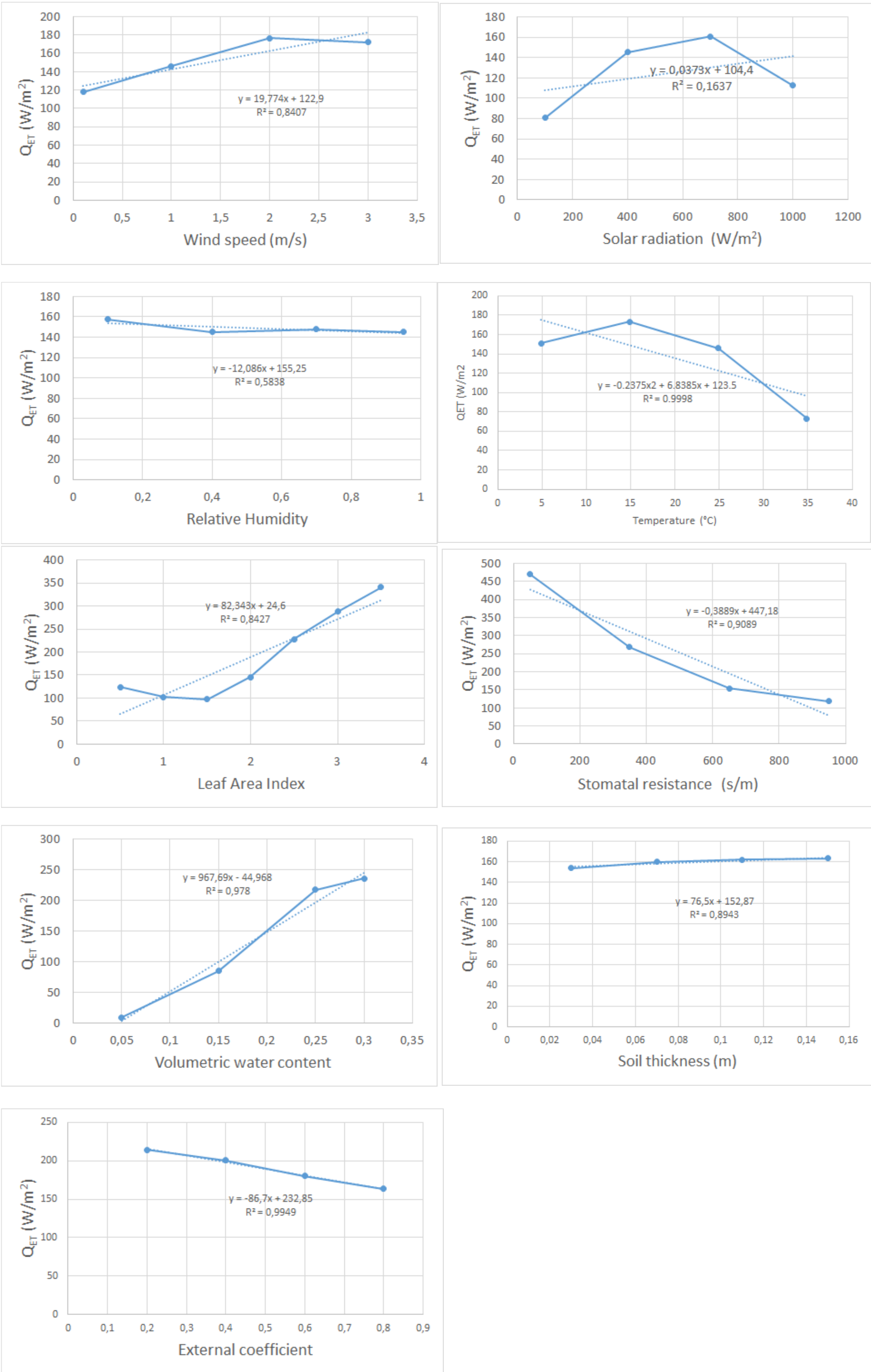

Figure 6. ET Sensitivity analyses.

This sensitivity analysis highlighted that the highest values of evapotranspiration were obtained with high volumetric water content in the substrate (0.25 and 0.30), reduced stomatal resistance (50 and 350 s/m), high values of LAI (2.5, 3.0 and 3.5), and with low values of external coefficient, i.e. incoming long and short wave radiation, (0.2 and 0.4). Where the radiation emitted from earth/atmosphere is terrestrial or longwave radiation and the radiation emitted from sun is solar or shortwave radiation. These results can be inferred by observing the value assumed for the different percentage between the minimum and maximum values of ET (ΔQ_{ET}). The volumetric water content is the variable with the largest difference (ΔQ_{ET} =96.3%) between the minimum and maximum value of evapotranspiration, from 8.8 to 235 W/m^2.

Stomatal resistance and LAI also produce considerable variations in the ET, with values between 469.5 and 118.5 W/m^2 (ΔQ_{ET} =74.8%) and between 340.6 and 97.4 W/m^2, (ΔQ_{ET} =71.4%), respectively.

In a similar manner, the variables with less influence on evapotranspiration process were identified. When substrate thickness and relative humidity vary, the evapotranspiration flux remains almost constant, with a ΔQ_{ET} variation of 5.8 and 7.8 %, respectively. Values of evapotranspiration lower than 145 W·m^{-2} are never reached whatever was the variations in relative humidity, substrate thickness, and long and short wave radiation.

Furthermore, Figure 6 shows that wind speed, volumetric water content, and leaf area index have a positive correlation with ET, i.e. the higher these values, the higher the ET. Otherwise, air temperature, external coefficients (long and short wave radiation), and stomatal resistance are characterized by a negative correlation with ET. Finally, relative humidity and soil thickness present a neutral correlation.

The performed elaboration allows to evidence as all the parameter variations can be represented by means of a second order polynomial regression, which shows rather high value of the correlation coefficient R^2. Therefore, this correlation could constitute a reference for comparing set of experimental results coming from different studies.

Moreover, a frequency analysis on the results coming from Tabares-Velasco and Srebric [62] was also carried out. It is possible to observe that the highest frequencies of Q_{ET} are in the range 100-149 and 150-199 Wm^{-2} (Figure 7, left). The cumulative curve (Figure 7, right) indicates that 90% of the values of Q_{ET} are lower than 249 Wm^{-2}.

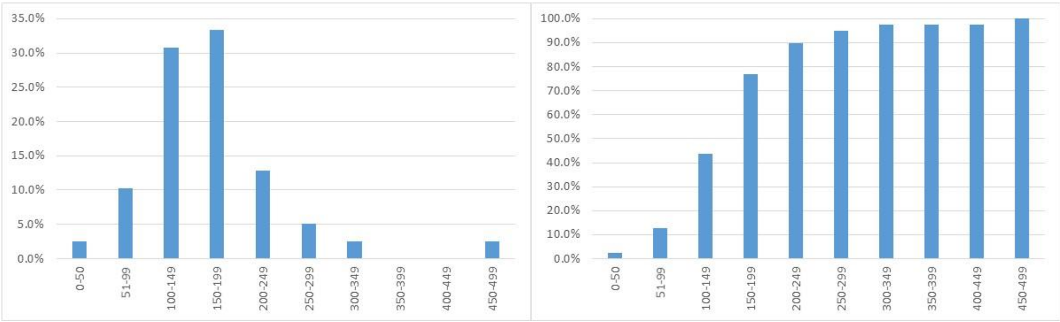

Figure 7. A frequency analysis of energy for evapotranspiration Q_{ET} (left) and the cumulative curve (right).

This section has highlighted which factors are influencing ET and how their variation has positively or negatively affect evapotranspiration. Moreover, after having analysed data from the literature the correlations, as well as the range of variation of ET found, helps in establishing a comparative framework between different researches.

7.9. Conclusions

The purpose of this study was to review the impact of ET on green roofs. Although most of the studies agree to consider evapotranspiration among the main factors affecting the behavior of green roofs, only few studies experimentally assessed evapotranspiration rates. The following general conclusions can be drawn:

- The experimental studies carried out have made use a wide variety of equipment and techniques for the measurement of ET. When the objective is directly to assess the evapotranspiration of green roofs, high precision load cells that determine the evolution of weight over time are the most widely used equipment.
- Many of the mathematical models used to evaluate the performance of green roofs take into account the latent heat flux due to evaporation of water from the substrate and transpiration of plants. However, only few models were validated considering experimental data of evapotranspiration rates, and in many cases, the experiments were conducted in laboratory conditions and for short periods. Therefore, more research that experimentally analyses all factors that affect the ET phenomenon under real conditions will help to fill the gap in the current state of the art.
- The high variability of technical-constructive solutions and climatic conditions affecting the energy performance of green roofs, the different units of measurement used to quantify evapotranspiration, the lack of information regarding the duration of the experiments, and the specific climatic conditions make it difficult to compare the results obtained from different studies. Thus,

some guidelines to develop a correct experimental methodology could help in providing better comparative analysis for future research.

- Some studies evaluated evapotranspiration in green roofs by comparing roofs with and without vegetation and by implementing different plant species. However, only few of them evaluated the evapotranspiration rate by varying the type of substrate. Finally, an important lack of studies considering the role of the drainage layer in the ET process of a green roof was also detected.
- There are geographic areas of the world with high potential ET rates where this phenomenon has not yet sufficiently evaluated for green roofs.
- There are no studies correlating ET with external surface temperatures of the green roof, although many studies determined that one of the main advantages of using green roofs is the reduction of surface temperatures and the consequent mitigation of the urban heat island effect.

Furthermore, the following are the specific conclusions:

- Load cells are the equipment that could be recommended for future studies to assess the evapotranspiration of green roofs in a direct and high precision way. They allow monitoring the evolution of the tray weights due to water loss over time in kg m^{-2} day^{-1} that is the most appropriate unit of measurements to estimate the evapotranspiration at any desired time-step.
- The sensitivity analysis highlighted that the highest values of evapotranspiration were achieved with high volumetric water content in the substrate, reduced stomatal resistance and high values of LAI.
- On one hand, the variation of the volumetric water content in the substrate causes the largest fluctuation between the minimum and maximum values of evapotranspiration. On the other hand, the variation in the substrate thickness and relative humidity showed the minimum variation on the heat flux, being the parameters that less affect the ET in a green roof.
- Here the importance of testing experimentally the ET process during enough extended periods of time, covering all the different seasons and climate conditions to correlate the ET with the main meteorological scenarios (e.g. sunny, cloudy, and rainy days) have to be highlighted.
- Moreover, further studies should be carried out to assess the evapotranspiration of different green roof solutions considering the influence of the drainage, as well as to investigate those geographic areas of the world, which has high potential for green roof evapotranspiration.

Globally, this review analysis provides valuable information for building companies, architects, engineers, designers and stakeholders, on the ET of various green roof solutions and the different materials used. In addition, this thesis chapter highlighted the principal gaps in the current literature that will lead researchers to perform new studies within this topic.

References

[1] M. Santamouris, Regulating the damaged thermostat of the cities - Status, impacts and mitigation challenges, Energy Build. 91 (2015) 43–56. doi:10.1016/j.enbuild.2015.01.027.
[2] H. Akbari, C. Cartalis, D. Kolokotsa, A. Muscio, A.L. Pisello, F. Rossi, M. Santamouris, A. Synnefa, N.H. Wong, M. Zinzi, Local climate change and urban heat island mitigation techniques – the state of the art, J. Civ. Eng. Manag. 22 (2016) 1–16. doi:10.3846/13923730.2015.1111934.
[3] M.T. Hoelscher, T. Nehls, B. Jänicke, G. Wessolek, Quantifying cooling effects of facade greening: Shading, transpiration and insulation, Energy Build. 114 (2016) 283–290. doi:10.1016/j.enbuild.2015.06.047.
[4] O. Buchin, M.T. Hoelscher, F. Meier, T. Nehls, F. Ziegler, Evaluation of the health-risk reduction potential of countermeasures to urban heat islands, Energy Build. 114 (2016) 27–37. doi:10.1016/j.enbuild.2015.06.038.
[5] F. Rosso, I. Golasi, V.L. Castaldo, C. Piselli, A.L. Pisello, F. Salata, M. Ferrero, F. Cotana, A. de Lieto Vollaro, On the impact of innovative materials on outdoor thermal comfort of pedestrians in historical urban canyons, Renew. Energy. 118 (2018) 825–839. doi:10.1016/j.renene.2017.11.074.
[6] S. Cascone, G. Sciuto, Recovery and reuse of abandoned buildings for student housing: A case study in Catania, Italy, Front. Archit. Res. (2018). doi:10.1016/j.foar.2018.08.004.
[7] U. Berardi, A cross-country comparison of the building energy consumptions and their trends, Resour. Conserv. Recycl. 123 (2017) 230–241. doi:10.1016/j.resconrec.2016.03.014.
[8] U. Berardi, The outdoor microclimate benefits and energy saving resulting from green roofs retrofits, Energy Build. 121 (2016) 217–229. doi:10.1016/j.enbuild.2016.03.021.
[9] M. Santamouris, Cooling the cities - A review of reflective and green roof mitigation technologies to fight heat island and improve comfort in urban environments, Sol. Energy. 103 (2014) 682–703. doi:10.1016/j.solener.2012.07.003.
[10] E. Ng, L. Chen, Y. Wang, C. Yuan, A study on the cooling effects of greening in a high-density city: An experience from Hong Kong, Build. Environ. 47 (2012) 256–271. doi:10.1016/j.buildenv.2011.07.014.
[11] K.X. Soulis, N. Ntoulas, P.A. Nektarios, G. Kargas, Runoff reduction from extensive green roofs having different substrate depth and plant cover, Ecol. Eng. 102 (2017) 80–89. doi:10.1016/j.ecoleng.2017.01.031.
[12] J.C. Berndtsson, Green roof performance towards management of runoff water quantity and quality: A review, Ecol. Eng. 36 (2010) 351–360. doi:10.1016/j.ecoleng.2009.12.014.
[13] R.A. Francis, J. Lorimer, Urban reconciliation ecology: The potential of living roofs and walls, J. Environ. Manage. 92 (2011) 1429–1437. doi:10.1016/j.jenvman.2011.01.012.
[14] D.B. Rowe, Green roofs as a means of pollution abatement, Environ. Pollut. 159 (2011) 2100–2110. doi:10.1016/j.envpol.2010.10.029.
[15] F. Olivieri, C. Di Perna, M. D'Orazio, L. Olivieri, J. Neila, Experimental measurements and numerical model for the summer performance assessment of extensive green roofs in a Mediterranean coastal climate, Energy Build. 63 (2013) 1–14. doi:10.1016/j.enbuild.2013.03.054.
[16] P. Bevilacqua, D. Mazzeo, N. Arcuri, Thermal inertia assessment of an

experimental extensive green roof in summer conditions, Build. Environ. 131 (2018) 264–276. doi:10.1016/j.buildenv.2017.11.033.

[17] A. Gagliano, M. Detommaso, F. Nocera, G. Evola, A multi-criteria methodology for comparing the energy and environmental behavior of cool, green and traditional roofs, Build. Environ. 90 (2015) 71–81. doi:10.1016/j.buildenv.2015.02.043.

[18] T.E. Morakinyo, K.W.D. Kalani, C. Dahanayake, E. Ng, C.L. Chow, Temperature and cooling demand reduction by green-roof types in different climates and urban densities: A co-simulation parametric study, Energy Build. 145 (2017) 226–237. doi:10.1016/j.enbuild.2017.03.066.

[19] I. Jaffal, S. Ouldboukhitine, R. Belarbi, A comprehensive study of the impact of green roofs on building energy performance, Renew. Energy. 43 (2012) 157–164. doi:10.1016/j.renene.2011.12.004.

[20] L.L.H. Peng, C.Y. Jim, Green-roof effects on neighborhood microclimate and human thermal sensation, Energies. 6 (2013) 598–618. doi:10.3390/en6020598.

[21] Y. Wang, F. Bakker, R. de Groot, H. Wörtche, Effect of ecosystem services provided by urban green infrastructure on indoor environment: A literature review, Build. Environ. 77 (2014) 88–100. doi:10.1016/j.buildenv.2014.03.021.

[22] C.Y. Jim, L.L.H. Peng, Weather effect on thermal and energy performance of an extensive tropical green roof, Urban For. Urban Green. 11 (2012) 73–85. doi:10.1016/j.ufug.2011.10.001.

[23] M. D’Orazio, C. Di Perna, E. Di Giuseppe, Green roof yearly performance: A case study in a highly insulated building under temperate climate, Energy Build. 55 (2012) 439–451. doi:10.1016/j.enbuild.2012.09.009.

[24] L.L.H. Peng, C.Y. Jim, Seasonal and diurnal thermal performance of a subtropical extensive green roof: The impacts of background weather parameters, Sustain. 7 (2015) 11098–11113. doi:10.3390/su70811098.

[25] S. Cascone, F. Catania, A. Gagliano, G. Sciuto, A comprehensive study on green roof performance for retrofitting existing buildings, Build. Environ. 136 (2018) 227–239. doi:10.1016/j.buildenv.2018.03.052.

[26] R. Castiglia Feitosa, S.J. Wilkinson, Attenuating heat stress through green roof and green wall retrofit, Build. Environ. 140 (2018) 11–22. doi:10.1016/j.buildenv.2018.05.034.

[27] C.Y. Jim, S.W. Tsang, Modeling the heat diffusion process in the abiotic layers of green roofs, Energy Build. 43 (2011) 1341–1350. doi:10.1016/j.enbuild.2011.01.012.

[28] C.Y. Jim, Assessing climate-adaptation effect of extensive tropical green roofs in cities, Landsc. Urban Plan. 138 (2015) 54–70. doi:10.1016/j.landurbplan.2015.02.014.

[29] O. Saadatian, K. Sopian, E. Salleh, C.H. Lim, S. Riffat, E. Saadatian, A. Toudeshki, M.Y. Sulaiman, A review of energy aspects of green roofs, Renew. Sustain. Energy Rev. 23 (2013) 155–168. doi:10.1016/j.rser.2013.02.022.

[30] A.B. Besir, E. Cuce, Green roofs and facades: A comprehensive review, Renew. Sustain. Energy Rev. 82 (2018) 915–939. doi:10.1016/j.rser.2017.09.106.

[31] V.L. Barradas, A. Tejeda-Martínez, E. Jáuregui, Energy balance measurements in a suburban vegetated area in Mexico City, Atmos. Environ. 33 (1999) 4109–4113. doi:10.1016/S1352-2310(99)00152-1.

[32] B.M. Wadzuk, M. Asce, D. Schneider, M. Feller, R.G. Traver, Evapotranspiration from a Green-Roof Storm-Water Control Measure, J. Irrig. Drain. Eng. 139 (2013) 995–1003. doi:10.1061/(ASCE)IR.1943-4774.0000643.

[33] C. Berretta, S. Poe¨, V. Stovin, Reprint of “Moisture content behaviour in extensive green roofs during dry periods: The influence of vegetation and substrate characteristics,” J. Hydrol. 516 (2014) 37–49. doi:10.1016/j.jhydrol.2014.04.001.

[34] D.J. Watson, Comparative Physiological Studies on the Growth of Field Crops: I. Variation in Net Assimilation Rate and Leaf Area between Species and Varieties, and within and between Years, Ann. Bot. 11 (1947) 41–76. doi:10.1093/oxfordjournals.aob.a083148.

[35] E. Voyde, E. Fassman, R. Simcock, J. Wells, Quantifying Evapotranspiration Rates for New Zealand Green Roofs, J. Hydrol. Eng. 15 (2010) 395–403. doi:10.1061/(ASCE)HE.1943-5584.0000141.

[36] L. Zhao, J. Xia, C. yu Xu, Z. Wang, L. Sobkowiak, C. Long, Evapotranspiration estimation methods in hydrological models, J. Geogr. Sci. 23 (2013) 359–369. doi:10.1007/s11442-013-1015-9.

[37] G.H. Hargreaves, R.G. Allen, History and evaluation of Hargreaves evapotranspiration equation, J. Irrig. Drain. Eng. 129 (2003) 53–63. doi:10.1061/(ASCE)0733-9437(2003)129:1(53).

[38] C.H.B. Priestley, R.J. Taylor, On the Assessment of Surface Heat Flux and Evaporation Using Large-Scale Parameters, Mon. Weather Rev. 100 (1972) 81–92. doi:10.1175/1520-0493(1972)100<0081:OTAOSH>2.3.CO;2.

[39] H.L. Penman, Natural Evaporation from Open Water, Bare Soil and Grass, Proc. R. Soc. A Math. Phys. Eng. Sci. 193 (1948) 120–145. doi:10.1098/rspa.1948.0037.

[40] D.E. Marasco, P.J. Culligan, W.R. McGillis, Evaluation of common evapotranspiration models based on measurements from two extensive green roofs in New York City, Ecol. Eng. 84 (2015) 451–462. doi:10.1016/j.ecoleng.2015.09.001.

[41] R.G. Allen, D. Raes, M. Smith, Crop evapotranspiration - Guidelines for computing crop water requirements - FAO Irrigation and drainage paper 56., (1998). doi:10.1016/j.eja.2010.12.001.

[42] D.M. Sumner, J.M. Jacobs, Utility of Penman-Monteith, Priestley-Taylor, reference evapotranspiration, and pan evaporation methods to estimate pasture evapotranspiration, J. Hydrol. 308 (2005) 81–104. doi:10.1016/j.jhydrol.2004.10.023.

[43] A. Jahanfar, J. Drake, B. Sleep, B. Gharabaghi, A modified FAO evapotranspiration model for refined water budget analysis for Green Roof systems, Ecol. Eng. 119 (2018) 45–53. doi:10.1016/j.ecoleng.2018.04.021.

[44] C.Y. Jim, S.W. Tsang, Biophysical properties and thermal performance of an intensive green roof, Build. Environ. 46 (2011) 1263–1274. doi:10.1016/j.buildenv.2010.12.013.

[45] C.Y. Jim, H. He, Coupling heat flux dynamics with meteorological conditions in the green roof ecosystem, Ecol. Eng. 36 (2010) 1052–1063. doi:10.1016/j.ecoleng.2010.04.018.

[46] P.C. Tabares-Velasco, J. Srebric, A heat transfer model for assessment of plant based roofing systems in summer conditions, Build. Environ. 49 (2012) 310–323. doi:10.1016/j.buildenv.2011.07.019.

[47] C.Y. Jim, S.W. Tsang, Ecological energetics of tropical intensive green roof, Energy Build. 43 (2011) 2696–2704. doi:10.1016/j.enbuild.2011.06.018.

[48] A.M. Coutts, E. Daly, J. Beringer, N.J. Tapper, Assessing practical measures to reduce urban heat: Green and cool roofs, Build. Environ. 70 (2013) 266–276. doi:10.1016/j.buildenv.2013.08.021.

[49] C.Y. Jim, L.L.H. Peng, Substrate moisture effect on water balance and thermal regime of a tropical extensive green roof, Ecol. Eng. 47 (2012) 9–23. doi:10.1016/j.ecoleng.2012.06.020.

[50] R.M. Lazzarin, F. Castellotti, F. Busato, Experimental measurements and numerical modelling of a green roof, Energy Build. 37 (2005) 1260–1267. doi:10.1016/j.enbuild.2005.02.001.

[51] L.S.H. Lee, C.Y. Jim, Thermal-cooling performance of subtropical green roof with deep substrate and woodland vegetation, Ecol. Eng. 119 (2018) 8–18.

doi:10.1016/j.ecoleng.2018.05.014.
[52] C. Feng, Q. Meng, Y. Zhang, Theoretical and experimental analysis of the energy balance of extensive green roofs, Energy Build. 42 (2010) 959–965. doi:10.1016/j.enbuild.2009.12.014.
[53] Y. He, H. Yu, N. Dong, H. Ye, Thermal and energy performance assessment of extensive green roof in summer: A case study of a lightweight building in Shanghai, Energy Build. 127 (2016) 762–773. doi:10.1016/j.enbuild.2016.06.016.
[54] P.C. Tabares-Velasco, J. Srebric, Experimental quantification of heat and mass transfer process through vegetated roof samples in a new laboratory setup, Int. J. Heat Mass Transf. 54 (2011) 5149–5162. doi:10.1016/j.ijheatmasstransfer.2011.08.034.
[55] S.E. Ouldboukhitine, R. Belarbi, R. Djedjig, Characterization of green roof components: Measurements of thermal and hydrological properties, Build. Environ. 56 (2012) 78–85. doi:10.1016/j.buildenv.2012.02.024.
[56] O. Schweitzer, E. Erell, Evaluation of the energy performance and irrigation requirements of extensive green roofs in a water-scarce Mediterranean climate, Energy Build. 68 (2014) 25–32. doi:10.1016/j.enbuild.2013.09.012.
[57] S.E. Ouldboukhitine, G. Spolek, R. Belarbi, Impact of plants transpiration, grey and clean water irrigation on the thermal resistance of green roofs, Ecol. Eng. 67 (2014) 60–66. doi:10.1016/j.ecoleng.2014.03.052.
[58] C.L. Tan, P.Y. Tan, N.H. Wong, H. Takasuna, T. Kudo, Y. Takemasa, C.V.J. Lim, H.X.V. Chua, Impact of soil and water retention characteristics on green roof thermal performance, Energy Build. 152 (2017) 830–842. doi:10.1016/j.enbuild.2017.01.011.
[59] Y. Tian, X. Bai, B. Qi, L. Sun, Study on heat fluxes of green roofs based on an improved heat and mass transfer model, Energy Build. 152 (2017) 175–184. doi:10.1016/j.enbuild.2017.07.021.
[60] S. Hodo-Abalo, M. Banna, B. Zeghmati, Performance analysis of a planted roof as a passive cooling technique in hot-humid tropics, Renew. Energy. 39 (2012) 140–148. doi:10.1016/j.renene.2011.07.029.
[61] S.W. Tsang, C.Y. Jim, Theoretical evaluation of thermal and energy performance of tropical green roofs, Energy. 36 (2011) 3590–3598. doi:10.1016/j.energy.2011.03.072.
[62] S.-E. Ouldboukhitine, R. Belarbi, I. Jaffal, A. Trabelsi, Assessment of green roof thermal behavior: A coupled heat and mass transfer model, Build. Environ. 46 (2011) 2624–2631. doi:10.1016/j.buildenv.2011.06.021.
[63] F.E. Boafo, J.-T. Kim, J.-H. Kim, Evaluating the impact of green roof evapotranspiration on annual building energy performance, Int. J. Green Energy. 14 (2017) 479–489. doi:10.1080/15435075.2016.1278375.
[64] C.M. Silva, M.G. Gomes, M. Silva, Green roofs energy performance in Mediterranean climate, Energy Build. 116 (2016) 318–325. doi:10.1016/j.enbuild.2016.01.012.
[65] S. Vera, C. Pinto, P.C. Tabares-Velasco, W. Bustamante, F. Victorero, J. Gironás, C.A. Bonilla, Influence of vegetation, substrate, and thermal insulation of an extensive vegetated roof on the thermal performance of retail stores in semiarid and marine climates, Energy Build. 146 (2017) 312–321. doi:10.1016/j.enbuild.2017.04.037.
[66] T.G. Theodosiou, Summer period analysis of the performance of a planted roof as a passive cooling technique, Energy Build. 35 (2003) 909–917. doi:10.1016/S0378-7788(03)00023-9.
[67] V. Azeñas, J. Cuxart, R. Picos, H. Medrano, G. Simó, A. López-Grifol, J. Gulías, Thermal regulation capacity of a green roof system in the mediterranean region: The effects of vegetation and irrigation level, Energy Build. 164 (2018) 226–238. doi:10.1016/j.enbuild.2018.01.010.

[68] G. Pèrez, J. Coma, I. Martorell, L.F. Cabeza, Vertical Greenery Systems (VGS) for energy saving in buildings: A review, Renew. Sustain. Energy Rev. 39 (2014) 139–165. doi:10.1016/j.rser.2014.07.055.

[69] H. Takebayashi, M. Moriyama, Surface heat budget on green roof and high reflection roof for mitigation of urban heat island, Build. Environ. 42 (2007) 2971–2979. doi:10.1016/j.buildenv.2006.06.017.

[70] R. Djedjig, S.-E. Ouldboukhitine, R. Belarbi, E. Bozonnet, Development and validation of a coupled heat and mass transfer model for green roofs, Int. Commun. Heat Mass Transf. 39 (2012) 752–761. doi:10.1016/j.icheatmasstransfer.2012.03.024.

[71] C.E. Seubert, C.S.T. Daughtry, D.A. Holt, M.F. Baumgardner, Aggregating Available Soil Water Holding Capacity Data for Crop Yield Models, 1984.

[72] C.J. Willmott, K. Matsuura, Willmott and Feddema’s Moisture Index Archive: Gridded Monthly Climatologies, (2001).

[73] M. Qin, G. Walton, R. Belarbi, F. Allard, Simulation of whole building coupled hygrothermal-airflow transfer in different climates, Energy Convers. Manag. 52 (2011) 1470–1478. doi:10.1016/j.enconman.2010.10.010.

[74] T. Susca, S.R. Gaffin, G.R. Dell’Osso, Positive effects of vegetation: Urban heat island and green roofs, Environ. Pollut. 159 (2011) 2119–2126. doi:10.1016/j.envpol.2011.03.007.

[75] P. Bevilacqua, J. Coma, G. Pérez, C. Chocarro, A. Juárez, C. Solé, M. De Simone, L.F. Cabeza, Plant cover and floristic composition effect on thermal behaviour of extensive green roofs, Build. Environ. 92 (2015) 305–316. doi:10.1016/j.buildenv.2015.04.026.

[76] Y. He, H. Yu, A. Ozaki, N. Dong, S. Zheng, Influence of plant and soil layer on energy balance and thermal performance of green roof system, Energy. 141 (2017) 1285–1299. doi:10.1016/j.energy.2017.08.064.

[77] K.L. Getter, D.B. Rowe, Media depth influences Sedum green roof establishment, Urban Ecosyst. 11 (2008) 361–372. doi:10.1007/s11252-008-0052-0.

[78] T. Takakura, S. Kitade, E. Goto, Cooling effect of greenery cover over a building, Energy Build. 31 (2000) 1–6. doi:10.1016/S0378-7788(98)00063-2.

[79] G. Peri, G. Rizzo, G. Scaccianoce, M. La Gennusa, P. Jones, Vegetation and soil – related parameters for computing solar radiation exchanges within green roofs: Are the available values adequate for an easy modeling of their thermal behavior?, Energy Build. 129 (2016) 535–548. doi:10.1016/j.enbuild.2016.08.018.

[80] P. Ferrante, M. La Gennusa, G. Peri, G. Rizzo, G. Scaccianoce, Vegetation growth parameters and leaf temperature: Experimental results from a six plots green roofs’ system, Energy. 115 (2016) 1723–1732. doi:10.1016/j.energy.2016.07.085.

[81] R. Kumar, S.C. Kaushik, Performance evaluation of green roof and shading for thermal protection of buildings, Build. Environ. 40 (2005) 1505–1511. doi:10.1016/j.buildenv.2004.11.015.

[82] T. Savi, S. Andri, A. Nardini, Impact of different green roof layering on plant water status and drought survival, Ecol. Eng. 57 (2013) 188–196. doi:10.1016/j.ecoleng.2013.04.048.

[83] N.D. VanWoert, D.B. Rowe, J.A. Andresen, C.L. Rugh, L. Xiao, Watering regime and green roof substrate design affect Sedum plant growth, HortScience. 40 (2005) 659–664. doi:10.2134/jeq2004.0364.

[84] A. Pianella, R.E. Clarke, N.S.G. Williams, Z. Chen, L. Aye, Steady-state and transient thermal measurements of green roof substrates, Energy Build. 131 (2016) 123–131. doi:10.1016/j.enbuild.2016.09.024.

[85] J. Coma, A. de Gracia, M. Chàfer, G. Pérez, L.F. Cabeza, Thermal characterization of different substrates under dried conditions for extensive

green roofs, Energy Build. 144 (2017) 175–180. doi:10.1016/j.enbuild.2017.03.031.
[86] J. Coma, G. Pérez, A. Castell, C. Solé, L.F. Cabeza, Green roofs as passive system for energy savings in buildings during the cooling period: use of rubber crumbs as drainage layer, Energy Effic. 7 (2014) 841–849. doi:10.1007/s12053-014-9262-x.
[87] G. Pérez, A. Vila, L. Rincón, C. Solé, L.F. Cabeza, Use of rubber crumbs as drainage layer in green roofs as potential energy improvement material, Build. Environ. 97 (2012) 347–354. doi:10.1016/j.apenergy.2011.11.051.
[88] L. Rincón, J. Coma, G. Pérez, A. Castell, D. Boer, L.F. Cabeza, Environmental performance of recycled rubber as drainage layer in extensive green roofs. A comparative Life Cycle Assessment, Build. Environ. 74 (2014) 22–30. doi:10.1016/j.buildenv.2014.01.001.
[89] K.L. Getter, D.B. Rowe, J.A. Andresen, I.S. Wichman, Seasonal heat flux properties of an extensive green roof in a Midwestern U.S. climate, Energy Build. 43 (2011) 3548–3557. doi:10.1016/j.enbuild.2011.09.018.
[90] T. Ayata, P.C. Tabares-Velasco, J. Srebric, An investigation of sensible heat fluxes at a green roof in a laboratory setup, Build. Environ. 46 (2011) 1851–1861. doi:10.1016/j.buildenv.2011.03.006.
[91] E. Alexandri, P. Jones, Developing a one-dimensional heat and mass transfer algorithm for describing the effect of green roofs on the built environment: Comparison with experimental results, Build. Environ. 42 (2007) 2835–2849. doi:10.1016/j.buildenv.2006.07.004.
[92] K. Richards, Adaptation of a leaf wetness model to estimate dewfall amount on a roof surface, Agric. For. Meteorol. 149 (2009) 1377–1383. doi:10.1016/j.agrformet.2009.02.014.
[93] S. Quezada-Garcìa, G. Espinosa-Paredes, M.A. Escobedo-Izquierdo, A. Vàzquez-Rodrìguez, R. Vàzquez-Rodrìguez, J.J. Ambriz-Garcìa, Heterogeneous model for heat transfer in Green Roof Systems, Energy Build. 139 (2017) 205–213. doi:10.1016/j.enbuild.2017.01.015.
[94] G. Rana, N. Katerji, Measurement and estimation of actual evapotranspiration in the eld under Mediterranean climate: a review, Eur. J. Agron. 13 (2000) 125–153. doi:10.1016/S1161-0301(00)00070-8.
[95] M. Banna, L. Pietri, B. Zeghmati, Turbulent mixed convection of heat and water vapor transfers in a two-dimensional vegetation canopy, Heat Mass Transf. Und Stoffuebertragung. 40 (2004) 757–768. doi:10.1007/s00231-003-0432-1.
[96] J. Levallius, Green roofs on municipal buildings in Lund - Modeling potential environmental benefits, Master Sci. Thesis, Lund Univ. Lund,. (2005). doi:10.1121/1.2934487.
[97] J.W. Deardorff, Efficient prediction of ground surface temperature and moisture, with inclusion of a layer of vegetation, J. Geophys. Res. 83 (1978) 1889. doi:10.1029/JC083iC04p01889.
[98] B.J. Choudhury, J.L. Monteith, A four-layer model for the heat budget of homogeneous land surfaces, Q. J. R. Meteorol. Soc. 114 (1988) 373–398. doi:10.1002/qj.49711448006.
[99] J.R. Philip, D.A. De Vries, Moisture movement in porous materials under temperature gradients, Eos, Trans. Am. Geophys. Union. 38 (1957) 222–232. doi:10.1029/TR038i002p00222.
[100] D.J. Sailor, A green roof model for building energy simulation programs, Energy Build. 40 (2008) 1466–1478. doi:10.1016/j.enbuild.2008.02.001.
[101] S. Frankenstein, G. Koenig, Fast All-Season Soil STrength (FASST) Cold Regions Research and Engineering Laboratory, (2004).
[102] M. Kottek, J. Grieser, C. Beck, B. Rudolf, F. Rubel, World map of the Köppen-Geiger climate classification updated, Meteorol. Zeitschrift. 15 (2006) 259–263. doi:10.1127/0941-2948/2006/0130.

8. Experimental set-up design to evaluate the evaporative cooling potential in extensive green roofs substrates in a continental Mediterranean climate

8.1. Introduction

Evapotranspiration cools the surface of the plants, reduces the heat flux toward the interior of the building and decreases the urban heat island effect. Furthermore, review studies on urban green spaces carried out by Besir and Cuce [1], Raji et al. [2] demonstrated that environmental benefits related to stormwater management, building energy usage, carbon sequestration and air pollution depend on the rate of water loss by evapotranspiration. Vera et al. [3] provided a critical review of more than 23 heat transfer vegetative roof models developed that have been used for building energy or urban modelling purposes. Findings included that evapotranspiration controlled the intensity of all other heat fluxes by modulating incoming/outgoing heat fluxes, depending on the plant and environmental conditions. In summer conditions, evapotranspiration can divert 70–86% of the net radiation when plants are well watered. Boafo et al. [4] evaluated the evapotranspiration effect of an extensive green roof on annual energy consumption of an office building. Increasing Leaf Area Index (LAI) from 20% to 100% cover increased evapotranspiration flux by 10.4% in summer and 80.2% in winter. These results show the importance of evapotranspiration in the reduction of thermal loads on a green roof. While several studies have documented a reduction in stormwater runoff volumes from green roofs, few have directly quantified rates of evapotranspiration in terms of passive cooling potential, although agreeing that green roofs mitigate high rooftop heating.

Evapotranspiration is the combined water vapor surface flux resulting from evaporation and plant transpiration. Evaporation is the transformation of water into vapor at the surface of the wet growing media while transpiration is the physiological process of transforming water into vapor at the plant surfaces, primarily leaves. This process occurs when there is a vapor pressure differential between the plants and surrounding air. Evapotranspiration is influenced by precipitation history (intensity, duration, inter-event times), climatic conditions (net radiation, temperature, humidity, wind), vegetation characteristics (species, leaf area index, stage of growth) and substrate properties (porosity, permeability, field capacity, capillary pressure-saturation relationship).

In a previous review study, Cascone et al. [5] reported that evapotranspiration rates can be obtained by direct measurement, or indirect approaches with mathematical models. Because the cooling effect is invisible and difficult to measure directly, many studies have calibrated empirical and analytical equations to evaluate evapotranspiration rates. In 1998, the Food and Agriculture Organization (FAO) standardized the equation elaborated by Penman and Monteith as the FAO model to calculate the evapotranspiration of an extensive land-surface fully covered by grass of uniform height in a well-watered condition. Jahanfar et al. [6] have reported that the FAO method underestimates evapotranspiration for green roof systems, especially during dry periods. The inaccuracy of evapotranspiration prediction methods in water-limited conditions is a significant gap in assessing the performance of green roof. Evapotranspiration rate can be directly evaluated by measuring water losses from a roof assembly. Previous research studies have quantified evapotranspiration with weighing lysimeters that directly measure water loss by using a load sensor or scale. Alternatively, a few studies have used soil water balance approach. The soil water balance is performed by tracking changes in the substrate water content that can be measured with probes based on different measurement methods.

In order to fill the literature gaps, this thesis chapter aims to develop an experimental set-up for the evaluation of passive cooling potential of green roofs improving the knowledge of the correlation between the evapotranspiration phenomenon and the thermal performance of an extensive green roof. To this end, a new experimental set-up was designed and built on the roof top of the CREA building at the University of Lleida (Spain). It allows to determine the latent heat flux, temperatures at different layers, moisture content of the substrate, and the specific microclimatic conditions of a green roof solution. Since evapotranspiration in green roofs strongly depends on the water content in the substrate, the passive cooling potential was evaluated by varying the amount of water supplied by irrigation system. Following the description of set-up design and implementation, first results from the experimental evaluation on passive cooling of green roofs are reported without vegetation (evaporation only).

8.2. State of the art

The evapotranspiration (ET) phenomena have recently draw increased the interest by the green roof research community because of its importance on heat and mass transfer phenomenon in a green roof. With the aim to design and build up a new set-up correctly, an extensive bibliographic analysis considering only experimental studies was carried out. Thus, the review will allow to identify the strengths and the elements to be improved in the design and implementation of the experimental set-up. The literature review concerns both methodology and experimental results from previous studies. Table 1 summarizes the used set-ups in previous studies and Table 2 shows the main analyzed results.

Table 1. Summary of previous experimental set-up design to measure green roof evapotranspiration.

Reference	Sample size	Plant specie	Substrate type	Irrigation regime	ET measurements	Other measurements
Tan et al. (2017)	1.0 × 1.0 m	Cyathula prostrata	Normal garden soil and proprietary lightweight soilless media consisting mainly of perlite and organic matter	1 h each day (approximately 12 L of water supplied per m^2)	Load cells	Surface temperatures Soil moisture
Ouldboukhitine et al. (2014)	0.61 × 0.61 m	Vinca Major (grass) Lolium Perenne (Periwinkle)	Proprietary blend containing a mix of gravel, sand, silt and clay	Saturated trays	Sensor balance	Air temperature Relative humidity Heat flux
Schweitzer and Erell (2014)	1.0 × 1.0 m	Pennisetum clandestinum Aptenia cordifolia Sesuvium verrucosum Halimione portulacoides	Mixture of vermiculite and a light-weight planting mix rich in compost	1- min pulses per day, for a total of 7 L of water (summer)	Mini-lysimeter	Air temperature Surface temperature
Coutts et al. (2013)	2.4 × 2.4 m	Sedum rubrotinctum	Coarse scoria-soil mixture	No irrigation (exp n.1) Saturated trays (exp n.2)	Portable closed-chamber	Soil heat flux Soil temperature Soil moisture
Ouldboukhitine et al. (2012)	3 m^2	Grass Sedum	Medium with high porosity	Saturated trays	Sensor balance	Thermal conductivities Water content Maximum water capacities Porosity
Tabares-Velasco and Srebric (2011)	1.3 ×1.14 m	S. spurium D. nubigenum	consisted mainly of expanded clay	Saturated trays	High-resolution platform Water content reflectometer	Incident incoming short-wave radiative fluxes Incident incoming long-wave radiation Heat fluxes Substrate and plant temperature

Table 2. Summary of previous experimental results of green roof evapotranspiration.

Reference	**Samples**	**Minimum value kg/(m^2×day)**	**Maximum value kg/(m^2×day)**
Tan et al. (2017)	Normal soil	2.0	6.0
	Artificial soil	2.0	6.0
	Artificial soil + water retention	4.0	7.0
Ouldboukhitine et al. (2014)	Periwinkle	0.5	5.0
	Grass	0.5	3.5
	Soil bare	0.5	3.0
Schweitzer and Erell (2014)	Soil moist	4.0	6.0
	Pennisetum	7.0	9.0
	Aptenia	3.0	6.0
	Sesuvium	6.5	7.5
	Halimione	7.5	4.0
Coutts et al. (2013)	Sedum	0.7	7.4
	Bare soil	0.7	9.8
Ouldboukhitine et al. (2012)	Sedum	N/A	5.0
	Grass	N/A	8.0
	Bare soil	N/A	4.2
Tabares-Velasco and Srebric (2011)	Exp. n.1*	1.1	4.6
	Exp. n.2*	1.4	3.5
	Exp n. 3*	3.3	4.0
	Exp. n.4*	1.6	4.2
	Exp. n.5*	1.8	4.9
	Exp. n.6*	0.9	1.9
	Exp. n.7*	1.4	6.0
	Exp. n.8*	2.1	4.9
	Exp. n.9*	1.4	5.3

* Tabares-Velasco and Srebric (2011) and Tabares-Velasco et al. (2012) provided a detailed experiment description

Many of the reviewed studies have used lysimeters or load cells to determine the ET behavior in green roofs.

Tan et al. [7] installed nine green roof plots measuring 1 m by 1 m on a fully exposed rooftop in Singapore. Each green roof plot consisted of identical arrangement made of 4 mm thick acrylic with height of 0.4 m. The nine green roof plots were divided into three treatment combinations through varying the substrate type (e.g. normal garden soil and proprietary lightweight soilless media consisting mainly of perlite and organic matter) and presence or absence of the water retention layer, with three replicates per treatment combination. All nine green roofs were planted with *Cyathula prostrata*. The authors measured ET by weighing the mass of the middle planters for each green roof plot using load cells characterized by a measurement range from 0 to 200 kg, at one-minute intervals. The plants were irrigated for 1 h each day (approximately 12 L of water supplied per m^2). Furthermore, surface temperatures were measured using thermocouple wires at different locations for all planter boxes and soil moisture sensors were embedded in the middle planters to monitor soil moisture content for each of the set-ups. On days with clear sky conditions, the results show that ET ranged from around 2 to 6 kg m^{-2} d^{-1}. ET for sample with water retention layer was maintained at around 4–6 kg m^{-2} d^{-1}, while for samples without the water retention layer plant ET decreased to approximately 2 kg m^{-2} d^{-1}, during which wilting was observed to have occurred.

Ouldboukhitine et al. [8] investigated the evapotranspiration for green roofs under controlled laboratory conditions. The laboratory facility test consisted of two superposed wind tunnels. The wind tunnel on the top simulated the outside conditions while the wind tunnel on the bottom simulated the indoor conditions. The prototype green roof trays were assembled from 61×61 cm metal trays, designed to fit the laboratory test equipment, using typical green roof construction materials. In particular, the growing media was a proprietary blend containing a mix of gravel, sand, silt and clay. These plant types were periwinkle (*Vinca Major*) and ryegrass (*Lolium Perenne*). Hydrologic transfer was measured using a sensor balance installed under each tray to track the weight loss by the trays due to water evapotranspired during the test period. The authors began the test by saturating the trays and then recorded the weight of the trays over time using the balance sensors installed under the trays. The results showed that the evapotranspiration for trays with vegetation was always greater than evaporation of trays with growing media only. After 48 h, trays with periwinkle recorded the highest evapotranspiration rate, about 5.0 kg, comparing to those with ryegrass, about 3.5 kg. Furthermore, the results showed that the thermal resistance of the tray without plants was about 0.8 m^2 K/W. However, in the presence of vegetation, the thermal resistance was about 0.92 m^2 K/W in the case of ryegrass and about 1.27 m^2 K/W in the case of periwinkle.

Schweitzer and Erell [9] evaluated cooling performance in conjunction with actual water requirements for different plant species used in green roofs. Four types of plants with different appearance and adaptation strategies were selected: *Pennisetum clandestinum*, *Aptenia cordifolia*, *Sesuvium verrucosum* and *Halimione portulacoides*.

The experiment was carried on the campus of Tel Aviv University. The primary test cells used in the experiment consisted of asbestos-cement cylinders 1 m in diameter and 1 m high, with a wall thickness of 2 cm. The green roof assembly consisted of a watertight wooden frame 5 cm deep with a 6 mm polycarbonate sheet serving as the bottom of the tray. The growing medium was a mixture of vermiculite and a light-weight planting mix rich in compost. In the first summer, each roof received eight 1-min pulses per day, for a total of 7 L of water. In winter, the schedule was altered to reduce the daily water supply to 4 L for each 1 m^3 roof model. The water requirements were measured at the beginning of the second summer period using mini-lysimeter measurements of sample trays. In addition, temperature was also measured above and below the roof of the test cells by means of copper-constantan thermocouples to allow an estimate of the thermal resistance of the assembly and of heat flux through it. There were substantial differences among the plant species, with *A. cordifolia* being the most economical, losing less than half as much water as the *P. clandestinum*, about 3 L m^{-2} compared to 7 L m^{-2}. This rate was less even than exposed moist soil, about 3.8 L m^{-2} per day.

Coutts et al. [10] examined the thermal performance of different roofs, focussing on green and cool roofs to help identify and compare the effectiveness of rooftop treatments to mitigate urban heat. Four experimental roofs 2.4 × 2.4 m wooden platforms erected on stilts at a height of 1 m were compared, inclined at a slope of 15°. As regards the green roofs, a sheet of steel was covered with a black poly membrane, and then overlaid with a sheet of plastic egg-cups, which act as small reservoirs. Over this was laid a geo textile layer and then a coarse scoria-soil mixture that was 0.15 m deep. Green roof was planted with the succulent vegetation type *Sedum rubrotinctum*. Drainage holes were located on the downward slope to allow runoff from the roofs. These roofs were instrumented with two soil heat flux plates at a depth of 0.08 m, soil temperature at three depths (0.04, 0.05 and 0.08 m), and one soil moisture probe at a depth of 0.08 m. A portable closed-chamber was used to measure evapotranspiration rates. A circular perspex chamber with a diameter of 300 mm and a height of 415 mm was used. Evapotranspiration measurements was determined from the change in the mass concentration of water over time using a rectangular hyperbola as a saturation function to determine the initial slope. Furthermore, the authors conducted an irrigation experiment to examine changes in evapotranspiration from higher soil moisture levels under clear, sunny conditions, the samples were heavily irrigated until free drainage was observed. The results demonstrated that maximum rates of evapotranspiration increased on green roof from a mean of around 100 W m^{-2} observed for the individual days, to a mean of around 260 W m^{-2} on green roof the day after irrigation.

Ouldboukhitine et al. [11] an evaluated evapotranspiration by performing an experiment where the green roof components are taken on the same scale as those used in green roof construction. An experimental device was set up to measure the amount of water lost by evapotranspiration. In the experiment, the green roof components were replicated in a tray and suspended in a traction-compression sensor balance (ZFA sensor of SCAIME, 200-kg capacity and 0.03% accuracy). The experiment began by saturating the tray with water. Using a gravimetric technique consisting of monitoring the evolution of the tray weights over time, the evolution of the water reserve of the substrate was determined, which represents the amount of evapotranspirated water. The daily ETP with a grass tray (2.34 mm) was larger than that with a Sedum tray (1.42 mm). The daily evapotranspiration for grass measured in this experiment (2.53 mm) was greater than that calculated by the Penman-Monteith equation (1.66 mm). This comparison showed that the modelled evapotranspiration required a correction. The corrected coefficient α was 1.37.

Tabares-Velasco and Srebric [12] designed and built a new apparatus, named ‘‘Cold Plate’’, to include laboratory-rated instrumentation and to allow simultaneous measurements of all heat and mass transfer processes on a green roof. The “Cold Plate” apparatus was located inside a full-scale environmental chamber to monitor and supply different environmental conditions. Underneath the green roof sample, a platform continuously measured sample weight to quantify the water loss rates. Evapotranspiration was measured by two different approaches: changes in weight of the green roof sample due to the water losses measured with a high-resolution platform and changes in substrate volumetric water content due to the water losses measured with a water content reflectometer. Other data acquisition sensors installed in tested green roof samples were: pyranometer, pyrgeometer, heat flux meters, thermistors and anemometers. The tested green roof samples consisted of planter boxes that were 1.3 m wide and 1.14 m long. The substrate depth was approximately 0.09 m and consisted mainly of expanded clay. Below the substrate, the samples had filter and drainage layer to filter and drain all excess water from the green roof samples. Three different green roof samples were tested: without plants, with *S. spurium*, and with *D. nubigenum*. Each experimental test started by watering the samples until saturation was reached at 48 and 24 h before starting the experiments. The results demonstrated that the curves had an elongated ‘‘S’’ shape with extremely low evapotranspiration rates when the water was scarce and high evapotranspiration rates when the water was abundant in the substrate. In the middle of the substrate water content range, the relationship was approximately linear. The green roof sample achieved the largest and nearly constant evapotranspiration rates, about 150 W m^{-2}, during the first two days, or when VWC was above 0.14. Therefore, the authors concluded that the substrate water content was the most important factor in determining the evapotranspiration rates. Furthermore, among all experiments, when the air speed was about 9 times higher than other experiments, evapotranspiration rates was the largest. An increase in the air speed from 0.1 m/ s to 1 m/s resulted in an increased evapotranspiration by 10–30%. From the same experimental apparatus, Tabares-Velasco and Srebric [13] developed a model that was validated with a detailed heat and mass transfer data set. Measurements of evapotranspiration rates by the gravimetric method were carried out, while simultaneously measuring the total energy balance on the green roof sample. Therefore, this data set provided an opportunity to calibrate the evapotranspiration model specifically for extensive green roofs. The validation showed that the model predicted most of the heat and mass transfer accurately, following the same trend as the experimental data, but it underestimated maximum evapotranspiration rates when samples are the wettest. Changing substrate conditions from driest to the wettest conditions showed increased evapotranspiration from 8 to 230 W/m^2.

Tabares-Velasco and Srebric [12] and Tabares-Velasco and Srebric [13] measured evapotranspiration by using both a high-resolution platform and a water content reflectometer. The total water losses measured from the substrate water balance method were 10–20% larger than the scale readings. Thus, the authors used evapotranspiration rates measured from the scale because the scale method is the only method that directly measures evapotranspiration and the substrate water balance is an indirect and less precise technique. Furthermore, in all the previous research, full scale green roofs cannot be accommodated. A relatively large width and depth compared to the sample thickness need to be selected to assure a one-dimensional heat flux through the sample. In addition, only the core part of the green roof sample must be used for thermal measurements because the surrounding part of the sample need to be used as a buffer zone where one-dimensional flux is less likely.

8.3. Materials and methods

8.3.1. <u>Experimental set-up</u>

Two weighing lysimeters are designed and assembled by GREiA research group from University of Lleida (Figure 1) to evaluate the evapotranspiration of green roofs under different irrigation scenarios. They are made of 3 cm section of plywood structure ($\lambda = 0.138$ W·m^{-1}·K^{-1}) with a total area of 4 m^2 (Figure 1.A) and reinforced below with rectangular laminated tubes (40 × 60 × 2 mm). Immediately after the plywood base, each lysimeter is insulated from the bottom part with 8 cm of XPS panels (λ = 0.036 $W \cdot m^{-1} \cdot K^{-1}$) and completely waterproofed with a bituminous dense layer (Figure 1.B), a drainage hole allows water runoff. The whole system is weighed with eight load cells (Figure 1.C) by using four of them in each lysimeter. Since a single load cell has a maximum load service of 450 kg, each lysimeter allows a total of 1,800 kg of service. Both lysimeters are completely equal and allow to test extensive and semi-intensive green roof samples of up to 250 mm depth, as can be seen in Figure 1.D.

The irrigation system is controlled by GARDENA devices (Model: 1885) that allows personalized daily irrigation schedules. The water distribution system consists in 14 auto-compensating dripping valves distributed in 4 rows (Ø 25 mm) every 50 cm (Figure 1.B).

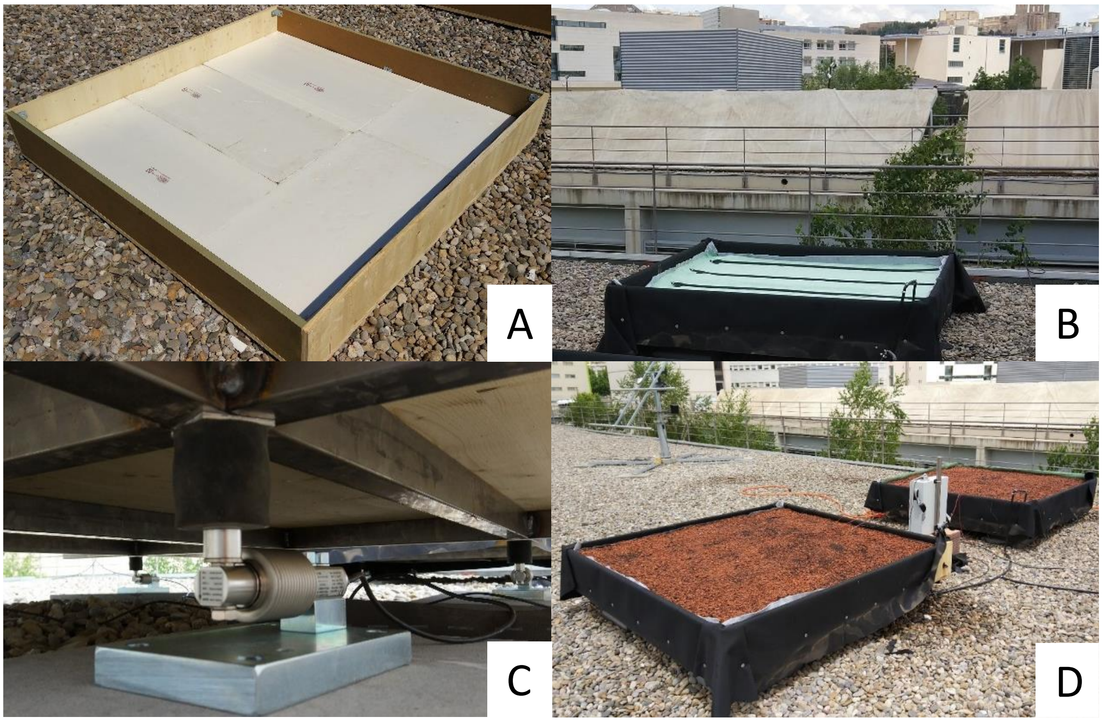

Figure 1. (A) Insulated plywood structure, (B) waterproof membrane (black), drip irrigation system, and anti-root membrane (green), (C) load cells and laminated steel tubes, (D) experimental set-up based on two identical lysimeters of 4 m^2.

8.3.2. Climate conditions

The experimental set-up is located on the rooftop of CREA building in the University of Lleida, Spain. The specific climate conditions are characterized as a continental Mediterranean (Cfa) according the Köppen-Geiger climate classification. The summers are dry and hot while winters are cold and foggy. The mean annual precipitation is 423 mm generally distributed between April-May and October-November. The mean temperature in Lleida is 15.2 ºC with a maximum mean temperature of 32 ºC in July and a minimum mean temperature of 1.5 ºC in January.

8.3.3. Instrumentation

Figure 2 shows the distribution of the sensors in both, the green roofs and the conventional flat roof that was used as a reference system. The following data was recorded at 5 min interval:

- Temperature between plywood and insulation (Point D in Figure 2) [˚C]
- Temperature between waterproof and drainage layers (Point C in Figure 2) [˚C]
- Temperature between drainage and substrate layers (Point B in Figure 2) [˚C]
- Temperature on the surface sample (Point A in Figure 2) [˚C]
- Volumetric water content in the substrate [%]
- Outdoor ambient temperature [˚C] and humidity [%] at the height of samples (60 cm)
- Global horizontal solar irradiance [W/m^2]
- Wind velocity [m/s]
- Rainfall [mm]
- Constant weight of samples [kg]

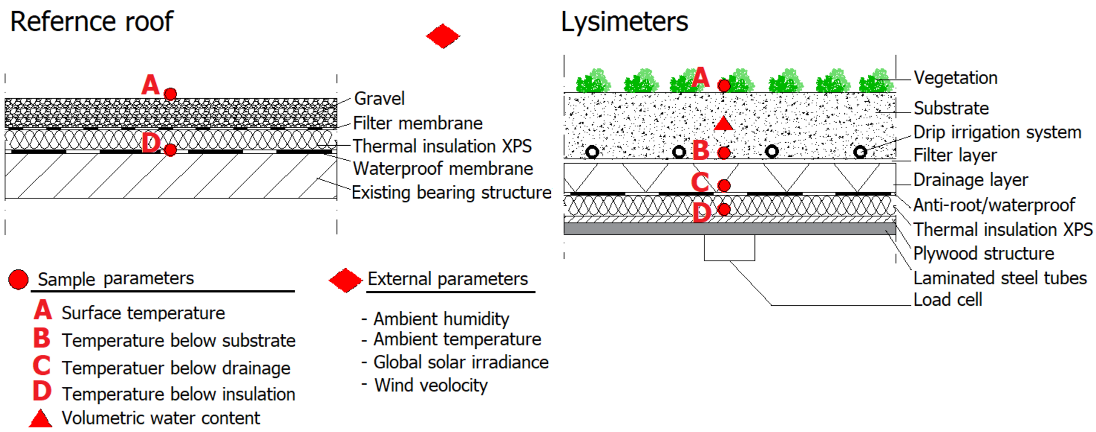

Figure 2. Distribution of the different sensors in the two lysimeters, and in the conventional reference roof.

Pt-100 DIN B probes (accuracy ± 0.3 ºC) are installed to measure the surface temperatures across the green roof section. The air temperature and humidity were measured with a TESTO transmitter (model 6651) with an accuracy of ±0.2 ºC, and ±1.7 %, respectively. To measure the wind velocity an anemometer AN046 (G.I.S Iberica) with an accuracy of ± 3% and 0.1 m/s of resolution is used. Volumetric water content is measured with Decagon EA-10 Soil moisture sensors with an accuracy of ±0.03 m^3/m^3 typical in mineral soils (± 3%), and ±0.02 m^3/m^3 in any porous medium (± 2%). A Middleton Solar pyranometer SK08 is used to capture the global solar irradiance. Finally, to measure the weigh evolution of the lysimeters the load cells

(UTILCELL Model 300) with accuracy class 3000 (minimum division of 30g) were used.

8.3.4. Green roofs

The extensive green roof consists of five different layers, from the top to the bottom: 80 mm of substrate, 2.4 mm of water distribution filter, 40 mm water retention layer, and 3 mm protective layer (Figure 3). Without considering plants, the total thickness of the system is about 130 mm and weighs approximately 83 kg/m^2 (dry) and 127 kg/m^2 (saturated) allowing up to 44 l/m^2 of water retention capacity.

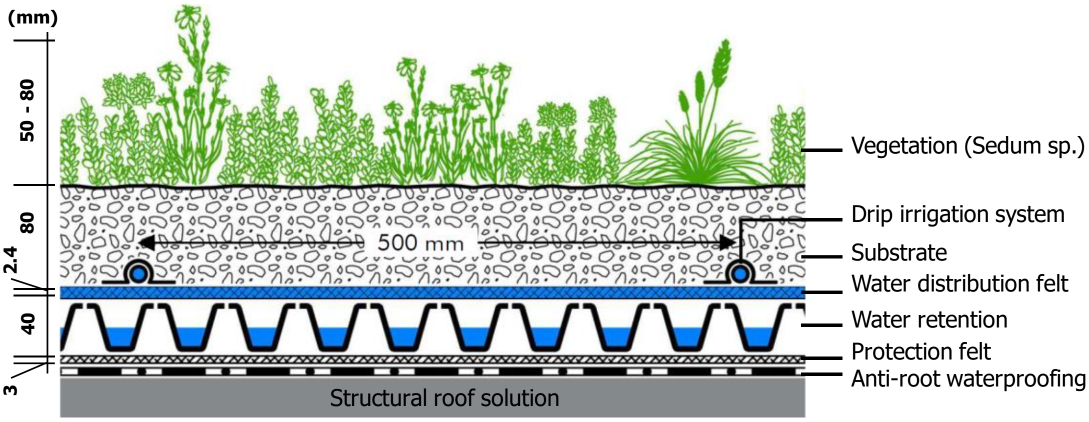

Figure 3. Detailed section of the extensive green roof system.

8.3.5. Water distribution and water retention layers

These are the two most important layers of the green roof system that manage the water available for plants. The water distribution felt (100% polyacrylic) spreads the water over the entire green roof surface and temporarily stores from 3 to 4 l/m^2 before release it into the retention layer. Once the felt is completely wet, the water permeability is approximately 20 L·m^{-2}·S^{-1}. Then, water comes into the retention layer allowing an extra storage of 5 l/m^2 in case of drought periods. In addition, the engineered design of water storage also contains air to have oxygen for a better root development.

8.3.6. Methodology of experiments

Two different types of experiments were carried out to evaluate the evaporative cooling potential of the specific substrate commonly used in extensive green roofs in a continental Mediterranean climate. Summer data was collected between 30th June and 18th September 2018.

8.3.6.1. Experiment 1

In this experiment the field capacity and the water evaporation of the substrate after simulating an intensive rainfall event was quantified. As starting point, the samples were irrigated before the sunrise until reach the saturated condition of the system.

Then, the lysimeters were evaluated under free floating conditions until the mean VWC of the substrate was 0 (dry condition). The total period of this experiment was from August 7th to 23th, 2018. It is important to highlight that there were no additional irrigations except the punctual natural precipitations.

8.3.6.2. Experiment 2

The aim of the second experiment is to obtain the maximum field capacity only using the drip irrigation system located below the substrate layer. This will help in evaluating the evaporation potential of the system by comparing two irrigation methods, the natural precipitations and the real maintenance irrigation to guarantee the survival of Sedum sp. in summer conditions. At the beginning of the experiment the samples were irrigated from the bottom part until reach the drainage layer saturation that occurred when water input and drained water were equal. Then, the system worked under free floating conditions until reach the dry condition.

8.4. Results

In addition to the weighing capacity of the lysimeters, all the experiments performed in this thesis chapter characterized the global horizontal solar irradiance [W m^{-2}], wind speed [m s^{-1}], relative humidity [%] and air temperature [ºC] because they are the principal meteorological parameters affecting the ET [kg m^{-2} day^{-1}] by removing water content from substrate and plants.

8.4.1. <u>Experiment 1</u>

8.4.1.1. Evaporation potential

Figure 4 shows the daily evolution of the ambient parameters that affect the ET in the set-up. The highest ET_{Rate} was 5.1 (kg m^{-2} day^{-1}) with a mean VWC of 15.5 % on August 7th, 2018, as expected, because it was the day of the rain simulation event. Notice that this date was the warmest day of the period with a mean daily temperature and solar radiation of 31 ºC and 451 W m^{-2}. During this experiment, there were three relevant natural rainfall events on August 8th, 12th, and 17th 2018 that have added 6.6, 3.6 and 3.5 (kg m^{-2} day^{-1}) into the system, respectively. The same rainy days, the bare substrate showed important evaporation rates about 3.8, 2.1 and 1 (kg m^{-2} day^{-1}), respectively, because the rainfall events occurred after 7:30 p.m. in all cases. In addition, the water stored during the evenings was the cause why the days after a rainfall event showed higher ET values than the days before (Figure 4). From saturated to dry conditions, the total evaporated water from the bare substrate in this period was 39.3 (kg m^{-2}) and the total water input (rain) was 15.9 (kg m^{-2}).

The negative water balance and the hot summer conditions directly affected the trend of VWC that showed a fast decrement in the first week despite received rainwater (Figure 4). The rain on August 8th increased the VWC from 11.9 to 13.3 %, while the rainfalls on 12th and 17th only cushioned the fast decrement of VWC. From August 20th on, the ET was below 1 (kg m^{-2} day^{-1}) and the VWC was almost 0%.

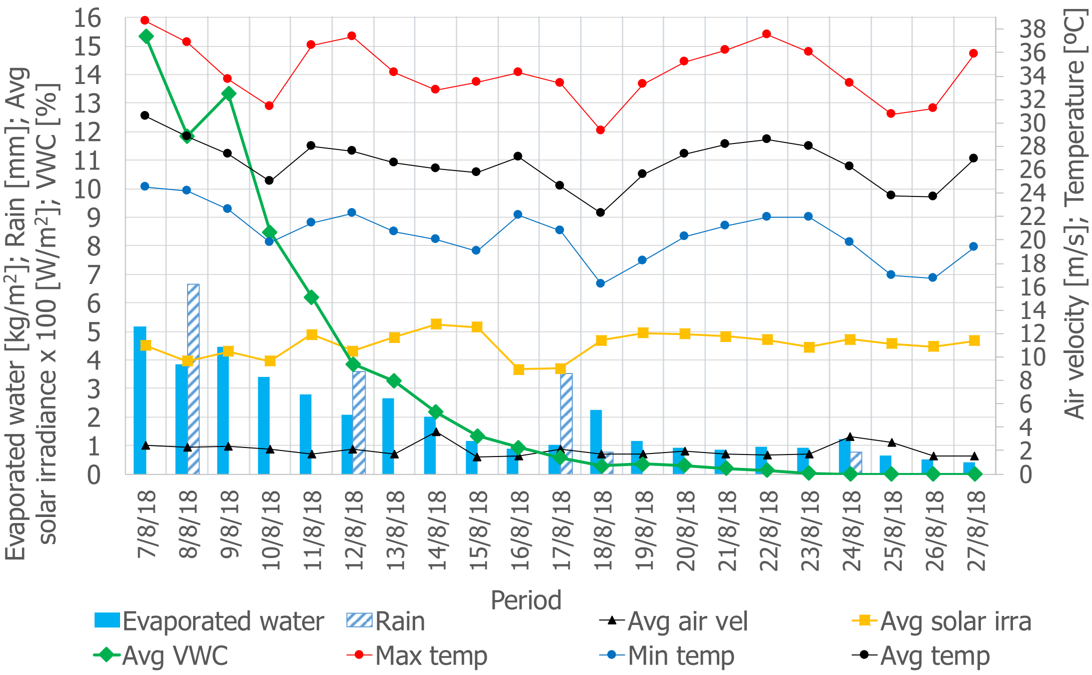

Figure 4. Water evaporation from saturated to dry conditions and daily ambient parameters along the experimental summer period.

Using the conversion table created by Cascone et al. [5], the total amount of water evaporated in this thesis chapter can be easily translated into energy and directly compared with the results from other similar studies.

Tabares-Velasco and Srebric [12] developed a laboratory setup that measures ET to quantify the heat and mass transfer in a vegetated green roof. The ET values obtained with a substrate water content of 0.15 (m^3/m^3) was approximately 150 (W/m^2) or 5.29 (kg m^{-2} day^{-1}). This result is really similar to those obtained in my experimental set-up under real conditions that was 5.1 (kg m^{-2} day^{-1}) with a mean VWC of 15.5 % on August 7th, 2018.

Higher values of ET were obtained in the study performed by Tan et al. [7] in small green roof plots of 1 m^2 on the National University of Singapore rooftop. The experiments were performed in a tropical rainforest climate (*Af*) according to the Köppen-Geiger climate classification. The substrate used is a 30 cm lightweight soilless consisting mainly of perlite and organic matter to improve soil water retention, and the vegetation is *Cyathula prostrata*. The nine analysed plots reached maximum

ET rates between 6 and 8 (kg m^{-2} day^{-1}) with a daily watering of 12 ($l \cdot m^{-2} \cdot day^{-1}$) where the maximum VWC have ranged between 0.22% and 0.35%. The higher and more constant VWC values were obtained in the plots with a 5 cm water retention layer. Finally, there is a lack of information about the specific location of the watering drip system into the green roof section.

Another study conducted by Chenot et al. [14] in a Mediterranean climate (Csa) shows similar ET values in comparison to the results obtained in experiment one of this thesis chapter. The aim of the study was to evaluate how substrate composition and depth affect the moisture behaviour and plant development in a Mediterranean context. A total of 96 trays of 1 m^2, varying the depth from 5 to 15 cm and the substrate composition with different % of coarse and fine materials, were tested in summer and autumn periods of 2016. A mean ET rate of 4.23 (kg m^{-2} day^{-1}) was obtained using the Thornthwaite method after a rainfall of 77.28 mm distributed along 18 days in summer (from June 17th to July 18th). The VWC in the samples were collected manually every two days after a rain event. The results showed a maximum moisture content of 12% and 8% in substrates of 5 cm and 15cm, respectively.

The substrate composition, thickness and vegetation, as well as the watering system are the two main technical differences when the results of previous mentioned studies are compared to those of the present thesis chapter. However, the values of moisture content and ET rates showed similar trends in all the studies such as fast decrements of VWC after a week from last rainfall or watering especially for the thinner substrates of 5 to 8 cm, and similar daily ET rates.

The experimental correlation between the daily evaporation and the VWC of the bare substrate is presented in Figure 5. This linear correlation confirms the similar expected results by Tabares-Velasco and Srebric [12] in their study in which they have stated that a linear relationship for evaporation and the bare substrate water content (without plants) could be obtained.

However, the same authors obtained a non-linear correlation between VWC and ET when used plants in laboratory experiments because of the different parameters affecting their water loss, such as photosynthesis and stomatal resistance.

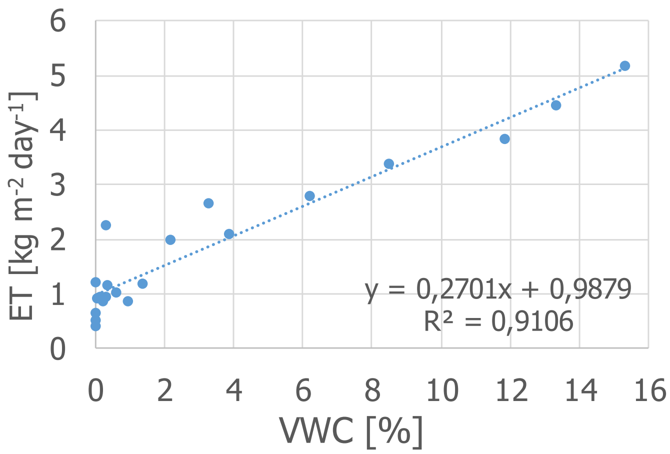

Figure 5. Experimental correlation of the daily evaporation rates and volumetric water content of the substrate.

8.4.1.2. Temperature evolution

The thermal performance of the substrate showed an important reduction of the surface temperatures by the addition of water at the beginning of the experiment, as expected (Figure 6). The gravel reference system registered higher daily peak temperatures of about 14 ºC in comparison to the saturated substrates. However, the fast reduction of moisture content after nine days, represented in Figure 6, had a direct impact in increasing the surface temperature of the substrate (Figure 6). From August 16th onwards, both substrates and gravel systems showed similar temperatures on the surface because of the low daily ET rates. Only from August 18th to 21st, there were small reductions of peak temperatures in the substrate compared to the gravel system due to the rainfall (3.5 mm) on 17 August.

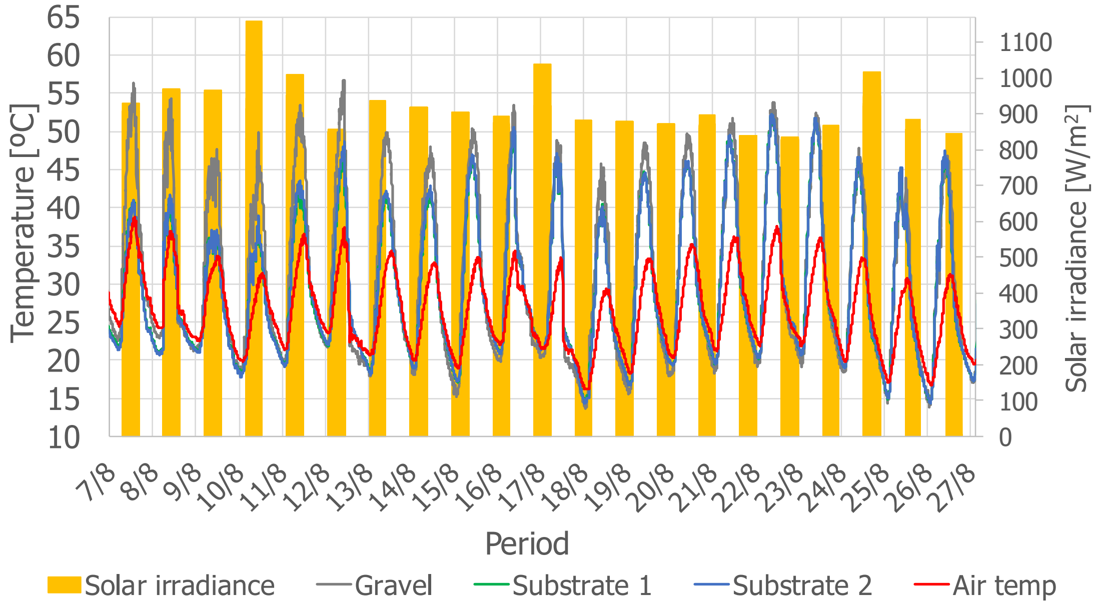

Figure 6. Thermal performance of the surface of substrate and gravel systems.

8.4.2. Experiment 2

8.4.2.1. Evaporation potential

According to Chenot et al. [14], the substrate moisture behaviour during summer dry periods in Avignon, South-eastern France (Csa), is influenced by the type of rainfall event (intensity, duration). In addition to these statements done by Chenot et al. 2017, the results presented in the experiment 2 of the present thesis chapter highlight the importance of the irrigation system. Figure 7 shows the evolution of VWC that registered a peak of 5.3% four days after the irrigation event. This value represents approximately one third of the maximum water content registered in experiment 1 (15.5%) that was saturated simulating an intense rainfall event. Thus, an important difference not only in the peak but also in the time lag of the VWC peak was observed when two different irrigation systems were compared. A delay of 4 days after the saturation of the system was observed in the moisture content peak.

Since the water input in experiment 2 is from drip watering system allocated below the substrate (Figure 7) instead of the outermost surface as in experiment 1, the water movement is mainly characterized by water sorption of the substrate and because of evaporation but not by precipitation. Thus, a drip irrigation system cannot provide the same water distribution to a substrate as a rainfall event.

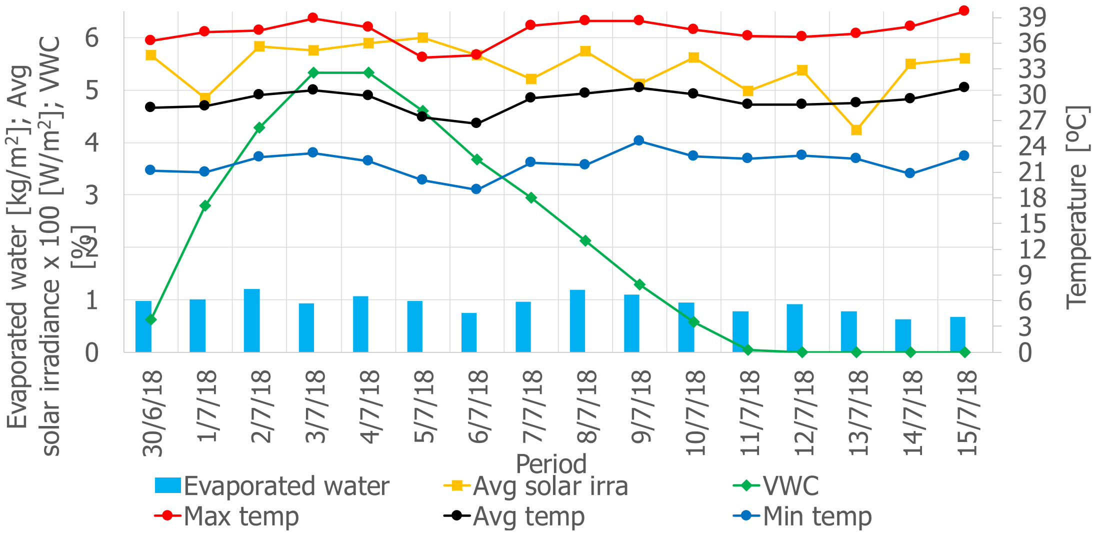

Figure 7. Water evaporation from saturated to dry conditions using internal drip irrigation system and daily ambient parameters along the experimental summer period.

The daily mean temperature of the air along this period was 28.9 ºC with a mean RH and solar irradiance of 60.2% and 321 W/m^2, respectively. The highest ET rate was 1.2 (kg m^{-2} day^{-1}) with a mean VWC of 5.5 % on July 8th, 2018. For this specific watering system, the water evaporation is limited because of the low VWC of the substrate. The incremental trend of VWC was not linear being 2.18% on July 1st, 1.49% on July 2nd, and 1.05% on July 3rd until reach the peak of 5.3% on July 4th. However, the VWC trend showed a linear decrement from the peak until reach the dry conditions with a daily reduction of about 0.75%.

8.4.2.2. Temperature evolution

Compared to the Experiment 1, where a higher quantity of water was provided by manual irrigation, the differences in temperatures are reduced in Experiment 2 (Figure 8). Substrate surface temperatures were always higher than both air temperatures and gravel roof. This is due to the white color of the gravels and their reflective capacity. In this Experiment, the water provided by the drip irrigation was not able to reduce substrate temperatures though the evaporation phenomena.

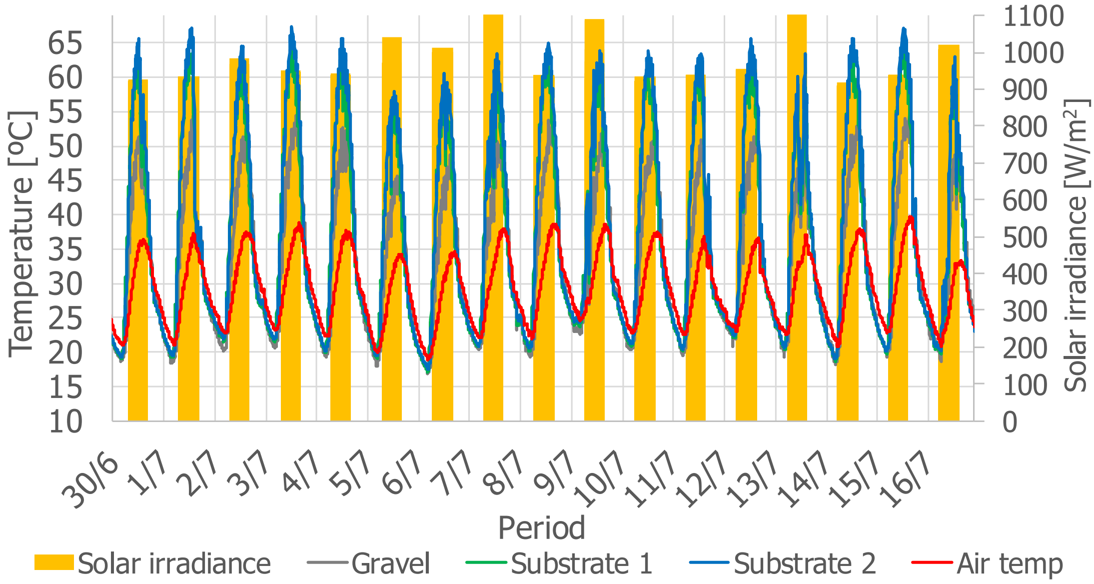

Figure 8. Thermal performance of the surface of substrate and gravel systems.

8.5. Conclusions

In this thesis chapter, an experimental set-up was developed for the evaluation of passive cooling potential of green roofs to improve the knowledge on the correlation between the evapotranspiration and thermal performance. The passive cooling potential was evaluated by varying the amount of water supplied by irrigation system. First results from the experimental evaluation on passive cooling of green roofs showed that when a high quantity of water was provided manually (Experiment 1), it increased the thermal performance of green roof. On the other hand, when the water was provided only by the drip irrigation system, the thermal performance is not so far from the gravel bare roof. It should be highlighted that these are only first results from the experimental set-up, mainly carried out to check that it works properly. The ongoing research will evaluate the cooling effect following the vegetation installation, comparing its thermal performance with the performance of green roof without vegetation. The second step of the research will be the comparison between the cooling effect of two different plant species, in order to identify the vegetation with the highest cooling potential in the continental Mediterranean climate.

References

[1] A.B. Besir, E. Cuce, Green roofs and facades: A comprehensive review, Renew. Sustain. Energy Rev. 82 (2018) 915–939. doi:10.1016/j.rser.2017.09.106.

[2] B. Raji, M.J. Tenpierik, A. Van Den Dobbelsteen, The impact of greening systems on building energy performance: A literature review, Renew. Sustain. Energy Rev. 45 (2015) 610–623. doi:10.1016/j.rser.2015.02.011.

[3] S. Vera, C. Pinto, P.C. Tabares-velasco, W. Bustamante, A critical review of heat and mass transfer in vegetative roof models used in building energy and urban enviroment simulation tools, Appl. Energy. 232 (2018) 752–764. doi:10.1016/j.apenergy.2018.09.079.

[4] F.E. Boafo, J.T. Kim, J.H. Kim, Evaluating the impact of green roof evapotranspiration on annual building energy performance, Int. J. Green Energy. 14 (2017) 479–489. doi:10.1080/15435075.2016.1278375.

[5] S. Cascone, J. Coma, A. Gagliano, G. Pérez, The evapotranspiration process in green roofs : A review, Build. Environ. 147 (2019) 337–355. doi:10.1016/j.buildenv.2018.10.024.

[6] A. Jahanfar, J. Drake, B. Sleep, B. Gharabaghi, A modified FAO evapotranspiration model for refined water budget analysis for Green Roof systems, Ecol. Eng. 119 (2018) 45–53. doi:10.1016/j.ecoleng.2018.04.021.

[7] C.L. Tan, P.Y. Tan, N.H. Wong, H. Takasuna, T. Kudo, Y. Takemasa, C.V.J. Lim, H.X.V. Chua, Impact of soil and water retention characteristics on green roof thermal performance, Energy Build. 152 (2017) 830–842. doi:10.1016/j.enbuild.2017.01.011.

[8] S.E. Ouldboukhitine, G. Spolek, R. Belarbi, Impact of plants transpiration, grey and clean water irrigation on the thermal resistance of green roofs, Ecol. Eng. 67 (2014) 60–66. doi:10.1016/j.ecoleng.2014.03.052.

[9] O. Schweitzer, E. Erell, Evaluation of the energy performance and irrigation requirements of extensive green roofs in a water-scarce Mediterranean climate, Energy Build. 68 (2014) 25–32. doi:10.1016/j.enbuild.2013.09.012.

[10] A.M. Coutts, E. Daly, J. Beringer, N.J. Tapper, Assessing practical measures to reduce urban heat: Green and cool roofs, Build. Environ. 70 (2013) 266–276. doi:10.1016/j.buildenv.2013.08.021.

[11] S.E. Ouldboukhitine, R. Belarbi, R. Djedjig, Characterization of green roof components: Measurements of thermal and hydrological properties, Build. Environ. 56 (2012) 78–85. doi:10.1016/j.buildenv.2012.02.024.

[12] P.C. Tabares-Velasco, J. Srebric, Experimental quantification of heat and mass transfer process through vegetated roof samples in a new laboratory setup, Int. J. Heat Mass Transf. 54 (2011) 5149–5162. doi:10.1016/j.ijheatmasstransfer.2011.08.034.

[13] P.C. Tabares-Velasco, J. Srebric, A heat transfer model for assessment of plant based roofing systems in summer conditions, Build. Environ. 49 (2012) 310–323. doi:10.1016/j.buildenv.2011.07.019.

[14] J. Chenot, E. Gaget, C. Moinardeau, R. Jaunatre, E. Buisson, T. Dutoit, Substrate composition and depth affect soil moisture behavior and plant-soil relationship on Mediterranean extensive green roofs, Water (Switzerland). 9 (2017) 1–16. doi:10.3390/w9110817.

Nomenclature

C_d Denominator constant that changes with reference type and calculation time step, s/m

C_n Numerator constant that changes with reference type and calculation time step, K mm s3 M/g/d or K mm s^3M/g/h

C_{pa} Specific heat of air at constant pressure, J/kg/°C

e_a Actual vapour pressure, kPa

e_s Saturation vapour pressure

E_g Evaporation rate on soil surface, kg/m^2/s

E_c Transpiration rate on plant canopy, kg/m^2/s

E_{et} Evapotranspiration rate, kg/m^2/s

ET Evapotranspiration rate, mm/h

ET_0 Reference evapotranspiration rate from a grass surface, mm/h

ET_{sz} Reference evapotranspiration rate from a standardized surface, mm/h

F Net heat flux, W/m^2

G Soil heat flux, W/m^2

H Sensible heat flux, W/m^2

K Dry soil thermal conductivity W/m/K

I_{ir} Total incoming long wave radiation, W/m^2

I_s Total incoming short wave radiation, W/m^2

L Latent heat flux, W/m^2

L_c Latent heat flux on plant canopy, W/m^2

L_g Latent heat flux on soil surface, W/m^2

L_{et} Latent heat flux from evapotranspiration, W/m^2

LAI Leaf area index, -

PET Potential ET rate, mm/h

q_{af} Vapour pressure of the air within plant canopy, Pa

q_c Vapour pressure of the air in contact with plants, Pa

q_g Vapour pressure of the air in contact with soil, Pa

Q_{ad} Energy transported by evapotranspirated water, W/m^2

Q_a Sensible heat flux to the air, W/m^2

Q_s Heat flux to the soil, W/m^2

Q_c Heat storage in the crop, W/m^2

Q_p Energy available for photosynthesis, W/m^2

R_n Net solar irradiance, W/m^2

R_s Incoming solar irradiation, MJ/m^2/d or MJ/m^2/h

r_a Aerodynamic resistance to transpiration, s/m

r_{sto}	Stomatal resistance to vapour diffusion, s/m
r_g	Aerodynamic resistance to evaporation on soil surface, s/m
T	Temperature, K
T_a	Mean monthly/daily/hourly air temperature, °C
TD	Mean maximum minus mean minimum temperature, °C/day
T_F	Mean monthly/daily/hourly air temperature, °F
u_2	Wind speed at 2m height, m/s
z	Height or depth, m
Greek letters	
α	Albedo, -
Δ	Slope of saturation vapour pressure with air temperature, kPa/°C
ε	Thermal emissivity, -
ε_1	View factor, -
γ	Thermodynamic psychometric constant, kPa/K
ρ_a	Air density, kg/m^3
ρ_{af}	Density of air within plant canopy, kg/m^3
λ	Latent heat of evaporation, MJ/kg
μ	Latent heat of vaporization of water, J/kg
σ	Stefan-Boltzmann constant, $W\ m^{-2}\ K^{-4}$
σ_f	Fractional vegetation coverage, -

General conclusions

The main results of the Ph.D. thesis are divided into numerical analysis and experimental research.

The results of numerical analyses are summarized in the following list:

1. The analysis carried out to assess the effect of different substrate-vegetation combinations on the energy performance of an extensive green roof and to identify those with the highest performance in the Mediterranean climate showed that solutions with the Salvia scored the highest during the summer period.
2. Only a few green roof configurations are suitable for the retrofitting of existing buildings, as their weight in saturated conditions does not exceed the load limit for roofs previously designed as walkable. All green roof solutions reduced energy consumption during both summer and winter. Considering this energy savings and material costs, an investment return time of between 13 and 18 years was estimated, depending on the technological solution.

The results of the experimental research are summarized in the following list:

1. The set-up at the University of Catania made it possible to evaluate the thermal performance of an innovative green roof and compare it with commercial solutions. First, the LCA analysis determined that the environmental impact of the production process of the recycled polyethylene granule used as drainage is mainly due to electricity consumption. The analysis of thermal behavior showed that the energy performance of the innovative solution is comparable with those of the conventional systems and is better than those of the traditional roof.
2. The high-precision scales below the green roof samples installed at the University of Lleida allowed to determine the evolution of weight over time, corresponding to a change in the water content in the green roof. First results from the experimental evaluation on passive cooling of green roofs showed that when a high quantity of water was provided manually, it increased the thermal performance of green roof. On the other hand, when the water was provided only by the drip irrigation system, the thermal performance is not so far from the gravel bare roof.

Future research developments will cover laboratory analysis of the thermo-physical properties of materials used in the experimental set-up at the University of Catania. The thermal conductivity of the materials for the drainage layer and substrate will be assessed as the water content changes, with attention to the recycled polyethylene granule and the substrate specially formulated for this research. In addition, the physical characteristics of the polyethylene grain in terms of minimum and maximum density, permeability and specific weight will be determined. A further study will aim at defining a mathematical model to validate experimental results. This model will be used to simulate the energy performance of the green roof on a building scale. Finally, regarding the correlation between evapotranspiration and the thermal behavior of the green roof, vegetation will be installed on a sample at the University of Lleida while in the other no vegetation will be installed.